Hunting for new physics in the primordial Universe

Wang, D.-G.

Hunting for New Physics in the Primordial Universe

Proefschrift

ter verkrijging van
de graad van Doctor aan de Universiteit Leiden,
op gezag van Rector Magnificus prof. mr. C.J.J.M. Stolker,
volgens besluit van het College voor Promoties
te verdedigen op 27 donderdag 2020
klokke 13:45 uur

door

Dong-Gang Wang
geboren te Guangrao, Shandong (China)
in 1991

Promotor:	Prof. dr. A. Achúcarro	
Co-promotor:	Prof. dr. Y.-F. Cai	(University of Science and Technology of China, Hefei, PRC)

Promotiecommissie:

Dr. E. Pajer	(University of Cambridge, UK)
Prof. dr. D. Roest	(University of Groningen)
Prof. dr. E. R. Eliel	
Prof. dr. K. E. Schalm	

Casimir PhD series, Delft-Leiden 2020-18
ISBN 978-90-8593-445-5
An electronic version of this thesis can be found at https://openaccess.leidenuniv.nl

The work in this thesis is funded by the Netherlands Organization for Scientific Research (NWO).

The cover is a sketch of the primordial era of the Universe. Time evolves from bottom to top. In chronological order, it shows the inflation stage, temperature anisotropies in the cosmic microwave background (image taken from the legacy release of the Planck satellite), and the formation of large scale structures (galaxy distribution image taken from the website of the Millennium Simulation Project). Examples of the new physics effects studied in this thesis are depicted by scalar field potentials, trajectories and a curved field space, while various Feynman diagrams correspond to some interesting physical processes during inflation.
The back cover is the first four lines of *Inquiries of Heaven* by Qu Yuan, a Chinese poet who lived during the Warring States period around 2300 years ago. The calligraphy was performed by Wang Chunliang, with the help of Wang Hongling.

To my parents

Contents

1 Introduction

At the dawn of time,
who was there to transmit the 'Dao'?
When the shape had not been stabilized,
by which means they could be explored?

The darkness and light are in chaos;
who could dive into the mysteries?
For this unique existence from nothing,
how to identify its pheno?

Inquiries of Heaven
Qu Yuan
(c. 340–278 BC)

In the past one hundred years, our understanding of the Universe has been tremendously improved. Cosmology, shifting away from speculative tones of philosophy and theology, has become a solid scientific subject, which can be analysed quantitatively and tested via precise experiments. The current research reveals that our Universe originated from the Big Bang 13.8 billion years ago and keeps expanding from then on. Furthermore not only the evolution history of the Universe, but also the matter distribution within it, can be described by scientific methods. With the latest advances, it has also become possible for the human being to give a natural and simple explanation for the origin of the Universe.

In the history of modern cosmology, the developments of fundamental physics played an important role. At the beginning, General Relativity reformulated our view of spacetime and provided the mathematical framework for describing the expansion of the Universe, which initiated the modern advance of cosmology. Later on, the hot Big Bang theory was constructed with the help of nuclear physics, thermodynamics and statistical physics. More significantly, the recent developments in *Quantum Field Theory* (QFT) have renovated our understanding for the origin of the Universe. The most important progress in this direction is the proposal of *cosmic inflation* as a possible consequence of QFT at extremely high energy scales of the primordial Universe [1–6]. This theory, positing an exponentially expanding phase at the very beginning of the Universe, successfully explains the very fine-tuned initial conditions of the hot Big Bang cosmology. Moreover, during inflation vacuum fluctuations of quantum fields are expected to generate seeds for galaxy formation, which explains the origin of cosmic structures. Thus there has been great theoretical interest in the inflation scenario in the past several decades.

On the other hand, the last century has also witnessed a rapid revolution in astronomy, which greatly changed the situation of observational cosmology. Now we have more and more data coming from various cosmological observations, which lead us into the era of precision cosmology. In particular, measures of temperature fluctuations in the cosmic microwave background (CMB) have provided a clean window for looking into the primordial perturbations generated in the very early Universe. As being tested by the CMB data more and more precisely [7, 8], cosmic inflation has been established as the leading paradigm of primordial cosmology. Furthermore, the upcoming experiments of large scale structure (LSS) surveys are expected to reveal more information about the early Universe in the near future.

Despite of the phenomenological success of inflation, it has also been realised for many years that there are some theoretical challenges, as it is notoriously difficult to embed inflation in more fundamental theories. Meanwhile, the idea of *Effective Field Theory* (EFT) provides a constructive approach, where the underlying microscopic details become irrelevant and an effective description may demonstrate the interesting physics in a model-independent way. Because of the high energy scale during inflation, typically we expect there would be some new physics, which may leave imprints in the primordial perturbations and become testable in cosmological observations. This line of thinking leads us to take inflation as a natural laboratory for probing fundamental physics at extremely high energy scales.

This thesis is a contribution to the hunting for new physics in the primordial Universe. One goal here is to trace observable effects in theoretically consistent theories of inflation. In particular I will dive into inflation with curved field spaces, which are generally expected in high energy physics theories. On the other hand, there will be also phenomenological studies directly motivated by observations. Here the main focus goes to one particularly important observable – primordial non-Gaussianity, which is expected to be a powerful tool for testing new physics effects.

The outline of the introduction is organized as follows. In Section 1.1, I will briefly review how new discoveries in fundamental physics have reformulated our understanding of the very early Universe. In particular, I will first introduce inflationary cosmology, including its historical origin, current status, and possible issues. Next, I will introduce the developments of cosmological perturbation theory and connections with astronomical observations. Section 1.2 turns to test new fundamental physics through primordial cosmology and focuses on two major frameworks. Firstly there will be a bird's eye review of multi-field inflation with a focus on the effects of curved field spaces. Next, I will present the idea of EFT and its applications in inflationary cosmology. After that there will be discussions on the current status and future directions. In the end the structure of the thesis will be outlined in Section 1.3. In this introduction, we use natural units with $\hbar = c = 1$ and set the Planck mass as $M_{\rm pl} \equiv (8\pi G)^{-1/2}$.

1.1 From fundamental physics to primordial cosmology

The advance of modern cosmology started from the theory of General Relativity which was proposed by Albert Einstein in 1915 [9]. This gravity theory suggests we live in a curved spacetime, while for our Universe on

the largest scales, the geometry can be described by a flat, homogeneous and isotropic Robertson-Walker metric

$$ds^2 = -dt^2 + a(t)^2 \left[dr^2 + r^2 \left(d\theta^2 + \sin^2\theta d\phi^2\right)\right] \ , \tag{1.1}$$

where $a(t)$ is the scale factor reflecting the expansion or contraction of the space. In 1927, Lemaître proposed the recession behaviour of galaxies in an expanding Universe [10], which was confirmed by Hubble's observation two years later [11]. After that the expansion of the Universe is established, and the expansion rate is characterized by the Hubble parameter $H \equiv \dot{a}/a$, where the dot denotes derivative with respect to the cosmic time t. Then from the Einstein field equation, one can derive the following Friedmann equations [10, 12]

$$3H^2 M_{\rm pl}^2 = \rho, \tag{1.2}$$

$$M_{\rm pl}^2 \dot{H} = -\frac{1}{2}(\rho + p) \ . \tag{1.3}$$

This setup, also known as the Friedmann-Lemaître-Robertson-Walker (FLRW) model, provides a quantitative description for the background dynamics of the Universe.

One particularly important solution of the Friedmann equations is the *de Sitter spacetime*, which was proposed by Willem de Sitter in 1917 [13, 14]. There an unconventional matter content with negative pressure $p = -\rho$ drives the Universe to expand exponentially $a(t) \propto e^{Ht}$. As we will discuss later, a potential-dominated vacuum energy in QFT may lead to this type of accelerating expansion, which plays an important role in the modern studies of primordial cosmology.

With information of the density ρ and pressure p of the matter components, we can reconstruct the expansion history of our Universe. Later *the hot Big Bang theory* proposed that our observable Universe originated from a small patch with a hot and dense state. Since the energy scales are extremely high in the early Universe, elementary particles are unbounded and nuclear physics effects become dominant. After the first several minutes of the Big Bang, free neutrons and protons formed the nuclei of light elements, which is called the *Big Bang Nucleosynthesis* (BBN) [15]. As the Universe expands and cools, nuclei and electrons were combined to form neutral atoms around 380000 years later. As a result, photons can travel freely through space from then on, and some of them remain in today's Universe. This relic radiation forms the so-called called *cosmic microwave background* (CMB).

The time evolution of the Universe is shown in Fig. 1.1 with energy scales. Both BBN and CMB, as the landmark predictions of the hot Big Bang theory, have been confirmed by observational experiments. In particular, astronomers precisely measured the light element abundance of BBN and the temperature of black body radiation from the CMB, which provides strong supporting evidence of the Big Bang origin of the Universe.

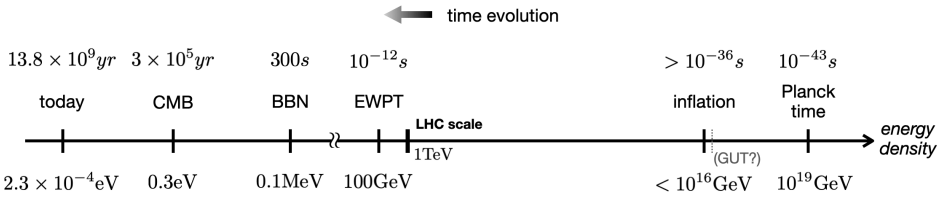

Figure 1.1: The evolution history of the Universe with energy scales. (EWPT, LHC and inflation will be discussed in the following sections.)

In spite of these successes, some unsolved puzzles remain in the hot Big Bang theory. The most famous one is the so-called *horizon problem*. In the Big Bang cosmology, the casually connected area of the Universe was much smaller than the physical size of today's observable Universe in the early times. This means that the homogeneous matter distribution we observe today were not correlated at the very beginning. Thus it is confusing why different casually disconnected areas shared the same properties during the Big Bang.

Another puzzle is the flatness problem, which questions why the spatial curvature of our Universe is negligible today. Since it is more natural to have a spatially curved Universe after the Big Bang expansion, the current observations of a zero spatial curvature may need fine tuning of the initial conditions. In addition, although the Universe is homogeneous and isotropic on the largest scales, there are also cosmic structures such as clusters, galaxies and stars. Their origin and distribution remain unexplained. In essence, these puzzles are all related the initial conditions of the Universe, which indicates that there may be an earlier phase before the hot Big Bang.

Meanwhile, if we go further back in time, and consider even earlier stages of the Universe, the energy density becomes much higher than the scale of particle colliders on earth, and the size of the observable Universe enters the unknown microscopic regime. According to our understanding of elementary particles in the subatomic world, quantum fields are expected to play an important role in this extreme environment. This consideration

led to studies on cosmic phase transitions and later the development of inflationary cosmology, which will be elaborated on in the following sections.

1.1.1 Cosmic inflation

Inflation was first introduced to solve the puzzles of the Big Bang cosmology in early 1980s by Alan Guth [1]. It assumes that around the initial 10^{-36} seconds, the Universe undergoes a quasi-de Sitter expansion. This exponentially accelerating period expands the Universe at least e^{60} times larger, and thus dilutes away the unwanted relics and possible spatial curvature at the very beginning. Meanwhile, as a result of the rapid accelerating expansion, the observable Universe today all comes from one casually connected region at the beginning of inflation. Therefore by the end of inflation, a flat, homogeneous and isotropic initial condition was naturally given for the following Big Bang expansion.

Historically inflation was also proposed as one possible consequence of QFT in the very early Universe. Here we will first review the early developments of inflation theory from the perspective of spontaneous symmetry breaking and cosmic phase transitions, and then move to its standard scenario and remaining issues.

1.1.1.1 Cosmic phase transition and inflation

Spontaneous symmetry breaking (SSB) is one of the most profound concepts in modern QFT. It corresponds to the situation where the theory obeys a certain symmetry, but the system in the lowest-energy vacuum state does not respect the same symmetry. One simple example is the breaking of a $U(1)$ symmetry in the following theory of a complex scalar field

$$\mathcal{L} = -\frac{1}{2}\partial_\mu\phi^*\partial^\mu\phi - \lambda(\phi^*\phi - v^2)^2 \tag{1.4}$$

where the potential has a Mexican hat form as shown in Fig. 1.2. As the minima of the potential are located at $|\phi| = v$, there are an infinite number of vacua in this theory. For each vacuum state, for instance $\phi = v$, it is no longer invariant under the $U(1)$ symmetry. Meanwhile it is convenient to parametrize the complex field as $\phi = \rho e^{i\theta}$. Then we find the radial field ρ is massive, and the angular direction θ turns out to be massless. This massless mode, or the angular direction in the circle of the minima, is called a Goldstone field, which is naturally associated with a shift symmetry $\theta \to \theta + const.$.

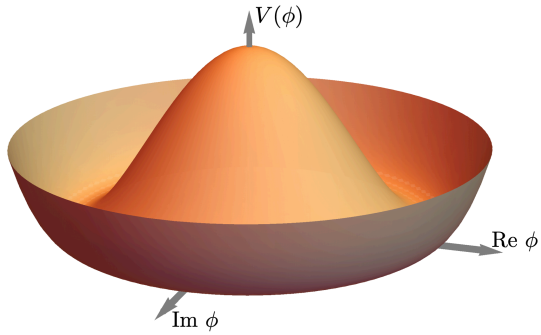

Figure 1.2: Mexican hat potential and SSB.

The concept of SSB played a central role in the construction of the Standard Model of particle physics, where a Higgs field is introduced to spontaneously break the gauge symmetry $SU(2) \times U(1)$ of the electroweak theory and unify the electromagnetic and weak interactions. Soon after, it was realized that the $SU(2)\times U(1)$ symmetry should be restored in the early Universe. As the energy is higher in the earlier stages, the finite-temperature effects in QFT will change the form of the Mexican hat potential, and the minimum is expected to become the point at the origin which respects the symmetry. Therefore, when the temperature goes down as the Universe expands, there should be a phase transition process in the early stage which evolves from the symmetric phase to the broken phase.

In the Standard Model of particle physics, the electroweak phase transition (EWPT) is not expected to dramatically change the course of the Big Bang expansion. However, there may be significant consequences if we consider another SSB process for a larger symmetry group which can unify the electroweak theory with the strong interaction with $SU(3)$ symmetry as well. This hypothetical theory, called Grand Unified Theory (GUT), although has not been verified in experiments, may lead to a drastic phase transition in the very early Universe.

The first proposal of cosmic inflation was realized in the first-order phase transition of a GUT theory. There at the beginning the scalar field, which is also called the inflaton, is supposed to be at the local minimum $\phi = 0$. This is a false vacuum as shown in the left panel of Fig. 1.3. As a consequence, the nonzero vacuum energy with $\rho_{\rm vac} \simeq V$ and negative pressure $p_{\rm vac} \simeq -V$ becomes dominant, which drives the de Sitter expansion of the Universe. Then as the Universe inflates, vacuum decay happens and the inflaton field

will move to the true minimum at the bottom of the potential via quantum tunnelling, initiating the following hot Big Bang expansion.

This first scenario was later named as "old inflation". However, this idea does not work, since a graceful exit from inflation is not provided here. As the vacuum decay leads to bubbles of the true vacuum in the Universe, the de Sitter expansion stops inside the bubbles, but still keeps going elsewhere. As a result, bubbles may never collide with each other to end inflation in the whole Universe.

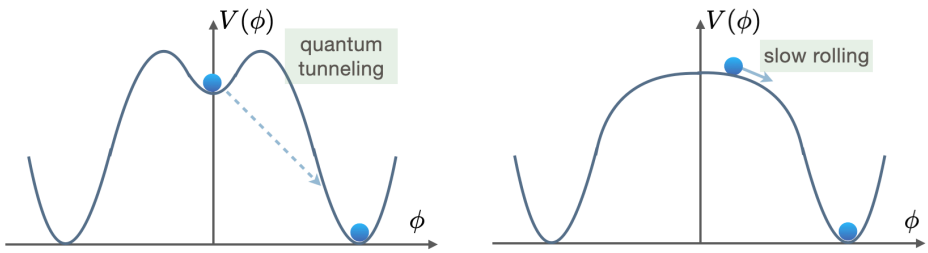

Figure 1.3: "Old inflation" (left) and "new inflation" (right) on cross-section profiles of the Mexican-hat-type potentials.

Soon after, the graceful exit problem was solved in the "new inflation" scenario proposed by Andrei Linde [2]. Instead of the first-order phase transition process with bubble nucleation in the old inflation, here a continuous GUT phase transition is considered. As shown in the right panel of Fig. 1.3, the scalar field rolls on a Coleman-Weinberg potential without barriers. Due to the effects of Hubble friction, the field velocity turns out to be quite slow, and the energy is dominated by the potential. As a result, a quasi-de Sitter expansion is provided and inflation gracefully ends in the whole Universe as the inflaton slowly rolls to the true minimum of the potential.

1.1.1.2 Slow-roll inflation

After the idea of "slow-roll" was proposed, physicists found it is not necessary to stick to GUT phase transitions, and many other models have shown similar behaviour but are less constrained than the new inflation. In general, they can be simply described by the following action with Einstein gravity and a canonically normailzed inflaton field

$$S = \int d^4x\sqrt{-g}\left[\frac{M_{\rm pl}^2}{2}\mathbf{R} - \frac{1}{2}(\partial\phi)^2 - V(\phi)\right] , \tag{1.5}$$

where the potential should satisfy the following slow-roll conditions

$$\epsilon_V \equiv \frac{M_{\rm pl}^2}{2}\left(\frac{\partial_\phi V}{V}\right)^2 \ll 1 \ , \qquad |\eta_V| \equiv M_{\rm pl}^2\frac{|\partial_{\phi\phi} V|}{V} \ll 1 \ . \tag{1.6}$$

As a result, a quasi-de Sitter expansion is supposed to be driven by the vacuum energy of the scalar field. This requirement, saying that the inflaton potential should be sufficiently flat, can be equivalently parameterized by using the Hubble slow-roll parameters as

$$\epsilon \equiv -\frac{\dot{H}}{H^2} \ll 1, \qquad \eta \equiv \frac{\dot{\epsilon}}{\epsilon H} \ll 1 \ . \tag{1.7}$$

It turns out that this slow-roll dynamics is an attractor in the phase space $(\phi, \dot{\phi})$, where non-slow-roll conditions will converge to it rapidly. Here the smallness of the first slow-roll parameter ϵ ensures that the kinetic energy of the inflaton is much smaller than the potential, such that accelerating expansion can happen, while $\eta \ll 1$ guarantees inflation will not end prematurely. This class of models are named as *single field slow-roll inflation*. Since current observations are in favor of these simplest models, they are regarded as the standard scenario of inflation.

In recent years, more accurate CMB data indicates a hierarchy between slow-roll parameters $\epsilon \ll \eta$. This has led to stronger constraints on slow-roll potentials, where inflating on a concave plateau is more favoured by observations. As a result, a subclass of slow-roll models with plateau-like potentials have been extensively investigated lately. Famous examples here include Starobinsky inflation [3], Higgs inflation [16] and α-attractors [17, 18].

1.1.2 Possible issues

From the phenomenological perspective, single field slow-roll scenario is very successful. Meanwhile its theoretical construction relies on the ultraviolet (UV) physics at higher energy scales. If we seriously look into these inflation models in a consistent UV theory, typically they turn out to be problematic [19]. Here I list several difficulties faced by the UV-completion of inflation and also some generic lessons that we can learn from these theoretical challenges.

1.1.2.1 η-problem

The most well-known challenge for single field slow-roll models is the so-called η-problem [20]. As the slow-roll parameter η is related to the mass

of the inflaton field via $\eta_V \simeq m_\phi^2/H^2$, the second condition in (1.6) can also be seen as a requirement that the Hubble parameter during inflation should be much larger than the mass scale of the inflaton field. This is fine if we only treat the scalar field at the classical level. However, in a complete theory with quantum fields, the effects of radiative corrections should also be taken into account. If we do so, the inflaton mass receives contributions from loop diagrams which are typically around or larger than the Hubble scale $\Delta m_\phi \gtrsim H^2$. As a result of this large correction, the second slow-roll condition will be violated

$$\Delta\eta_V \simeq \frac{\Delta m_\phi^2}{H^2} \gtrsim 1, \tag{1.8}$$

thus the inflaton potential can no longer stay sufficiently flat to sustain long enough inflation.

Generally speaking, this is a problem for most of the slow-roll models. As the characteristic energy scale during inflation is given by the Hubble parameter, we expect there is always a hierarchy between H and m_ϕ in the system, which may generically spoil the flatness of the slow-roll potential. Therefore the η-problem can be seen as the hierarchy problem of inflation and is essentially the same as the one of the Higgs field in particle physics, where with a UV cutoff for new physics, the radiative correction to the Higgs mass is expected to be much larger than the measured value in Large Hadron Collider (LHC) [1].

In order to solve this problem and avoid a certain level of fine-tuning, usually it becomes necessary to impose some symmetries for the inflaton field. A concrete example is realized in natural inflation [21], where an approximate shift symmetry of a pseudo-Goldstone field is introduced to protect the flatness of the potential. We shall elaborate on this issue in Section 1.2.2.3 where its connections with SSB and implications for the effective theory will be discussed.

1.1.2.2 Swampland conjectures

If we care about the embedding of inflation within quantum gravity, there have been some speculative criteria called swampland conjectures which might tell whether a low-energy effective theory of inflation can emerge from

[1] According to the modern understanding of QFT, the hierarchy problem can be universal for scalar fields. In general spinor and gauge fields are protected by chiral symmetries and gauge symmetries respectively, thus will not be affected by quantum corrections, but this is not generically the case for scalar field theories.

UV-complete theories or not. Although rigorous proofs are still missing, these conjectures may give some hints about theoretical constructions of inflation models. Here are two famous examples:

- *Swampland distance conjecture.* To ensure the validity of the effective description, the field excursion distance during inflation is conjectured to be smaller than the Planck scale [22], *i.e.*

$$\Delta\phi \lesssim cM_{\rm pl} \ , \tag{1.9}$$

  where c is a $\mathcal{O}(1)$ constant. This is also related to the well-studied Weak Gravity Conjecture [23] which has got indications from various perspectives recently. If it is generally true, many inflation models with super-Planckian field excursion ($\Delta\phi > M_{\rm pl}$) might be problematic.

- *Swampland de Sitter conjecture.* This one supposes scalar field potentials in consistent effective theories ought to satisfy the following condition [24]

$$\left|\frac{\nabla V}{V}\right| \gtrsim \frac{1}{M_{\rm pl}}\mathcal{O}(1) \ . \tag{1.10}$$

  Basically it means the slope of the potentials should be quite steep. Compared with the distance conjecture, the de Sitter conjecture is in tension with all the single field inflation models, but it is also controversial. So far there is still no solid supporting evidence from quantum gravity theories.

1.1.2.3 Other challenges and alternatives to inflation

Besides the issues above, some other theoretical considerations may challenge inflationary cosmology as a whole. For instance, it has been shown that in inflationary spacetimes geodesics are incomplete towards the past direction, thus one expects a cosmic singularity [25]. On the other hand, the physical wavelength of some quantum fluctuations during inflation can be much smaller than the Planck length (trans-Planckian) at the beginning, thus one may worry if the analysis of perturbation is valid [26]. These issues, though not fatal, motivate us to also consider alternative paradigms for the primordial Universe.

Bouncing cosmologies provide a simple solution for the singularity problem and the trans-Planckian problem [27, 28]. In this class of paradigms the Universe was contracting at the beginning, and then transited to the Big

Bang expansion through a bouncing phase. A particular example is called *matter bounce cosmology* [29–31], where the contracting phase is dominated by the pressureless matter. In Chapter 6, I will study the distinguishable predictions from matter bounce models and also look into their difficulties.

1.1.3 Cosmological perturbation theory

Besides inflation, cosmological perturbation theory is another great achievement of primordial cosmology in the past several decades [32–34]. There a natural and elegant explanation is given for the origin of inhomogeneous structures in the Universe.

For the analysis of a perturbation mode k in a cosmic background, one particularly important length scale is the Hubble radius H^{-1}, which is also the curvature scale of the FLRW spacetime. Since for the de Sitter Universe, the Hubble radius is the size of the so-called event horizon as well, we also refer it as the horizon scale in this thesis. When the physical wavelength of this mode is larger than this scale, it is called "superhorizon" ($a/k \gg H^{-1}$); correspondingly "subhorizon" refers to the regime where perturbations have shorter wavelengths than this curvature scale ($a/k \ll H^{-1}$).

According to the cosmological perturbation theory, microscopic quantum fluctuations during inflation were stretched outside of the horizon by the rapid accelerating expansion (which is called horizon-exit), and then the primordial perturbations were generated. After inflation, these tiny inhomogeneities re-entered the horizon, which led to the anisotropies of temperature fluctuations in the CMB, and also provided the seeds for macroscopic objects like galaxies and clusters. We briefly introduce the basic formulation here with the standard results of single field slow-roll inflation.

1.1.3.1 Primordial perturbations

In the primordial Universe, there are two types of metric perturbations that are relevant to today's cosmological observations. The first one is the curvature perturbation $\mathcal{R}(t, \mathbf{x})$, which is the scalar component in the perturbed metric; while the second one are the tensor modes, also known as the primordial gravitational waves $h_{ij}(t, \mathbf{x})$.

During inflation, the curvature perturbation is generated by the quantum fluctuations of the inflaton field $\delta\phi$. At the beginning these fluctuations are in the subhorizon regime and do not feel the spacetime curvature, thus they are well described by the vacuum state as in the flat spacetime, which is called the Bunch-Davies initial condition. As inflation stretches these fluctu-

ations exponentially, their physical wavelengths become superhorizon, and a quantum-to-classical transition happens. After this horizon-exit process, the inflaton fluctuations acquire a typical size of $\delta\phi = H/(2\pi)$. This sources the generation of primordial curvature perturbation on superhorizon scales with a frozen amplitude $\mathcal{R} = \frac{H}{\dot{\phi}}\delta\phi$.

More specifically, one may begin with perturbing the action (1.5) of slow-roll inflation, and then derive the quadratic action of scalar perturbations

$$S_2 = \int d^4x a^3 \epsilon \left[\dot{\mathcal{R}}^2 - \frac{1}{a^2}(\partial_i \mathcal{R})^2\right] . \tag{1.11}$$

As we see, there is no mass term for $\mathcal{R}$, which indicates its conservation on superhorizon scales. It is more convenient to work with the Fourier mode in momentum space. After canonical quantization and solving the linear equation of motion, we derive the following approximate solution for the mode function in the de Sitter limit

$$\mathcal{R}_k = \frac{H}{\sqrt{4\epsilon k^3}}(1 + ik\tau)e^{-ik\tau}, \tag{1.12}$$

where τ is the conformal time defined by $d\tau \equiv dt/a(t)$. This provides a good description for both the Bunch-Davies vacuum state $\mathcal{R}_k \sim 1/\sqrt{k}$ inside the horizon ($-k\tau \gg 1$) and the superhorizon evolution $\mathcal{R}_k \sim k^{-3/2}$ ($-k\tau \ll 1$).

A similar story goes for the generation of primordial gravitational waves: during inflation tensor fluctuations are also stretched to macroscopic scales and freeze after horizon-exit. But here the tensor perturbations $h_{ij}(t, \mathbf{x})$ come from the vacuum of gravitons, instead of the inflaton fluctuations. We may also write down its quadratic action

$$S_2 = \frac{M_{\rm pl}^2}{4} \int d^4x \; a^3 \left[\dot{h_{ij}}^2 - \frac{1}{a^2}(\partial_k h_{ij})^2\right] , \tag{1.13}$$

while the solution of the mode function follows as

$$h_{ij} = \frac{iH}{\sqrt{2k^3}}(1 + ik\tau)e^{-ik\tau}e_{ij} \tag{1.14}$$

where e_{ij} is the polarization tensor. As a result, a stochastic background of gravitational waves is expected after inflation.

1.1.3.2 Cosmological observables from the primordial Universe

The statistics of primordial perturbations is well captured by the correlation functions, which are also the major observational targets in today's

cosmological experiments. Here we list some of the important observables for the primordial cosmology.

- *Primordial power spectrum.* The power spectra of perturbations, which are the Fourier transformation of two-point correlation functions, are the leading observables for the primordial cosmology. Again we use single field slow-roll inflation as an example, then with the solution (1.12) for the curvature perturbation, the prediction for its power spectrum at the end of inflation becomes

$$P_{\mathcal{R}}(k) \equiv \frac{k^3}{2\pi^2} \left|\mathcal{R}_k\right|^2 = \frac{H^2}{8\pi^2 M_{\rm pl}^2 \epsilon} \ , \tag{1.15}$$

  where H and ϵ ought to be evaluated at the time of horizon-exit τ_* of the k-mode given by $k = aH$ (or $-k\tau_* = 1$ equivalently). This spectrum is nearly scale-invariant, but taking into account the evolution of H and ϵ during inflation, we find it has a slight red tilt with less power on smaller scales. Usually a spectral index is defined to describe this mild scale-dependence

$$n_s - 1 \equiv \frac{d\ln P_{\mathcal{R}}}{d\ln k} = -2\epsilon - \eta, \tag{1.16}$$

  where the definitions of the Hubble slow-roll parameters (1.7) have been used to get the single field result. The prediction of a nearly scale-invariant power spectrum from single field slow-roll inflation is in agreement with the current CMB observations [7].

  Similarly we can define the power spectrum of primordial gravitational waves, and the single field slow-roll prediction follows directly

$$P_t(k) \equiv \frac{k^3}{2\pi^2} \left|h_{ij}^*(k) h^{ij}(k)\right|^2 = \frac{2H^2}{\pi^2 M_{\rm pl}^2} \ . \tag{1.17}$$

  This stochastic background of gravitational waves has not been detected yet, which is the major target for the on-going and future observational measurements on the B-mode polarization of the CMB and also other gravitational wave experiments. Usually the tensor-to-scalar ratio is defined to represent the amplitude of this spectrum

$$r \equiv \frac{P_t}{P_{\mathcal{R}}} \ , \tag{1.18}$$

while its latest constraint comes from the Planck satellite $r < 0.064$ [7]. Also this power spectrum has a slight red tilt, and we define the tensor spectral index as

$$n_t \equiv \frac{d\ln P_t}{d\ln k}, \tag{1.19}$$

which can be shown to equal -2ϵ in single field slow-roll models.

- *Primordial non-Gaussianity.* Power spectra can capture the properties of Gaussian statistics successfully, on the other hand, a wealth of interesting information may exist in the non-Gaussian statistics [35–38]. Thus after measuring the power spectrum, a lot of efforts have been carried out in the studies of primordial non-Gaussianities. Usually we look into higher order correlation functions for possible deviations from Gaussian distribution. One major observable here is the primordial bispctrum of curvature perturbations, which is the Fourier transform of the three-point correlation function

$$\langle \mathcal{R}_{\mathbf{k_1}} \mathcal{R}_{\mathbf{k_2}} \mathcal{R}_{\mathbf{k_3}} \rangle \equiv (2\pi)^3 \delta^{(3)}(\mathbf{k_1} + \mathbf{k_2} + \mathbf{k_3}) B_{\mathcal{R}}(k_1, k_2, k_3) \ . \tag{1.20}$$

The three momenta must add up to zero by translation invariance and therefore they form a triangle. As we can see here, the bispectrum can have many possible shapes as functions of three momenta and also overall sizes. Usually a shape function $\mathcal{S}(k_1, k_2, k_3)$ is introduced to represent the various templates, and for each shape there is a non-linear parameter $f_{\rm NL}$ describing the size of the non-Gaussian signal

$$B_{\mathcal{R}}(k_1, k_2, k_3) = \frac{18}{5} f_{\rm NL} \mathcal{S}(k_1, k_2, k_3) P_{\mathcal{R}}^2. \tag{1.21}$$

The typical templates include local, equilateral and folded shapes, while the size of the local non-Gaussianity has got the tightest observational constraint from CMB observations $f_{\rm NL}^{\rm local} = -0.9 \pm 5.1$.

Besides the shape function, another informative channel is the triangle configurations of momenta, such as the squeezed limit with $k_1 \ll k_2 = k_3$. The behaviours of the bispectrum at different triangle limits are supposed to encode information about various physical effects during inflation. One famous example is *Maldacena's consistency relation of single field inflation*, where the squeezed bispectrum is associated with the scalar spectral index as follows [39, 40]

$$\lim_{k_1 \ll k_2 = k_3} B_{\mathcal{R}}(k_1, k_2, k_3) = \frac{(2\pi)^4}{4k_1^3 k_3^3} P_{\mathcal{R}}(k_1) P_{\mathcal{R}}(k_3) \frac{d\ln P_{\mathcal{R}}(k_3)}{d\ln k_3} \tag{1.22}$$

Since this result is caused by the gravitational interactions during inflation, it is expected to be the minimal amount of non-Gaussianity generated, which is known as the gravitational floor. This relation was supposed to be valid for all the single field inflation models with Bunch-Davies vacuum. However, later a counterexample was constructed in non-attractor inflation [41–43]. Chapter 5 shall carefully reexamine the violation of the consistency relation in this class of non-standard models.

Although it is difficult to detect in observations, the rich phenomenology of primordial non-Gaussianity makes it a very powerful tool to probe new physics in the primordial Universe. In this thesis, besides Chapter 5, Chapter 4 will study the imprints on the squeezed bispectrum from inflationary models with more complicated internal field spaces, while Chapter 6 will investigate the non-Gaussian signals from one alternative scenario to inflation.

- *Other future opportunities.* Current CMB observations show that primordial curvature perturbations on very large scales are nearly scale-invariant and Gaussian, which is consistent with the single-field slow-roll scenario. Meanwhile there are still many possibilities to deviate from these standard predictions. One is called primordial features, which correspond to deviations from the nearly scale-invariance of the power spectrum, such as oscillating wiggles. Another possibility is called anomalies, which correspond to possible deviations from the statistical isotropy of the primordial perturbations, such as hemispherical asymmetry and cold spot indicated by the latest CMB data. These observables, which will be further constrained by future CMB and LSS experiments, provide opportunities for testing inflation from different perspectives.

  Finally, one recent topic is primordial black holes (PBHs) which are hypothetical objects formed in the early Universe. Since they may originate from enhanced curvature perturbations with wavelengths much shorter than the cosmological scales today, one can also probe the small-scale power spectrum via the tighter and tighter observational constraints on PBHs [44]. In order to generate PBHs which are of observational interest, it is also important to investigate natural mechanisms of amplifying curvature perturbations during inflation. One attempt in this direction is the proposal of *sound speed resonance*, where the small scale perturbations are efficiently enhanced

by parametric resonance effects during inflation [45, 46]. It remains an open question if this idea can be naturally realized in consistent theories.

1.2 From primordial cosmology to fundamental physics

High energy physics aims to explore the fundamental laws of the microscopic world, which contributes to the greatest ambition of theoretical physics – a *theory of everything*, bringing together quantum mechanics and general relativity. From the experimental perspective, the traditional approach to high energy physics is using colliders to search for new particles. However the energy scale that can be reached by LHC is around 1TeV which is far below the Planck scale where quantum gravity effects are expected to dominate. At the current stage, it also becomes more and more difficult to achieve higher energy through particle collider experiments.

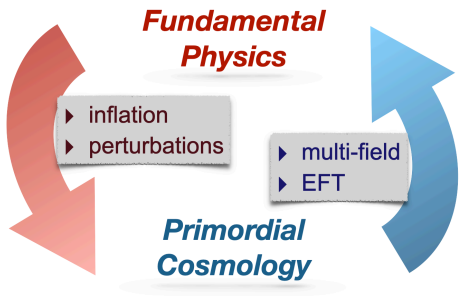

Figure 1.4: The interplay between fundamental physics and primordial cosmology.

Meanwhile, cosmology provides us a unique chance to peek into the new physics effects. In the last section, we have seen how fundamental physics tremendously changed the status of cosmology and helped with the development of inflationary cosmology. Notably inflation may also provide the highest energy scales in our Universe which can be probed via experiments. In this sense, cosmic inflation can be seen as a natural high energy laboratory for testing fundamental theories. In the following I shall elaborate on two major frameworks for this purpose.

1.2.1 Multi-field inflation in a nutshell

Although single field slow-roll models play the leading role in inflationary cosmology, we should also notice that in high energy theories typically there

are multiple fields. This leads to studies on multi-field inflation. One particularly interesting question is whether other fields would lead to observable consequences. Furthermore, these additional fields and their interactions with the inflaton are typically associated with particles, field space and fundamental symmetries during inflation. In this sense, multi-field inflation provides powerful techniques for us to study the effects of these interesting physics.

Meanwhile, another motivation for studying multi-field inflation comes from the theoretical challenges of single field models in more fundamental theories. As we discussed in Section 1.1.2, these unsolved issues may put constraints on the UV completion of single field inflation. While the η-problem may be solved by assuming internal symmetries, it is still less clear how to avoid the issues from swampland conjectures. Here multi-field models may provide a natural solution [47, 48]. For instance, if the inflaton trajectory is turning in a multi-dimensional field space, its geodesic distance can remain sub-Planckian while the excursion range is larger than $M_{\rm pl}$, and inflating on a steep potential would also become possible because of the centrifugal force.

In the following I will approach multi-field inflation via the covariant formalism [49–53] and classify representative models into different regimes. After that there will be general discussions on a recent topic in this direction – inflation with a curved field manifold.

1.2.1.1 The covariant formalism

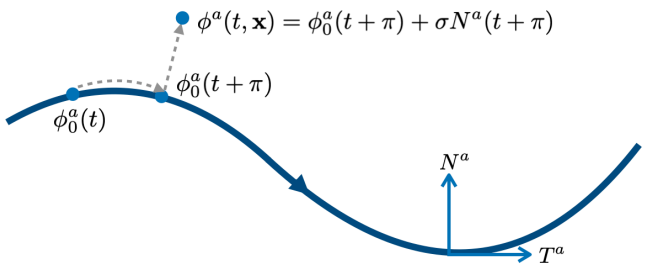

Figure 1.5: A generic inflaton trajectory with tangent and normal vectors in a two-dimensional field space, and the corresponding perturbations π and σ along and orthogonal to the trajectory respectively.

The starting point for many multi-field models is the following action

with a set of scalar fields ϕ^a and Einstein gravity

$$S = \int d^4x\sqrt{-g}\left[\frac{M_{\rm Pl}^2}{2}\mathbf{R} - \frac{1}{2}G_{ab}(\phi)g^{\mu\nu}\partial_\mu\phi^a\partial_\nu\phi^b - V(\phi)\right] , \qquad (1.23)$$

where $G_{ab}(\phi)$ is an internal field space metric. In a flat FLRW Universe, the background equations of this system can be written as

$$D_t\dot{\phi}_0^a + 3H\dot{\phi}_0^a + V^a = 0 , \qquad 3H^2 = \frac{1}{2}\dot{\phi}_0^{\,2} + V , \qquad (1.24)$$

where $D_t \equiv \dot{\phi}^a\nabla_a$ is the field space covariant derivative with respect to cosmic time and $V_a = \nabla_a V$ is the gradient of the potential. Notice that the latin field indices are manipulated with the internal space metric G_{ab}, e.g. $V^a = G^{ab}V_b$. The rolling motion of the inflaton forms a trajectory in the multi-dimensional field space. Here let us consider the two-field case as a simple example. As shown in Fig. 1.5, at each point of the trajectory we can define the tangent and normal unit vectors

$$T^a \equiv \frac{\dot{\phi}^a}{\dot{\phi}_0}, \qquad N_a \equiv \sqrt{\det G}\,\epsilon_{ab}T^b , \qquad (1.25)$$

where $\dot{\phi}_0 \equiv \sqrt{G_{ab}\dot{\phi}_0^a\dot{\phi}_0^b}$ is the proper inflaton field velocity, and ϵ_{ab} is the Levi-Civita antisymmetric symbol with $\epsilon_{12} = 1$. Now we can define one particularly important parameter – the turning rate Ω of the trajectory as:

$$\Omega \equiv -N_a D_t T^a \qquad (1.26)$$

Projecting the field equations of motion along the tangent and normal directions, we get respectively

$$\ddot{\phi}_0 + 3H\dot{\phi}_0 + V_T = 0 , \qquad (1.27)$$

$$V_N = \dot{\phi}_0\Omega , \qquad (1.28)$$

where $V_T = T^aV_a$ and $V_N = N^aV_a$. The second equation shows the balancing between the centrifugal force and the gradient of the potential in the normal direction. As we see here, if $\Omega = 0$, which corresponds to the situation the trajectory is a geodesic in the field space, the field dynamics simply returns to the single field case. Thus for multi-field behaviour, one major difference from the single field one is a nonzero turning rate (or non-geodesic motion equivalently [52]).

Now let us turn to the analysis of perturbations. There are two types of scalar perturbations in multi-field inflation: the adiabatic perturbation along the trajectory and the isocurvature perturbation σ orthogonal to the trajectory. As shown in Fig. 1.5, the deviation along $\phi_0^a(t)$ can be parametrized by a fluctuation in time π, which corresponds to the curvature perturbation through $\mathcal{R} = H\pi$. At the linear order, we can decompose the field perturbations as

$$\delta\phi^a = \delta\phi_\parallel T^a + \sigma N^a \ , \tag{1.29}$$

where $\delta\phi_\parallel = \dot{\phi}_0\pi$. Then the quadratic action in terms of curvature perturbation $\mathcal{R}$ and σ can be derived as

$$S_2 = \int d^4x a^3 \left[\epsilon\left(\dot{\mathcal{R}} - \frac{2\Omega}{\sqrt{2\epsilon}}\sigma\right)^2 - \frac{\epsilon}{a^2}(\partial_i\mathcal{R})^2 + \frac{1}{2}\left(\dot{\sigma}^2 - \frac{1}{a^2}(\partial_i\sigma)^2\right) - \frac{1}{2}\mu^2\sigma^2\right] \ , \tag{1.30}$$

Here let us look into two important terms in this action. The first one is the derivative interaction term $\dot{\mathcal{R}}\sigma$. As we see, this term means that when the trajectory has a nonzero turning rate, the two perturbation modes are coupled to each other. As a result, there is conversion from isocurvature to curvature perturbations on superhorizon scales. This is the key feature of multi-field effects. On the other hand, generally the isocurvature modes have a mass μ^2. It can be expressed as

$$\mu^2 = V_{NN} + \epsilon\mathbb{R}H^2 + 3\Omega^2 \ , \tag{1.31}$$

where $V_{NN} = N^a N^b \nabla_a \nabla_b V$ and $\mathbb{R}$ is the Ricci scalar of the field space. Thus there are three different contributions: the Hessian of the potential in the normal direction, the field space curvature and the turning effect. This mass term, which provides a new scale during inflation, plays an important role in the studies of multi-field models. Based on the size of μ^2 relative to the Hubble scale, most of the models in the literature can be classified into three different regimes.

- $\mu \ll H$. This is the regime with light isocurvature fields. Typically this class of models can generate local type non-Gaussiantiy. Many previous works, such as the curvaton scenario [54, 55], focus on the situation where curvature and isocurvature perturbations are decoupled during inflation while the remaining isocurvature modes convert into adiabatic ones in post-inflation stages. Another well-studied situation is the slow-roll slow-turn models with $\Omega \ll H$ where $\mathcal{R}$ and σ are weakly coupled.

- $\mu \sim \mathcal{O}(H)$. This is the so-called quasi-single field regime with massive isocurvature fields [56–58]. Usually with a nonzero Ω, the primordial non-Gaussianity here has an intermediate shape between local and equilateral configurations, and the squeezed limit of the bispectrum also demonstrates a rich phenomenology related to the new mass scale. This regime has been extensively investigated in the framework of cosmological collider physics [59] in the past several years. We shall give more discussion about this direction in Section 1.2.3.

- $\mu \gg H$. This corresponds to the heavy field regime. In general, the heavy field here can be integrated out and then one may get a single-field effective theory with a reduced sound speed of the inflaton [52, 60–62]. The non-Gaussianity here has an equilateral shape as the result of the sound speed effect.

1.2.1.2 The recent revival of interest: curved field space

For inflation model building, most of the previous efforts were focused on the potential of the scalar fields, as it plays the central role of driving inflation. Meanwhile, it is worth noticing that besides the potential, there is another free function in the action (1.23) – the field space metric G_{ab}. If we consider inflation models from various UV theories, such as string theory, supergravity or nonlinear sigma model (NLSM)[2], typically they result in a metric function with curved geometry. One particularly interesting question is the role of this internal field space in inflation models.

This direction has drawn a lot of attention in the recent research of multi-field inflation. For instance, it is shown that for models with a negatively curved field manifold, a tachyonic instability caused by the field space curvature may deflect the background trajectory near the end of inflation, which is known as *geometrical destabilization* [63–67]. In another scenario called *hyperinflation* [68–72], as a consequence of the hyperbolic geometry, the multi-field evolution demonstrates a nontrival attractor behaviour on a steep potential. The first part of this thesis mainly focuses on two classes of models with curved field manifold. Here are some brief discussions.

The first one is the *inflationary α-attractors* [17, 18, 73–77]. Originated from the so-called Kahler potential of supergravity theories, the hyperbolic geometry plays a significant role in this class of models. There the inflaton potential is stretched to be of the plateau-like form by the effects of the

[2]See Section 1.2.2.3 for discussions about the realization of a curved field manifold in a NLSM.

curved field space, and as a result various single-field models yield universal predictions on the spectral index and tensor-to-scalar ratio which are favoured by the latest CMB observations. As the hyperbolic space has two-dimensions, α-attractors are multi-field models in principle. Chapter 2 will present the first two-field analysis and further demonstrate the role of the curved field space there.

The second class is called the *ultralight isocurvature scenario* [78–82]. These models explore one particular corner of multi-field inflation, where the additional field is massless and vigorously interacts with the inflaton. There the isocurvature modes freeze after horizon-exit, and source the growth of curvature perturbations on superhorizon scales. As a result, the final curvature perturbations at the end of inflation are mainly contributed by the isocurvature sourcing effects, and one still recovers a single-field like phenomenology. Chapter 3 will present a specific realization of this scenario – shift-symmetric orbital inflation.

After these models, one may wonder if there is any unified description of inflationary curved field space. Lately there have been studies of the multi-field background attractor behaviour within various models [83–86], but the perturbation analysis is still unclear. Just like in many multi-field models, predictions from these ones with curved field space usually are also model-dependent. And it remains a difficult question to figure out the observational signatures of the field space geometry. Chapter 4 provides an attempt toward this investigation, where the role of the internal manifold on the additional massive field is considered. For the further study, a more systematic and comprehensive approach to different curved field space scenarios may rely on the effective field theory of inflation.

1.2.2 Effective field theory approaches

In the theoretical studies of inflation, the top-down approach aims to build consistent models from UV-complete theories. However, it turns out to be quite difficult as we discussed in Section 1.1.2, and the model predictions may depend on specific constructions. Besides that, our current understanding of inflation has already taught us a lot about its consistent realizations in general. Thus one can also take the bottom-up approach, and the idea of effective field theory (EFT) provides a constructive framework, where a low energy theory may describe interesting physics in a model-independent way. Here I will introduce the concept of EFT and then discuss its applications in inflationary cosmology.

1.2.2.1 The philosophy of EFT

The physics of natural phenomena comes with many scales. The idea of EFT indicates that there are different theories describing the physics at distinct scales respectively, and for the physics of a certain scale, the EFT may not need information from other scales. In this sense, an EFT will be sufficient for describing a low-energy system after we integrate out (coarse-grain) the high energy physics (microscopic details). Moreover, operators in the EFT can be uniquely determined by fundamental symmetries at play. Therefore EFT provides a constructive approach of parametrizing our ignorance at UV scales and studying the low-energy physics with limited information.

In modern physics, there are many interesting and successful EFTs, with or without UV-completions, such as the Fermi theory of weak interactions, the chiral perturbation theory of pions and the low energy description of superconductivity. As an explicit and simple example, here let us look into *spontaneous symmetry breaking* (SSB) again and show how the low-energy physics in the broken phase can be described by an EFT of Goldstone fields.

Consider a set of scalar fields Σ whose action is invariant under a global symmetry G. The corresponding group transformation is $\Sigma \to e^{i\theta^A T^A}\Sigma$, where T^A are the generators of G and θ^A are parameters. If the vacuum of the theory is located at a nonzero value $\langle\Sigma\rangle = \bar{\Sigma}$ which is invariant under the transformation of a subgroup H, but changes under other remaining symmetry transformations, then this vacuum state spontaneously breaks the symmetry of G to the subgroup H. These remaining group elements of the broken symmetry (denoted by the generators t^a) form the so-called *coset* – G/H.

In general the symmetry breaking pattern is more complicated than the simplest $U(1)$ breaking example discussed at the beginning of Section 1.1.1.1. But the Mexican hat potential may also help us gain some intuition here. Suppose a UV toy model for this SSB is described by the following linear sigma model Lagrangian

$$\mathcal{L} = -\frac{1}{2}\partial\Sigma^\dagger\partial\Sigma - \lambda\left(\Sigma^\dagger\Sigma - f^2\right)^2 \ . \tag{1.32}$$

where f is the symmetry breaking scale[3] associated with the vacuum expectation value (vev) $\bar{\Sigma}$. In this case the coset space G/H corresponds to the vacua defined by $\Sigma^\dagger\Sigma = f^2$ in which the massless Goldstone fields

[3]In the case of a pseudo-Golstone field whose shift symmetry is explicitly broken, f is usually known as the axion decay constant.

live. There is also a "radial" direction which is supposed to be heavy and represent high energy physics in the system.

Now let us look at the low-energy state around the vev $\bar{\Sigma}$. Without losing generality, the scalar fields can be conveniently parameterized as

$$\Sigma = (\bar{\Sigma} + \sigma)U(\pi), \quad \text{with } U(\pi) = e^{it^a\pi^a} \ . \tag{1.33}$$

where π^a are Goldstone fields living in the coset space and σ represents fluctuations along the heavy "radial" direction. Since at low energies the heavy physics related to σ becomes irrelevant, the unitary matrix-valued field $U(\pi)$ contains all the information of Goldstones. Since the mass terms are forbidden, with only derivative terms, the leading order Lagrangian of the Goldstones' EFT follows as

$$\mathcal{L}^0_{\text{eff}} = -\frac{f^2}{4}\text{Tr}[\partial_\mu U^\dagger \partial^\mu U] \ . \tag{1.34}$$

This is also well known as a *non-linear sigma model* (NLSM) which has a *curved* target manifold. We can further expand the Lagrangian in terms of π^a

$$\mathcal{L}^0_{\text{eff}} = -\frac{f^2}{2}\partial_\mu\pi^a\partial^\mu\pi^a + \frac{f^2}{6}\partial_\mu\pi^a\partial^\mu\pi^b\left(\pi^a\pi^b - \delta^{ab}\pi^c\pi^c\right) + ... \tag{1.35}$$

It is impressive to notice that we are only guided by the symmetry breaking pattern to derive the low-energy interacting Lagrangian (1.35) for Goldstones, while knowledge about the heavy radial modes is not used. In other words, it does not matter whether the UV physics is described by the toy model in (1.32) or other setup, while an EFT from symmetry argument provides good descriptions for Goldstone fields at low energy.

A concrete example of the above EFT formalism is the chiral perturbation theory, where pions turn out to be the pseudo-Goldstone fields of the SSB in quantum chromodynamics (QCD). Even if we do not know anything about QCD, the low-energy pions' interactions are well determined by the symmetry breaking pattern there. See Ref. [87] for more detailed discussion.

This approach of EFT is known as the Callan-Coleman-Wess-Zumino (CCWZ) coset construction [88, 89]. Through this example, we see low-energy physics can be mostly insensitive to the underlying microscopic details, while symmetries strongly constrain the form of the EFT and a model-independent description becomes possible.

1.2.2.2 EFTs in cosmology

When we apply EFT in the studies of inflationary cosmology, there can be different approaches. Here we mainly discusses two major ones.

- *EFT of background fields.* From the effective theory point of view, the action (1.5) of slow-roll models can be seen as the leading order approximation below some cutoff scales. In this sense higher order non-renormalizable operators, though suppressed, may also appear and show possible imprints of UV physics. The EFT of background fields provide a systematic way to study these perturbative corrections to the single-field slow-roll scenario [90].

  The key guideline for writing down these EFT operators is symmetry. As we discussed in Section 1.1.2.1, in order to avoid the η-problem, the inflaton field is expected to be protected by an approximate shift symmetry, thus the inflaton should appear with derivatives in the EFT operators. As a result, the leading extension in the single field scenario minimally coupled to gravity is to add a dimension-8 operator

  $$\frac{(\partial\phi)^2(\partial\phi)^2}{\Lambda_k^4}. \tag{1.36}$$

  This leads to the so-called *k-essence* theory where the kinetic term has a non-standard form[4] [91, 92]. In order to ensure the perturbativity of the EFT expansion, here this cutoff scale should satisfy the condition $\Lambda_k > \dot{\phi}$.

  If we consider operators with coupling to an additional field σ, again due to the symmetry argument, the leading order operator that we can write down is expected to be a dimension-5 one [93]

  $$\frac{(\partial\phi)^2\sigma}{\Lambda_s}. \tag{1.37}$$

  This operator, which is linear in σ, can also be seen as an equivalent description of non-geodesic trajectories in field space. Meanwhile the next-to-leading order correction is a dimension-6 operator, whose effects have been neglected in previous studies. Chapter 4 will give a more detailed discussion on this topic.

[4] In a general form the k-essence Lagrangian can be written as $P(X,\phi)$ with $X = (\partial\phi)^2$.

- *EFT of fluctuations.* Another approach to EFT of inflation is to put aside background theories and directly look into perturbations' behaviour. The starting point here is the observation that the background evolution in cosmology usually breaks the time translation symmetry, and the resulting Goldstone field is identified with the adiabatic perturbation. In this approach, one can write down all the possible operators of perturbations with the remaining spatial translation symmetry, thus it provides the most general description of single field inflation [94]. For instance, this EFT approach can also describe strongly coupled models, such as DBI inflation [95, 96], which are beyond the perturbative EFT expansion of the background field approach. However, in this framework one cannot trace the background information of inflation which may contain some important new physics, such as the internal symmetries of the inflaton field. Meanwhile a multi-field extension of this EFT has been investigated in Ref. [97]. But it remains an open question how to implement the recently discovered multi-field models with curved field manifold [98].

1.2.2.3 Inflation in coset space: a new type of EFT

As we discussed in Section 1.1.2.1, in order to avoid the η-problem, *symmetries are expected to play an important role for inflation.* In many fundamental constructions, the inflaton candidate is a pseudo-Goldstone boson protected by an internal symmetry. One direct consequence is that inflation is related to some spontaneous symmetry breaking process, and the inflaton evolves in a coset space defined by the symmetry breaking pattern[5].

Natural inflation provides the first and the simplest realization of this idea, in which the inflaton is a so-called axion associated with the breaking of a U(1) symmetry, and a soft explicit symmetry breaking generates a slow-roll potential for the axion field [21]. However, later it was realized that there a super-Planckian axion decay constant makes the effective description invalid [99]. Meanwhile in high energy theories, it is more natural to have more complicated symmetry breaking patterns, where the non-abelian coset spaces G/H are curved, and multiple (pseudo-)Goldstone fields will be involved besides the inflaton.

There are many interesting questions to be explored in this direction.

[5]This differs from the original proposals from phase transition discussed in Section 1.1.1.1. From the example of Mexican hat potential, inflation models around early 1980s correspond to the radial field, while inflation in coset space concerns the angular directions associated with the Goldstones.

For instance, the behaviour of the running inflaton in a general coset space G/H may have implications for inflation. This line of thinking was pioneered by the studies of *spontaneous symmetry probing* [100], where as one Goldstone field rolls in a non-abelian coset, the not-running Goldstones are found to become massive. This can be seen by considering a time-dependent configuration $\pi^1 = ct$ in the example of EFT with the broken symmetry in Section 1.2.2. After some algebra the effective Lagrangian (1.35) yields

$$\mathcal{L}^0_{\rm eff} = -\frac{f^2}{2}\left[\partial_\mu\pi^1\partial^\mu\pi^1 + \partial_\mu\pi^i\partial^\mu\pi^i + c^2\pi^i\pi^i\right] + ... \tag{1.38}$$

where π^i are the Goldstones transverse to the running π^1 and they acquire masses. The implications of this effect on inflation will be explored in Chapter 4. In addition, with the CCWZ coset construction, a new type of EFT of inflation is expected from symmetry breaking patterns. Differing from the background and fluctuations EFTs, this one may be able to systematically track spontaneously broken internal symmetries during inflation. Inflation in coset space may also link a wide range of topics, such as curved field space, UV realizations and phenomenologies. This thesis will briefly touch some of the above topics, while more systematic investigation remains for future work [101].

1.2.3 Hunting for new physics in the primordial Universe

With multi-field inflation and EFT as powerful frameworks, now we can move forward to investigate new physics effects in the primordial Universe. To achieve this purpose, *model-independence* is also important. In the literature, there has been a large menu of inflation models with various phenomenologies. Generic conclusions will be impossible if predictions rely on some specific models. Therefore for testing new physics, one particular difficulty is to figure out the relation between theories and observable imprints, independent of models.

One interesting attempt in this direction is the *cosmological collider physics* program [59], which searches for observational signals of heavy particles during inflation in primordial non-Gaussianity. Not relying on a specific model, it is found that the squeezed limit of the primordial bispectrum contains information about these extra particles: there the oscillation pattern is uniquely determined by their masses; while the angular dependence of the bispectrum measures the spin. Although the signals usually are quite small, if detected, they would provide a clean channel and reveal a lot information about the possible new particles in the extreme environment of

inflation. Lately this has been further extended to the proposal of cosmological bootstrap, which provides a systematic formalism for calculating inflationary correlation functions from symmetries [102].

Meanwhile it is interesting to notice one major difference between QFTs in particle physics and cosmology. The former usually has a static vacuum expectation value, while in cosmology field configurations are typically time-dependent. For instance, during inflation there is an excursion of the inflaton in the field space because of the slow-roll dynamics. This indicates that besides adopting the traditional strategy of collider physics, there may be novel approaches which are more suitable for searching for new physics in cosmology. For instance, with the excursion trajectory of the inflaton field, we may be able to probe properties related to the internal spaces, such as their geometries and underlying fundamental symmetries. There have been some pioneer works in this direction [103, 104], but systematic understanding is still unclear, which deserves future investigation.

1.3 The outline of the thesis

This thesis consists of two parts. Part I mainly focuses on multi-field inflation with curved field spaces, while in Part II I investigate the phenomenology of primordial non-Gaussianity in both inflation models and alternatives to inflation.

- **Part I. Excursion in curved field spaces.**

  Chapter 2 performs a study on multi-field α-attractors. α-attractors are a class of inflation models characterised by a hyperbolic field space, which have multiple fields involved in general. We present the first two-field analysis of this class of models and find surprisingly that due to the underlying hyperbolic geometry, the universal predictions of single field α-attractors are robust, even when multifield effects are significant. This work, together with geometric destabilisation [63], hyperinflation [68] and several others by other authors around the same time, initiated the revival of interest in multi-field models with curved field space. It is a collaborative project with Ana Achúcarro, Renata Kallosh, Andrei Linde and Yvette Welling [75].

  Chapter 3 proposes a new class of multi-field attractors called shift-symmetric orbital inflation, where the inflaton trajectory is turning significantly in field space, but the model predictions still mimic the single-field ones. In particular, we have demonstrated that, contrary

to expectations in the literature, the primordial non-Gaussianity for these models is small and compatible with current bounds. This work was done with Ana Achúcarro, Ed Copeland, Oksana Iarygina, Gonzalo Palma and Yvette Welling [79].

Chapter 4 tackles a more general question: are there observational signatures related to the scale of field space curvature? Here I approach this question in the context of "quasi-single field inflation/ cosmological collider physics". Meanwhile the relation between the EFT of background fields and inflationary curved field spaces are discussed. Remarkably, I have found that the field space curvature can naturally lead to the running of the scaling index in the squeezed scalar bispectrum, and thus modify the collider signals in non-Gaussianity. This project was done by myself [105].

- **Part II. Tracing primordial triangles.**

  Chapter 5 revisits non-Gaussianities of non-attractor inflation. We show that previous calculations of the primordial bispectrum in non-attractor inflation were incomplete. Through careful analysis, we find that the transition process after the non-attractor phase, which had been previously neglected, always plays an important role. By examining the violation of Maldacena's consistency relation in this class of models, we worked out the first complete and detailed calculation of non-Gaussianity in the "non-attractor to slow-roll" transition. This was a joint project with Yi-Fu Cai, Xingang Chen, Mohammad Hossein Namjoo, Misao Sasaki and Ziwei Wang [106].

  Chapter 6 is about non-Gaussianities in alternatives to inflation, focusing on the distinctive features. In particular, we have calculated the primordial bispectrum in the matter bounce scenario with a general single scalar field. Here the non-Gaussian phenomenology of the matter bounce cosmology is extended to the cases with a small sound speed. Our results also lead to a "no-go" theorem which rules out many alternative models just using current observational constraints. This was a collaboration with Yi-Fu Cai, Yubin Li and Jerome Quintin [107].

Excursion in curved field spaces

2 Universality of multi-field α-attractors

Abstract: We study a particular version of the theory of cosmological α-attractors with $\alpha = 1/3$, in which both the dilaton (inflaton) field and the axion field are light during inflation. The kinetic terms in this theory originated from supergravity has a hyperbolic geometry. We show that because of the underlying negatively curved moduli space in this theory, it exhibits double attractor behavior: their cosmological predictions are stable not only with respect to significant modifications of the dilaton potential, but also with respect to significant modifications of the axion potential: $n_s \simeq 1 - \frac{2}{N}$, $r \simeq \frac{4}{N^2}$. We also show that the universality of predictions extends to other values of $\alpha \lesssim \mathcal{O}(1)$ with general two-field potentials. Our results support the idea that inflation involving multiple, not stabilized, light fields on a hyperbolic manifold may be compatible with current observational constraints for a broad class of potentials.

Keywords: inflation, supersymmetry and cosmology

Based on[1]:

A. Achúcarro, R. Kallosh, A. Linde, D.-G. Wang, Y. Welling
Universality of multi-field α-attractors
JCAP 1804 (2018), no. 04 028, [arXiv:1711.09478].

[1]Here section 2.2 has been trimmed, while a new appendix 2.C on the stabilization of the "rolling on the ridge" trajectories is added.

2.1 Introduction

UV embeddings of inflation typically contain multiple scalar fields beside the inflaton. If the additional fields are stabilized, we can integrate them out to find effectively single field inflation. On the other hand, if the additional fields remain light during inflation, we should take into account the full multi-field dynamics. Planck [108, 109] puts tight constraints on these inflationary models, therefore we should understand which model-building ingredients are important to ensure compatibility with the data. In particular, both the geometry of field space and the curvature of the inflationary trajectory play a very important role in determining the observables. In this paper we focus on the special role played by hyperbolic geometry.

A notable example are the α-attractor models, a relatively simple class of inflationary models that have a single scalar field driving inflation. In the simplest supergravity embedding of these models, the potential depends on the complex scalar $Z = \rho\, e^{i\theta}$, where Z belongs to the Poincaré disk with $|Z| = \rho < 1$ and the kinetic terms read[2]

$$3\alpha \frac{\partial_\mu \bar{Z} \partial^\mu Z}{(1 - Z\bar{Z})^2} + ... \tag{2.1}$$

In many versions of these models, the field θ is heavy and stabilized at $\theta = 0$, so that the inflationary trajectory corresponds to the evolution of the single field ρ. An important property of these models is that their cosmological predictions are stable with respect to considerable deformations of the choice of the potential of the field ρ: $n_s \approx 1 - \frac{2}{N}$, $r \approx \frac{12\alpha}{N^2}$ [17, 18, 74, 110–115]. These predictions are consistent with the latest observational data for $\alpha < O(10)$.

In the single-field realizations, the universality of these predictions can be ultimately traced back to the radial stretching introduced by the geometry (2.1) as we approach the boundary $\rho \sim 1$. On the other hand it is clear that, in the two-field embedding in terms of Z, the stretching also affects the "angular" θ-direction and this begs the question whether perhaps there is a regime where the predictions for the inflationary observables are also fairly insensitive to the details of the angular dependence of the potential. In this paper we answer this question in the affirmative for sufficiently small $\alpha \lesssim O(1)$.

A particularly interesting case is $\alpha = 1/3$, where a class of supergravity embeddings are known to possess an additional symmetry, which makes

[2] Alternatively, $3\alpha \frac{\partial T \partial \bar{T}}{(T+\bar{T})^2}$, where $T = \frac{1+Z}{1-Z}$.

both ρ and θ light [74]. This means we cannot integrate out the angular field and we have to take into account the full multi-field dynamics. We will show that, in contrast with the naive expectation, the cosmological predictions of the simplest class of such models are very stable not only with respect to modifications of the potential of the field ρ, but also with respect to strong modifications of the potential of the field θ. Importantly, we have to account for the full multi-field dynamics [49–52, 61, 116–118] in order to obtain the right results[3]. The predictions coincide with the predictions of the single-field α-attractors for $\alpha = 1/3$: $n_s \approx 1 - \frac{2}{N}$, $r \approx \frac{4}{N^2}$. It was emphasized in [74] that for $3\alpha = 1$, the geometric kinetic term

$$\frac{dZd\bar{Z}}{(1 - Z\bar{Z})^2} \tag{2.2}$$

has a fundamental origin from maximal $\mathcal{N} = 4$ superconformal symmetry and from maximal $\mathcal{N} = 8$ supergravity. Also the single unit size disk, $3\alpha = 1$, leads to the lowest B-mode target which can be associated with the maximal supersymmetry models, M-theory, string theory and N=8 supergravity, see [113, 114] and [115].

More generally, we will also show that, for sufficiently small values of $\alpha < O(1)$, the class of potentials exhibiting universal behaviour becomes very broad, and in particular it includes potentials with $\frac{1}{\rho}V_\theta \sim V_\rho \sim V$.

Our results lend support to the tantalizing idea, recently explored in some detail in [78] and building on earlier works in [120–124], that multi-field inflation on a hyperbolic manifold may be compatible with current observational constraints *without the need to stabilize all other fields besides the inflaton.* Since axion-dilaton moduli systems with the geometry (2.1) are ubiquitous in string compactifications, this observation could have important implications for inflationary model building.

Although at first sight the universality found here resembles a similar result obtained in the theory of multi-field conformal attractors [125] for $\alpha = 1$, the reason for our new result is entirely different. In the model studied in [125], the light field θ evolved faster than the inflaton field, so it rapidly rolled down to the minimum of the potential with respect to the field θ, and the subsequent evolution became the single-field evolution driven by the inflaton field. The observable e-folds are in the latter, single-field regime. On the other hand, in the class of models to be discussed in our paper, the angular velocity $\dot{\theta}$ is exponentially suppressed, due to the hyperbolic geometry, and inflation proceeds (almost) in the radial direction.

[3] See [119] for a recent review and references there.

The angular field will *not* roll down to its minimum, but instead it is "*rolling on the ridge*". This is illustrated in Figures 2.3 and 2.4. Nevertheless, the trajectory is curved and the inflationary dynamics is truly multi-field.

Multi-field models of slow-roll inflation based on axion-dilaton systems have been studied for some time [126, 127]. However, it is only fairly recently that the very important role played by the hyperbolic geometry for multi-field inflation is being recognized (see, e.g. [63, 68, 69, 74, 78, 80, 121, 128]). Unlike in previous works, here we choose to be agnostic about the potential, and derive the conditions that will guarantee universality of the inflationary predictions for the two-field system.

The paper is organized as follows. In Section 2.2 we present a new supergravity embedding of the $\alpha = 1/3$ two-field model with a light, non-stabilized, angular field, as an anti-D3 brane induced geometric inflationary model. We study its inflationary dynamics, and elaborate on the "rolling on the ridge" behaviour in Section 2.3. Next, we work out the universal predictions for primordial perturbations in Section 2.4, and leave the details of the full multi-field analysis for Appendix 2.B. We extend this result to general values of α and work out the constraints on the potential to ensure the universality of the predictions in Section 2.5 and Appendix 2.A. Section 2.6 is for summary and conclusions.

2.2 α-attractors and their supergravity implementations

There are several different formulations of α-attractors in supergravity. One of the first formulations [18] was based on the theory of a chiral superfield Z with the Kähler potential corresponding to the Poincaré disk of size 3α,

$$K = -3\alpha \ln(1 - Z\bar{Z} - S\bar{S}) \ , \tag{2.3}$$

and superpotential

$$W = S\, f(Z)(1 - Z^2)^{\frac{3\alpha-1}{2}} \ , \tag{2.4}$$

where $f(Z)$ is a real holomorphic function. It is possible to make the field S vanish during inflation, either by stabilizing it, or by making it nilpotent [129]. Either way, the kinetic term for Z is

$$3\alpha \frac{dZ d\bar{Z}}{(1 - Z\bar{Z})^2}. \tag{2.5}$$

The field Z can be represented as $e^{i\,\theta} \tanh \frac{\varphi}{\sqrt{6\alpha}}$, where φ is a canonically normalized inflaton field. In the simplest models of this class, the mass of

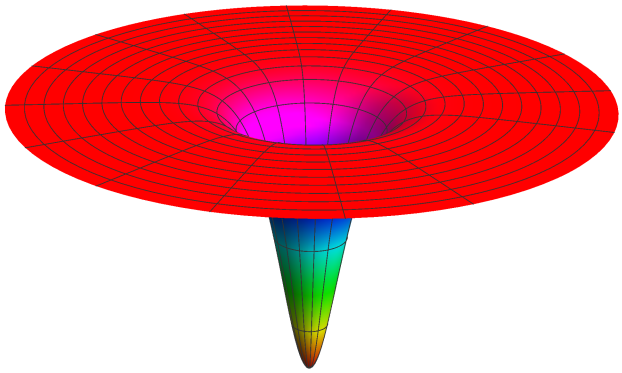

Figure 2.1: The θ-independent $3\alpha = 1$ T-model potential $V(\varphi) = m^2 \tanh^2 \frac{\varphi}{\sqrt{2}}$.

the field θ in the vicinity of $\theta = 0$ during inflation is given by

$$m_\theta^2 = 2V \left(1 - \frac{1}{3\alpha}\right), \tag{2.6}$$

up to small corrections proportional to slow roll parameters. In particular, for the simplest models with $\alpha > 1/3$ one finds $m_\theta^2 > 0$, which means that the field θ is stabilized at $\theta = 0$. Meanwhile for $\alpha > 2/5$ one has $m_\theta^2 = V/3 \geqslant H^2$ where H is the Hubble constant. This means that the field θ for $\alpha \geqslant 2/5$ is strongly stabilized, and the only dynamical field during inflation is the inflaton field φ with the potential

$$V = \left|f(\tanh \frac{\varphi}{\sqrt{6\alpha}})\right|^2. \tag{2.7}$$

Meanwhile for $3\alpha \approx 1$ one finds that during inflation $|m_\theta^2| \ll H^2$. As an example, the potential V for $f(Z) = mZ$ does not depend on θ at all:

$$V = m^2 \tanh^2 \frac{\varphi}{\sqrt{6\alpha}} \ , \tag{2.8}$$

see Figure 2.1.

These specific models with $3\alpha = 1$ with light, non-stabilized fields θ have drawn a lot of attention recently. Therefore it would be interesting to revisit all versions of these models, including the extensions with θ-dependence of the potential. While the details of a supergravity construction are presented in the original paper [75], in general the resulting scalar potential $V(Z, \bar{Z})$

is a function of Z and $\bar{Z}$ which is regular at the boundary $Z\bar{Z} = 1$ and which vanishes at the minimum at $Z = 0$.

In the simplest cases, where V is a function of $Z\bar{Z}$, it does not depend on the angular variable θ, just as the potential in the theory (2.3) (2.4) for $3\alpha = 1$ shown in Figure 2.1. For more general potentials, V may depend on θ, and the potentials can be quite steep with respect to ρ and θ.

The key feature of this class of models, as well as of the models (2.3) (2.4) for $3\alpha = 1$, is that they describe hyperbolic moduli space corresponding to the Kähler potential $K = -\ln(1 - Z\bar{Z})$, with the metric of the type encountered in the description of an open universe, see Equation (2.12) below. As we will see, the slow roll regime is possible for these two classes of theories even for very steep potentials, because of the hyperbolic geometry of the moduli space.

2.3 Dynamics of multi-field α-attractors

Now we come to study inflation with the above theoretical construction. Our starting point is

$$g^{-1}\mathcal{L} = \frac{dZd\bar{Z}}{(1 - Z\bar{Z})^2} - V(Z, \bar{Z}) \ . \tag{2.9}$$

The complex variable on the disk can be expressed as

$$Z = \rho\, e^{i\theta} \ , \tag{2.10}$$

where ρ is the radial field and θ is the angular field. In general, the potential $V(\rho, \theta)$ in these variables can be quite complicated and steep. For simplicity, in the following we assume the potential vanishes at the origin $Z = 0$ and is monotonic along the radial direction of the unit disk[4], *i.e.* $V_\rho \geqslant 0$. One natural possibility is $V_\rho \sim V_\theta/\rho \sim V$, which at first glance cannot yield sufficient inflation. However, the hyperbolic geometry of the moduli space makes slow roll inflation possible even if the potential is quite steep.

To see this, and to connect this to a more familiar canonical field φ in $3\alpha = 1$ attractor models where the tanh argument is $\varphi/\sqrt{6\alpha}$, we can use the following relation

$$\rho = \tanh \frac{\varphi}{\sqrt{2}} \ . \tag{2.11}$$

[4]We study other interesting cases with non-monotonic potential, such as the Mexican hat potential and natural inflation with hyperbolic geometry in another work [77].

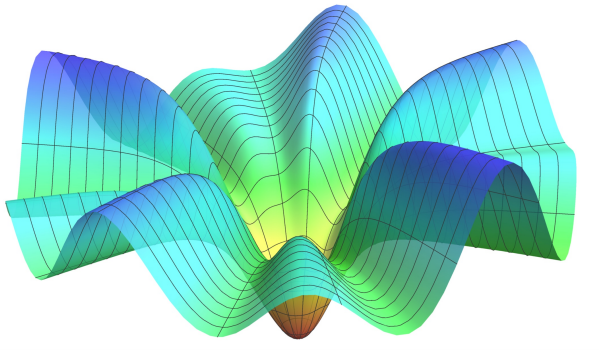

Figure 2.2: A stretched potential with angular dependence

Therefore, our cosmological models with geometric kinetic terms are based on the following Lagrangian of the axion-dilaton system

$$g^{-1}\mathcal{L} = \frac{1}{2}(\partial\varphi)^2 + \frac{1}{4}\sinh^2(\sqrt{2}\varphi)(\partial\theta)^2 - V(\varphi,\theta)\ , \tag{2.12}$$

where some choice of the potentials $V(\varphi,\theta)$ will be made depending on both moduli fields. In terms of this new field φ, the corresponding potential near the boundary $\rho = 1$ is exponentially stretched to form a plateau, where φ field becomes light and slow-roll inflation naturally occurs. If we further assume the potential is a function of the radial field only, then we recover the T-model as shown in Figure 2.1. Generally speaking, the potential may also depend on θ, and have ridges and valleys along the radial direction. One simple example is shown in Figure 2.2. Although the θ field can appear heavy in the unit disk coordinates, after stretching in the radial direction, the effective mass in the angular direction is also exponentially suppressed for $\varphi \gg 1$.

For a cosmological spacetime, the background dynamics is described by equations of motion of two scalar fields

$$\ddot{\varphi} + 3H\dot{\varphi} + V_\varphi - \frac{1}{2\sqrt{2}}\sinh\left(2\sqrt{2}\varphi\right)\dot{\theta}^2 = 0\ , \tag{2.13}$$

$$\ddot{\theta} + 3H\dot{\theta} + \frac{V_\theta}{\frac{1}{2}\sinh^2(\sqrt{2}\varphi)} + \frac{2\dot{\theta}\dot{\varphi}}{\frac{1}{\sqrt{2}}\tanh(\sqrt{2}\varphi)} = 0\ , \tag{2.14}$$

and the Friedmann equation

$$3H^2 = \frac{1}{2}(\dot{\varphi}^2 + \frac{1}{2}\sinh^2\sqrt{2}\varphi\ \dot{\theta}^2) + V(\varphi,\theta)\ , \tag{2.15}$$

where $H \equiv \dot{a}/a$ is the Hubble parameter. In such a two-field system with potential as shown in Figure 2.2, one may expect that the inflaton will first roll down from the ridge to the valley, and then slowly rolls down to the minimum along the valley. In the following we will demonstrate, due to the magic of hyperbolic geometry, the dynamics of moduli fields is totally different from this naive picture.

2.3.1 Rolling on the ridge

In single-field α-attractor models, inflation takes place near the edge of the Poincaré disk with $\rho \to 1$ (or equivalently $\varphi \gg 1$). Here we also focus on the large-φ regime where the potential in the radial direction is stretched to be very flat. As a consequence, the radial derivative of the potential is exponentially suppressed

$$V_\varphi \simeq 2\sqrt{2} V_\rho e^{-\sqrt{2}\varphi} \ . \tag{2.16}$$

After a quick relaxation, the fields can reach the slow-roll regime with the Hubble slow-roll parameters

$$\epsilon \equiv -\frac{\dot{H}}{H^2} = \frac{\dot{\varphi}^2 + \frac{1}{2}\sinh^2(\sqrt{2}\varphi)\dot{\theta}^2}{2H^2} \ll 1 \ , \qquad \eta \equiv \frac{\dot{\epsilon}}{H\epsilon} \ll 1. \tag{2.17}$$

Thus the kinetic energy of fields is much smaller than the potential, and the $\dot{\theta}\dot{\varphi}$ term in (2.13) is subdominant. Moreover, we assume that the field accelerations $\ddot{\varphi}$ and $\ddot{\theta}$ can be neglected with respect to the potential gradient. The equation of motion for θ is then simplified to

$$\frac{\dot{\theta}}{H} \simeq -8\frac{V_\theta}{V} e^{-2\sqrt{2}\varphi}. \tag{2.18}$$

This gives us the velocity in the angular direction, which is highly suppressed in the large-φ regime. Substituting the above result in the equation of motion for φ (2.13), we can see that the centrifugal term proportional to $\dot{\theta}^2$ is also suppressed by $e^{-2\sqrt{2}\varphi}$. Thus for $\varphi \gg 1$ this term can be neglected compared to V_φ. Therefore the equation of motion for φ is approximately

$$3H\dot{\varphi} + V_\varphi \simeq 0 \ , \tag{2.19}$$

which is the same as the single field case with slow-roll conditions. Similarly we get the field velocity in the radial direction $\dot{\varphi} \sim e^{-\sqrt{2}\varphi}$, which is much larger than the angular velocity $\dot{\theta}$. This is the main reason for the difference

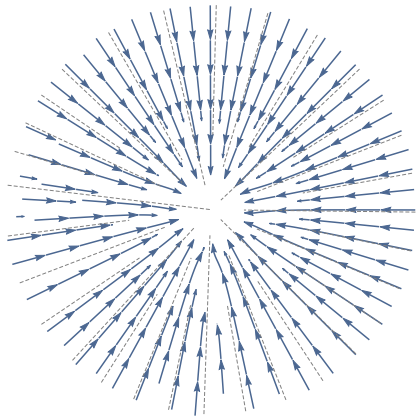

Figure 2.3: The stream of φ and θ fields on the potential with random angular dependence shown in Figure 2.2. The dashed gray lines show the radial directions, while the blue arrows correspond to the field flow, starting at $\varphi_i = 10$.

between the slow-roll regime in the present set of models, and in the multi-field conformal attractors studied in [125]. In the conformal attractors, the field θ was rapidly rolling down, whereas here instead of rolling down to the valley first, the scalar fields are *rolling on the ridge* with almost constant θ.

To see this counter-intuitive behaviour clearly, we can look at the flow $(\dot{\varphi},\ \dot{\theta})$ in the polar coordinate system. The numerical result of the flow of the fields is shown in Figure 2.3 for the potential from Figure 2.2. As we see, although the potential *looks* chaotic in the angular direction, the fields always roll to the minimum along the ridge, no matter where they start.

However, it is crucial to emphasize that, although $\dot{\theta}$ is highly suppressed and θ is nearly constant, the angular motion is still quite important. In the curved field manifold, since the angular distance is also stretched for large φ, the proper velocity in the angular direction is given by $\frac{1}{\sqrt{2}}\sinh(\sqrt{2}\varphi)\dot{\theta}$. We are encouraged to define a new parameter γ as the ratio between the *physical* angular and radial velocity

$$\gamma \equiv \frac{\sinh(\sqrt{2}\varphi)\,\dot{\theta}}{\sqrt{2}\,\dot{\varphi}} \simeq \frac{V_\theta}{V_\rho}, \tag{2.20}$$

where in the last step we have used large-φ and slow-roll approximations. Since θ hardly evolves and $\rho \simeq 1$ for $\varphi \gg 1$, γ is nearly constant during most period of inflation. This parameter captures the deviation from the single

field scenario. For instance, let us look at the potential slow-roll parameter in the radial direction

$$\epsilon_\varphi \equiv \frac{1}{2}\left(\frac{V_\varphi}{V}\right)^2 \simeq \frac{\dot{\varphi}^2}{2H^2} \ , \tag{2.21}$$

which is the same with the single field one. Then in our model the full Hubble slow-roll parameter (2.17) is approximately given by

$$\epsilon = (1+\gamma^2)\epsilon_\varphi \ . \tag{2.22}$$

Thus a nonzero γ demonstrates the contribution of the angular motion in the evolution of the two-field system. Furthermore, depending on the form of the potential, γ can be $\mathcal{O}(1)$ as we shall show in a toy model later. In such cases, the physical angular motion is comparable to the radial one, and the multi-field effects is particularly important[5].

In summary, for multi-field α-attractors, there are two subtleties caused by the hyperbolic field space. First of all, the two-field evolution *looks* like the single field case without turning behaviour in the field space. On the other hand, the straight trajectory is an illusion, and the *multi-field* effect can still be significant. In Section 2.4, we will show how these surprising behaviours lead us to the universal predictions for primordial perturbations.

Concluding this subsection, we wish to further explain why "*rolling on the ridge*" is a quite general behaviour in multi-field α-attractors. Besides the aforementioned approximations, importantly we also neglect the centrifugal term in (2.13). Strictly speaking, this requires

$$V_\varphi \gg \frac{1}{2\sqrt{2}}\sinh\left(2\sqrt{2}\varphi\right)\dot{\theta}^2, \tag{2.23}$$

which in the large-φ regime is equivalent to the following condition of the potential

$$\frac{V_\rho}{V} \gg \frac{4}{3}\left(\frac{V_\theta}{V}\right)^2 e^{-\sqrt{2}\varphi} \ . \tag{2.24}$$

Now we can see, near the boundary of the disk, unless the angular dependence of the potential is exponentially stronger than the radial one, the above condition always holds true and the system evolves as we describe above. Finally let us stress that we have to ensure all our approximations are valid. We collect all conditions on the potential in Appendix 2.A. A natural choice of the potential with $V_\rho \sim V_\theta/\rho \sim V$ certainly satisfies these conditions.

[5]To see the importance of multi-field behaviour, another way is to look at the nonzero turning parameter, which we will discuss in Appendix 2.B.

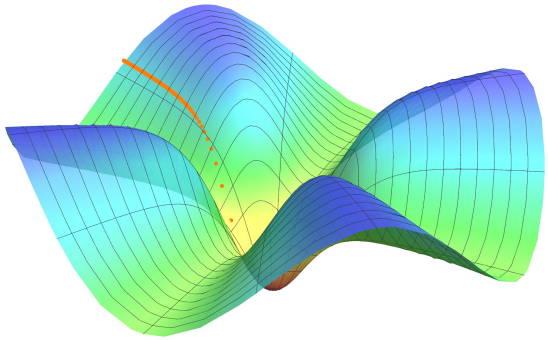

Figure 2.4: Rolling on the ridge: the form of the potential is given by the toy model (2.26) with $A = 0.2$, $n = 4$ and initial angle $\theta_i = \pi/8$; the orange dots show a typical background trajectory, while the interval between the neighboring dots corresponds to one e-folding time.

2.3.2 A toy model

Before moving to the calculation of perturbations, let us work out a toy model to further confirm the above analysis. Consider the following potential on the unit disk

$$V(Z, \bar{Z}) = V_0 \left[Z\bar{Z} + A(Z^n + \bar{Z}^n) \right] \ . \tag{2.25}$$

To ensure that it is monotonic in the radial direction of the unit disk we need $A \leqslant \frac{1}{n}$. Then the condition (2.24) is certainly satisfied. In terms of φ and θ, the potential is given by

$$V(\varphi, \theta) = V_0 \tanh^2 \left(\frac{\varphi}{\sqrt{2}} \right) \left[1 + 2A \cos(n\theta) \tanh^{n-2} \left(\frac{\varphi}{\sqrt{2}} \right) \right] \ . \tag{2.26}$$

For demonstration, in the following we take $n = 4$, $A = 0.2$ and the initial angle $\theta_i = \pi/8$. We solve the background evolution of this two field system numerically. Figure 2.4 shows the field trajectory on the toy model potential. We can see that the inflaton is rolling on the ridge with nearly constant θ.

Using the full numerical solution, we can check the validity of the large-φ and slow-roll approximations by looking at the evolution of background parameters. For example, within our analytical treatment, the γ parameter is given by (2.20) as

$$\gamma \simeq -\frac{nA \sin(n\theta)}{1 + nA \cos(n\theta)} \ . \tag{2.27}$$

It is nearly constant, since $\theta \simeq \theta_i$ during inflation. And the above choice of parameter values gives us $\gamma \simeq -0.8$, which agrees well with the numerical

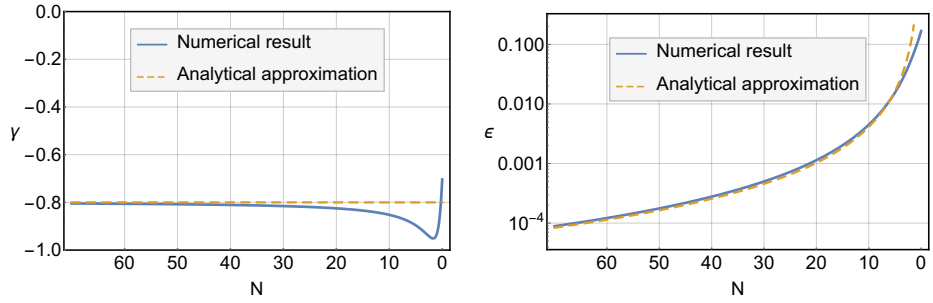

Figure 2.5: The evolution of γ and ϵ in the toy model (2.26) with $A = 0.2$, $n = 4$ and initial angle $\theta_i = \pi/8$.

result as shown in Figure 2.5. Next, let us look at the slow-roll parameter ϵ. Solving (2.19) gives us its behaviour in terms of e-folding number as

$$\epsilon \simeq \frac{1+\gamma^2}{4N^2} \ , \tag{2.28}$$

where (2.22) is used. As shown in Figure 2.5, this provides a good approximation until the last several e-foldings of inflation, where $\varphi \gg 1$ is not valid any more. It is interesting to notice that, during inflation the scalar field mainly rolls in the large-φ region, outside of which inflation would end very quickly. Therefore, the approximation $\varphi \gg 1$ does give a good description for the background dynamics. In the following section and in Appendix 2.B, we will come back to this toy model, and use it as an example to demonstrate other aspects of multi-field α-attractors.

2.4 Universal predictions of α-attractors

One of the most important properties of single field α-attractor inflation is the universal prediction for observations. For $\alpha \lesssim \mathcal{O}(1)$ and a broad class of potentials, as long as $V(\rho)$ is non-singular and rising near the boundary of the Poincaré disk, the resulting scalar tilt and tensor-to-scalar ratio converge to

$$n_s = 1 - \frac{2}{N} \quad \text{and} \quad r = \frac{12\alpha}{N^2}, \tag{2.29}$$

where $N \sim 50 - 60$ is the number of e-folds for modes we observe in the CMB.

One interesting question is whether the universal predictions are still valid in the multi-field regime. In multi-field scenarios the curvature perturbation is sourced by the isocurvature modes on superhorizon scales, thus

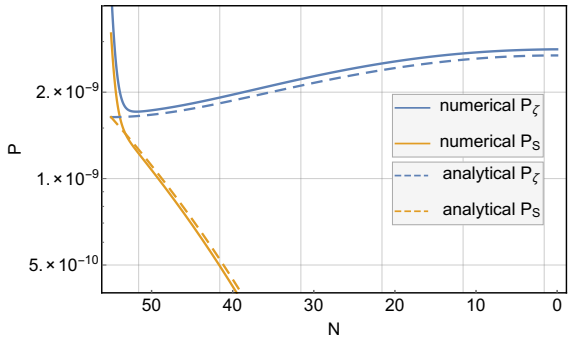

Figure 2.6: The evolution of curvature power spectrum P_ζ and isocurvature power spectrum $P_\mathcal{S}$ for perturbation modes which exit the horizon at $N = 55$. We use the toy model (2.26) with $A = 0.2$, $n = 4$ and initial angle $\theta_i = \pi/8$. The analytical solutions here are based on calculations in Appendix 2.B.

their evolution is typically non-trivial and yields totally different results for n_s and r. As we show above, the angular dependence in the α-attractor potentials indeed leads to multi-field evolution. For the toy model we studied, the behaviour of perturbations can be computed using the numerical code `mTransport` [130]. We focus on one single k mode for curvature and isocurvature perturbations, and show their evolution in Figure 2.6. As expected, the curvature perturbation is enhanced during inflation, while the isocurvature modes decay. Therefore, naively one expects there would be corrections to the single field α-attractor predictions due to the multi-field effects.

In the following we will show that, surprisingly, the universal predictions are still valid in the multi-field regime. We use the δN formalism to derive the inflationary predictions for the multi-field α-attractor models studied in this paper. A full analysis of the perturbations is left for Appendix 2.B, where the evolution of the coupled system of curvature and isocurvature modes is solved via the first principle calculation .

The δN formalism [131–135] is an intuitive and simple approach to solve for the curvature perturbation in multi-field models. At the end of inflation, regardless of the various field trajectories, the amplitude of curvature perturbations is only determined by the perturbation of the e-folding number N, which is caused by the initial field fluctuations. Therefore, without studying details of the coupled system of curvature and isocurvature modes, as long as we know how the number of e-foldings N depends on the initial value of the two fields, the curvature perturbation can be calculated.

Let us therefore consider how the initial φ and θ determine N. In this paper, we define the e-folding number as the one counted backwards from the end of inflation, thus $dN = -Hdt$. In terms of N, the slow-roll equation (2.19) becomes

$$\frac{d\varphi}{dN} \simeq 2\sqrt{2}e^{-\sqrt{2}\varphi}\frac{V_\rho}{V} \ . \tag{2.30}$$

Since in the large φ regime $\rho \to 1$ and V_ρ/V is nearly constant for a given trajectory, the equation above yields the e-foldings from the end of inflation as

$$N = \frac{1}{B}e^{\sqrt{2}\varphi} + C(\theta) \ , \tag{2.31}$$

where $B \equiv 4V_\rho/V$ and $C(\theta)$ is an $\mathcal{O}(1)$ integration constant which can be fixed by setting $N = 0$ at the end of inflation. Thus, both two fields affect the duration of inflation as expected in multi-field models. By this expression, we can use the δN formalism to find curvature perturbation at the end of inflation

$$\zeta = \delta N = \frac{\partial N}{\partial \varphi}\delta\varphi + \frac{\partial N}{\partial \theta}\delta\theta = \frac{\sqrt{2}e^{\sqrt{2}\varphi}}{B}\delta\varphi + \left(C_\theta - \frac{B_\theta}{B^2}e^{\sqrt{2}\varphi}\right)\delta\theta \ . \tag{2.32}$$

As we see here, $\frac{\partial N}{\partial \varphi}$ and $\frac{\partial N}{\partial \theta}$ can be comparable to each other. However, one should keep in mind that θ field is non-canonical, thus to estimate the field fluctuation amplitudes at horizon-exit, one should consider the canonically normalized ones: $\delta\varphi$ and $\frac{1}{\sqrt{2}}\sinh(\sqrt{2}\varphi)\delta\theta$. Approximately in the large-φ region we have the following relation

$$\delta\varphi \simeq \frac{e^{\sqrt{2}\varphi}}{2\sqrt{2}}\delta\theta \simeq \frac{H}{2\pi} \ . \tag{2.33}$$

From here, we find that the field fluctuation $\delta\theta$ is exponentially suppressed, compared to the one from $\delta\varphi$. So we only need to take into account the first term in equation (2.32). In addition, equation (2.21) yields $\epsilon_\varphi = B^2e^{-2\sqrt{2}\varphi}/4$, which further simplifies the δN formula to $\zeta \simeq \delta\varphi/\sqrt{2\epsilon_\varphi}$. In the end, the power spectrum of curvature perturbation can be expressed as

$$P_\zeta \equiv \frac{k^3}{2\pi^2}|\zeta_k|^2 \simeq \frac{H^2}{8\pi^2\epsilon_\varphi} \ . \tag{2.34}$$

It is interesting to note that this result does not depend on any parameters related to the multi-field effects (such as γ). Using (2.21) and (2.31), we also get $\epsilon_\varphi \simeq 1/(4N^2)$, which has the same behaviour with the single-field potential slow-roll parameter ϵ_V. Thus the power spectrum above is

coincident with the single-field one. Then the predictions of scalar tilt and tensor-to-scalar ratio follow directly

$$n_s - 1 \simeq -\frac{2}{N} \quad \text{and} \quad r \simeq \frac{4}{N^2} \ . \tag{2.35}$$

These results are further confirmed by solving the full evolution of perturbations as shown in Appendix 2.B.

The δN calculation above also demonstrates the counter-intuitive properties of multi-field α-attractors. As we show in Section 2.3, the stretching effects of hyperbolic geometry not only flattens the potential in the radial direction, but also suppresses the angular velocity $\dot{\theta}$. At the level of perturbations, the similar effect occurs to the field fluctuations in the angular direction. While the canonically normalized angular field fluctuation has the same amplitude with $\delta\varphi$, the original field perturbation $\delta\theta$ is exponentially suppressed. Therefore, only the radial field fluctuation $\delta\varphi$ contributes to the final result.

Furthermore, the above results do not depend on the initial values of θ, which correspond to different field trajectories as shown in Figure 2.3. Certainly their respective e-folding number N and ϵ_φ can be different from each other. However, the N-dependence of ϵ_φ is the same for all the "rolling on the ridge" trajectories. Thus regardless of various initial values of θ, the multi-field α-attractors yield the same universal predictions for n_s and r.

Typically, another prediction in multi-field inflation is large local non-Gaussianity, which is disfavoured by the latest data [109]. Therefore it is also worthwhile to estimate the size of the bispectrum in our model. Here we expand the δN formula to the second order in field fluctuations

$$\zeta = \delta N = \frac{\partial N}{\partial \varphi}\delta\varphi + \frac{\partial N}{\partial \theta}\delta\theta + \frac{1}{2}\frac{\partial^2 N}{\partial \varphi^2}\delta\varphi^2 + \frac{1}{2}\frac{\partial^2 N}{\partial \theta^2}\delta\theta^2 + \frac{\partial^2 N}{\partial\theta\partial\varphi}\delta\theta\delta\varphi \ . \tag{2.36}$$

In principle, there are two contributions here: one captured by the δN expansion, and another one caused by field interactions of $\delta\varphi$ and $\delta\theta$. However, for the same reason shown in (2.33), the $\delta\theta$-related terms in the expansion (2.36) are highly suppressed. Moreover, since there is no large coupling between field fluctuations, we expect that the second contribution to the bispectrum will also be negligible. As a result, the local non-Gaussianity is approximately given by $\delta\varphi$ terms in (2.36)

$$f_{\rm NL} \simeq \frac{5}{6}\,\frac{\partial^2 N}{\partial\varphi^2}\Big/\left(\frac{\partial N}{\partial\varphi}\right)^2 \simeq \frac{5}{6N} \ , \tag{2.37}$$

which is coincident with the single field consistency relation $f_{\rm NL} = -\frac{5}{12}(n_s - 1)$ [39, 40]. Again, we find the multi-field α-attractor prediction returns to the single field one, which further demonstrates the scope of universality.

2.5 Universality conditions for more general α

Our investigation was stimulated by the realization that α-attractors have particularly interesting interpretation in supergravity models with $\alpha = 1/3$. A significant deviation from $\alpha = 1/3$ typically either makes the field θ tachyonic, or strongly stabilizes it at $\theta = 0$, which results in a single-field inflation driven by the field φ, see e.g. (2.6). One may wonder, however, what happens if we consider a more general class of two-field α-attractors, which may or may not have supergravity embedding[6], and concentrate on their general features related to the underlying hyperbolic geometry.

For general α, the canonically normalized field in the radial direction is defined by $\rho = \tanh(\varphi/\sqrt{6\alpha})$, which leads to the following kinetic term

$$\frac{1}{2}\,(\partial\varphi)^2 + \frac{3\alpha}{4}\sinh^2\left(\sqrt{\frac{2}{3\alpha}}\varphi\right)(\partial\theta)^2\,. \tag{2.38}$$

The equations of motion (2.13) and (2.14) also change accordingly, see (2.47) and (2.48). Similarly as in Section 2.4, in the slow-roll and large-φ approximations these equations reduce to

$$\frac{\dot\theta}{H} \simeq -\frac{8}{3\alpha}\frac{V_\theta}{V}e^{-2\sqrt{\frac{2}{3\alpha}}\varphi}\,, \qquad 3H\dot\varphi \simeq -\frac{2\sqrt{2}}{\sqrt{3\alpha}}V_\rho e^{-\sqrt{\frac{2}{3\alpha}}\varphi}\,. \tag{2.39}$$

As we see, the angular motion is also exponentially suppressed, compared to the radial one. So the rolling on the ridge behaviour is not unique for $\alpha = 1/3$, but quite general for any $\alpha \lesssim \mathcal{O}(1)$. Similarly to (2.24), we get the following condition to ensure its validity

$$\frac{V_\rho}{V} \gg \frac{4}{9\alpha}\left(\frac{V_\theta}{V}\right)^2 e^{-\sqrt{\frac{2}{3\alpha}}\varphi}\,, \tag{2.40}$$

which can be satisfied easily by many choices of potential, generalizing the bound (2.24) to other values of α. Therefore, the results follow directly just like we find in Section 2.3. For example, the ratio of proper velocities

$$\gamma = \frac{\sqrt{\frac{3\alpha}{2}}\sinh\left(\sqrt{\frac{2}{3\alpha}}\varphi\right)\dot\theta}{\dot\varphi} \tag{2.41}$$

[6] Ref. [136] provides a supergravity embedding for the more general $\alpha < 1$ models.

is still nearly constant, while ϵ_φ evolves as

$$\epsilon_\varphi \simeq \frac{3\alpha}{4N^2} \ . \tag{2.42}$$

Repeating the same δN calculation for perturbations, we get $N \simeq 3\alpha e^{\sqrt{2/3\alpha}\varphi}/B$ and

$$\zeta = \delta N \simeq \frac{1}{\sqrt{2\epsilon_\varphi}}\delta\varphi, \tag{2.43}$$

which lead to the universal predictions (2.29) for generic α. Therefore in a broader class of α-attractors without supersymmetry, adding angular dependence to the potential will not modify the universal predictions either. Importantly, in order to validate the various assumptions we make to obtain the universal predictions, we need the potential to satisfy certain conditions. The most non-trivial condition is already given in (2.40). The additional constraints on the potential come from *assuming* the slow-roll, 'slow-turn' and large φ approximation. We give more detail about these approximations and collect the constraints on the potential in Appendix 2.A. Some of the conditions should also be satisfied for single field α-attractors. The smaller α becomes, the more pronounced the stretching of the hyperbolic field metric gets and it will be more likely to be within the large φ regime $\varphi \gtrsim \sqrt{\frac{3\alpha}{2}}$ and the slow-roll regime at the same time. Finally, there are some additional constraints on the potential because of the multi-field nature of our class of models. In particular, if we want to have suppressed field accelerations, we need to satisfy the slow-roll and the slow-turn conditions given in (2.49d) - (2.49f). A natural choice of the potential with $\frac{V_\theta}{\rho V} \sim \frac{V_\rho}{V} \sim \frac{V_{\theta\theta}}{\rho^2 V} \sim \frac{V_{\theta\rho}}{\rho V} \sim \frac{V_{\rho\rho}}{V} \sim 1$, evaluated at the boundary $\rho \sim 1$ amply satisfies all conditions for $\alpha \lesssim O(1)$.

2.6 Summary and Conclusions

In this paper we have studied the inflationary dynamics and predictions of a class of α-attractor models where both the radial and the angular component of the complex scalar field $Z = \rho\, e^{i\theta}$ are light during inflation. We concentrated on the special case $\alpha = 1/3$, where the model has a supergravity embedding with a high degree of symmetry from $\mathcal{N} = 4$ superconformal or $\mathcal{N} = 8$ supergravity. However, our results may have more general validity under the conditions specified in Appendix A. Under the weak assumptions that the potential is monotonic in the radial coordinate, and the angular

gradient is not exponentially larger than the radial gradient (2.24), we find exactly the same predictions as in the theory of the single field α-attractors:

$$n_s - 1 \simeq -\frac{2}{N} \quad \text{and} \quad r \simeq \frac{12\alpha}{N^2} \ . \tag{2.44}$$

Universality of these predictions may make it difficult to distinguish between different versions of α-attractors by measuring n_s. However, from our perspective this universality is not a problem but an advantage of α-attractors, resembling universality of several other general predictions of inflationary cosmology, such as the flatness, homogeneity and isotropy of the universe, and the flatness, adiabaticity and gaussianity of inflationary perturbations in single field inflationary models.

The hyperbolic field metric plays a key role in finding these universal results. Let us summarize how we arrived at our new result and stress how the hyperbolic geometry dictates the analysis.

- First, the hyperbolic geometry effectively stretches and flattens the potential in the radial direction to a shape independent of the original radial potential. Independent - as long as the potential obeys the condition (2.24). The amplitude of this shape, however, varies along the angular direction.

- Next, the angular velocity $\dot{\theta}$ is exponentially suppressed, due to the hyperbolic geometry, and inflation proceeds (almost) in the radial direction. The inflaton is "*rolling on the ridge*" in the $(\varphi,\ \theta)$ plane. This is illustrated in Figures 2.3 and 2.4.

- The straight radial trajectory is an illusion, since the *physical* velocity in the axion θ direction is typically of the same order as the radial velocity. The angle between the inflationary trajectory and the radial direction is nonzero and practically constant in this regime. Moreover, although the field is following the gradient flow, the trajectory is curved in the hyperbolic geometry. Therefore, the perturbations are coupled and the multi-field effects have to be taken into account.

- Then, we use the δN formalism to compute the power spectrum of curvature perturbations (confirmed by a fully multi-field analysis in Appendix 2.B). The typical initial θ perturbations are very small and have a negligible effect on the number of efolds. However, the initial value of θ of a given trajectory determines how much a perturbation in the radial direction affects the number of efolds, since the trajectory

is curved. At the same time the initial value of θ determines the renormalization of the slow-roll parameter ϵ. *These two effects cancel exactly*, leaving us with the same predictions as the single field α-attractors. Also the non-Gaussianity calculation recovers the single field result $f_{\rm NL} \simeq -\frac{5}{12}(n_s - 1)$.

- Finally, in Section 2.5 and Appendix 2.A, we relax the condition $\alpha = 1/3$ and simply assume the hyperbolic geometry (2.1) with smooth potentials. We identify the conditions on the potential in order to exhibit the universal behaviour discussed in our paper, see (2.49). For $\alpha \lesssim O(1)$ these conditions are amply satisfied by a broad class of potentials $V(\rho, \theta)$, including natural ones without a hierarchy of scales: $\frac{V_\theta}{\rho V} \sim \frac{V_\rho}{V} \sim \frac{V_{\theta\theta}}{\rho^2 V} \sim \frac{V_{\theta\rho}}{\rho V} \sim \frac{V_{\rho\rho}}{V} \sim 1$, evaluated at the boundary $\rho \sim 1$.

In conclusion, the main result of our investigation is the stability of predictions of the cosmological α-attractors with respect to significant modifications of the potential in terms of the original geometric variables Z. Whereas the stability with respect to the dependence of the potential on the radial component of the field Z is well known [18], the stability with respect to the angular component of the field Z is a novel result which we did not anticipate when we began this investigation.

Our results could have important implications for constructing UV completions of inflation. We have confirmed again that multi-field models of inflation can be perfectly compatible with the current data, in particular when the additional fields are very light. This lends support to the idea that it is not always necessary to stabilize all moduli fields in order to have a successful model of inflation.

Appendix

2.A Constraints on the potential

In this Appendix we collect the conditions the potential has to obey in order to validate our approximations for any value of α. Let us first recap some relevant definitions and equation for general α. First of all, our three

radial variables are given by φ and

$$R(\varphi) \equiv \sqrt{\frac{3\alpha}{2}} \sinh\left(\sqrt{\frac{2}{3\alpha}}\varphi\right), \quad \rho \equiv \tanh\left(\frac{\varphi}{\sqrt{6\alpha}}\right). \tag{2.45}$$

We introduced the radial variable $R(\varphi)$ because it appears naturally in the *physical* angular velocity $R(\varphi)\dot{\theta}$. The kinetic term can now be written in three equivalent ways

$$\begin{aligned} \frac{1}{2}\frac{(\partial\rho)^2 + \rho^2(\partial\theta)^2}{(1-\rho^2)^2} &= \frac{1}{2}(\partial\varphi)^2 + \frac{3\alpha}{4}\sinh^2\left(\sqrt{\frac{2}{3\alpha}}\varphi\right)(\partial\theta)^2 \\ &= \frac{1}{2}(\partial\varphi)^2 + \frac{1}{2}R(\varphi)^2(\partial\theta)^2. \end{aligned} \tag{2.46}$$

The equations of motion are generalized to

$$\ddot{\varphi} + 3H\dot{\varphi} + V_\varphi - \frac{1}{2}\sqrt{\frac{3\alpha}{2}}\sinh\left(2\sqrt{\frac{2}{3\alpha}}\varphi\right)\dot{\theta}^2 = 0\ , \tag{2.47}$$

$$\ddot{\theta} + 3H\dot{\theta} + \frac{V_\theta}{\frac{3\alpha}{2}\sinh^2\left(\sqrt{\frac{2}{3\alpha}}\varphi\right)} + \frac{2\dot{\theta}\dot{\varphi}}{\sqrt{\frac{3\alpha}{2}}\tanh\left(\sqrt{\frac{2}{3\alpha}}\varphi\right)} = 0\ . \tag{2.48}$$

Now we are ready to collect all constraints on the potential. In our derivation we *assume* that we can neglect $\ddot{\varphi}$ and that we can take the large-φ approximation. Moreover, it is important that we can neglect the centrifugal term proportional to $\dot{\theta}^2$ in Equation (2.47). We use the gradient flow to estimate the size of $\dot{\theta}$, and this leads to the first constraint (2.49a). For consistency, we have to ensure the validity of: ncy, we have to ensure the validity of:

- The slow-roll approximation, which gives rise to the next four constraints (2.49b) - (2.49e). This approximation ensures that the field velocities are small and that we can neglect their acceleration pointing along the corresponding field direction as well.
- The slow-turn approximation, which allows us to neglect the field accelerations pointing along the *other* field direction. If we can assume gradient flow for θ this leads to the condition (2.49f).
- The large-φ approximation, which requires us not to go to the extreme limit of a very shallow radial potential. We want to inflate sufficiently

far from the origin in order to obtain enough efolds of inflation, such that we can use the large-φ approximation. In our analysis we work for simplicity with potentials $\left(\frac{V_\rho}{V}\right)^2 \gtrsim \frac{\alpha}{4}$ so this is automatically satisfied.

$$\frac{V_\rho}{V} \gg \frac{4}{9\alpha}\left(\frac{V_\theta}{V}\right)^2 e^{-\sqrt{2/3\alpha}\varphi}, \tag{2.49a}$$

$$\epsilon_\varphi \equiv \frac{1}{2}\left(\frac{V_\varphi}{V}\right)^2 = \frac{4}{3\alpha}\left(\frac{V_\rho}{V}\right)^2 e^{-2\sqrt{2/3\alpha}\varphi} \ll 1, \tag{2.49b}$$

$$\epsilon_\theta \equiv \frac{1}{2}\left(\frac{V_\theta}{RV}\right)^2 = \frac{4}{3\alpha}\left(\frac{V_\theta}{V}\right)^2 e^{-2\sqrt{2/3\alpha}\varphi} \ll 1, \tag{2.49c}$$

$$\eta_\varphi \equiv \frac{1}{3}\frac{V_{\varphi\varphi}}{V} = \frac{8}{9\alpha}\frac{V_{\rho\rho}}{V}e^{-2\sqrt{2/3\alpha}\varphi} \ll 1 \tag{2.49d}$$

$$\eta_\theta \equiv \frac{1}{3}\frac{V_{\theta\theta}}{R^2V} = \frac{8}{9\alpha}\frac{V_{\theta\theta}}{V}e^{-2\sqrt{2/3\alpha}\varphi} \ll 1, \tag{2.49e}$$

$$\omega_\phi \equiv \frac{V_{\theta\varphi}}{3RV}\frac{V_\theta}{RV_\varphi} = \frac{V_{\theta\rho}}{V}\frac{V_\theta}{V_\rho}\frac{8}{9\alpha}e^{-2\sqrt{2/3\alpha}\varphi} \ll 1. \tag{2.49f}$$

Please note that all constraints have to be evaluated at $\rho \sim 1$, i.e. at $\varphi \gg 6\alpha$. Our conditions are satisfied for simplest potentials, because in the large-φ regime all slow-roll and slow-turn parameters are exponentially suppressed. For instance, natural potentials which satisfy $\frac{V_\theta}{\rho V} \sim \frac{V_\rho}{V} \sim \frac{V_{\theta\theta}}{\rho^2 V} \sim \frac{V_{\theta\rho}}{\rho V} \sim \frac{V_{\rho\rho}}{V} \sim 1$ at the boundary $\rho \sim 1$, amply obey the conditions.

2.B Full analysis of perturbations

In this Appendix, we give a detailed study of turning trajectories in multi-field α-attractors and work out the full evolution of curvature and isocurvature perturbations.

2.B.1 Covariant formalism and large-φ approximations

For a general multi-field system spanned by coordinate ϕ^a with field metric G_{ab}, the equations of motion in the FRW background can be simply written as

$$D_t\dot{\phi}^a + 3H\dot{\phi}^a + V^a = 0\ , \qquad 3H^2 = \frac{1}{2}\dot{\Phi}^2 + V \tag{2.50}$$

where D_t is the covariant derivative respect to cosmic time and $\dot{\Phi}^2 \equiv G_{ab}\dot{\phi}^a\dot{\phi}^b$. To describe the multi-field effects, it is convenient to define the

tangent and orthogonal unit vectors along the trajectory as

$$T^a \equiv \frac{\dot{\phi}^a}{\dot{\Phi}} \ , \qquad N_a \equiv \sqrt{\det G}\epsilon_{ab}T^b \ , \tag{2.51}$$

where ϵ_{ab} is the Levi-Civita symbol with $\epsilon_{12} = 1$. The rate of turning for the background trajectory is defined as

$$\Omega \equiv -N_a D_t T^a = \frac{V_N}{\dot{\Phi}} \ , \tag{2.52}$$

where for the second equality we have used the background equations of motion and $V_N = N^a \nabla_a V$ is the gradient of the potential along the normal direction of the trajectory. This quantity, which vanishes in single field models, is particularly important for the multi-field behaviour and evolution of perturbations. A dimensionless turning parameter is introduced as

$$\lambda \equiv -\frac{2\Omega}{H} \ . \tag{2.53}$$

Another important parameter is the field mass along the orthogonal direction defined as

$$V_{NN} \equiv N^a N^b \nabla_a \nabla_b V \ . \tag{2.54}$$

Now let us come back to our model with coordinates $\phi^a = (\varphi, \theta)$ and hyperbolic field metric

$$G_{ab} = \begin{pmatrix} 1 & 0 \\ 0 & \frac{1}{2}\sinh^2(\sqrt{2}\varphi) \end{pmatrix} \ . \tag{2.55}$$

The Ricci scalar of this manifold is a negative constant $\mathbb{R} = -2$. By the definitions above, after some algebra, λ and V_{NN} here can be written into the following form

$$\lambda = \frac{1}{\epsilon H^3}\frac{1}{\sqrt{2}}\sinh(\sqrt{2}\varphi)\left[\ddot{\varphi}\dot{\theta} - \ddot{\theta}\dot{\varphi} - \frac{2\dot{\theta}\dot{\varphi}^2}{\frac{1}{\sqrt{2}}\tanh(\sqrt{2}\varphi)} - \frac{1}{2\sqrt{2}}\sinh\left(2\sqrt{2}\varphi\right)\dot{\theta}^3\right] \ , \tag{2.56}$$

$$\begin{aligned} V_{NN} \ = \ & \frac{1}{\dot{\Phi}^2}\left(\frac{V_{\theta\theta}\dot{\varphi}^2 + \frac{\sqrt{2}}{4}\sinh(2\sqrt{2}\varphi)V_\varphi\dot{\varphi}^2}{\frac{1}{2}\sinh^2(\sqrt{2}\varphi)} + 2\dot{\theta}\dot{\varphi}\left[\frac{\sqrt{2}V_\theta}{\tanh(\sqrt{2}\varphi)} - V_{\theta\varphi}\right]\right. \\ & \left. + \frac{1}{2}\sinh^2(\sqrt{2}\varphi)V_{\varphi\varphi}\dot{\theta}^2\right) \ . \end{aligned} \tag{2.57}$$

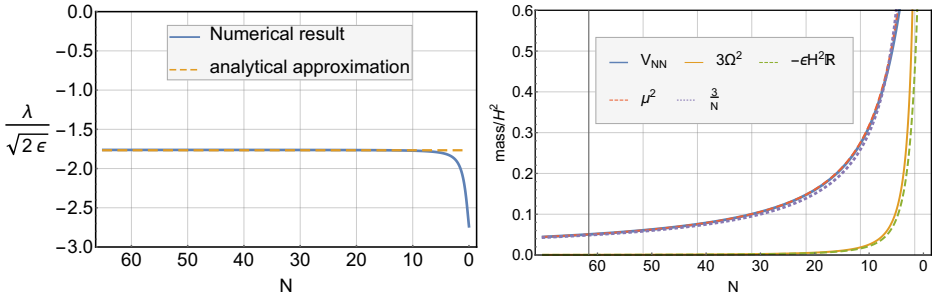

Figure 2.7: The evolution of the dimensionless turning parameter $\frac{\lambda}{\sqrt{2\epsilon}}$ and entropy masses. Here we use the toy model potential (2.26) with $n = 4$, $A = 0.2$ and $\theta_i = 8/\pi$.

These expressions look very complicated, but in the large-φ regime they can be efficiently simplified. First of all, since γ in (2.20) is nearly constant, we can use this parameter to replace $\dot{\theta}$ by $\dot{\varphi}$ in these expressions, for example $\dot{\Phi}^2 = (1+\gamma^2)\dot{\varphi}^2$. Then we can use the relations of background quantities presented in Section 2.4 to further simplify the result. Finally the turning parameter λ can be expressed as

$$\lambda = \frac{-1}{\epsilon H^3}(1+\gamma^2)\frac{\sqrt{2}\gamma\dot{\varphi}^3}{\tanh(\sqrt{2}\varphi)} \simeq \frac{2\sqrt{2}\gamma}{(1+\gamma^2)^{1/2}} \cdot \sqrt{2\epsilon}\ , \tag{2.58}$$

where the large φ approximation is used in the last step. Therefore, at $\varphi \gg 1$, $\lambda/\sqrt{2\epsilon}$ is nearly constant. Similarly, we can work out the approximated expression for V_{NN}. Here we use the toy model potential for demonstration, which yields

$$V_{NN} \approx V_0 B e^{-\sqrt{2}\varphi}. \tag{2.59}$$

Therefore, V_{NN} is nearly zero at the beginning of inflation, but then grows up as φ rolls to the center. These analytical approximations are checked by using numerical solution of the toy model. In Figure 2.7 we show the numerical results versus the analytical ones for $n = 4$, $A = 0.2$ and $\theta_i = 8/\pi$. Indeed we see that $\frac{\lambda}{\sqrt{2\epsilon}}$ remains constant until the very end of inflation, where the large-φ approximation breaks down.

2.B.2 Primordial Perturbations

With the analytical approximations developed above, now we can move to study the behaviour of perturbations. In particular, we would like to derive the analytical expression for the power spectrum of curvature perturbations.

At the linear level, the curvature perturbation ζ and the isocurvature modes σ are defined as

$$\delta\phi^a = \sqrt{2\epsilon}\zeta T^a + \sigma N^a \tag{2.60}$$

And their full equations of motion in terms of e-foldings are given by

$$\frac{d}{dN}\left(\frac{d\zeta}{dN} - \frac{\lambda}{\sqrt{2\epsilon}}\sigma\right) + (3 - \epsilon + \eta)\left(\frac{d\zeta}{dN} - \frac{\lambda}{\sqrt{2\epsilon}}\sigma\right) + \frac{k^2}{a^2H^2}\zeta = 0, \tag{2.61}$$

$$\frac{d^2\sigma}{dN^2} + (3 - \epsilon)\frac{d\sigma}{dN} + \sqrt{2\epsilon}\lambda\left(\frac{d\zeta}{dN} - \frac{\lambda}{\sqrt{2\epsilon}}\sigma\right) + \frac{k^2}{a^2H^2}\sigma + \frac{\mu^2}{H^2}\sigma = 0\ , \tag{2.62}$$

where μ^2 is the entropy mass of the isocurvature perturbations given by

$$\mu^2 \equiv V_{NN} + \epsilon H^2\mathbb{R} + 3\Omega^2\ . \tag{2.63}$$

Thus besides V_{NN}, the turning effects and the curvature of the field manifold also contribute to the entropy mass. But in multi-field α-attractors here, as shown in Figure 2.7, μ^2 is mainly controlled by the V_{NN} term. Then by (2.59) and the solution of φ in (2.31), we get

$$\frac{\mu^2}{H^2} \approx \frac{V_{NN}}{H^2} \approx 3Be^{-\sqrt{2}\varphi} \approx \frac{3}{N}, \tag{2.64}$$

which provides a good analytical approximation as shown in Figure 2.7.

The exact solutions of the full equations (2.61) and (2.62) can be obtained only through numerical method, as we have shown in Figure 2.6. But notice that the leading effect here comes from the coupled evolution of curvature and isocurvature modes after horizon-exit. Thus for the analytical approximations, we can focus on super-horizon scales. There the isocurvature equation of motion reduces to

$$3\frac{d\sigma}{dN} + \frac{\mu^2}{H^2}\sigma \simeq 0. \tag{2.65}$$

If we focus on the mode that exits horizon at N_* with amplitude σ_*, then we get the following solution for its evolution

$$\sigma(N) \approx \sigma_*\frac{N}{N_*}\ . \tag{2.66}$$

Remember that e-folding number is counted backwards from the end of inflation. Thus this solution shows the decay of the isocurvature perturbation outside of the horizon. The evolution of the normalized isocurvature

power spectrum $P_{\mathcal{S}}$ is shown in Figure 2.6, where $\mathcal{S} = \sigma/\sqrt{2\epsilon}$. As we see, the analytical approximation above successfully captures the super-horizon decay, compared with the numerical result.

Next, we look at the curvature perturbation, which after horizon-exit is sourced by the the isocurvature modes in the following way

$$\frac{d\zeta}{dN} = \frac{\lambda}{\sqrt{2\epsilon}}\sigma. \tag{2.67}$$

Also for the mode exits horizon at N_* with amplitude ζ_*, we get the solution

$$\zeta(N) = \zeta_* + \int_{N_*}^{N} dN' \, \frac{\lambda}{\sqrt{2\epsilon}}\sigma(N'). \tag{2.68}$$

As we noticed in (2.58), $\lambda/\sqrt{2\epsilon}$ is nearly constant, thus it can be seen as unchanged after horizon-exit $\lambda/\sqrt{2\epsilon} = \lambda_*/\sqrt{2\epsilon_*}$. Meanwhile, notice that since σ is almost massless in the large-φ regime, one has the relation $\sqrt{2\epsilon_*}\zeta_* \simeq \sigma_* \simeq H/(2\pi)$. Then the evolution of ζ is given by

$$\zeta(N) = \zeta_* + \frac{\lambda_*}{2}\frac{N^2 - N_*^2}{N_*}\zeta_*. \tag{2.69}$$

These two contributions are uncorrelated with each other, since they come from the different parts of the quantized fluctuations. Thus finally we can write down the power spectrum at the end of inflation ($N = 0$)

$$\begin{aligned} P_\zeta = P_\zeta^{(1)} + P_\zeta^{(2)} &= \frac{H^2}{4\pi^2}\frac{1}{2\epsilon_*}\left(1 + \frac{\lambda_*^2 N_*^2}{4}\right) \\ &= \frac{H^2}{8\pi^2\epsilon_*}\left(1+\gamma^2\right) = \frac{H^2}{8\pi^2\epsilon_{\varphi *}}, \end{aligned} \tag{2.70}$$

where we used the relation (2.22), the expression of λ (2.58), and $\epsilon_\varphi \simeq 1/(4N^2)$. Therefore, we recover the same result as we got in δN calculation.

It is interesting to note that, although the turning effects play an important role in the intermediate calculation, they vanish in the final answer. There are two effects on the curvature perturbation in multi-field α-attractors: first, the growth on super-horizon scales gives an enhancement factor $\left(1+\gamma^2\right)$; secondly, due to the motion in the θ direction, the slow-roll parameter ϵ is also enhanced by the same amount. Thus as a consequence, these two changes cancel each other, and the final power spectrum of curvature perturbation here becomes the same as the single field result.

2.C Geometrical stabilization of α-attractors

Now let us look at the three contributions to the isocurvature mass. For field spaces with a Ricci scalar $\mathbb{R} < 0$, the second term in (2.63) is negative. As inflation goes on, ϵ increases and thus the second term may become dominant, which leads to a negative entropy mass. As a result one gets a tachyonic instability here and the inflaton direction is destabilized. This effect of a negatively curved field space is dubbed as geometrical destabilization [63]. This phenomenon can end inflation prematurely, or separate inflation into two stages, in both cases modifying the standard predictions of single field models.

For α-attractors with unstabilized extra fields, at first sight, geometrical destabilization seems to be a problem. For instance, in the $U(1)$-symmetric potential without angular dependence, one has $V_{\theta\theta} = 0$ and thus it looks like the Ricci curvature term would contribute a negative μ^2. However, in the following we shall show that this naive guess fails since the Christoffel symbol term in V_{NN} is always positive and larger than the negative Ricci term. To be more specific, let us look at the field space metric in (2.55). The Ricci scalar of this manifold is a negative constant $\mathbb{R} = -\frac{4}{3\alpha}$, while we also get the following Christoffel symbol term

$$\Gamma^{\varphi}_{\theta\theta} = -\frac{1}{2}\sqrt{\frac{3\alpha}{2}}\sinh\left(2\sqrt{\frac{2}{3\alpha}}\varphi\right) \ . \tag{2.71}$$

Now we take the simplest case as an example, where inflaton only rolls in the radial direction, i.e. $\dot{\theta} = 0$. In this case we have $\Omega = 0$ and

$$T^a = (1, 0), \qquad N^a = (0, \frac{1}{\sqrt{\frac{3\alpha}{2}}\sinh\left(\sqrt{\frac{2}{3\alpha}}\varphi\right)}). \tag{2.72}$$

Therefore, the entropy mass can be expressed as

$$\begin{aligned} \mu^2 &= \frac{V_{\theta\theta} - \Gamma^{\varphi}_{\theta\theta}V_{\varphi}}{\frac{3\alpha}{2}\sinh^2(\sqrt{\frac{2}{3\alpha}}\varphi)} - \frac{2\dot{\varphi}^2}{3\alpha} \\ &\simeq \frac{V_{\theta\theta}}{\frac{3\alpha}{2}\sinh^2(\sqrt{\frac{2}{3\alpha}}\varphi)} + \sqrt{\frac{4\epsilon}{3\alpha}}V - \frac{4\epsilon}{\alpha}V \\ &\simeq \frac{V_{\theta\theta}}{\frac{3\alpha}{2}\sinh^2(\sqrt{\frac{2}{3\alpha}}\varphi)} + \frac{1}{N}V - \frac{3}{N^2}V \ . \end{aligned} \tag{2.73}$$

In the second step, we used slow-roll and large-φ approximations, and $\epsilon \simeq 3\alpha/(4N^2)$ was used in the last step. These approximations are valid as long as inflation is not close to the end, *i.e.* $N \gg 1$. As we see, for the situation where the angular direction of the potential is not stabilized, *e.g.* $V_{\theta\theta} = 0$ in the $U(1)$-symmetric case, the second term from the Christoffel symbol is still larger than the negative curvature term. Thus the entropy direction is automatically stabilized during inflation.

Even if we consider a tachyonic mass in the angular direction $V_{\theta\theta} < 0$, which is the case on the top of the ridges in multi-field α-attractors, we find that the Christoffel terms from the hyperbolic manifold always give leading and positive contributions to the entropy mass. This further confirms the observation in Fig. 2.7, where V_{NN} is always the dominating contribution in μ^2. Therefore, instead of geometrical destabilization, the hyperbolic geometry of α-attractors helps us stabilize the "rolling on the ridge" trajectories.

3 Shift-symmetric orbital inflation

Abstract: We present a new class of two-field inflationary attractor models, known as *'shift-symmetric orbital inflation'*, whose behaviour is strongly multi-field but whose predictions are remarkably close to those of single-field inflation. In these models, the field space metric and potential are such that the inflaton trajectory is along an 'angular' isometry direction whose 'radius' is constant but *arbitrary*. As a result, the radial (isocurvature) perturbations away from the trajectory are exactly *massless* and they freeze on superhorizon scales. These models are the first exact realization of the 'ultra-light isocurvature' scenario, previously described in the literature, where a combined shift symmetry emerges between the curvature and isocurvature perturbations and results in primordial perturbation spectra that are entirely consistent with current observations. Due to the turning trajectory, the radial perturbation sources the tangential (curvature) perturbation and makes it grow linearly in time. As a result, only one degree of freedom (*i.e.* the one from isocurvature modes) is responsible for the primordial observables at the end of inflation, which yields the same phenomenology as in single-field inflation. In particular, isocurvature perturbations and local non-Gaussianity are highly suppressed here, even if the inflationary dynamics is truly multi-field. We comment on the generalization to models with more than two fields.

Keywords: multi-field inflation, cosmological perturbation theory

Based on:

A. Achúcarro, E. Copeland, O. Iarygina, G. Palma, D.-G. Wang, Y. Welling
Shift-symmetric orbital inflation: single field or multi-field?
Phys. Rev. D Rapid Communications, **102**, 021302(R) (2020), [arXiv:1901.03657].

3.1 Introduction

Single field slow roll inflation is the leading explanation for the observations through the CMB [7] that primordial perturbations are very close to Gaussian and adiabatic, yet embedding it in an ultraviolet complete theory such as string theory is notoriously difficult. Moduli fields arising from string compactifications require stabilizing to realize single field inflation [19], and large field excursions test the validity of using four dimensional effective theories[1].

One may therefore wonder whether there are multi-field inflationary scenarios with a phenomenology similar to that of single field inflation. Most of the previous studies on multi-field inflation focus on the slow-roll slow-turn regime, where the isocurvature and curvature perturbations are weakly coupled, therefore one may get single-field like phenomenology unsurprisingly. Meanwhile, models with significant multi-field turning behaviour are commonly considered to be problematic. In the usual understanding of this regime, light fields during inflation may lead to isocurvature perturbations and local non-Gaussianity tightly constrained by current observations. However, it has been suggested recently that inflation with non-stabilized light fields on an axion-dilaton system can be compatible with the latest CMB data [75, 78, 120–124]. In particular, it was pointed out in [78] that, when the perturbations orthogonal to the trajectory are *massless* but efficiently *coupled* to the inflaton, the isocurvature modes are dynamically suppressed. This is the "ultra-light isocurvature" scenario.

In this paper we provide for the first time a family of exact models of inflation in which the multi-field effects are significant, but the phenomenology remains similar to single field inflation. The models combine two ingredients: First, the inflaton trajectory proceeds along an isometry direction of the field space, so it is Orbital Inflation in the sense of [81, 82]. This ensures time independence of the coupling between the radial and tangential inflationary perturbations. Second, the trajectory can have an *arbitrary* radius (within some range described below), and a constant radius is proven to be a neutrally stable attractor. Hence, isocurvature perturbations become exactly massless. The two ingredients, combined, guarantee that the sourcing of the curvature perturbation is sustained over many e-folds of inflationary expansion. The action for the perturbations inherits a symmetry

[1]The recent swampland debate highlights the importance of finding viable scenarios for inflation that are not strictly single-field. See, for instance, the discussion in [47] as compared to [24, 137]

between background solutions that is not manifest in the potential or in the Lagrangian. We show that, at the end of inflation, only the isocurvature degree of freedom is responsible for the generation of primordial observables, but perturbations still remain adiabatic and Gaussian. We call this scenario *shift-symmetric orbital inflation*.

Crucially this scenario provides a new direction to explore inflation and a potential resolution to some of the problems faced by the embedding of inflation in string theory. That is, in the construction of inflationary models wherein every modulus is stabilized except for the inflaton, one could be missing less restrictive realizations of inflation compatible with current observational constraints. We set $\hbar = c = 1$ and the reduced Planck mass $M_p \equiv (8\pi G)^{-1/2} = 1$, where G is Newton's contant.

3.2 A toy model

To illustrate the idea, we first consider the following Lagrangian in flat field space with polar coordinates (illustrated in Fig. 3.1)

$$\mathcal{L} = \frac{1}{2}\left[\rho^2(\partial\theta)^2 + (\partial\rho)^2\right] - \frac{1}{2}m^2\left(\theta^2 - \frac{2}{3\rho^2}\right). \tag{3.1}$$

The potential has a monodromy in the angular coordinate, and although it is unbounded at $\rho \to 0$, inflation only takes place in the physically consistent regime where $V(\rho, \theta) > 0$. Moreover, as shown in the perturbation analysis below, our study is restricted to radii that cannot be too small. Therefore, we only care about the local form of the potential close to the inflationary trajectory, which we assume is captured well by (3.1). In general, it is difficult to solve the background equations analytically in such a system. However, this model has the following exact neutrally stable solutions at any radius (see Fig. 3.1)

$$\rho = \rho_0, \quad \dot{\theta} = \pm\sqrt{\frac{2}{3}}\frac{m}{\rho_0^2}. \tag{3.2}$$

The Friedmann equation becomes $H^2 = m^2\theta^2/6$ on the attractor, where H is the Hubble parameter, and the first slow-roll parameter is $\epsilon \equiv -\dot{H}/H^2 = \frac{2}{\rho_0^2\theta^2}$. This trajectory is nongeodesic in field space, with turning effects that depend on the radius κ of the trajectory. Note that here $\kappa = \rho_0$ but, if the field space geometry is curved, κ will be a more general function of ρ_0.

The situation is reminiscent of circular orbits in a spherically symmetric gravitational field, where the centripetal force stabilizes the radial direction,

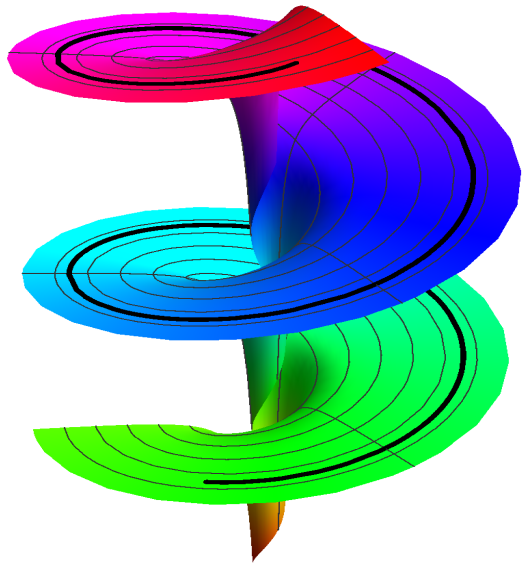

Figure 3.1: The toy model potential $V(\rho, \theta)$ given in (3.1) together with a typical inflationary trajectory indicated with the solid black line.

and the inflaton can circle at any radius with the corresponding angular velocity. For the field system on the cosmological background, only the isometric circular orbits appear, and we need to break the shift symmetry of θ in the potential to overcome the Hubble friction. We can label each solution by a continuous parameter c with the corresponding map

$$\rho_c = \rho_0 + c, \quad \left(\theta_c^2\right)' = \frac{\left(\theta_0^2\right)'}{(1 + c/\kappa)^2}, \tag{3.3}$$

where the prime $'$ denotes a derivative with respect to efolds $d/dN = d/(Hdt)$. This transformation identifies all the trajectories in (3.2) and hints at the existence of a shift symmetry for the perturbations. In flat gauge, the isocurvature perturbation σ is associated with $\delta\rho$ and the curvature perturbation $\mathcal{R}$ with $\frac{\rho}{\sqrt{2\epsilon}}\delta\theta$, which equals $\frac{1}{4}\rho^2\delta\left(\theta^2\right)$ in this toy model. To find the effect of the transformation on the perturbations, we split $\rho = \rho_0 + \sigma$ and $\left(\theta^2\right)' = \left(\theta_0^2\right)'(1 - \mathcal{R}')$. This allows us to determine how a small c changes σ and $\mathcal{R}'$. In the long wavelength limit every transformed set of perturbations $(\sigma_c, \mathcal{R}'_c)$ provide a new solution to the equations of motion. This is because homogeneous perturbations map background solutions onto each other. Therefore, we expect the following *symmetry* for linearized pertur-

bations

$$\sigma \to \sigma + c, \quad \mathcal{R}' \to \mathcal{R}' + \frac{2}{\kappa}c. \tag{3.4}$$

Given the shift symmetry of σ, the isocurvature perturbation is expected to be massless and freeze after horizon-exit. Meanwhile, the symmetry also indicates that $\mathcal{R}$ has a growing solution that is dictated by the constant σ on superhorizon scales.

To get an intuitive notion of the perturbations behavior, we employ the δN formalism [131–135]. From the Friedmann equation and the exact solution (3.2), the number of efolds until the end of inflation is $N = \rho^2\theta^2/4 - 1/2$. The curvature perturbation at the end of inflation is

$$\mathcal{R}(k_*) = \delta N \simeq \frac{1}{\sqrt{2\epsilon_*}}(\rho\delta\theta)_* + \frac{2N_*}{\kappa}\delta\rho_*, \tag{3.5}$$

where $(\rho\delta\theta)_*$ and $\delta\rho_*$ are field fluctuations with typical amplitude $\frac{H_*}{2\pi}$ at horizon-exit of the k_* mode. This yields the following power spectrum of curvature perturbations

$$P_{\mathcal{R}}(k_*) \simeq \frac{H_*^2}{4\pi^2}\left(\frac{1}{2\epsilon_*} + \frac{4N_*^2}{\kappa^2}\right). \tag{3.6}$$

Here the first contribution has an adiabatic origin, just like in the single-field models, and the second term corresponds to the conversion from isocurvature to curvature modes on superhorizon scales. When the radius of the trajectory is small enough, namely $8\epsilon_* \ll \kappa^2 \ll 8\epsilon_* N_*^2 \approx 4N_*$, the second term in (3.6) dominates. Then the final power spectrum becomes $P_{\mathcal{R}}(k_*) \simeq H_*^2 N_*^2/(\pi^2\kappa^2)$, which is generated by one single degree of freedom – the isocurvature mode.

3.3 Shift-symmetric orbital inflation

To construct generic models with the above properties, we begin with an axion-dilaton system in a non-trivial field manifold (θ, ρ) with kinetic term $K = -\frac{1}{2}\left(f(\rho)\partial_\mu\theta\partial^\mu\theta + \partial_\mu\rho\partial^\mu\rho\right)$. This field space, of curvature $\mathbb{R} = f_\rho^2/2f^2 - f_{\rho\rho}/f$, arises generically from UV completions of inflation in quantum gravity or from an effective field theory (EFT) viewpoint. To realize shift-symmetric orbital inflation, we assume the inflationary trajectory to be isometric, *i.e.* along the θ direction at *any* (constant) radius in field space. The potential can be derived by generalizing the Hamilton-Jacobi

formalism [131, 138–140] to a two-field system. It has the general form

$$V = 3H^2 - 2\frac{H_\theta^2}{f(\rho)}, \tag{3.7}$$

where H is a function of θ only, $H_\theta \equiv dH/d\theta$ and $f(\rho) > 0$. The model (3.1) is recovered for $H \propto \theta$ and $f(\rho) = \rho^2$, corresponding to a flat field space parametrized by polar coordinates. This non-linear system admits exact solutions

$$\dot{\theta} = -2\frac{H_\theta}{f}, \qquad \rho = \rho_0. \tag{3.8}$$

Thus the inflaton moves in an orbit of constant radius, as ensured by the Hamilton-Jacobi formalism. As in the toy model, this trajectory is not along a geodesic. Here the tangent and normal vectors to the trajectory are $\mathcal{T}^a = 1/\sqrt{f}(1,0)$ and $\mathcal{N}^a = (0,1)$, and the radius of the turning trajectory is a constant given by $\kappa = 2f/f_\rho$. It follows that all these trajectories are *neutrally stable*: a small perturbation orthogonal to a given orbital trajectory will bring us to one of the neighbouring trajectories. The attractor behaviour is explicitly demonstrated in the appendix of the original paper.

3.4 Analysis of perturbations

In flat gauge, the comoving curvature perturbation $\mathcal{R}$ is defined as the projection of the field perturbation along the inflationary trajectory $\mathcal{R} = \frac{1}{\sqrt{2\epsilon}}\mathcal{T}_a\delta\phi^a$, and the isocurvature perturbation σ corresponds to the orthogonal projection $\sigma = \mathcal{N}_a\delta\phi^a$. Then for generic multi-field models, the quadratic action of perturbations takes the following form [78]

$$S^{(2)} = \frac{1}{2}\int d^4x a^3 \left[2\epsilon\left(\dot{\mathcal{R}} - \frac{2H}{\kappa}\sigma\right)^2 + \dot{\sigma}^2 - \mu^2\sigma^2 + \dots\right], \tag{3.9}$$

where ellipses stand for the gradient terms $-(\partial_i\sigma)^2 - 2\epsilon(\partial_i\mathcal{R})^2$. The interaction between curvature and isocurvature modes is given by the term $a^3(8\epsilon H/\kappa)\dot{\mathcal{R}}\sigma$. To guarantee perturbative analysis we require that $\sqrt{8\epsilon}/\kappa \ll 1$ [78, 141]. The mass of entropy perturbations is defined as $\mu^2 \equiv V_{NN} + \epsilon H^2\left(\mathbb{R} + 6/\kappa^2\right)$, where the first term is obtained from the standard Hessian of the potential $V_{NN} \equiv \mathcal{N}^a\mathcal{N}^b\left(V_{ab} - \Gamma^c_{ab}V_c\right)$, the second and third terms correspond to the field space curvature and turning contributions respectively.

For shift-symmetric orbital inflation, we expect the isocurvature perturbations to be exactly massless, as in the toy model, and this is confirmed by

using (3.8) to show $\mu^2 = 0$. This implies that the quadratic action (3.9) has the combined shift symmetry (3.4), as in the toy model. The power spectra of perturbations in the massless limit can be directly estimated from the coupled evolution of perturbations [78]. When $\mu = 0$, the linearized system simplifies in the superhorizon limit, yielding

$$\mathcal{R}_k' = \frac{2}{\kappa}\sigma_k, \qquad \sigma_k = \frac{H_*}{2\pi}, \tag{3.10}$$

where $*$ denotes evaluation at the time of horizon crossing. That is, on superhorizon scales the isocurvature perturbation quickly becomes a constant, and it sources the growth of $\mathcal{R}$. At the end of inflation, the primordial curvature perturbation can be expressed as $\mathcal{R}_k = \mathcal{R}_* + 2N_*\sigma_k/\kappa$, where the first term is the curvature perturbation amplitude at horizon-exit, and the second term comes from the isocurvature source. Thus these two contributions are uncorrelated with each other, and the dimensionless power spectrum for $\mathcal{R}$ is given by

$$P_{\mathcal{R}} = \frac{H_*^2}{8\pi^2\epsilon_*}\left(1 + \mathcal{C}\right), \tag{3.11}$$

where $\mathcal{C} = 8\epsilon_* N_*^2/\kappa^2$ represents the contribution from isocurvature modes. This result agrees with the δN calculation for the toy model given in (3.6). The full calculation via the in-in formalism gives the same answer up to subleading corrections [78]. Note that the power spectrum is completely determined by the isocurvature perturbations if $\mathcal{C} \gg 1$, which corresponds to trajectories with a small radius κ or, equivalently, significant turning effects with $8\epsilon_* \ll \kappa^2 \ll 8\epsilon_* N_*^2$. Thus at the end of inflation, curvature perturbations are highly enhanced compared to the ones at horizon-exit. Meanwhile, the isocurvature power spectrum for $\mathcal{S} \equiv \sigma/\sqrt{2\epsilon}$ remains unchanged as $P_{\mathcal{S}} = \frac{H_*^2}{8\pi^2\epsilon_*}$. Therefore, the amplitude of the isocurvature perturbation is dynamically suppressed, *i.e.* $P_{\mathcal{S}}/P_{\mathcal{R}} \simeq 1/\mathcal{C} \ll 1$. The details of how $P_{\mathcal{S}} \neq 0$ can generate isocurvature components in the CMB are rather model-dependent, and one cannot automatically claim that a suppressed ratio $P_{\mathcal{S}}/P_{\mathcal{R}}$ is compatible with observations. However, if $\mathcal{R}$ and $\mathcal{S}$ contributed similarly to the curvature and isocurvature components in the CMB, the result is compatible with current constraints.

3.5 Phenomenology

We now turn to the observational predictions of shift-symmetric orbital inflation. For any positive $\mathcal{C}$, from (3.11), the tensor-to-scalar ratio can be

expressed as $r = 16\epsilon_*/(1+\mathcal{C})$, and the scalar spectral index is $n_s - 1 \equiv \frac{d\ln P_\mathcal{R}}{d\ln k} = -2\epsilon_* - \eta_* + (d\mathcal{C}/dN)/(1+\mathcal{C})$, where we used $d\ln k = dN$. Note that $\frac{\partial N_*}{\partial N} = -1$, since N_* counts the number of efolds backwards. These predictions depend on the function $H(\theta)$. As in single field inflation, this function determines how slow-roll parameters ϵ and $\eta \equiv \epsilon'/\epsilon$ scale with N_*.

For concreteness, we consider models with $H \sim \theta^p$. Solving (3.8) for $\theta(N)$ yields[2] $\epsilon_* \simeq p/(2N_*)$ and $\eta_* \simeq 1/N_*$. The predictions for n_s and r are therefore well approximated by

$$n_s - 1 \simeq -\frac{p+1}{N_*} - \frac{4p}{\kappa^2 + 4pN_*}, \quad r \simeq \frac{8p\kappa^2}{N_*\kappa^2 + 4pN_*^2}. \tag{3.12}$$

We plot these results against the Planck 1σ and 2σ contours [7] in Fig. 3.2. N_* is taken to be between 50 and 60, and the radius κ^2 varies between 1 and 10^5. The purple region is for $p = 1$, corresponding to the toy model (3.1), and we also show the predictions for $p = 0.5$ (red region), $p = 0.2$ (yellow region) and $p = 0.1$ (green region).

Notice that n_s and r only depend on the value of κ and are therefore insensitive to the details of the field metric. When $\kappa \to \infty$ one recovers the predictions of chaotic inflation with $V \propto \phi^{2p}$. Meanwhile as κ decreases, predictions are pushed downwards and to the left in this $n_s - r$ diagram. Therefore, in the case of power-law potentials only for small p do the predictions remain within the Planck contours. The interesting regime here is still the case with significant turning (small κ or $\mathcal{C} \gg 1$), where the final power spectrum $P_\mathcal{R} \simeq \frac{H_*^2 N_*^2}{\pi^2\kappa^2}$ mainly has an isocurvature origin. Then the tensor-to-scalar ratio is given by $r = 2\kappa^2/N_*^2 = 16\epsilon_*/\mathcal{C}$, which is suppressed. The spectral index reduces to $n_s - 1 = -(p+2)/N_*$ which, for small p, lies in the sweet spot $n_s = 0.9649 \pm 0.0042$.

Another important observable is primordial non-Gaussianity, which is currently bounded by Planck through $f_{\rm NL}^{\rm loc} = 0.8 \pm 5$ [109]. There are examples in the literature of how $\mathcal{O}(1)$ local non-Gaussianity can arise in multi-field models, especially when the coupling between isocurvature and curvature modes is large [57, 142–144] - see [145] for a review. There are also examples of how small levels of non-Gaussianity can arise in multifield models [146–148]. However, in most cases a detailed analytic understanding of the size of the non-Gaussianity is lacking because the associated dynamics is non-linear and complicated. This is not the case in

[2] We note that for $0 < p < 1$ this toy model is not well defined as $\theta \to 0$, as can be seen in (3.7). This is not a problem as the inflationary period we are interested in occurs before that point is reached. The true underlying potential would have to be completed in some way. This is similar to case with say axion monodromy.

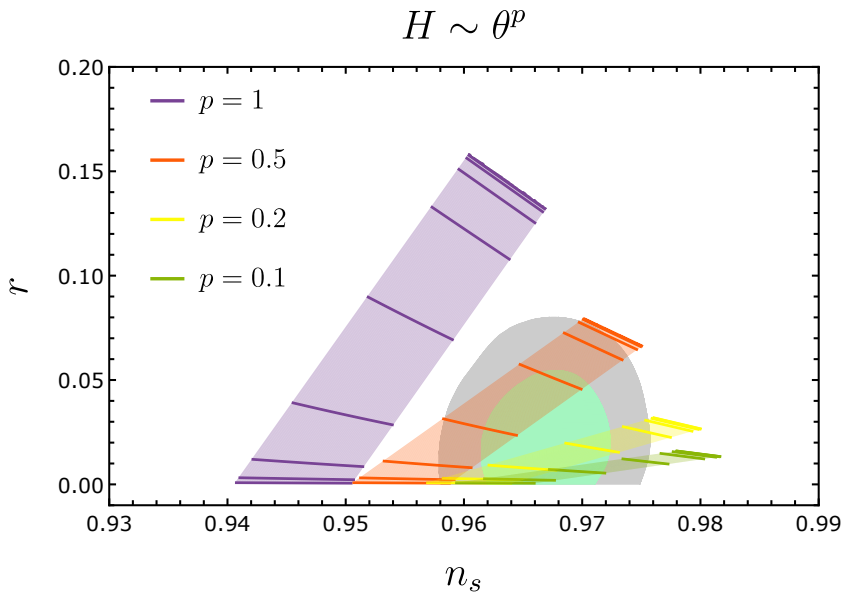

Figure 3.2: The analytical predictions (3.12) for (n_s, r) compared to the *Planck* 1σ and 2σ contours [7]. We show the predictions for wavenumbers which cross the horizon $50-60$ efolds before the end of inflation. The predictions for $n_s - r$ depend on the value of $\kappa \in [1, 1000]$, where the values $(1, 2, 4, 8, 16, 32, 64, 128, 256)$ are depicted with thick lines (from bottom to top).

shift-symmetric orbital inflation, where we find that we can both easily satisfy the Planck constraint and crucially understand its origin analytically. The amplitude of local non-Gaussianity can be determined using the δN formalism. In a generic multi-field inflation model with curved field manifold, we have $f_{\rm NL}^{\rm loc} = \frac{5}{6} G^{ab} G^{cd} N_a N_c N_{bd} / (G^{ab} N_a N_b)^2$ [142, 149], where $G_{ab} = \mathrm{diag}\{f(\rho), 1\}$ is the field space metric, N_a and N_{ab} are derivatives of N with respect to the fields (θ, ρ). To gain some analytical understanding, here we still focus on models with $H \sim \theta^p$, where N can be expressed as $N = f(\rho)\theta^2/4p - p/2$. The amplitude of local non-Gaussianity then follows

$$f_{\rm NL}^{\rm loc} = \frac{5}{12}\eta_* \left[1 - \frac{\mathcal{C}^2}{(1+\mathcal{C})^2}\frac{\kappa^2 \mathbb{R}}{2}\right], \tag{3.13}$$

where we used the relation $\mathcal{C} = 2p^2/(\epsilon_* \kappa^2)$. When $\kappa \to \infty$, we have $\mathcal{C} \to 0$ and $\mathcal{C}^2\kappa^2 \to 0$. Thus the second term in (3.13) vanishes, which leads to the single field result $f_{\rm NL}^{\rm loc} = 5\eta_*/12$ as expected. The enhancement of non-Gaussianity is possible in the intermediate regime $\mathcal{C} \sim \mathcal{O}(1)$, where the

transfer from isocurvature to adiabatic modes is inefficient. In that case, $f_{\rm NL}^{\rm loc} \sim -5p\mathbb{R}/12$ can be large if the field space is highly curved.

For the interesting regime with $\mathcal{C} \gg 1$, the δN expansion is dominated by N_ρ and $N_{\rho\rho}$. This then leads to what, at first sight, appears as the counterintuitive result that $f_{\rm NL}^{\rm loc}$ is negligible and slow-roll suppressed

$$f_{\rm NL}^{\rm loc} \simeq \frac{5}{6}\frac{N_{\rho\rho}}{N_\rho^2} = \frac{5}{12}\eta_* \left(1 - \frac{\kappa^2\mathbb{R}}{2}\right). \tag{3.14}$$

This is the same as happened in the calculation of the power spectrum: the contribution to the curvature perturbation sourced by the isocurvature modes dominates the final result. The bispectrum is found to be slow-roll suppressed, just like in single field inflation, but there are small corrections from the field space curvature, which violates Maldacena's consistency relation [39, 40]. We have recently confirmed this result via a scaling symmetry approach in [80].

3.6 Discussions

We have proposed a class of multi-field inflationary models that demonstrate a new type of attractor trajectory along the isometry direction in field space. Here the isocurvature modes become massless and freeze on super-horizon scales. Moreover, when the turning effects become significant, the curvature perturbations keep growing after horizon-exit and thus isocurvature modes are dynamically suppressed. As a consequence, these multi-field models yield the single-field-like phenomenology favored by observations.

Additional isocurvature perturbations will either decay if they are massive or freeze if they are light. Therefore, although our computations were done in a simple two-field setting, we expect the conclusions will continue to hold in multi-field extensions with more than two fields, provided that the number of additional light isocurvature fields is not too large.

We have shown and explained how in shift-symmetric orbital inflation, a negligible amount of local non-Gaussianity is produced. Here the isocurvature degree of freedom can be the dominant contribution to the bispectrum, but in such cases $f_{\rm NL}$ is slow-roll suppressed. This result teaches us a generic lesson: that in multi-field models, even if the isocurvature-to-adiabatic conversion is very efficient, the resulting non-Gaussianity can still be suppressed. A large coupling between curvature and isocurvature modes enhances the transfer of non-Gaussianity, but for this transfer to generate large non-Gaussianity, one needs sizable self-interactions affecting

the isocurvature field during horizon crossing [57, 141]. In this class of scenarios, however, the shift symmetry along the radial direction (3.4) has a role in suppressing the self-interactions of the isocurvature field (see [80]). Therefore, it is perfectly fine to study multi-field models with significant and sustained turning trajectories, without worrying about generating large non-Gaussianity.

Our model has important implications on the realization of inflation in UV-complete theories. Contrary to what is usually assumed, and as emphasized in [78], it is not always necessary to stabilize all compactification moduli, or to have a large mass hierarchy between the inflaton and other fields. The most problematic effects usually associated with multi-field effects – the generation of isocurvature perturbations and non-Gaussianity at unacceptable levels – cancel each other in the shift-symmetric orbital scenario [3]. From an EFT point of view this can be traced back to the effect of derivative interactions among the curvature and isocurvature perturbations that are absent in single-field inflation. These are unavoidable on curved trajectories and curved field spaces and, therefore, ubiquitous in string compactifications.

[3] As already emphasized, large isocurvature perturbations at the end of inflation do not necessarily imply large isocurvature components in the CMB, the details of which are rather model dependent. Nevertheless, in this class of models the potentially significant generation of isocurvature modes in the CMB is automatically alleviated by the mechanism at play.

4 Inflationary massive fields with a curved field manifold

Abstract: Massive fields during inflation provide an interesting opportunity to test new physics at very high energy scales. Meanwhile in fundamental realizations, the inflationary field space typically has a curved geometry, which may leave detectable imprints in primordial observables. In this paper we study an extension of quasi-single field inflation where the inflaton and the massive field belong to a curved field manifold. Because of the nontrivial field space curvature, the massive field here can get significant mass corrections of order the Hubble scale, thus the quasi-single field predictions on primordial non-Gaussianity are affected. We derive the same result in an equivalent approach by using the background effective field theory of inflation, where a dimension-6 operator is identified to play an important role and its cutoff scale is associated with the curvature scale of the field space. In addition, due to the slow-roll evolution of the inflaton, this type of mass correction has intrinsic time-dependence. Consequently, the running mass modifies the scaling behaviour in the squeezed limit of the scalar bispectrum, while the resulting running index measures the curvature of the internal field space. Therefore the minimal setup of a massive field within curved field space during inflation may naturally lead to new observational signatures of the field space geometry.

Keywords: Inflation, primordial non-Gaussianity, effective field theory

Based on:

D.-G. Wang
On the inflationary massive fields with a curved field manifold
JCAP 2001 (2020), no. 01 046, [arXiv:1911.04459].

4.1 Introduction

Cosmic inflation, which provides a good description of the very early Universe [7, 8], can also be seen as a physics laboratory at extremely high energy scales. Through primordial perturbations, we can trace the imprints left by fundamental physics during inflation in astronomical observations, such as the cosmic microwave background (CMB) and large scale structure (LSS) surveys. Moreover primordial non-Gaussianity, which encodes the field interactions during inflation, is believed to be one of the most powerful tools for testing new physics effects [35, 37, 150, 151]. Therefore it is phenomenologically interesting to work out various non-Gaussian templates from inflation theories for future observations. From this point of view, one well-studied example is *quasi-single field inflation* (QSFI) [56–58, 152–154], where the extra fields during inflation with mass of $\mathcal{O}(H)$ can leave unique signatures in the primordial bispectrum of curvature perturbation. This idea has been further developed into model-independent frameworks for probing primordial physics, such as the proposals of cosmological collider physics [59, 102, 155–161] and primordial standard clocks [162–165].

Meanwhile, another important question in the primordial cosmology is the physical realizations of inflation in more fundamental theories. From this theoretical perspective, one common observation is that the resulting low-energy effective theories of inflation are typically associated with a curved field manifold. For instance, it could be the moduli field space arising in string compactifications, or the coset field space of (pseudo-)Goldstones after spontaneous symmetry breaking. This theoretical consideration leads to the studies on *inflation with curved field space*. Recently there has been a revival of interest in this direction, and the representative works include α-attractors [17, 18, 73, 74] and their multi-field extensions [75–77, 166–168], geometrical destabilization [63–67, 83], ultra-light isocurvature scenario [78, 80] and orbital inflation [79, 81, 82], hyperinflation [68–72], the two-field regime of axion monodromy [169], and the analysis of new multi-field attractors [84–86]. Usually in the curved field manifold the inflaton trajectory may demonstrate turning dynamics (or equivalently non-geodesic motion in the field space). It has also been suggested that such kind of multi-field behaviour may be free from some possible problems faced by single field inflation [47, 48, 170]. Moreover, richer phenomenology emerges in this class of multi-field models, which could be interesting for future observational detections.

Having various models of inflation with curved field space, now one may

ask a more generic question: considering that the field space curvature is associated to a new energy scale during inflation, then what are the *observational signatures of this curvature scale*? One attempt in this direction was lately performed in Ref. [171], where the generic cubic action is derived for the multi-field system with curved field space, and after a heavy field is integrated out, the geometrical effects manifest in the effective cubic action of curvature perturbations. The question remains, if there are other observable imprints uniquely left by the geometry of the internal space during inflation.

In this paper, we attack the above question in the context of QSFI, by focusing on the behaviour of a massive field living in a curved field manifold of inflation. The main results are summarized as follows:

- We extend the QSFI model to the case where the inflaton and the massive field span a curved field space with a nontrivial metric. Using the covariant formalism of multi-field inflation, we perform the background and perturbation analysis of this two-field system. Due to the presence of the non-trivial field space curvature, the massive field gets mass corrections which can be comparable to (or even larger than) the "bare" mass. Then we provide one simple realization of QSFI with significant curved field space effects. Furthermore, through this concrete case study, we explicitly demonstrate how the curvature of the field space is related to an energy scale during inflation.

- Next, we investigate the background effective field theory (EFT) of inflation with the dimension-five (dim-5) and dimension-six (dim-6) mixing operators. This EFT approach, which has been widely adopted in the studies of massive fields, provides an alternative description for the curved field space system. We explicitly bridge the gap between these two languages. In particular, the dim-6 operator in the EFT can give a significant contribution to the mass of the extra field, thus has the same effects as the curved field space. Moreover, this correction to the "bare" mass is essentially time-dependent, and we further consider the running behaviour of the final isocurvature mass.

- Finally, we study the phenomenological consequences of the curved field space on QSFI predictions. As is known, the mass of the additional field leaves a unique scaling signature in the squeezed limit of the scalar bispectrum. Here the curved field space may result in two modifications: *i)* the field space curvature contribution corrects

the original "bare" mass, thus changes the predictions in the scaling index; *ii)* the time-dependence of this mass correction leads to the running of the scaling in the squeezed bispectrum. Therefore through the phenomenology of the running isocurvature mass, we can find the observational signatures left by the field space curvature.

The time dependence of the isocurvature mass μ is divided into three different regimes: running within $\mu < 3H/2$ and $\mu > 3H/2$, and also running through $\mu = 3H/2$. To search for new predictions, we work out the modified scaling behaviour of the squeezed bispectrum caused by them one by one. In the first two cases, the modification corresponds to the running of the scaling index in the power-law and oscillatory signals respectively, while the third case demonstrates a transition behaviour between these two types of signals. Implications for non-Gaussianity observations are discussed.

Some of the results, for instance the field space curvature contribution to the mass of the extra field, have been noticed in different setups, such as geometrical destabilization [63] (for negative correction, also see the early discussion in Ref. [53]) and spontaneous symmetry probing [100] (for positive correction). Here we look into more generic cases of this contribution, and find it illuminating to further interpret the curved field space effects from the perspective of inflationary massive fields. In addition, the correspondences among several different research topics are clarified. Other results, such as the curved field space modifications to QSFI and the running phenomenology of μ^2, were not discussed in the previous studies.

The outline of the paper is as follows. In Section 4.2 we study the massive field within a curved field space during inflation via the multi-field analysis, and demonstrate the effects of the field space curvature in a concrete example. In Section 4.3 we take the background EFT approach to reexamine QSFI, and identify the role of a dim-6 operator and its connection with curved field space. Section 4.4 focuses on the phenomenology, where the consequences of the running isocurvature mass are investigated in detail. We summarize in Section 4.5 with discussions on future works .

4.2 When quasi-single field inflation meets a curved field space

QSFI corresponds to one particular regime of inflation models, where the extra fields besides the inflaton are massive and thus generate isocurvature pertubations with a mass around the Hubble scale H. The original model

of QSFI in Ref. [56, 57] is described by the following matter Lagrangian

$$\mathcal{L}_m = -\frac{1}{2}\rho^2(\partial\theta)^2 - \frac{1}{2}(\partial\rho)^2 - V(\rho) - V_{sr}(\theta) \ , \tag{4.1}$$

where the radial field ρ is taken to be massive and stabilized around $\rho = \rho_0$, with $V''(\rho_0) \sim \mathcal{O}(H^2)$. Meanwhile the angular field θ plays the role of the inflaton, which is slowly rolling on a nearly flat potential along the angular direction. In this section, we shall extend this model, and consider the situation while the inflaton and the massive field are living in a curved field manifold.

The curved field space generically arises in the low-energy effective theory of inflation, whose action with a scalar sector and Einstein gravity can be formulated as

$$S = \int d^4x\sqrt{-g}\left[\frac{M_{\rm pl}^2}{2}\mathbf{R} - \frac{1}{2}G_{ab}(\phi)g^{\mu\nu}\partial_\mu\phi^a\partial_\nu\phi^b - \mathcal{V}(\phi)\right] \ . \tag{4.2}$$

Notice that besides the spacetime metric $g_{\mu\nu}$, an internal field space metric $G_{ab}(\phi)$ of a non-linear sigma model also appears. Generally speaking, the inflaton field here corresponds to one particular trajectory in the multi-dimensional field space. Thus in addition to the adiabatic perturbations along this inflaton trajectory, the isocurvature perturbations in the orthogonal direction are also present. To be specific, we consider an axion-dilaton system spanned by $\phi^a = (\theta, \rho)$ with the field space metric

$$G_{ab} = \begin{pmatrix} f(\rho) & 0 \\ 0 & 1 \end{pmatrix} \ , \tag{4.3}$$

which yields a non-trivial kinetic mixing for the two scalar fields. Here the axion θ can be seen as an "angular" field, while the dilaton field ρ corresponds to the "radial" direction in this internal space. The non-trivial geometry of this internal manifold is characterized by the Ricci curvature scalar

$$\mathbb{R} = \frac{f'(\rho)^2}{2f(\rho)^2} - \frac{f''(\rho)}{f(\rho)} \ , \tag{4.4}$$

which is of mass dimension -2. With the choice of the potential, QSFI can be easily realized in this multi-field system[1]. One direct extension of the

[1]One can construct exact models of QSFI with curved field space by using the extended Hamilton-Jacobi formalism, as done in orbital inflation [81, 82]. This approach is not adopted here.

original model yields the following two-field Lagrangian

$$\mathcal{L}_m = -\frac{1}{2}f(\rho)(\partial\theta)^2 - \frac{1}{2}(\partial\rho)^2 - V(\rho) - V_{sr}(\theta) \ , \tag{4.5}$$

where again θ is the inflaton and ρ is the massive field. Thus the original model can be seen as a special case of the above setup with $f(\rho) = \rho^2$, where the field space is flat and described by the polar coordinate. Next, with the help of multi-field techniques, we shall investigate the QSFI with a general metric function $f(\rho)$.

4.2.1 The multi-field analysis of the massive field

For inflaton trajectories in a curved field space, the covariant formalism of multi-field inflation [49–53] provides a powerful tool to describe the background dynamics and perturbations. Consider a turning trajectory with $\rho = \rho_0$, then the field velocity of the canonically normalized inflation is given by $\dot{\phi}^2 = G_{ab}\dot{\phi}^a\dot{\phi}^b = f(\rho)\dot{\theta}^2$, where the dot denotes the derivative with respect to the cosmic time. Thus we can build the tangent and normal unit vectors of this trajectory

$$T^a \equiv \frac{\dot{\phi}^a}{\dot{\phi}} = \frac{1}{\sqrt{f(\rho_0)}}(1,0) \ , \qquad N^a = (0,1) \ . \tag{4.6}$$

Also the turning rate is defined as

$$\Omega \equiv -N_a D_t T^a = \frac{f'(\rho_0)}{2\sqrt{f(\rho_0)}}\dot{\theta} \ , \tag{4.7}$$

where D_t is the covariant derivative of the field space with respect to cosmic time. In general a geodesic trajectory in the field space yields $\Omega = 0$, thus the turning parameter measures the deviation from a geodesic [52]. For the flat field metric $f(\rho) = \rho^2$, it simply yields $\Omega = \dot{\theta}$. With these notations, the background equations of motion (EoMs) $D_t\dot{\phi}^a + 3H\dot{\phi}^a + V^a = 0$ become

$$\ddot{\phi} + 3H\dot{\phi} + V_T = 0 \ , \qquad \Omega\dot{\phi} = V_N \ , \tag{4.8}$$

where $V_T = T^a\nabla_a V_{sr}$ and $V_N = N^a\nabla_a V$, with ∇_a being the covariant derivative of the field space. The first equation captures the slow-roll dynamics, while the second one describes the balance between the turning and the centrifugal force. Meanwhile the slow-roll parameters here are given by

$$\epsilon \equiv -\frac{\dot{H}}{H^2} = \frac{\dot{\phi}^2}{2M_{\rm pl}^2H^2} = \frac{f(\rho_0)\dot{\theta}^2}{2M_{\rm pl}^2H^2} \ , \qquad \eta \equiv \frac{\dot{\epsilon}}{H\epsilon} = 2\epsilon \ . \tag{4.9}$$

Now let us describe the behaviour of perturbations using the background parameters above. At the linear level, we can define the curvature perturbation ζ and the isocurvature modes σ as $\delta\phi^a = \sqrt{2\epsilon}\zeta T^a + \sigma N^a$. Expanding (4.2) to the second order, we get the general form of the quadratic action

$$S_2 = \int d^4x a^3 \left[\epsilon \left(\dot{\zeta} - \frac{2\Omega}{\sqrt{2\epsilon}}\sigma \right)^2 - \frac{\epsilon}{a^2}(\partial_i \zeta)^2 + \frac{1}{2}\left(\dot{\sigma}^2 - \frac{1}{a^2}(\partial_i \sigma)^2 \right) - \frac{1}{2}\mu^2\sigma^2 \right] . \tag{4.10}$$

Here notice that at the quadratic level, the interaction between ζ and σ is given by the turning parameter Ω. From the EoM of perturbations, this coupling corresponds to the conversion from isocurvature to curvature modes on superhorizon scales. For a geodesic trajectory ($\Omega = 0$), the curvature and isocurvature perturbations are decoupled. In this work we mainly focus on the weakly coupled regime, *i.e.* $\Omega/H \ll 1$. Another interesting result of the covariant formalism is the isocurvature mass, which in general can be expressed as

$$\mu^2 = V_{NN} + \frac{1}{2}\dot{\phi}^2\mathbb{R} + 3\Omega^2 \ . \tag{4.11}$$

Here the first term is the Hessian of the potential in the normal direction $V_{NN} = N^a N^b \nabla_a \nabla_b V$. For the turning trajectory along the θ direction, we simply get $V_{NN} = V''(\rho_0)$, which can be seen as the "bare" mass of the radial field, and is the one usually considered in QSFI. The second and third terms are the contributions from field space curvature and turning rate. Since we work in the weakly coupled regime with $\Omega \ll H$, thus the last term contribution can be neglected for $\mu^2 \sim \mathcal{O}(H^2)$.

The main focus of this paper is the second term in (4.11). This field space curvature contribution can be tracked back to the kinetic term of the the two-field system in (4.5). Naively speaking, when we derive the perturbed Lagrangian, the σ field mass has contributions from the second order expansion of $f(\rho)$, which is related to the Ricci scalar in (4.4). This is a unique correction in the quantum field theory with time-dependent background. Thus for inflation, it is always accompanied by the inflaton field velocity $\dot{\phi}^2$, whose magnitude can be estimated from the current observations[2]: $\dot{\phi}^2 \simeq 10^7 H^4$. Therefore unless the field space curvature is extremely small, the second term in (4.11) should not be neglected.

In the following we shall demonstrate in a case study that the field space curvature is typically associated with a new energy scale during in-

[2]In the weakly coupled regime of QSFI, since the massive field correction to the final power spectrum of ζ is small, the single field prediction $P_\zeta = H^4/(4\pi^2\dot{\phi}^2)$ remains valid approximately. Then from the observational result $P_\zeta \simeq 2\times10^{-9}$ [7], one gets $\dot{\phi}^2 \simeq 10^7 H^4$.

flation, and for natural choices of this scale, the curvature term in μ^2 can be comparable to or even larger than the V'' term.

4.2.2 A concrete example: inflation in coset space

In order to avoid the η-problem [20], the low-energy effective theories of inflation are usually supposed to be described by (pseudo-)Goldstone bosons protected by an (approximate) internal symmetry, such that the slow-roll potential is free from quantum corrections. Consequently the inflaton may roll in a *non-abelian coset space* G/H defined by the symmetry breaking pattern. While the details of a relevant project will be presented in a future paper [101], here let us look at two simplest cases of coset space with nontrivial geometries which have been considered before in Ref. [172, 173].

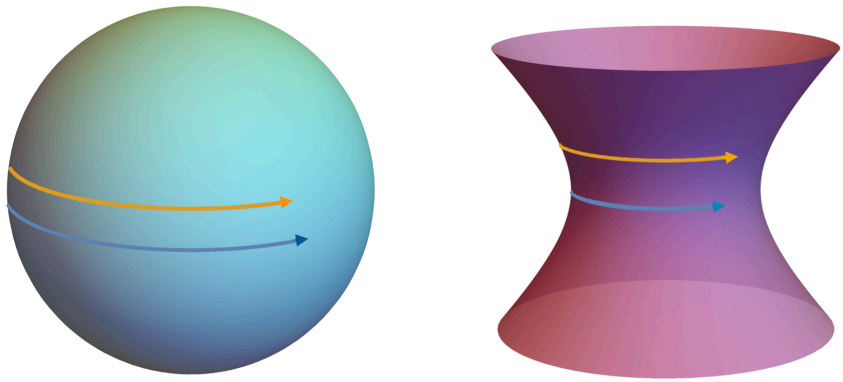

Figure 4.1: The $SO(3)/SO(2)$ (left) and $SO(2,1)/SO(2)$ (right) coset spaces, with the corresponding geodesic trajectories (blue curves) and examples of possible deviations (orange curves).

- $SO(3)/SO(2)$. This coset space is a 2d-sphere defined by $\phi_1^2+\phi_2^2+\phi_3^2 = R^2$ in the three-dimensional Euclidean space, where the constant R is the radius of the spherical surface. Thus it is convenient to use the spherical coordinates

$$\phi_1 = R\cos\varrho\cos\theta\ , \qquad \phi_2 = R\cos\varrho\sin\theta\ , \qquad \phi_3 = R\sin\varrho\ , \tag{4.12}$$

  where θ and ϱ are two Goldstone fields in the coset. As a result, the line element of this field space becomes $ds^2 = R^2\left(d\varrho^2+\cos^2\varrho d\theta^2\right)$. If we canonically normalize ϱ by redefining $\rho = R\varrho$, then the kinetic

term of the two Goldstones is expressed as

$$K = -\frac{1}{2}(\partial\rho)^2 - \frac{1}{2}R^2\cos^2\left(\frac{\rho}{R}\right)(\partial\theta)^2 \ , \tag{4.13}$$

which corresponds to the system in (4.5) with $f(\rho) = R^2\cos^2(\rho/R)$. This field space has a positive constant curvature with $\mathbb{R} = 2/R^2$.

- $SO(2,1)/SO(2)$. This non-compact coset yields a 2d-hyperbola defined by $\phi_1^2 + \phi_2^2 - \phi_3^2 = R^2$ in the three-dimensional Minkowski space, as shown in Fig. 4.1. We use the following field coordinates

$$\phi_1 = R\cosh\varrho\cos\theta \ , \quad \phi_2 = R\cosh\varrho\sin\theta \ , \quad \phi_3 = R\sinh\varrho \ . \tag{4.14}$$

Again the coset space is spanned by the Goldstone fields θ and ϱ, with the line element $ds^2 = R^2\left(d\varrho^2 + \cosh^2\varrho d\theta^2\right)$. Using the field redefinition $\rho = R\varrho$, we get the Goldstone kinetic term as

$$K = -\frac{1}{2}(\partial\rho)^2 - \frac{1}{2}R^2\cosh^2\left(\frac{\rho}{R}\right)(\partial\theta)^2 \ , \tag{4.15}$$

which has $f(\rho) = R^2\cosh^2(\rho/R)$. This is a hyperbolic space[3] with a negative constant curvature given by $\mathbb{R} = -2/R^2$.

As we see from these two examples, the Ricci scalar is determined by the radius R of the field space, which corresponds to the symmetry breaking scale in this setup. Now we take into account the motion of the inflaton by assuming a slow-roll potential which softly breaks the shift symmetry. Let us first consider the geodesic trajectories in these field spaces, which can be related to the spontaneous symmetry probing solutions discussed in Ref. [100].

In the $SO(3)/SO(2)$ coset, the geodesic is a trajectory along the maximal circle, as shown by the blue curve in the left panel of Fig. 4.1. Here without losing generality we take it to be the equator with $\rho = 0$, and the canonically normalized inflaton ϕ is driven by a slow-roll potential in the θ direction, with $\phi = R\theta$. If there is no explicit symmetry breaking for the ρ field, naively this Goldstone is supposed to be massless. However, because of the rolling of another Goldstone θ, the "not-rolling" Goldstone ρ acquires a mass [100]

$$m_\rho^2 = \dot{\theta}^2 = \frac{\dot{\phi}^2}{R^2} \ , \tag{4.16}$$

[3]One can connect this with the hyperbolic field space in α-attractors with $\mathbb{R} = -2/(3\alpha)$, and there α is related to the radius of curvature by $\alpha = R^2/3$.

which is exactly the second term in (4.11). From here we can explicitly see that, the curved field space contribution to the isocurvature mass is associated with the internal curvature scale. For $R \sim \dot{\phi}/H \simeq 3600H$, this contribution is $\mathcal{O}(H^2)$; while for $R \sim M_{\rm pl}$ it becomes slow-roll suppressed as $\sim \epsilon H^2$.

For the non-compact coset $SO(2,1)/SO(2)$, let us consider the inflaton trajectory that is also along the θ direction, then for the field space in (4.15) the geodesic motion is given by $\rho = 0$, which is the blue curve in the right panel of Fig. 4.1. Here the ρ field also acquires a similar mass correction from the rolling of the inflaton in the hyperbolic field space. But this is a tachyonic contribution $-\dot{\phi}^2/R^2$, since the field space curvature is negative. Thus to stabilize the isocurvature perturbation during inflation, one needs to break the shift symmetry and engineer a potential in the ρ direction.

Now we consider small deviations from the geodesics, for which $\Omega/H \ll 1$ and thus the curvature and isocurvature perturbations are weakly coupled. This can be easily achieved by perturbing the above geodesics away from the equator[4], such as the orange trajectories in Fig. 4.1. For the spherical space case, the trajectory is taken to be the latitude line $\rho = \delta$, where δ parametrizes the deviation. Then (4.7) yields $\Omega \simeq -(\delta/R)\dot{\theta}$ which can be much smaller than H for $\delta \ll R$. Similarly in the hyperbolic field space, a non-geodesic trajectory with $\rho = \delta$ yields $\Omega \simeq (\delta/R)\dot{\theta}$. Since these deviations from the geodesics are kept to be small, the field space curvature contribution to μ^2 discussed above remains valid. Therefore these isometry trajectories in the coset space provide simple realizations of QSFI with curved field manifold.

In summary, from the above example we identify that $\mathbb{R} \sim 1/R^2$, where the curvature radius R can be seen as the energy scale describing the curved field space geometry. Moreover, it may lead to significant contribution to the isocurvature mass

$$\mu^2 \simeq V''(\rho_0) + \frac{\dot{\phi}^2}{2}\mathbb{R} = V''(\rho_0) \pm \frac{\dot{\phi}^2}{R^2} \ , \tag{4.17}$$

which should not be neglected. For certain ranges of the curvature scale, this correction could be comparable to or even larger than the Hubble scale, which may dominate μ^2 in QSFI. As a result, the model predictions of QSFI

[4]A potential in the ρ direction is needed for this type of toy model trajectories. Here we keep agnostic about the specific form of the potential, and consider the consequences of this non-geodesics motion directly.

for primordial non-Gaussianities would be affected, which we shall explore in detail in Section 4.4.

Before concluding this section, we would like to mention another interesting observation: in (4.11) the second term $\dot{\phi}^2\mathbb{R}/2$ is *time-dependent* during inflation, since the inflaton field velocity $\dot{\phi}^2 = 2\epsilon H^2 M_{\rm pl}^2$ is evolving. Although it is a small effect, when the field space curvature contribution is non-negligible, we may expect running behaviour for the isocurvature mass, which we shall describe in detail at the end of the next section.

4.3 The EFT of background fields revisited

In this section we reexamine QSFI via the background EFT of inflation. Usually to achieve the slow-roll evolution and the nearly scale-invariant primordial perturbations, the inflaton field is believed to be protected by an (approximate) shift-symmetry. Based on this argument, one can construct the EFT of background fields for inflation without the knowledge of microphysical realizations [90], which provides a model-independent framework for studying physics in the primordial Universe.

Here we are mainly interested in the coupling between the extra-fields and the inflaton (denoted as φ in this section). Since the massive field ρ does not respect the shift symmetry, the leading contribution to the mixing between the inflaton and ρ is given by a dimension-five (dim-5) operator in the EFT expansion

$$\mathcal{L}^5_{\rm int} = -\frac{1}{2\Lambda_1}(\partial\varphi)^2\rho \ , \tag{4.18}$$

where Λ_1 is the cutoff scale. This operator, which has been elaborately investigated in the studies of QSFI and related topics [59, 93, 174, 175], is the leading order term in the EFT expansion. Realistically higher order terms should also be present. In the following we shall show how one could connect *the background EFT* with the *curved field space* in QSFI, and then focus on the role of a dimension-six (dim-6) operator

$$\mathcal{L}^6_{\rm int} = \pm\frac{1}{2\Lambda_2^2}(\partial\varphi)^2\rho^2 \ , \tag{4.19}$$

which can introduce the same effects as the field space curvature. The connection has also been noticed in geometrical destabilization [63], while in the current work we bridge the gap explicitly and highlight the generic effects for massive fields.

4.3.1 Bridging the background EFT with curved field spaces

Let us begin with the following EFT Lagrangian of two background fields

$$\mathcal{L}_m = -\frac{1}{2}\left(1 + c_1\frac{\rho}{\Lambda} + c_2\frac{\rho^2}{\Lambda^2}\right)(\partial\varphi)^2 - \frac{1}{2}(\partial\rho)^2 - \frac{1}{2}m^2\rho^2 - V_{\rm sr}(\varphi)\ . \quad (4.20)$$

where Λ is an overall cutoff for the dim-5 and dim-6 operators. The dimensionless coefficients c_1 and c_2 with $|c_{1,2}| \leqslant 1$ are introduced to represent their relative size and signs, thus $\Lambda_1 = \Lambda/c_1$ and $\Lambda_2 = \Lambda/\sqrt{|c_2|}$. Furthermore these two mixing operators are considered to be perturbative corrections to the single field slow-roll inflation, *i.e.* $\rho/\Lambda \ll 1$. Notice that the system has the same form with (4.5), while in the curved field space language these two operators yield a non-trivial field space metric function

$$f(\rho) = 1 + c_1\frac{\rho}{\Lambda} + c_2\frac{\rho^2}{\Lambda^2}\ . \quad (4.21)$$

Thus the EFT in (4.20) can be seen as the expansion of a curved manifold Lagrangian around a fixed trajectory with constant ρ. From (4.4) we also get the Ricci curvature as

$$\mathbb{R} \simeq -\frac{2c_2 - c_1^2/2}{\Lambda^2} + \mathcal{O}\left(\frac{\rho}{\Lambda}\right)\ . \quad (4.22)$$

As we see, since the curvature contains the second order derivative of the metric, the dim-6 operator will play a role here in general.

First let us look at the background dynamics. The EoM of the ρ field, which is the centrifugal force equation in (4.8), yields the stabilized value for the massive field at $\rho = \rho_0$[5]

$$\frac{1}{2}\left(c_1\frac{1}{\Lambda} + 2c_2\frac{\rho_0}{\Lambda^2}\right)\dot\varphi^2 = m^2\rho_0 \quad \Rightarrow \quad \frac{\rho_0}{\Lambda} = \frac{c_1}{2}\frac{\dot\varphi^2/\Lambda^2}{m^2 - c_2\,(\dot\varphi^2/\Lambda^2)}\ . \quad (4.23)$$

To ensure the validity of EFT, one needs $\rho_0/\Lambda \ll 1$. Then the canonically normalized inflaton is just $\phi = f(\rho_0)\varphi$ with $f(\rho_0) \simeq 1$. Also there is a turning rate given by[6]

$$\Omega^2 \simeq \frac{1}{4}\left(c_1 + 2c_2\frac{\rho_0}{\Lambda}\right)^2\frac{\dot\varphi^2}{\Lambda^2} + \mathcal{O}\left(\frac{\rho_0}{\Lambda}\right)\ , \quad (4.24)$$

[5]Note here ρ_0 depends on the inflaton velocity, thus strictly speaking it is not a constant. See Ref. [81, 82] for models with exactly constant ρ_0.

[6]In the expansion we also consider the possibility for a hierarchy between c_1 and c_2, such as $c_1 \sim c_2(\rho_0/\Lambda)$.

thus the curvature and isocurvature perturbations are coupled at the linear level. The weak coupling condition $\Omega/H \ll 1$ here implies that $|c_1 + 2c_2(\rho_0/\Lambda)|(\dot{\varphi}/\Lambda) \ll 2H$. The isocurvature mass follows from (4.11) as

$$\begin{aligned}\mu^2 &\simeq m^2 + \left[c_1^2 - c_2 + 3c_2^2\left(\frac{\rho_0}{\Lambda}\right)^2 + 3c_1c_2\left(\frac{\rho_0}{\Lambda}\right)\right]\left(\frac{\dot{\varphi}}{\Lambda}\right)^2 \\ &\simeq m^2 + \left(\frac{c_1^2}{4} - c_2\right)\left(\frac{\dot{\varphi}}{\Lambda}\right)^2, \end{aligned} \tag{4.25}$$

where in the second approximation the weak coupling condition is used. Here the ρ field "bare" mass m^2 gets corrections from the mixing operators due to the time-dependent background of the inflaton field.

Now we comment on the role of the dim-5 operator. At the background level, this operator contains a tadpole for ρ which contributes to stabilize the massive field . If we switch it off by setting $c_1 = 0$, the centrifugal force equation (4.23) yields $\rho_0 = 0$ and the trajectory becomes a geodesic with $\Omega = 0$. Thus this operator is important for the non-geodesic motion of the inflaton, and leads to the mixing between curvature and isocurvature perturbations. Also it contributes to the left diagram in Fig. 4.2 for the scalar bispectrum in QSFI, thus its size can be related to the amplitude of the non-Gaussian signals. Meanwhile the cutoff scale of this operator is constrained in the weakly coupled regime. If we turn off the dim-6 operator by setting $c_2 = 0$, the weak coupling condition $|c_1|(\dot{\varphi}/\Lambda) \ll 2H$ yields a lower bound on $\Lambda_1 = \Lambda/c_1$. As a result, the dim-5 operator itself gives negligible corrections to the isocurvature mass which simply reduces to the "bare" one $\mu^2 \simeq m^2$.

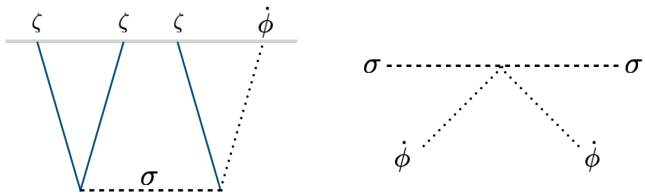

Figure 4.2: Different roles of dim-5 and dim-6 operators shown in Feynman diagrams.

4.3.2 On the role of the dimension-6 operator

As a next-to-leading order correction, usually the dim-6 operator in (4.19) is supposed to be sub-dominant. For instance, it contributes to the scalar bis-

pectrum through loop diagrams, which turns out to be negligible [59, 160]. But as discussed above (and also pointed out in Ref. [63, 160, 176] previously), this operator may give nontrivial corrections to the isocurvature mass. One can interpret this effect by the right diagram in Fig. 4.2, where the two inflaton legs are taken to be the background, and then the extra field get mass corrections through this operator.

To show its effects explicitly, let us consider the situation where the massive field enjoys an approximate $\mathbb{Z}_2$ symmetry, such that the coefficients of two mixing operators satisfy

$$|c_1| \ll |c_2| = 1. \tag{4.26}$$

Thus the overall cutoff scale Λ coincides with the one for the dim-6 operator Λ_2, and there is a hierarchy: $\Lambda_1 \gg \Lambda_2$. The Ricci scalar becomes $\mathbb{R} \simeq -2c_2/\Lambda^2$. In the curved field space analogy, this case corresponds to the small deviations from the equator ($\rho = 0$) in the coset space discussed in Section 4.2.2. For instance, in the $SO(3)/SO(2)$ system (4.13), suppose the massive field is stabilized around $\rho = \rho_b \ll R$ by a potential $V(\rho) = m^2(\rho - \rho_b)^2/2$. If we look at a local patch of the spherical surface around the latitude $\rho = \rho_b$, then the metric function there can be expanded as

$$R^2 \cos^2\left(\frac{\rho}{R}\right) = R^2\left[1 - 2\frac{\rho_b}{R}\frac{\rho - \rho_b}{R} - \frac{(\rho - \rho_b)^2}{R^2}\right] + ... \tag{4.27}$$

By redefining $\rho - \rho_b \to \rho$ and $R\theta \to \varphi$, we recover the EFT Lagrangian in (4.20) with $\Lambda = R$, $c_1 = -2\rho_b/R$ and $c_2 = -1$. Similarly the $SO(2,1)/SO(2)$ example can also be formulated into the Background EFT language, with $\Lambda = R$ as well, but $c_1 = 2\rho_b/R$ and $c_2 = 1$ instead. As we see here, *the cutoff scale* Λ *of the dim-6 operator plays the role of the curvature scale of the field space*, while the sign of c_2 denotes if it is positively or negatively curved.

The background dynamics of this hierarchical system follows directly. Because of the small but nonzero dim-5 operator, the massive field gets deviated from the potential minimum by the centrifugal force (4.23). Since $|c_1| \ll 1$, we find it easy to guarantee $\rho_0/\Lambda \ll 1$, and thus the EFT description is justified. Notice that, while the size of the dim-5 operator is still constrained by the weak coupling condition, there is more freedom for the cutoff scale of the dim-6 operator. One particularly interesting regime for QSFI is for $\dot{\varphi}^2/\Lambda^2 \sim H^2$, which corresponds to $\Lambda \sim 3000H$ by considering $\dot{\varphi}^2 \simeq \dot{\phi}^2 \simeq 10^7 H^4$. The isocurvature mass becomes

$$\mu^2 \simeq m^2 - c_2 \left(\frac{\dot{\varphi}}{\Lambda}\right)^2 = m^2 - 2c_2\epsilon H^2 \left(\frac{M_{\rm pl}}{\Lambda}\right)^2 \ , \tag{4.28}$$

where in the second equality we introduced the slow-roll parameter ϵ. The second term, which represents the contribution from the dim-6 operator, can be comparable with (or even larger than) the "bare" mass m^2, and thus should not be neglected. This expression has the same form with (4.17) in terms of the field space curvature. Thus for $c_2 = 1$, this correction is negative, which is equivalent to the hyperbolic field space case; while $c_2 = -1$ makes the massive field heavier and corresponds to the positively curved field space.

Moreover, as we briefly mentioned at the end of Section 4.2, this correction to μ^2 is time-dependent due to the rolling behaviour of the inflaton[7]. Now let us formulate the running behaviour of the isocurvature mass more specifically. If we consider the evolution of ϵ from the time denoted by the number of e-folds N_l, then as long as $N - N_l$ is not too big we have

$$\epsilon(N) \simeq \epsilon(N_l) + \epsilon'(N_l)(N - N_l) = \epsilon_l \left[1 + \eta_l (N - N_l)\right] , \tag{4.29}$$

with $\epsilon_l = \epsilon(N_l)$ and $\eta_l = \eta(N_l)$. Correspondingly the time dependence of μ^2 in (4.28) can be parametrized as

$$\mu^2(N) = \mu_l^2 + \lambda(N - N_l)H^2 \ , \tag{4.30}$$

where $\mu_l^2 = m^2 - 2c_2\epsilon_l H^2 (M_{\rm pl}/\Lambda)^2$ is the isocurvature mass at the time of N_l, and λ is the running parameter expressed in both the curved field space and the EFT languages as

$$\lambda = \eta_l \frac{\dot{\phi}^2}{2H^2}\mathbb{R} = -\eta_l \frac{c_2}{H^2}\frac{\dot{\varphi}^2}{\Lambda^2} \ . \tag{4.31}$$

As expected, typically the time-dependence is small and suppressed by η_l. We estimate the size of λ in the conformal limit of inflation $\epsilon \ll \eta$ [177]. This hierarchy between slow-roll parameters[8] is indicated by the observational

[7] This is similar to what happens for geometrical destabilization [63], where the running isocurvature mass with negative $\mathbb{R}$ may lead to tachyonic instability, which ends inflation prematurely or initiates a sidetracked phase [66, 83]. Here instead of $\mu^2 < 0$, we are interested in both the positive- and negative-running behaviour in the stable (QSFI) regime with $\mu^2 \sim \mathcal{O}(H^2)$, and mainly focus on its effects on the large-scale modes which can be probed by CMB or LSS surveys.

[8] It can be achieved by taking $V_{\rm sr}(\varphi)$ to be the plateau-like potentials, such as Starobin-

upper bound on the tensor-to-scalar ratio $r = 16\epsilon < 0.064$ and the observed value of the scalar tilt $n_s = 1 - \eta - 2\epsilon = 0.9649 \pm 0.0042$ [7], which also yields $\eta \simeq 0.035$. Then the running parameter in (4.31) is mainly controlled by the cutoff scale Λ. For $\Lambda \sim 3000H$, and thus $\dot{\varphi}^2/(H^2\Lambda^2) \sim \mathcal{O}(1)$, we get $|\lambda| \lesssim 0.1$. In principle a larger running can be achieved by lowering Λ, but then for the interest of QSFI one may need fine tune the correction in (4.28) against the "bare" mass such that $\mu^2 \sim \mathcal{O}(H^2)$.

4.4 Phenomenology of the running isocurvature mass

With the above analysis of massive fields living in curved field space, the goal of this section is to investigate the phenomenological consequences of a nontrivial field space curvature in QSFI, and focus on the effects of the running isocurvature mass.

First of all, let us briefly review the phenomenology of QSFI. To characterize primordial non-Gaussianity, the bispectrum of curvature perturbation is usually defined as

$$\langle \zeta_{\mathbf{k_1}} \zeta_{\mathbf{k_2}} \zeta_{\mathbf{k_3}} \rangle \equiv (2\pi)^3 \delta^{(3)}(\mathbf{k_1} + \mathbf{k_2} + \mathbf{k_3}) B_\zeta(k_1, k_2, k_3) \ . \tag{4.32}$$

We are particularly interested in the squeezed configurations of the momentum triangles formed by two short modes $k_1 = k_2 = k_s$ and one long mode $k_3 = k_l$, with $k_l \ll k_s$. One of the most interesting results in QSFI is that, the scaling behaviour of the bispectrum in this squeezed limit is uniquely determined by the isocurvature mass as follows [57, 58, 154]

$$\lim_{k_l \ll k_s} B_\zeta \propto \frac{1}{k_l^3 k_s^3} \left(\frac{k_l}{k_s}\right)^{3/2-\nu} \quad \text{for} \quad \mu < \frac{3H}{2} \tag{4.33}$$

$$\lim_{k_l \ll k_s} B_\zeta \propto \frac{1}{k_l^3 k_s^3} \left(\frac{k_l}{k_s}\right)^{3/2} \cos\left[\nu \ln\left(\frac{k_l}{k_s}\right) + \delta_\nu\right] \quad \text{for} \quad \mu > \frac{3H}{2} \tag{4.34}$$

where the scaling index ν is a function of the isocurvature mass

$$\nu = \sqrt{\frac{9}{4} - \frac{\mu^2}{H^2}} \ , \tag{4.35}$$

and δ_ν is a phase factor depending on ν. Here $\mu = 3H/2$ is the critical mass which divides the isocurvature mass spectrum into light and heavy regimes.

sky inflation [3] and α-attractors [17, 18, 73, 74], where the slow-roll parameters evolve as $\epsilon \sim 1/N^2$ and $\eta \simeq 2/N$.

Notice that in our notation, $0 < \nu < 3/2$ for $\mu < 3H/2$, and it becomes imaginary when $\mu > 3H/2$. Therefore through this observational channel of non-Gaussianities, one can measure the mass of the additional field in a model-independent manner.

Intuitively, the above scaling can be understood from the superhorizon behaviour of the massive field [58]. During inflation, the EoM of the isocurvature mode is

$$\sigma_k'' + \frac{k^2}{a^2H^2}\sigma_k + 3\sigma_k' + \frac{\mu^2}{H^2}\sigma_k = 0 \ , \tag{4.36}$$

where primes denote derivatives with respect to the number of e-folds N. For QSFI, we are mainly interested in the regime $\mu/H \sim \mathcal{O}(1)$. Thus on the superhorizon scales ($k \ll aH$), the second term is sub-dominant compared with the mass term. Approximately the EoM above becomes the one for a damped oscillator $\sigma_k'' + 3\sigma_k' + (\mu^2/H^2)\sigma_k \simeq 0$, and for a constant μ^2 it has two decaying solutions

$$\sigma_k(N) \propto e^{-(3/2\pm\nu)(N-N_k)} \ . \tag{4.37}$$

Here N_k is the e-folds when σ_k mode exits the horizon. For the light field case ($\mu < 3H/2$), the solution with minus sign dominates, and it corresponds to the underdamped decay. For the heavy field case ($\mu > 3H/2$), the imaginary ν leads to the overdamped oscillations. Now we consider the modulation of a long wavelength mode (k_l) on the short wavelength modes (k_s). Suppose that the k_l-mode exits the horizon at N_l, then later when the k_s-modes exit the horizon at N_s, the amplitude of the k_l-mode already decays by

$$\sigma_{k_l}(N_s) = \sigma_{k_l}(N_l)e^{-(3/2\pm\nu)(N_s-N_f)} = \sigma_{k_l}(N_l)\left(\frac{k_l}{k_s}\right)^{3/2\pm\nu} \ , \tag{4.38}$$

where in the second equality $e^{N_s-N_f} = k_s/k_l$ is used. As a result, the modulation of the long wavelength mode on the k_s modes will inherit this decayed amplitude. When $\mu < 3H/2$, the decaying solution with minus sign gives the power-law scaling in (4.33). While for $\mu > 3H/2$, ν is imaginary and the scaling can be written into the oscillatory form in (4.34).

For QSFI with curved field space, we first notice that the scaling behaviour of the squeezed bispectrum is determined by the full isocurvature mass. Thus when the field space curvature contribution to μ^2 is significant, what we measure in the non-Gaussianity observation is no longer the "bare"

mass of the additional field, since the scaling index ν in (4.35) is changed by this nontrivial mass correction[9]. It is also possible that in μ^2 the dominant contribution comes from the field space curvature term. For instance, in the example of inflation in coset space discussed in Section 4.2.2, the Goldstone field in the normal direction of the inflaton trajectory has a zero "bare" mass, but can still become massive due to the curved field space effect. In this sense the QSFI predictions based on the "bare" mass will be corrected, though it is difficult to distinguish these two mass contributions from each other. However, the time-dependence of the field space curvature term may break the degeneracy, which we shall study in the rest of this section.

Let us take the parametrization in (4.30) as our starting point. Before horizon-exit, since in (4.36) the second term dominates, the evolution of σ_k is barely affected by the running mass. Thus the conventional mode function with a Bunch-Davies initial condition provides a good description. This is also shown in the shaded regions of Figs. 4.3 and 4.4, where the full numerical solutions with running mass agree with dashed grey curves very well in the subhorizon regime. But the superhorzion evolution of σ_k differs from the conventional case with a constant mass. For simplicity, we define a rescaled mode function as

$$\widetilde{\sigma}_k = e^{3N/2}\sigma_k \ . \tag{4.39}$$

Then for the k_l mode which exits the horizon at e-folds N_l, the superhorizon EoM can be approximately written into the following form

$$\widetilde{\sigma}''_{k_l} - \left[\nu_l^2 - \lambda(N - N_l)\right]\widetilde{\sigma}_{k_l} = 0 \ , \tag{4.40}$$

where the scaling index at N_l is given by the isocurvatue mass at that time $\nu_l^2 = 9/4 - \mu_l^2/H^2$. This equation has the following analytical solution with two Airy functions

$$\widetilde{\sigma}_{k_l} = C_1 \mathrm{Ai}\left[\frac{\nu_l^2 - \lambda(N - N_l)}{(-\lambda)^{2/3}}\right] + C_2 \mathrm{Bi}\left[\frac{\nu_l^2 - \lambda(N - N_l)}{(-\lambda)^{2/3}}\right] \ , \tag{4.41}$$

where C_1 and C_2 are two integration constants determined by the initial condition. In the following we shall explore the behaviour of this solution in three different regimes, and their modification on the scaling of the squeezed bispectrum.

[9]Similar correction has been noticed in the context of cosmological colliders as a contamination [157, 158].

4.4.1 Running in the $\mu < 3H/2$ regime

First, let us look at the situation where the isocurvature mass is running in the $\mu < 3H/2$ regime, which means $\nu_l^2 - \lambda(N - N_l) > 0$. Since μ^2 varies slowly, in most cases the EoM (4.40) can be solved by the WKB approximation. More specifically the adiabatic condition here is given by

$$\nu_l^2 - \lambda(N - N_l) \gg (|-\lambda|)^{2/3} \ . \tag{4.42}$$

This breaks down when the isocurvature mass is running close to $3H/2$, which we leave for consideration in Section 4.4.3. Then the first order WKB solution of the rescaled mode function follows as

$$\widetilde{\sigma}_k(N) = \frac{\widetilde{\sigma}_k(N_l)}{\left[1 - \frac{\lambda}{\nu}(N - N_1)\right]^{1/4}} \exp\left(\int_N^N \sqrt{\nu_l^2 - \lambda(N' - N_l)}\, dN'\right) \ , \tag{4.43}$$

where

$$\int_N^N \sqrt{\nu_l^2 - \lambda(N' - N_l)}\, dN' \ = \ \frac{2}{3}\frac{1}{\lambda}\nu_l^3 - \frac{2}{3}\frac{1}{\lambda}\left[\nu_l^2 - \lambda(N - N_l)\right]^{3/2} . \tag{4.44}$$

We can get the same solution by taking the asymptotic expansion of Airy functions in Eq. (4.41). The evolution of the rescaled mode function is shown in the left panel of Fig. 4.3 for the negative running case, and in the left panel of Fig. 4.4 (the first 10 e-folds there) for $\lambda > 0$. We see that, the WKB solutions agree with the full numerical results of Eq. (4.36). Moreover, on superhorizon scales, they deviate from the results with constant masses, and thus are expected to modify the scaling behaviour in the squeezed bispectrum.

To show the phenomenological effects more explicitly, we further consider the situation with $\nu_l^2 \gg |\lambda(N - N_l)|$, then the series expansion of (4.44) yields

$$\nu_l \cdot (N - N_l) - \frac{1}{4\nu_l}\lambda(N - N_l)^2 + ... \tag{4.45}$$

Then the superhorizon decay of the isocurvature mode function is approximately given by

$$\sigma_{k_l}(N) = \sigma_{k_l}(N_l) e^{-(3/2-\nu_l)(N-N_l) - \frac{1}{4\nu_l}\lambda(N-N_l)^2} \ . \tag{4.46}$$

Therefore one can easily get its amplitude at N_s when the short wavelength modes exit the horizon. Similar with the situation in (4.38), the long mode modulation yields the squeezed limit accordingly, and here the scaling is modified to be

$$\lim_{k\ll k} B_\zeta \propto \frac{1}{k_l^3 k_s^3}\left(\frac{k_l}{k_s}\right)^{3/2-\nu+\alpha\,\ln(k/k)} , \quad \text{with } \alpha_\nu \equiv \frac{\lambda}{4\nu_l} = \frac{1}{4\nu_l}\epsilon_l M_{\rm pl}^2 \mathbb{R}\cdot\eta_l . \tag{4.47}$$

We notice that the running index α_ν leads the bispectrum to interpolate between the scalings given by the mass μ_l and the mass $\mu(N_s)$. When the curvature is positive, μ^2 increases and $\alpha_\nu > 0$. If we fix k_l, then for small k_s the bispectrum is closer to the local shape, and it moves towards the equilateral scaling when k_s increases. For negative $\mathbb{R}$, the running of the scaling index with k_s would be the opposite.

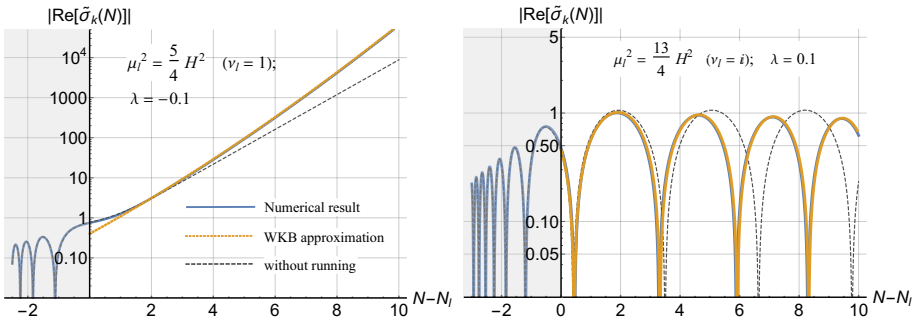

Figure 4.3: The evolution of the rescaled isocurvature mode function for cases with: negative-running mass in the $\mu < 3H/2$ regime (left panel) and positive-running mass in the $\mu > 3H/2$ regime (right panel). In both figures, the blue curves are the full numerical solutions of $\tilde{\sigma}_k$, the orange dotted lines are the WKB approximation on superhorizon scales, and the dashed grey lines are the solutions with constant masses ($\lambda = 0$). The shaded parts correspond to the subhorizon regime.

4.4.2 Running in the $\mu > 3H/2$ regime

Next we turn to study the heavy field case. In this regime, ν_l is imaginary and the running isocurvature mass satisfies $\nu_l^2 - \lambda(N - N_l) < 0$. Similarly we take the WKB approximation and leave its violations for the next subsection, while here the adiabatic condition becomes

$$|\nu_l^2 - \lambda(N - N_l)| \gg (|-\lambda|)^{2/3} . \tag{4.48}$$

Under this, (4.40) yields the following oscillating WKB solutions

$$\widetilde{\sigma}_k(N) \to \frac{C_\pm}{|\nu_l^2 - \lambda(N - N_1)|^{1/4}} \exp\left(\pm i \int_N^N \sqrt{|\nu_l^2 - \lambda(N - N_l)|}\, dN\right) , \tag{4.49}$$

whose real part can be further simplified into

$$\mathrm{Re}\,\widetilde{\sigma}_k(N) \propto \frac{1}{\left|\nu_l^2-\lambda(N-N_1)\right|^{1/4}}\,\cos\left[i\frac{2}{3\lambda}\left|\nu_l^2-\lambda(N-N_l)\right|^{3/2}-i\frac{2\nu_l^3}{3\lambda}+\delta_l\right]\,. \tag{4.50}$$

Here δ_l depends on ν_l and the initial conditions. Again this can also be obtained by taking the asymptotic expansion of Eq. (4.41). The result of the positive running mass is in the right panel of Fig. 4.3, and the right panel of Fig. 4.4 (the first 7 e-folds there) shows the ones for the negative running mass. We find good agreement with numerical results. As we can see, the positive running decreases the oscillation period while the negative running increases it. This can be shown more clearly if we take $|\nu_l|^2 \gg |\lambda(N-N_l)|$ and expand the above solution. The superhorizon isocurvature mode function follows as

$$\mathrm{Re}\,\sigma_k(N) \propto e^{-\frac{3}{2}(N-N)}\cos\left[i\nu_l(N-N_l)\left(1-\frac{\lambda}{4\nu_l^2}(N-N_l)\right)+\delta_l\right]\,. \tag{4.51}$$

Again considering its modulation on the k_s-mode at N_s, we get the following scaling behaviour in the squeezed bispectrum

$$\lim_{k\ll k} B_\zeta \propto \frac{1}{k_l^3 k_s^3}\left(\frac{k_l}{k_s}\right)^{3/2}\cos\left[i\nu_l\ln\left(\frac{k_l}{k_s}\right)-i\alpha_\nu\ln^2\left(\frac{k_l}{k_s}\right)+\delta_l\right]\,,\ \text{with}\ \alpha_\nu\equiv\frac{\lambda}{4\nu_l}\,. \tag{4.52}$$

Notice here like ν_l, the running index α_ν is also imaginary and can be expressed as $\alpha_\nu = -i\epsilon_l M_{\rm pl}^2\mathbb{R}\cdot\eta_l/(4|\nu_l|)$. Therefore due to the field space curvature, the oscillatory signal in the heavy field regime of QSFI would also be modified.

4.4.3 Running through $\mu = 3H/2$

Now we consider the situation where the WKB approximation breaks down. This corresponds to the cases when the isocurvature mass runs through $\mu = 3H/2$, and thus $\nu_l^2 - \lambda(N-N_l) \simeq 0$.

Let us first take a look at the numerical results in Fig. 4.4. For a positive λ, the isocurvature field runs from the light field regime to the heavy field regime, and the superhorizon behaviour of σ_k demonstrates a smooth transition from the overdamped decay to the underdamped oscillation (left panel). On the other hand, for the negative running, μ^2 drops below the critical mass, and then the mode function transits from the oscillatory form to the exponential decay (right panel).

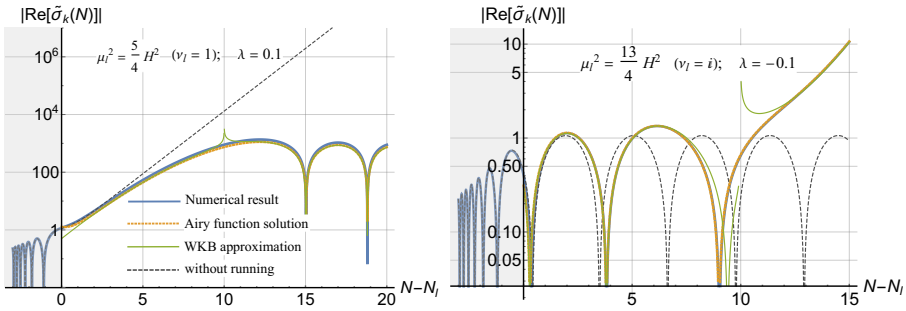

Figure 4.4: The evolution of the rescaled isocurvature mode function for cases with: positive-running mass from $\mu < 3H/2$ to $\mu > 3H/2$ (left panel) and negative-running mass from $\mu > 3H/2$ to $\mu < 3H/2$ (right panel). In both figures, the blue curves are the full numerical solutions of $\tilde{\sigma}_k$, the orange dotted lines are the superhorizon solutions using Airy functions, the WKB approximations are given by the green curves, and the dashed grey lines describe the evolution with constant masses ($\lambda = 0$). The shaded parts correspond to the subhorizon regime.

We can clearly see that the WKB solution becomes invalid when the mass runs close to $3H/2$. However, the analytical solutions (4.41) with two Airy functions still holds true in this transition regime, and provides a good description for the mode function. It is also interesting to notice that, the mathematics describing the transition between underdamped decay and overdamped oscillation is the same with the semi-classical approximation in quantum mechanics [178], where the wave function is oscillating in the classically allowed region and decaying in the tunnelling regime. Therefore the critical mass $\mu = 3H/2$ here can be seen as a "turning point" where the WKB approximation cannot be valid.

For the squeezed limit of the bispectrum, this transition behaviour of the superhorizon mode function may leave distinct imprints, with a combination of power-law and oscillatory signals. Thus in this case, the deviation from the standard QSFI predictions could be large, and can be seen as a new template for the squeezed bispectrum. But for detectability, we need to be lucky such that the transition behaviour just occurs for the perturbation modes that correspond to our observational window. Or it is also possible that, future observations for different scales may help us to find the hint of this signature. For instance, if an oscillatory signal is detected by large scale experiments (such as CMB), while we observe power-law scaling of the squeezed bispectrum on small scales (such as LSS and CMB distortions), then it would indicate a negative running isocurvature mass caused by a hyperbolic-type field space.

In summary, the running of the isocurvature mass leads to the running in the scaling of the squeezed bispectrum, and the running index α_ν measures the curvature of the field space. With the above analysis, we close this section by giving two final remarks:

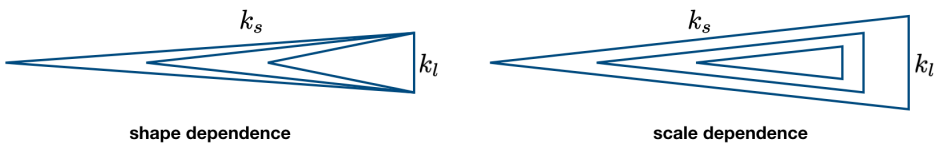

Figure 4.5: Two types of squeezed configurations of momentum triangles. The bispectrum may only depend on the shapes (left), or there is dependence on the size as well (right).

Shape-dependence & scale-dependence. In the standard QSFI with constant mass, one interesting fact is that, although the squeezed limit depends on the ratio of k_l/k_s, the full bispectrum is still scale-invariant. That is to say, if we rescale three momenta but keep their ratio fixed, which corresponds to the transformation to a similar triangle, then the bispectrum remains unchanged. Meanwhile the nontrivial scaling behaviour in (4.33) and (4.34) can be seen as a function of the various squeezed configurations. For instance, if we fix the long wavelength mode k_l, and let k_s vary, the bispcetrum becomes different. Thus this result is shape-dependent. For a running isocurvature mass, as we can see from (4.47) and (4.52) the shape dependence remains. Furthermore the bispectrum here also becomes scale-dependent. If we rescale three wavenumbers together, for instance $k_l \to \kappa k_l$ and $k_s \to \kappa k_s$, then the new scaling index ν_κ should be determined by the μ_κ^2 when the rescaled long wavelength mode κk_l exits the horizon

$$\nu_\kappa = \sqrt{\frac{9}{4} - \frac{\mu_\kappa^2}{H^2}} \simeq \nu_l - \frac{\lambda}{2\nu_l}(N_\kappa - N_l) \ . \tag{4.53}$$

Notice that the scale-dependent running index here $\tilde{\alpha}_\nu \equiv d\nu_l/(dN) = -\lambda/(2\nu_l)$ differs from the ones parametrizing shape-dependence in (4.47) and (4.52). This is because, a running isocurvature mass would continuously affect the superhorizon evolution of σ_{k_l}, which plays an important role for the shape-dependence; while the scale-dependence is controlled by the mass at different times, thus the running can be simply obtained by taking derivative of μ^2.

Implications on the scale-dependent bias. In the LSS observations, the halo overdensity δ_h tracing galaxy distribution and the dark matter density

contrast δ_m are related by the bias b through $\delta_h = b\delta_m$. It has been shown that, signals in the squeezed limit of the primordial scalar bispectrum can lead to a scale-dependent component in the bias $b^{\rm NG}$, which becomes dominant on large scales [179, 180] (see Ref. [181] for a recent review). Thus this scale-dependent halo bias provides an observational opportunity for the detection of the modified scaling behaviour studied above. In the conventional QSFI models, the scaling signals in (4.33) and (4.34) respectively imply $b^{\rm NG}(k) \propto k^{-1/2-\nu}$ and $b^{\rm NG}(k) \propto k^{-1/2}\cos(i\nu \ln k)$. Accordingly the squeezed bispectra with running in (4.47) and (4.52) yield

$$b^{\rm NG}(k) \propto k^{-1/2-\nu-\alpha\,\ln k} \quad \text{and} \quad b^{\rm NG}(k) \propto k^{-1/2}\cos(i\nu_l \ln k - i\alpha_\nu \ln^2 k)\ , \tag{4.54}$$

which suggests that, besides ν, the running index α_ν can also be set as a free parameter for the data analysis of future LSS surveys.

4.5 Conclusion and discussion

In this paper we explore the implications of nontrivial internal spaces in the context of inflationary massive fields. Here QSFI is generalized to curved field manifold, and then analyzed by using both the multi-field techniques and the background EFT approach. Through the multi-field analysis, we show that the field space curvature could contribute significantly to the isocurvature mass in QSFI, thus modify its predictions on non-Gaussianity. Meanwhile the same result is also derived in the EFT of the background fields, where a dim-6 operator is identified to generate the same effects as the curved field space. We build the connection between these two different but equivalent approaches, and further demonstrate that the cutoff scale of the dim-6 operator is associated with the curvature scale of the field space.

Moreover, as a result of the slow-roll dynamics of the inflaton field, the field space curvature contribution to the isocurvature mass is time-dependent in nature. We perform the first analysis on phenomenological consequences of the running isocurvature mass, and find new features in the scaling of the squeezed scalar bispectrum. Besides the power-law and oscillatory signals of QSFI in the light and heavy mass regimes, the time-dependence of the isocurvature mass leads to running behaviour in the squeezed scaling. If the field space is positively curved, the isocurvature mass increases, which leads to the positive running in the squeezed scaling. While for the field space with negative curvature, the running becomes negative. Also a transition signal between the power-law and oscillatory scalings is discovered when the mass runs through $\mu = 3H/2$. These modifications to the previous results of QSFI provide new templates for detecting

primordial non-Gaussianity. Therefore in future observations, through the precise measurement of running behaviours in the squeezed bispectrum, we may be able to probe the geometry of the internal field space during inflation.

This work can also be seen as the first step towards several possible directions for future research. First of all, it is interesting to study the implications on cosmological collider physics [59]. Our results indicate that, due to the time-dependent background of the inflaton field, higher dimension operators may become non-negligible for the collider signals. While the current work can be directly applied to heavy scalar particles, it is worth investigating similar effects of particles with spins, whose "bare" mass may also be corrected by higher order EFT operators mixing with the inflaton.

Next, considering that one of our main motivations is to probe field space curvature during inflation model-independently, the current results are not sufficiently general and unique yet. For instance, in principle it is possible to engineer other models of QSFI with running isocurvature mass, which would lead to similar phenomenology degenerate with the geometrical effects[10]. Thus we are encouraged to explore the truly unique signatures of the curved field space with more generalities.

Finally, the running scaling signals in the squeezed limit of the scalar bispectrum have implications for observations, which deserve a closer look. For example, the observability of these signals and the fitting of the running index using CMB and LSS data remain to be investigated.

[10]The analysis of the time-dependent isocurvature mass starting from the parametrization (4.30) can be seen as an independent part of this paper, which is also of phenomenological interest in contexts beyond curved field space. Though one may wonder if other constructions are as simple and natural as the one considered here.

Tracing primordial triangles

5 Revisiting non-Gaussianity from non-attractor inflation

Abstract: Non-attractor inflation is known as the only single field inflationary scenario that can violate non-Gaussianity consistency relation with the Bunch-Davies vacuum state and generate large local non-Gaussianity. However, it is also known that the non-attractor inflation by itself is incomplete and should be followed by a phase of slow-roll attractor. Moreover, there is a transition process between these two phases. In the past literature, this transition was approximated as instant and the evolution of non-Gaussianity in this phase was not fully studied. In this paper, we follow the detailed evolution of the non-Gaussianity through the transition phase into the slow-roll attractor phase, considering different types of transition. We find that the transition process has important effect on the size of the local non-Gaussianity. We first compute the net contribution of the non-Gaussianities at the end of inflation in canonical non-attractor models. If the curvature perturbations keep evolving during the transition - such as in the case of smooth transition or some sharp transition scenarios - the $\mathcal{O}(1)$ non-Gaussianity generated in the non-attractor phase can be completely erased by the subsequent evolution, although the consistency relation remains violated. In extremal cases of sharp transition where the super-horizon modes freeze immediately right after the end of the non-attractor phase, the original non-attractor result can be recovered. We also study models with non-canonical kinetic terms, and find that the transition can typically contribute a suppression factor in the squeezed bispectrum, but the final local non-Gaussianity can still be made parametrically large.

Keywords: Inflation, primordial non-Gaussianity, cosmological perturbation theory

Based on:

Y.-F. Cai, X. Chen, M. H. Namjoo, M. Sasaki, D.-G. Wang, Z. Wang
Revisiting non-Gaussianity from non-attractor inflation models
JCAP 1805 (2018), no. 05 012, [arXiv:1712.09998].

5.1 Introduction

Inflationary cosmology is the leading paradigm of the very early universe [1–6], in which the universe has experienced a primordial phase of quasi-de Sitter expansion. The simplest inflation model is realized by a canonical scalar field slowly rolling along a sufficiently flat potential. The associated perturbation theory successfully predicted a nearly scale-invariant power spectrum of primordial curvature perturbation, which is favoured by the latest cosmic microwave background (CMB) observations [108, 182]. Moreover, it is widely acknowledged that the primordial non-Gaussianity, which encodes information about the very early universe, could be a powerful tool to discriminate different inflation models or alternative scenarios [35–38]. Remarkably, there is a consistency relation for non-Gaussianity in single-field slow-roll inflation models pointed out by Maldacena [39, 40]. The consistency relation states that the amplitude of the primordial non-Gaussianity in squeezed configuration - where the wavelength of one mode is much larger than the other two in the three point correlation fucntion - is proportional to the spectral index of the power spectrum of scalar perturbations, *i.e.* $f_{\rm NL} = 5(1-n_s)/12$. Accordingly, the observation of the almost scale invariant power spectrum of linear perturbation indicates extremely small amount of nonlinear correlations in squeezed limit. As a result, one expects that the simplest inflation model in terms of single slow-roll scalar field would be ruled out if any squeezed limit non-Gaussianity could be detected.

It is, however, interesting to notice that there exists a nontrivial inflationary scenario, dubbed as non-attractor inflation [41–43, 183–185], that can violate Maldecena's consistency relation even in the framework of single scalar field with Bunch-Davies initial states. This is due to the fact that curvature perturbations generated from quantum fluctuations during the non-attractor phase are dominated by the growing modes at super-Hubble scales, of which the behaviour is much similar to the matter bounce cosmology [28–30] rather than the cosmology of slow-roll inflation. Accordingly, similar to the matter bounce cosmology [107, 186], large amount of *local non-Gaussianity* - which contributes dominantly to the squeezed limit bispectrum - can be achieved in non-attractor inflation models. Ref. [42] considers a simple model with canonical kinetic term which predicts $f_{\rm NL} \simeq 5/2$. The idea is then further generalized to the models with non-canonical kinetic terms in [43, 184, 185] where it has been shown that the non-Gaussianity can be arbitrarily large. Inspired by this unconventional

behaviour of primordial perturbations, many studies have been devoted to understand the possible violation of the consistency relation during the non-attractor phase from a variety of theoretical perspectives [103, 187–189].

Furthermore, it is important to notice that the non-attractor inflation alone is not phenomenologically viable [190]. Namely, without a conventional attractor phase, the non-attractor inflation does not provide enough e-folds or cannot fit the COBE normalization of the density perturbations. For a more realistic consideration, the phase of non-attractor inflation shall be regarded as some initial stage of the whole inflationary era, and a phase transition from non-attractor to the slow-roll attractor evolution becomes essential for this class of models. Therefore, the non-attractor inflation model consists of at least three different kinds of phases: the non-attractor phase, the transition phase, and the slow-roll phase. We shall define these phases more explicitly in models we study. During the transition phase, modes that exited the horizon may not freeze, the main focus of this paper is to understand how the transition process would influence primordial non-Gaussianities generated in the non-attractor phase.

In this work, we revisit primordial non-Gaussianities from non-attractor inflation by focusing on the impact of the *non-attractor to attractor transition*. We begin with a detailed analysis of the non-attractor inflation model with a canonical scalar field, which was previously studied in Ref. [42, 190]. Here the transition processes are classified into two different cases, depending on whether the background evolution around the transition is smooth or sharp. We first apply the in-in formalism to study the bispectrum in these two cases separately. For the smooth transition, our calculation shows that the non-Gaussianity generated in the non-attractor phase *cannot* survive through the transition to the slow-roll attractor phase. So the value $f_{\rm NL} = 5/2$ generated during the non-attractor phase returns to ~ 0 (slow-roll-suppressed) in the slow-roll phase, and the net contribution to the local $f_{\rm NL}$ is negligible as in the slow-roll attractor case. The situation is more complicated in the sharp transition. After a detailed analysis on the background and perturbations, we find that, in general the non-Gaussianity generated in the non-attractor phase is also suppressed after the transition. But in extremal cases where the curvature perturbations freeze out immediately at the transition time, the original result $f_{\rm NL} \simeq 5/2$ can be recovered. We confirm all these results by employing the simple and intuitive calculation of the δN formalism. Note that despite the non-trivial evolution of non-Gaussianity during the transition phase, the consistency relation is still violated even though the amplitude of non-Gaussianity might be slow-roll

suppressed. This is a consequence of the fact that the curvature perturbation modes keep evolving after they crossed the Hubble horizon; in contrast with the conventional, slow-roll models where curvature perturbation is conserved on super-horizon scales.

We further study the transition process in the non-attractor inflation model driven by a non-canonical scalar field, as constructed in [43, 184]. The background evolution shows that, the inflaton field first becomes canonical before the cosmological system enters into the phase of slow-roll attractor through a smooth transition phase. The difference between these models and the above canonical model is that now we have two types of terms in the non-canonical models. The first type behaves very similarly to the interaction term in the canonical model, and it does not contribute to large local non-Gaussianity either when a smooth transition is taken into account. However, the non-canonical models have another set of qualitatively different terms. These second type of terms are unique due to the presence of the non-canonical kinetic terms. The contribution to large local non-Gaussianity from these terms do not get exactly erased by the smooth transition period, but instead gets an additional suppression factor. Since the suppression factor and the amplitude of primordial non-Gaussianity generated in the non-attractor phase are independent of each other, the large local non-Gaussianity is still possible for certain model parameters. So the main conclusions of [43, 184] remain unchanged.

The paper is organized as follows. In Section 5.2 we study the canonical model of non-attractor inflation. After reviewing previous works, we focus on the detailed transition process from the initial non-attractor phase to the subsequent phase of slow-roll attractor. Then we elaborate on the behaviour of local non-Gaussianity in two different cases – smooth transition and sharp transition, via both in-in formalism and δN formalism. In Section 5.3 we generalize the study of the non-attractor inflation to models with non-canonical kinetic terms, where we only consider smooth transition case. The detailed transition process in these models is shown by full analysis of the background dynamics. After that, we estimate the size of the non-Gaussianity and find a suppression effect caused by the background evolution of the transition process. We summarize our conclusions with a discussion in Section 5.4. Throughout the paper we take the convention of the reduced Planck mass to be $M_{\rm pl}^2 = 1/8\pi G = 1$.

5.2 The canonical model

In this section we revisit the calculation of primordial non-Gaussianities in the model of canonical non-attractor inflation, and show how the different transition processes may change the non-Gaussianity generated in the non-attractor phase.

5.2.1 The non-attractor phase and local non-Gaussianity

The canonical non-attractor model is constructed by assuming that the inflaton's potential is almost a constant, i.e. for sufficiently large regime one has $V(\phi) \simeq V_0$ [41, 42]. Accordingly, the background equations in this model are given by

$$\ddot{\phi} + 3H\dot{\phi} \simeq 0 \ , \qquad 3H^2 = \frac{1}{2}\dot{\phi}^2 + V \simeq V_0 \ , \tag{5.1}$$

where a dot denotes the derivative with respect to cosmic time t, and $H \equiv \dot{a}/a$ is the Hubble parameter. This leads to the following behaviour for the slow-roll parameters

$$\epsilon \equiv -\frac{\dot{H}}{H^2} = \frac{\dot{\phi}^2}{2H^2} \propto a^{-6} \ , \qquad \eta \equiv \frac{\dot{\epsilon}}{H\epsilon} = -6 \ . \tag{5.2}$$

As shown in the above equation, the slow-roll parameter ϵ decays very quickly during the non-attractor phase, and thus, one can take the limit $\epsilon \to 0$ as a good approximation here. As a result, the Hubble parameter H is nearly constant during the non-attractor phase and in terms of conformal time τ the scale factor takes $a \simeq -1/(H\tau)$. In addition, the second slow-roll parameter η is of order $\mathcal{O}(1)$.

For the primordial curvature perturbation $\mathcal{R}$, we define $z \equiv a\sqrt{2\epsilon}$ and $u_k \equiv z\mathcal{R}_k$. Then at the linear level, the perturbation variable u_k is governed by the Mukhanov-Sasaki equation

$$u_k'' + \left(k^2 - \frac{z''}{z}\right) u_k = 0 \ , \tag{5.3}$$

where the prime denotes the derivative to conformal time τ. Following the standard treatment, the effective mass can be written as $z''/z \simeq (\nu^2 - 1/4)/\tau^2$, where for $\epsilon \ll 1$, ν is given by

$$\nu^2 = \frac{9}{4} + \frac{3}{2}\eta + \frac{1}{4}\eta^2 + \frac{\dot{\eta}}{2H} + \mathcal{O}(\epsilon) \ . \tag{5.4}$$

In the non-attractor stage, $\eta = -6$, and thus, $\nu = 3/2$. Consequently, Eq. (5.3) yields the mode function of curvature perturbation as follows,

$$\mathcal{R}_k(\tau) = \frac{u_k}{z} = \frac{H}{\sqrt{4\epsilon k^3}}(1 + ik\tau)e^{-ik\tau} \ , \tag{5.5}$$

which looks the same as the one in the lowest order slow-roll approximation. But notice that ϵ is rapidly evolving here in contrary to the slow-roll case. After Hubble-exit, one can get a scale-invariant power spectrum of primordial curvature perturbation, of which the form takes $P_{\mathcal{R}}(k) \equiv \frac{H^2}{8\pi^2\epsilon}$. However, since $\epsilon \propto a^{-6}$, the amplitude of curvature perturbation grows as $\mathcal{R}_k \propto a^3$ at super-Hubble scales. As a result, the final form of the power spectrum ought to be evaluated after the end of the non-attractor phase.

In order to calculate the non-Gaussianity, one needs to study the three-point correlation function of primordial curvature perturbation

$$\langle \mathcal{R}_{\mathbf{k_1}} \mathcal{R}_{\mathbf{k_2}} \mathcal{R}_{\mathbf{k_3}} \rangle \equiv (2\pi)^3 \delta^{(3)}(\mathbf{k_1} + \mathbf{k_2} + \mathbf{k_3}) B_{\mathcal{R}}(k_1, k_2, k_3) \ . \tag{5.6}$$

At the squeezed limit $k_1 \simeq k_2 \gg k_3$, the bispectrum $B_{\mathcal{R}}$ can be expressed as

$$B_{\mathcal{R}}(k_1, k_2, k_3) = (2\pi)^4 \frac{1}{k_1^3 k_3^3} P_{\mathcal{R}}(k_1) P_{\mathcal{R}}(k_3) \frac{3}{5} f_{\rm NL} \ , \tag{5.7}$$

where $f_{\rm NL}$ is the amplitude of non-Gaussianity in squeezed limit. The consistency relation, predicts $f_{\rm NL} \simeq \frac{5}{12}(1 - n_s)$ which we will see is violated in non-attractor models. Notice that the local shape has the same scaling behaviour in squeezed limit, although it is well defined in any configuration [37]. The non-Gaussianity that is generated during the non-attractor phase is indeed in the local shape but we are only interested in the squeezed limit (which tells us whether the consistency relation is violated or not); therefore we will not discuss non-Gaussianities in general configurations.

Ref. [42] uses two methods to compute the size of local non-Gaussianity. The first method focuses on the non-attractor phase alone. Because the contributions from the terms in cubic Lagrangian are slow-roll suppressed in this phase, Ref. [42] focuses on the contribution from a field-redefinition term in

$$\mathcal{R} = \mathcal{R}_n + \frac{\eta}{4}\mathcal{R}_n^2 + \frac{1}{H}\mathcal{R}_n \dot{\mathcal{R}}_n \ , \tag{5.8}$$

which yields

$$f_{\rm NL} = -\frac{5}{4}(\eta + 4) = \frac{5}{2} \tag{5.9}$$

at the end of the non-attractor phase τ_e. If these perturbations got frozen immediately at the end of this phase and were carried along to the attractor

slow-roll phase, we would end up with this order-one non-Gaussianity. However, the transition from the non-attractor phase to the slow-roll phase may not be an instant process and the process is not generically an attractor solution either. It turns out that the evolution of modes at the super-horizon scales can be non-negligible during this transition period.

The second method used in Ref. [42] indeed considers this transition, but treating it as an instant process. In this method, the field redefinition term no longer contributes because the parameter η should now be evaluated at the end of inflation instead of at the end of the non-attractor phase. This value of η is negligible. The corresponding contribution should now, equivalently, come from an interaction term in the cubic Lagrangian,

$$S_3 \supset \int dt d^3x \frac{a^3\epsilon}{2}\dot{\eta}\mathcal{R}^2\dot{\mathcal{R}} \ . \tag{5.10}$$

as correctly considered in Ref. [42]. The bispectrum coming from this interaction term is

$$\begin{aligned} B_{\mathcal{R}}(k_1,k_2,k_3) &= -2\Im\mathcal{R}_{k_1}(\tau_0)\mathcal{R}_{k_2}(\tau_0)\mathcal{R}_{k_3}(\tau_0)\int_{-\infty}^{\tau_0} d\tau a^2\epsilon\eta' \\ &\quad \times \left[\mathcal{R}^*_{k_1}(\tau)\mathcal{R}^*_{k_2}(\tau)\mathcal{R}^{*\prime}_{k_3}(\tau) + \text{perm.}\right] \ , \end{aligned} \tag{5.11}$$

where τ_0 is the conformal time after which the super-horizon curvature perturbation as well as the corresponding bispectrum cease evolving. We also remind that τ_e denotes the end of the non-attractor phase. The η parameter goes from -6 to nearly zero and then the coefficient η' can be comparably large. If the transition is approximated as an instant process that takes place suddenly at the time τ_e when the non-attractor phase ends [42], then one may expect $\tau_0 = \tau_e$ and the behaviour of η during the transition period can be approximated by a step function

$$\eta = -6\left[1 - \theta(\tau - \tau_e)\right] \ . \tag{5.12}$$

As a result, the interaction term (5.10) leads to

$$\lim_{k_3/k_1\to 0} B_{\mathcal{R}}(k_1,k_2,k_3) = (2\pi)^4 \frac{1}{4k_1^3k_3^3} P_{\mathcal{R}}(k_1)P_{\mathcal{R}}(k_3)\int d\tau\eta' \ , \tag{5.13}$$

and the value $f_{\rm NL} = 5/2$ will be recovered. However, one may still wonder whether this conclusion holds true if we consider a complete transition process. In the next subsections, we will study various transition cases in details, and show that, for a smooth transition the actual contribution from (5.10) is negligible; while the $\mathcal{O}(1)$ local non-Gaussianity can be recovered from a sharp transition.

5.2.2 The non-attractor to slow-roll transitions

The reason that the ultra-slow-roll inflation with a constant potential cannot be a complete model (even if we impose an abrupt cutoff and start the reheating instantly in the non-attractor phase) is that, after $40 \sim 60$ efolds, the density perturbation cannot produce the observed value.[1] So a transition to a slow-roll phase is needed. In the following, we construct a model that describes such a transition. The advantage of our model is that the exact analytical solutions can be obtained, in which the inflaton field begins the evolution in the non-attractor phase and then joins the slow-roll phase gradually.

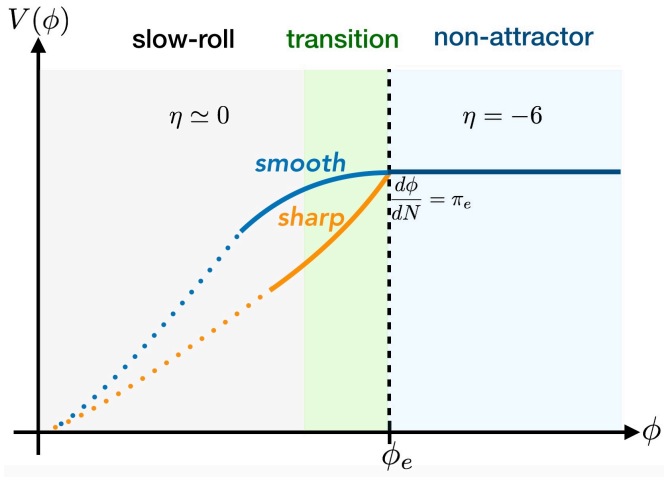

Figure 5.1: A sketch plot of the potentials of non-attractor inflation with smooth and sharp transitions. Note that the inflaton rolls from right to left, i.e. ϕ is decreasing during the evolution.

Suppose that the non-attractor phase ends at $\phi_e = \phi(\tau_e)$, and after that, a slow-roll potential $V(\phi)$ is attached to the constant one. Since the transition process is very short and the inflaton field excursion is very tiny, during this period, the attached slow-roll potential can be expanded as follows,

$$V(\phi) = V(\phi_e) + \sqrt{2\epsilon_V} V(\phi_e)(\phi - \phi_e) + \frac{1}{2}\eta_V V(\phi_e)(\phi - \phi_e)^2 + \dots \,. \quad (5.14)$$

[1] If we require only the non-attractor inflation to solve the flatness and horizon problems, the total number of efolds of the non-attractor phase should be $40 \sim 60$ efolds, at the end of which the value of ϵ would be diminishingly small. To fit the COBE normalization, H would be diminishingly small and ruled out already.

Here we have introduced the potential slow-roll parameters

$$\epsilon_V \equiv 1/2(V'(\phi_e)/V(\phi_e))^2 \text{ and } \eta_V \equiv V''(\phi_e)/V(\phi_e),$$

which are expected to be small constants such that the slow-roll dynamics can be triggered after the transition. Accordingly, one can sketch the possible form of potentials depending on different values of parameters which correspond to different types of transition, as shown in Figure 5.1. We may distinguish two extreme possibilities: if we require the derivative of the potential to be continuous, then $\epsilon_V = 0$ and thus the transition is *smooth*; whereas for other cases, such as $\sqrt{2\epsilon_V} \gtrsim |\eta_V|$, we get *sharp* transition. Note that by considering the above potential we restricted ourselves to the case with continuous potential and the positivity of the second term also implies that the inflaton rolls-down instead of jumping up. By the end of this section, however, we will discuss how the results may change by considering non-standard cases of discontinuous potential or negative slope. Finally, notice that the above additional potential in a single field model of inflation, breaks the internal shift symmetry explicitly; therefore even the generalized consistency relations [103, 189] are not applicable, unless if the bispectrum does not evolve when the potential (5.14) switches on.

In this type of inflation model, initially the inflaton field rolls along the constant potential $V = V_0$ for $\phi > \phi_e$, which we define as the *non-attractor phase*. After the inflaton field reaches ϕ_e, the potential becomes (5.14), on which inflation transits to the slow-roll attractor. We define this period as the *transition phase*, as shown by the light green region in Figure 5.1. Using e-folding number N as variable (with the convention $dN = Hdt$), the background equations become

$$\frac{d^2\phi}{dN^2} + 3\frac{d\phi}{dN} + 3\sqrt{2\epsilon_V} + 3\eta_V(\phi - \phi_e) \simeq 0 \ , \quad \text{and} \quad 3H^2 \simeq V(\phi_e) \ , \tag{5.15}$$

where we have assumed that the Hubble parameter is a constant. Without losing generality, we can set $N = 0$ at ϕ_e and the field velocity at the same moment is introduced to be π_e, then we have the following analytical solution

$$\phi = \frac{s-3-h}{s(s-3)}\pi_e e^{\frac{1}{2}(s-3)N} - \frac{s+3+h}{s(s+3)}\pi_e e^{-\frac{1}{2}(s+3)N} + \frac{2\pi_e h}{s^2-9} + \phi_e \ , \tag{5.16}$$

$$\pi \equiv \frac{d\phi}{dN} = e^{-3N/2}\left[\pi_e \cosh\left(\frac{s}{2}N\right) - \frac{3+h}{s}\sinh\left(\frac{s}{2}N\right)\right] \ , \tag{5.17}$$

with the parameters

$$s \equiv \sqrt{9 - 12\eta_V} \simeq 3 - 2\eta_V \ , \quad h \equiv 6\sqrt{2\epsilon_V}/\pi_e \ , \tag{5.18}$$

being introduced. Notice that in our convention $\pi_e < 0$ (because ϕ is decreasing throughout the evolution) and hence $h < 0$. After some simple algebra, the slow-roll parameters defined in (5.2) during the transition are given by

$$\epsilon(N) = \frac{\pi_e^2}{2} e^{-3N} \left[\cosh\left(\frac{s}{2}N\right) - \frac{3+h}{s} \sinh\left(\frac{s}{2}N\right) \right]^2 \ , \tag{5.19}$$

$$\eta(N) = s - 3 - \frac{2s(3+s+h)}{e^{sN}(s-3-h) + 3 + s + h} \ . \tag{5.20}$$

We can see from the above that, as N increases, η goes from $-6-h$ to $-2\eta_V$ during the transition.

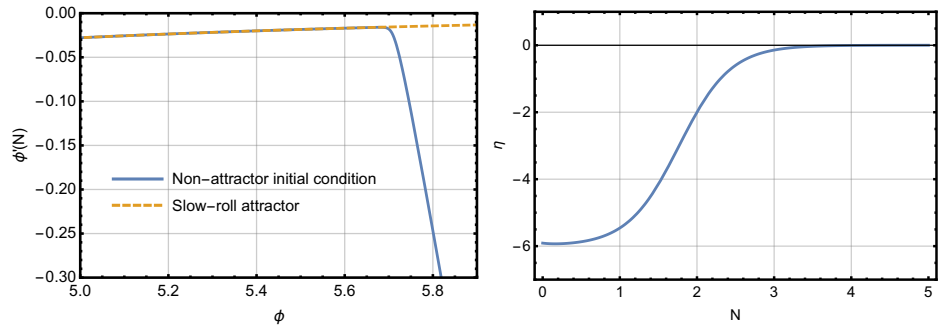

Figure 5.2: Smooth transition. Left Panel: the phase space diagram of non-attractor to slow-roll transition on a plateau-like potential. Right Panel: the evolution of η parameter during the transition.

Note that, the background evolutions in smooth and sharp transitions behave manifestly different, and h is a crucial parameter to characterize their difference. For the smooth transition, $h \to 0$, and thus at the beginning of the transition phase $\eta = -6$, which continuously follows the non-attractor phase and then smoothly evolves to the slow-roll attractor. Figure 5.2 shows this behaviour via the phase space diagram and the evolution of η, where the smooth transition is depicted by the numerical solution of the non-attractor initial condition on a plateau-like potential[2].

[2]See Section 5.2.3.1 for more discussions about this implementation.

For the sharp transition, h is a negative constant determined by the field velocity π_e at the end of the non-attractor phase. From (5.19) we see that, when the attractor is reached after the sharp transition, we have $\epsilon_0 \simeq \epsilon_V$ with $\epsilon_0 = \pi_0^2/2$, where π_0 is the field velocity $\frac{d\phi}{dN}$ during the slow-roll phase. Therefore, the parameter h can be described also by the ratio between π_0 and π_e

$$h \equiv 6\sqrt{2\epsilon_V}/\pi_e \simeq 6\sqrt{2\epsilon_0}/\pi_e = -6\pi_0/\pi_e \ . \tag{5.21}$$

From the relative magnitudes of π_e and π_0, it is straightforward to see that, the value of $|h|$ can be of order unity or even bigger, and there are three possible cases in sharp transition: $h < -6$, $h = -6$ and $-6 < h < 0$, as shown in the phase space diagram in Figure 5.3. Consequently at the beginning of the transition $\eta = -6 - h$ can be quite large, which differs from its value during the non-attractor phase (where it is $\eta = -6$). Thus there is a sudden change of η at the transition time, from -6 to $-6-h$, as shown by the numerical examples in the right panel of Figure 5.3. For the later convenience, we formulate the evolution of η around τ_e as

$$\eta = -6 - h\theta(\tau - \tau_e) \ , \quad \tau_{e_-} < \tau < \tau_{e_+} \ . \tag{5.22}$$

Therefore, typically a sharp transition process consists of an instant transition at the beginning and a following period of relaxation described by (5.16) – (5.20). One special case is $h = -6+2\eta_V \simeq -6$, where inflaton joins the slow-roll attractor immediately after the instant transition and there is no relaxation process. However, it still differs from the oversimplified case in (5.12). As we shall show in Section 5.2.4, this realistic instant transition does not imply immediate freezing of the curvature perturbation (i.e. $\tau_0 \neq \tau_e$), and the evolving super-horizon mode after the instant transition can still modify the non-Gaussianity generated during the non-attractor phase.

With these background solutions of transitions, in the following we shall perform a detailed study of non-Gaussianities. The in-in formalism is applied in Section 5.2.3 and 5.2.4, for smooth and sharp transitions respectively. In Section 5.2.5, we further confirm the in-in results in both cases via δN formalism.

5.2.3 Non-Gaussianity in a smooth transition

In this subsestion, we focus on in-in calculation of the smooth transition case, which corresponds to the limit $\epsilon_V \to 0$ in the potential (5.14), and

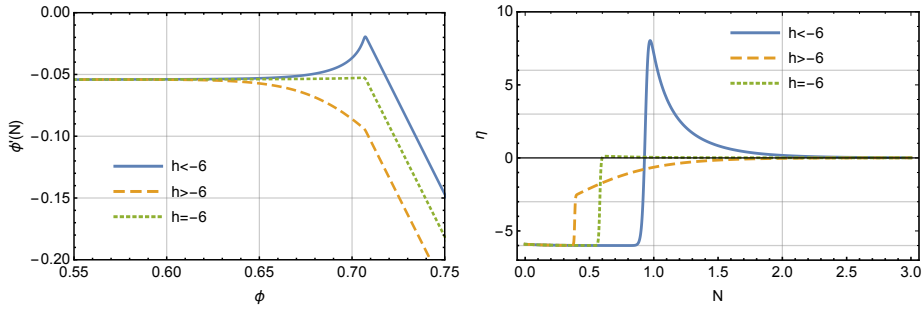

Figure 5.3: Sharp transition. Left Panel: the phase space diagram of sharp transition for three different cases. Right Panel: the evolution of η parameter during the sharp transition.

demonstrate that there is a cancellation for the local non-Gaussianity generated during the non-attractor stage. Then in Section 5.2.3.1, we confirm this conclusion by the numerical study of a realistic model. At last, in Section 5.2.3.2, we perform an extended analysis to show that this conclusion holds true for smooth transition in general.

Before the in-in calculation, we should first check the behaviour of the mode function during the transition, which is governed by the Mukhanov-Sasaki equation (5.3) and the index ν in (5.4). Even though η and $\dot{\eta}$ varies dramatically during the transition, surprisingly the exact solution (5.19) and (5.20) gives us $\nu^2 = 9/4 - 3\eta_V$, which is constant and the same as the result in slow-roll attractors[3]. Therefore, the mode function in (5.5) still applies here as the leading order approximation, and the resulting power spectrum in this period is still nearly scale-invariant. We should further remark that, the curvature perturbation still evolves during the transition, and should be fixed after the slow-roll attractor is reached. That is to say the final amplitude of the power spectrum is $P_{\mathcal{R}}(k) \equiv \frac{H^2}{8\pi^2\epsilon_0}$, where ϵ_0 is the ϵ in the slow-roll stage.

With this analytical description of the smooth transition, now let us look at the bispectrum caused by the cubic interaction term (5.10). We can substitute the mode function (5.5) into the in-in integral in (5.11). Notice that, even though ϵ is small, it varies fast during the transition, thus

$$\mathcal{R}_k'(\tau) = \frac{H}{\sqrt{4\epsilon k^3}} k^2 \tau e^{-ik\tau} - \frac{\eta}{2} aH \frac{H}{\sqrt{4\epsilon k^3}} (1 + ik\tau) e^{-ik\tau} \ , \tag{5.23}$$

[3]In Section 5.2.3.2, we shall show that the cancellation giving this result of ν^2 is not a coincidence.

where the second term is due to the ϵ's evolution[4]. Taking the squeezed limit $k_1 = k_2 = k \gg k_3$, we get

$$B_{\mathcal{R}}(k_1,k_2,k_3) = -\frac{(2\pi)^4}{4k_1^3k_3^3}P_{\mathcal{R}}^2 \Im \int_{-\infty}^{\tau_0} d\tau \frac{\eta'}{\sqrt{\epsilon/\epsilon_0}} e^{2ik(\tau-\tau_0)} \times \left[\frac{1-ik\tau}{k\tau} + \frac{3\eta}{4}\frac{(1-ik\tau)^2}{k^3\tau^3}\right](1+ik\tau_0)^2 \quad (5.24)$$

Since η' is negligible during the non-attractor and slow-roll phase, we only need to compute this integral during the transition process (from τ_e to τ_0). As mentioned earlier, the evolution of the bispectrum after τ_0 is suppressed, as is well-known in the attractor case where the super-horizon curvature perturbation freezes out. Since we are mainly interested in the perturbation modes which exit the Hubble radius during the non-attractor phase, we can use $|k\tau_e| < |k\tau_0| \ll 1$. Thus the leading order contribution of the above bispectrum becomes

$$B_{\mathcal{R}}(k_1,k_2,k_3) = -\frac{(2\pi)^4}{4k_1^3k_3^3}P_{\mathcal{R}}^2 \int_{\tau_e}^{\tau_0} d\tau \frac{\eta'}{\sqrt{\epsilon/\epsilon_0}} \left[1 + \frac{\eta}{2} - \frac{\eta}{2}\left(\frac{\tau_0}{\tau}\right)^3\right] . \quad (5.25)$$

Plugging in the analytical expressions for ϵ and η in (5.19) and (5.20), we find after the transition

$$\frac{3}{5}f_{\rm NL} \simeq -\frac{\sqrt{2\epsilon_0}}{\pi_e}\frac{\eta_V}{2} . \quad (5.26)$$

Here $\sqrt{2\epsilon_0}$ can be expressed as the field velocity $\frac{d\phi}{dN}$ at the beginning of the slow-roll phase τ_0, thus $\sqrt{2\epsilon_0} \ll |\pi_e|$. As a result, the local non-Gaussianity becomes negligible after the transition.

If we compare this calculation with the result (5.13) in the instant transition approximation, we can just identify $\tau = \tau_0$ and $\epsilon = \epsilon_0$ in (5.25) using the step function (5.12) for η. However, here when we compute the smooth transition explicitly, the third term in the bracket becomes negligible, since $\tau_0/\tau < 1$ during the transition. And we have seen that there is a cancellation between the first two terms, in contrast with the instant transition approximation which gives order one result. This cancellation is also demonstrated numerically as follows.

[4]This contribution was neglected in the calculation of [190], see Eq.(4.15) there.

5.2.3.1 Numerical study on a plateau-like potential

In a realistic case, non-attractor inflation can be seen as imposing the ultra-slow-roll initial condition on a plateau-like inflaton potential (such as Starobinsky inflation [3] and α-attractors [17, 18]). In such a situation, the smooth transition to slow-roll attractor occurs automatically. In addition, due to the scale-invariant power spectrum generated in the initial non-attractor phase, the primordial perturbations can be suppressed on large scales, which is favored by current CMB observations [190].

Now we study the background evolution of this realistic model numerically, and then further check the analytical results above. Consider the following potential of Starobinsky inflation [3]

$$V(\phi) = V_0 \left(1 - e^{-\sqrt{2/3}\phi}\right)^2 \ , \tag{5.27}$$

which is very flat for large ϕ. In the slow-roll attractor, the field velocity satisfies $\dot{\phi}_{sr} = -V'/(3H)$. However, if inflation starts with a much larger velocity $|\dot{\phi}| \gg |\dot{\phi}_{sr}|$ on this very flat potential, initially it would be in the non-attractor phase. Solving the background equations numerically, we get the results shown in Figure 5.2. As we can see from the phase space diagram and the evolution of η, this realistic model indeed has a non-attractor initial phase, and then it will join the slow-roll attractor very quickly.

With this numerical solution, we can go back to do the full computation for the integral in (5.24), not only for the perturbation which exit the Hubble radius before the transition (non-attractor modes), but also for those small scale modes (slow-roll modes). The final bispectrum receives contributions from both terms in (5.24). The numerical result of local $f_{\rm NL}$ as a function of k is shown in Figure 5.4. As we see, if we only consider one contribution, the local non-Gaussianity is $\mathcal{O}(1)$ for the non-attractor modes, and then it vanishes for the slow-roll modes. However, when we combine these two contributions together, they cancel each other and yield vanishing $f_{\rm NL}$ even for non-attractor modes. This result confirms the analytical calculation above.

In summary, both analytical and numerical calculation of the smooth transition process show that, there is a mysterious cancellation happening during this transition period. In the following subsection, we shall understand this cancellation in a more general way.

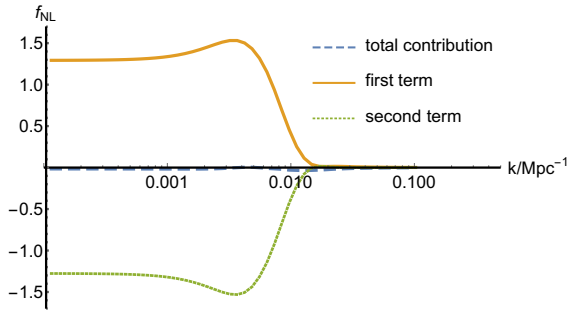

Figure 5.4: The cancellation in the in-in integral (5.24).

5.2.3.2 A more general analysis:

To understand what is going on during a smooth transition, we present a more general analysis as follows. First of all, let us remind of the background equations

$$\ddot{\phi} + 3H\dot{\phi} + V'(\phi) = 0 \ , \qquad 3H^2 = \frac{1}{2}\dot{\phi}^2 + V(\phi) \ , \tag{5.28}$$

Here the potential is required to have a slow-roll attractor, but for now we do not assume any slow-roll conditions. Then using the background equations and the Hubble "slow-roll" parameters defined in (5.2), the second and third order derivatives of the slow-roll potential can be exactly expressed as

$$\begin{aligned} V'' &= \left(6\epsilon - \frac{3}{2}\eta - \frac{\eta^2}{4} + \frac{5}{2}\epsilon\eta - 2\epsilon^2 - \frac{\dot{\eta}}{2H}\right) H^2 \ , \\ V''' &= \frac{1}{\sqrt{2\epsilon}}\left(9\epsilon\eta - \frac{3\dot{\eta}}{2H} - \frac{\eta\dot{\eta}}{2H} + 3\epsilon\eta^2 + \frac{3\epsilon\dot{\eta}}{H} - 9\epsilon^2\eta \right. \\ &\qquad \left. - \frac{\ddot{\eta}}{2H^2} - 12\epsilon^2 + 4\epsilon^3\right) H^2 \ , \end{aligned} \tag{5.29}$$

which respectively correspond to the inflaton mass and self-coupling. Note that these derivatives of the potential should be suppressed so that the slow-roll attractor is possible. Due to this requirement, some useful combinations of η and $\dot{\eta}$, that we will soon encounter, should be much smaller than unity, even though η and $\dot{\eta}$ can be individually large during the non-attractor and transition stages. One consequence of this observation is the behaviour of the effective mass in the Mukhanov-Sasaki equation (5.3). As we mentioned in the last subsection, the coefficient $\nu^2 - 9/4$ there is always small, even

during the transition where η and $\dot{\eta}$ are big. Now we see this parameter is directly related to inflaton mass

$$\nu^2 - \frac{9}{4} = -\frac{V''}{H^2} + \mathcal{O}(\epsilon) \ , \tag{5.30}$$

which does not care if inflation is in the attractor or not.

With this knowledge, let us look at the cubic interaction term (5.10) again. In our in-in calculation above, one subtlety is caused by the evolution behaviour of $\dot{\mathcal{R}}$. We can remove it via integration by part, and express (5.10) as

$$-\int dtd^3x \frac{d}{dt}\left(\frac{a^3\epsilon\dot{\eta}}{6}\right)\mathcal{R}^3 + \text{surface term} \ . \tag{5.31}$$

Since there is no more time derivative on $\mathcal{R}$, the only important effect lies in the cubic coupling. Here we are encouraged to introduce the effective coupling as

$$\frac{1}{6a^3\epsilon}\frac{d}{dt}\left(a^3\epsilon\dot{\eta}\right) = \frac{H^2}{3}\left(\frac{3\dot{\eta}}{2H} + \frac{\eta\dot{\eta}}{2H} + \frac{\ddot{\eta}}{2H^2}\right) \ . \tag{5.32}$$

Again it looks like due to the drastic variation of η, these terms could be large during the transition. However, if we plug in our analytical and numerical solutions in the last section, this combination is shown to be negligible. Interestingly, they are also present in V''', and can be written as

$$\frac{1}{6a^3\epsilon}\frac{d}{dt}\left(a^3\epsilon\dot{\eta}\right) = -\frac{1}{3}\sqrt{2\epsilon}V''' + \mathcal{O}(\epsilon)H^2 \ . \tag{5.33}$$

Therefore the contribution from this term is always small, no matter how big η and $\dot{\eta}$ are during the transition. The presence of V''' is not a coincidence here. In the flat gauge, the operator which contributes to the cubic Lagrangian (5.10) comes from the self-interaction of field fluctuations

$$\mathcal{L}_3 \subset \frac{a^3}{6}V'''\delta\phi^3 = \frac{a^3\epsilon}{3}\sqrt{2\epsilon}V'''\mathcal{R}^3 \ . \tag{5.34}$$

Taking the decoupling limit, we have

$$V''' = \frac{1}{\sqrt{2\epsilon}}\left(-\frac{3\dot{\eta}}{2H} - \frac{\eta\dot{\eta}}{2H} - \frac{\ddot{\eta}}{2H^2} + \mathcal{O}(\epsilon)\right)H^2 \ . \tag{5.35}$$

And after integration by parts, the self-interaction term exactly gives us the cubic term (5.10).

In summary, for a smooth non-attractor to slow-roll transition, as long as we have a slow-roll potential (V''' is small), the non-Gaussianities would be always small. The cubic interaction term (5.10), which was previously thought to contribute sizable $f_{\rm NL}$ in the instant transition approximation, actually never contributes in the realistic smooth transition case. However, this argument may not work in sharp transition cases. There the potential is unsmooth around the transition, which may yield large V'''. Furthermore, the unconventional behaviour of the mode function will add extra complications. These issues of the sharp transition will be addressed in the next subsection.

5.2.4 Non-Gaussianity in a sharp transition

As we discussed previously, the background of sharp transition differs from the smooth transition case. Now we come to study the effect of a sharp transition on the evolution of perturbations, especially on the local non-Gaussianity. The sharp transition corresponds to the case where the second term in the potential (5.14) is also important. In this subsection, we shall study the case $\sqrt{2\epsilon_V} \gtrsim |\eta_V|$. The form of the potential (5.14) can be invalid after the inflaton field evolves to sufficiently large distances from the transition point. But we can assume that the slow-roll limit is already reached before that happens so that we do not need to keep track of perturbations any more.

First of all, unlike the smooth transition case, the behaviour of the mode function in the sharp transition is more complicated. If we look at the Mukhanov-Sasaki equation and the index ν in (5.4), the analytical solution of the sharp transition (5.19) and (5.20) still gives us $\nu^2 = 9/4 - 3\eta_V$. However, due to the sudden change of η at the transition time τ_e, one cannot simply continue using the initial mode function (5.5) after τ_e. Here when the transition happens, the matching condition requires the mode function and its first derivative to be continuous, i.e. $\mathcal{R}(\tau_{e_-}) = \mathcal{R}(\tau_{e_+})$ and $\mathcal{R}'(\tau_{e_-}) = \mathcal{R}'(\tau_{e_+})$. This gives us the following behaviour of curvature perturbation after τ_e

$$\mathcal{R}_k(\tau) = \alpha_k \frac{H}{\sqrt{4\epsilon k^3}}(1+ik\tau)e^{-ik\tau} + \beta_k \frac{H}{\sqrt{4\epsilon k^3}}(1-ik\tau)e^{ik\tau} \ , \tag{5.36}$$

$$\begin{aligned} \mathcal{R}_k'(\tau) &= \alpha_k \left[\frac{H}{\sqrt{4\epsilon k^3}}k^2\tau e^{-ik\tau} + \frac{\eta}{2\tau}\frac{H}{\sqrt{4\epsilon k^3}}(1+ik\tau)e^{-ik\tau}\right] \\ &\quad +\beta_k \left[\frac{H}{\sqrt{4\epsilon k^3}}k^2\tau e^{ik\tau} + \frac{\eta}{2\tau}\frac{H}{\sqrt{4\epsilon k^3}}(1-ik\tau)e^{ik\tau}\right] \ , \end{aligned} \tag{5.37}$$

where

$$\alpha_k = 1 + i\frac{h}{4k^3\tau_e^3}(1+k^2\tau_e^2)\ , \qquad \beta_k = -ih(1+ik\tau_e)^2\frac{e^{-2ik\tau_e}}{4k^3\tau_e^3}\ . \tag{5.38}$$

We can easily check the long wavelength behaviour of the mode function after τ_e

$$\mathcal{R}_k(\tau) \simeq \frac{6-h}{6}\frac{H}{\sqrt{4\epsilon k^3}} + \frac{\tau^3}{6\tau_e^3}\frac{H}{\sqrt{4\epsilon k^3}} \qquad \text{for } k\to 0\ . \tag{5.39}$$

This solution satisfies the super-horizon EoM: $\ddot{\mathcal{R}} + (3+\eta)H\dot{\mathcal{R}} = 0$. At the time τ_0 of the slow-roll stage, we get the freezed amplitude

$$\mathcal{R}_k(\tau_0) \simeq \frac{6-h}{6}\frac{H}{\sqrt{4\epsilon_0 k^3}} = \left(1+\sqrt{\frac{\epsilon_0}{\epsilon_e}}\right)\frac{H}{\sqrt{4\epsilon_0 k^3}}\ . \tag{5.40}$$

For large values of $|h|$ the above relation reduces to $\mathcal{R}_k(\tau_0) \simeq \frac{H}{\sqrt{4\epsilon_e k^3}}$ which is similar to the mode function at the transition time τ_e. Thus, for $|h| \gg 1$, the final power spectrum does not change much by the transition and we have $P_{\mathcal{R}} \simeq \frac{H^2}{8\pi^2\epsilon_e}$. Therefore, we expect to recover the previously calculated non-Gaussianity $f_{\rm NL} = 5/2$ in the $|h| \gg 1$ limit where the mode function is assumed to freeze instantly after transition. We will confirm this expectation explicitly below. Note also that, in the $h = -6$ case with only instant transition, the super-horizon modes still evolve from τ_e to τ_0, as can be seen from (5.39). This shows that a realistic instant transition to the slow-roll evolution (which corresponds to $h = -6$) does not imply an instant freezing of the mode function, thus we do not expect to recover $f_{\rm NL} = 5/2$ after this transition. On the other hand, for $|h| \gg 1$, the adiabatic limit is reached instantly and the mode function freezes out immediately whereas the background evolution experiences a transition period before it relaxes to the slow-roll dynamics.

For the sharp transition, the in-in integral in the bispectrum (5.11) can be divided into two nontrivial pieces : one is the contribution from the instant transition at τ_e, where η can be approximated by the step function as in (5.22); and the other one is the relaxation period from τ_e to τ_0, which is described by the analytical solution in Section 5.2.2.

For the first piece, the integral goes from τ_{e_-} to τ_{e_+}. At τ_{e_-}, the mode function is described by (5.5), and $\eta = -6$. At τ_{e_+}, the mode function is given by (5.36), and $\eta = -6-h$. Thus taking the squeezed limit and focusing on perturbation modes which exit the Hubble radius during the

non-attractor phase, we can write this contribution to the bispectrum as

$$\begin{aligned}\lim_{k_3/k\to 0} B^a_{\mathcal{R}}(k,k,k_3) &= -\Im\mathcal{R}_k(\tau_0)^2\mathcal{R}_{k_3}(\tau_0)\int_{\tau_{e_-}}^{\tau_{e_+}} d\tau a^2\epsilon\eta' \\ &\quad\times\left[\mathcal{R}^*_k(\tau_{e_-})\mathcal{R}^*_k(\tau_{e_-})\mathcal{R}^{*\prime}_{k_3}(\tau_{e_-})\theta(\tau_e-\tau)\right. \\ &\quad\left.+\mathcal{R}^*_k(\tau_{e_+})\mathcal{R}^*_k(\tau_{e_+})\mathcal{R}^{*\prime}_{k_3}(\tau_{e_+})\theta(\tau-\tau_e)+\text{perm.}\right] \\ &= \frac{(2\pi)^4}{k_1^3k_3^3}P^2_{\mathcal{R}}\int_{\tau_{e_-}}^{\tau_{e_+}} d\tau\frac{-\eta'}{4}\frac{h\,(h+12)}{(h-6)^2} \\ &\quad\times\left[\theta(\tau_e-\tau)+\theta(\tau-\tau_e)\right]. \end{aligned} \tag{5.41}$$

Then via (5.22), the integral above yields

$$\begin{aligned}&\int_{\tau_{e_-}}^{\tau_{e_+}} d\tau\frac{h}{4}\frac{h\,(h+12)}{(h-6)^2}\theta'(\tau-\tau_e)\left[\theta(\tau_e-\tau)+\theta(\tau-\tau_e)\right] \\ &\quad=\frac{h^2}{4}\frac{h+12}{(h-6)^2}\,,\end{aligned} \tag{5.42}$$

where in the last step we took an integration by parts to reduce the integral to boundary terms.

The second part of the integral corresponds to the relaxation process after τ_e. Substituting the mode function (5.36) and (5.37) into (5.11), its contribution to the squeezed bispectrum is given by

$$\begin{aligned}\lim_{k_3/k\to 0} B^b_{\mathcal{R}}(k,k,k_3) &= \frac{(2\pi)^4}{k_1^3k_3^3}P^2_{\mathcal{R}}\int_{\tau_e}^{\tau_0} d\tau\frac{-\eta'}{8}\sqrt{\frac{\epsilon_0}{\epsilon}}\Bigg[2+\eta \\ &\quad+\frac{2h}{6-h}\frac{\tau^3}{\tau_e^3}(4+\eta)+\frac{h^2}{(6-h)^2}\frac{\tau^6}{\tau_e^6}(6+\eta)\Bigg]\end{aligned} \tag{5.43}$$

Using the analytical solution during the relaxation (5.16) and (5.17), the above integral becomes

$$\begin{aligned}&\int_{\tau_e}^{\tau_0} d\tau\frac{-\eta'}{8}\sqrt{\frac{\epsilon_V}{\epsilon}}\left[2+\eta+\frac{2h}{6-h}\frac{\tau^3}{\tau_e^3}(4+\eta)+\frac{h^2}{(6-h)^2}\frac{\tau^6}{\tau_e^6}(6+\eta)\right] \\ &\quad=-\frac{h}{4}\frac{6h+h^2+12\eta_V}{(6-h)^2}\,,\end{aligned} \tag{5.44}$$

where we used $\epsilon_0\simeq\epsilon_V$ which holds in the sharp transition with $\sqrt{2\epsilon_V}\gtrsim|\eta_V|$.

Adding these two contributions together, we get

$$\frac{3}{5}f_{\rm NL}=\frac{3h(h-2\eta_V)}{2(h-6)^2}\,. \tag{5.45}$$

As we see, the amplitude of local non-Gaussianity is mainly determined by the h parameter in sharp transition case. For $|h| \gg 1$, it yields the maximum value $f_{\rm NL} \simeq 5/2$, which recovers the result in the initial non-attractor phase. For the instant transition ($h = -6$), we get a reduced value $f_{\rm NL} = 5/8$. In general, the sharp transition suppresses the amount of local non-Gaussianity generated during the non-attractor phase. The extremal case is $h \to 0$, where we have negligible contribution $\frac{3}{5} f_{\rm NL} = -h\eta_V/12$, similar to the smooth transition result.

Concluding the subsection, we remark that the sharp transition of non-attractor inflation is different from the inflationary feature models, where due to the kink or step on the potential, one may have a short non-slow-roll period which connects two slow-roll stages before and after the local feature. Since initially inflation is on the slow-roll attractor, long wavelength modes will remain constant during the non-slow-roll period. Therefore these feature models cannot result in nontrivial local non-Gaussianity for large scale perturbations, and the consistency relation is still valid. The reason is that once the mode is frozen in the adiabatic limit it remains so regardless of what may happen after, because a constant is a solution of the EoM for the super-horizon mode function. However, in the sharp transition here, because of the initial non-attractor phase, long wavelength modes may continue to evolve on super-horizon scales. As a consequence, local non-Gaussianity can be modified on large scales due to the transition.

Related to this issue, it is also known that the presence of sharp feature on potential will generate scale-dependent oscillatory signals in power spectrum and non-Gaussianities (See e.g. [37] for a review). The argument is very general and should apply here as well. However, this sinusoidal oscillation starts to appear around the scale $k \sim 1/\tau_e$ and has a wavelength $\Delta k \sim 1/\tau_e$. So they appear at much shorter scales than what we are interested in in this paper.

5.2.5 δN calculation

The δN formalism [131–135, 142, 191] is a simple and intuitive approach to the non-linear behaviour of curvature perturbations. Based on the separate universe assumption, it mainly captures the super-horizon effects of the perturbation modes, thus it just provides what we need for the calculation of local non-Gaussianity. For non-attractor inflation, one extra subtlety one should take care of is that the number of e-folds N does not only depend on the initial field value ϕ, but also on the initial field velocity π [42]. In the following, via δN formalism we give a unified calculation of local non-

Gaussianity that captures both smooth and sharp transition cases, and recovers the in-in results in Section 5.2.3 and 5.2.4 in two extreme limits.

For the non-attractor phase, the number of e-folds N can be easily worked out. As in Section 5.2.2, we set $N = 0$, $\phi = \phi_e$ and $d\phi/dN = \pi_e$ at the end of the non-attractor phase, then the background equations (5.1) yield the following non-attractor solution in terms of e-folding number N

$$\phi(N) = \phi_e + \frac{\pi_e}{3}\left(1 - e^{-3N}\right) \ , \qquad \pi(N) \equiv \frac{d\phi}{dN} = \pi_e e^{-3N} \ . \tag{5.46}$$

Next we can invert this solution and obtain the e-folds of the non-attractor phase in terms of the initial ϕ and π

$$N_i = -\frac{1}{3}\ln\left[\frac{\pi}{\pi + 3\left(\phi - \phi_e\right)}\right] = -\frac{1}{3}\ln\frac{\pi}{\pi_e} \ , \tag{5.47}$$

where in the second equality we used the following relation of the non-attractor phase

$$3\left[\phi(N) - \phi_e\right] + \pi(N) = \pi_e. \tag{5.48}$$

For the subsequent transition and slow-roll stages, the analytical solutions are already worked out in (5.16) and (5.17). Here we need to study the evolution until the end of the transition, where the slow-roll attractor is reached. Let us set $N = N_f$ and $\phi = \phi_f$ at that time. Then N_f is big, and (5.16) yields the following approximation

$$\phi_f \simeq \frac{s-3-h}{s(s-3)}\pi_e e^{\frac{1}{2}(s-3)N_f} + \frac{2\pi_e h}{s^2-9} + \phi_e \ , \tag{5.49}$$

which gives us

$$\begin{aligned} N_f &\simeq \frac{2}{s-3}\ln\left[\frac{s(s-3)}{s-3-h}\left(\frac{\phi_f - \phi_e}{\pi_e} - \frac{2h}{s^2-9}\right)\right] \\ &= \frac{2}{s-3}\ln\left[\frac{1}{-2\eta_V\pi_e - 6\sqrt{2\epsilon_V}}\right] + const. \end{aligned} \tag{5.50}$$

In the second equality, we separate out the parts unrelated with initial condition (ϕ, π) as a constant. Note here, due to the relation (5.48), π_e and also h are determined by the initial ϕ and π in the non-attractor phase.

Finally, the total e-folding number from the non-attractor phase to the slow-roll stage counted backward in time is given by

$$N(\phi,\pi) = N_f - N_i = \frac{2}{s-3}\ln\left[\frac{1}{-2\eta_V\pi_e - 6\sqrt{2\epsilon_V}}\right] + \frac{1}{3}\ln\frac{\pi}{\pi_e} + const. \tag{5.51}$$

The δN formula is simply given by

$$\delta N = \frac{\partial N}{\partial \phi}\delta\phi + \frac{\partial N}{\partial \pi}\delta\pi + \frac{1}{2}\frac{\partial^2 N}{\partial \phi^2}\delta\phi^2 + \frac{\partial^2 N}{\partial\phi\partial\pi}\delta\phi\delta\pi + \frac{1}{2}\frac{\partial^2 N}{\partial \pi^2}\delta\pi^2 \ . \quad (5.52)$$

Since $\delta\phi$ is approximately constant on super-horizon scales, $\delta\pi$ is exponentially suppressed and thus can be neglected. As a result, from (5.51) we get

$$\begin{aligned} \delta N &= \left(\frac{\partial N_f}{\partial\phi} - \frac{\partial N_i}{\partial\phi}\right)\delta\phi + \frac{1}{2}\left(\frac{\partial^2 N_f}{\partial\phi^2} - \frac{\partial^2 N_i}{\partial\phi^2}\right)\delta\phi^2 \quad (5.53) \\ &= \left(-\frac{1}{\pi_e} + \frac{3}{3\sqrt{2\epsilon_V} + \eta_V\pi_e}\right)\delta\phi \\ &\quad + \left[\frac{3}{2\pi_e^2} - \frac{9\eta_V}{2(3\sqrt{2\epsilon_V} + \eta_V\pi_e)^2}\right]\delta\phi^2 \ , \quad (5.54) \end{aligned}$$

where again we used the initial condition dependence of $\pi_e(\phi,\pi)$ from (5.48). And the local non-Gaussianity directly follows

$$\frac{3}{5}f_{\rm NL} = \frac{1}{2}\frac{\partial^2 N}{\partial\phi^2}\Bigg/\left(\frac{\partial N}{\partial\phi}\right)^2 = \frac{3\left[4(\eta_V-3)\eta_V + h^2 + 4\eta_V h\right]}{2(2\eta_V + h - 6)^2} \quad (5.55)$$

This calculation is valid for both smooth transition ($h \to 0$) and sharp transition ($h \neq 0$). As we discussed previously, η_V is always small, but $|h|$ can be large for the sharp transition. Thus similar with the in-in result (5.45), when $|h| \gg 1$, we recover $f_{\rm NL} = 5/2$. For the smooth transition or sharp transition with small h, we get $f_{\rm NL} \simeq -5\eta_V/6 = 5\eta_0/12$, where η_0 is the second Hubble slow-roll parameter in the slow-roll stage. Note that this also agrees with the full in-in calculation. In such cases, the in-in result from cubic interaction term (5.10) is sub-dominant, and thus the leading contribution comes from the field redefinition (5.8), which yields the same result as above.

We close this section by some concluding remarks. It is interesting to discuss the implications of our results on the consistency relation violation in canonical non-attractor inflation. As we know, the power spectrum generated in the non-attractor phase is scale-invariant with $n_s - 1 = 0$. However, the final result (5.55) yields nonzero value for $f_{\rm NL}$ after the transition. Even in the smooth transition case where $f_{\rm NL}$ is slow-roll suppressed, we do not have $f_{\rm NL} = \frac{5}{12}(1-n_s)$. Therefore, the consistency relation is still violated in the non-attractor inflation with full consideration of the transition process.

It is also interesting to notice that $f_{\rm NL} = 5/2$ is the maximum non-Gaussianity that one can obtain from such a model irrespective of the details of the transition period. This upper bound holds true even if one considers either a bump potential (where the slope at the transition point is negative) or a step potential (where the potential is discontinuous). That is, although the final $f_{\rm NL}$ as a function of parameters is clearly different for these cases, its value cannot exceed the $f_{\rm NL}$ that is generated purely during the non-attractor phase. In terms of δN formalism, there can be two contributions to the final non-Gaussianity: one from the non-attractor e-folds N_i in (5.51), another one from N_f. When N_i terms are the dominant contribution in the δN expansion (5.53), we recover the $\mathcal{O}(1)$ non-Gaussianity of the non-attractor phase. In the opposite limit, where N_f terms are dominating, it turns out that the non-Gaussianity is small. This is an interesting observation without rigorous proof. But we remark that the N_f part of the evolution is basically the case with non-slow-roll initial condition on a slow-roll potential, which is generically expected to yield small non-Gaussianity, as we argued in Section 5.2.3.2. Thus if N_f terms dominate in δN expansion (5.53), we expect a slow-roll suppressed $f_{\rm NL}$. As a consequence, the upper bound is given by the non-attractor result $f_{\rm NL} = 5/2$ when N_i terms contribute.

5.3 Models with non-canonical kinetic terms

After studying the transition in the canonical ultra-slow-roll inflation, it is also interesting to re-examine the non-canonical model presented in [43, 184]. We will discuss the background evolution in details. However, since this model cannot be considered as a realistic model of inflation due to the fine tuning of its initial conditions, we study the perturbations only in a specific limit where the analytic calculation is still tractable.

In this model the non-attractor inflation is realized by a k-essence field with the following Lagrangian

$$\mathcal{L} = P(X,\phi) = X + \frac{X^\alpha}{M^{4\alpha-4}} - V(\phi)\ , \qquad V(\phi) = V_0 + v\phi^\beta\ , \tag{5.56}$$

where $X = -\frac{1}{2}(\partial\phi)^2$, and α, M, V_0, v, β are free parameters. In this model, the sound speed c_s is given by

$$c_s^2 \equiv \frac{P_{,X}}{P_{,X} + 2XP_{,XX}} = \frac{1 + \alpha\left(\frac{X}{M^4}\right)^{\alpha-1}}{1 + \alpha(2\alpha-1)\left(\frac{X}{M^4}\right)^{\alpha-1}}. \tag{5.57}$$

The following variables are also defined here for future reference:

$$\Sigma \equiv XP_{,X} + 2X^2P_{,XX} = \frac{XP_{,X}}{c_s^2}\,, \tag{5.58}$$

$$\lambda \equiv X^2P_{,XX} + \frac{2}{3}X^3P_{,XXX} = \frac{XP_{,X}}{c_s^2}(1-c_s^2)\frac{2\alpha-1}{6}\,. \tag{5.59}$$

To the best of our knowledge, so far this is the only model which can give us $f_{\rm NL}^{\rm local} \gg 1$ in single-field inflation with Bunch-Davies initial state. In this section, we will give a detailed analysis for the transition process in this model, and perform the full calculation to test whether large non-Gaussianity remains or not.

5.3.1 Background evolution of k-essence non-attractor model

First of all, let us focus on the background dynamics of this model. The equation of motion for inflaton can be written as

$$\left(\frac{\ddot{\phi}}{c_s^2} + 3H\dot{\phi}\right)\left[1+\alpha\left(\frac{X}{M^4}\right)^{\alpha-1}\right] + V_\phi = 0\,. \tag{5.60}$$

From the above equation and (5.57) we can see that one important parameter here for the evolution is the ratio X/M^4. For $X \gg M^4$, this model is non-canonical with $c_s^2 \simeq 1/(2\alpha-1)$; but for $X \ll M^4$, it returns to the canonical case. In this model initially the inflaton field climbs up the hilltop potential, with the kinetic energy dominated by the non-canonical term. Later on, as X decreases dramatically in the non-attractor phase, the system would go from the non-canonical regime to the canonical regime.

For k-essence field, the slow-roll parameters are expressed as

$$\epsilon \equiv -\frac{\dot{H}}{H^2} = \frac{XP_{,X}}{H^2}\,, \tag{5.61}$$

$$\eta \equiv \frac{\dot{\epsilon}}{H\epsilon} \simeq \frac{\ddot{\phi}}{H\dot{\phi}}\left(1+\frac{1}{c_s^2}\right)\,. \tag{5.62}$$

As we know, a non-attractor phase happens when $\epsilon \propto a^{-6}$ and $\eta \simeq -6$. In the original papers [43, 184], an ansatz $\phi(t) \propto a^\kappa$ was used to get the initial non-attractor stage. This was achieved by letting the V_ϕ term compete with the $\ddot{\phi}$ and $\dot{\phi}$ terms in the equation of motion (5.60). And the following conditions for parameter choices are required

$$\beta = 2\alpha\,, \quad \kappa = \frac{\eta}{2\alpha}\,, \quad v = -\frac{M^4}{c_s^2}\left(\frac{V_0\kappa^2}{6M^4}\right)^\alpha\left(1+\frac{3c_s^2}{\kappa}\right)\,. \tag{5.63}$$

However, it is still not clear how the system transits to the attractor phase in details. In the following we perform a full numerical study of the "non-attractor to slow-roll" transition in the k-essence model. Before that, we summarize the generic behaviour for the evolution first:

The main results of the numerical solution are shown in Figure 5.5. At the beginning, since the potential is tuned to accommodate with the ansatz as shown in (5.63), inflation occurs in the phase with $\eta = -6$, while $X \gg M^4$ gives a small sound speed. We call this initial stage the *non-attractor I*. Then as the inflaton approaches the hilltop, the V_ϕ term in (5.60) becomes subdominant, and thus the equation of motion becomes $\ddot{\phi} + 3Hc_s^2\dot{\phi} \simeq 0$, which according to (5.62) yields

$$\eta = -3(c_s^2 + 1) \ . \tag{5.64}$$

Since the inflaton field is still non-canonical ($c_s \ll 1$), we have $\eta \simeq -3$. We dub this period as the *non-attractor II* phase. Next, X continues decreasing and becomes smaller than M^4, then the canonical term in $P(X, \phi)$ begins to dominate the kinetic energy of inflaton. After that, the scalar field becomes canonical, and we call this moment the *canonical transition*. And from (5.64), we see the system goes to the canonical non-attractor regime with $\eta = -6$. This stage has the same behaviour with the canonical non-attractor model, and is called *non-attractor III* here. Finally, the following transition to the slow-roll attractor is the same as what we discussed in Section 5.2. As we see, the "non-attractor to slow-roll" transition is much more complicated in the non-canonical model. One important feature is that there is also a canonical transition prior to the slow-roll attractor phase. This qualitative description is confirmed by the numerical analysis below.

Numerical Study.

Following the choice of parameter values in [43, 184], here we take $\alpha =$

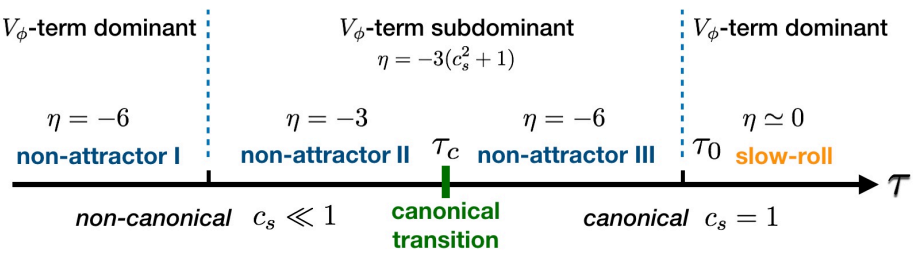

Figure 5.5: The transition process in the k-essence non-attractor model.

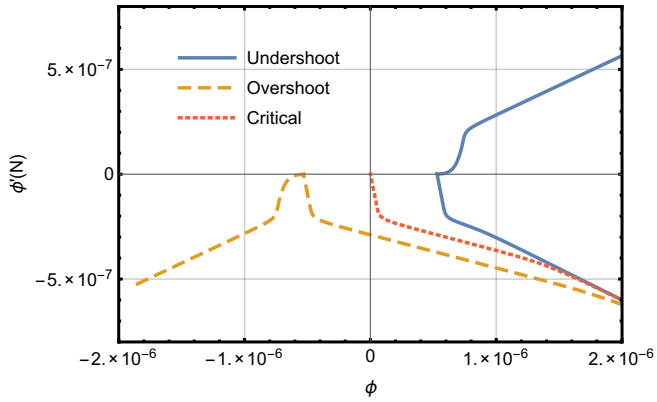

Figure 5.6: The phase space diagram $(\phi, \frac{d\phi}{dN})$ for the k-essence non-attractor model.

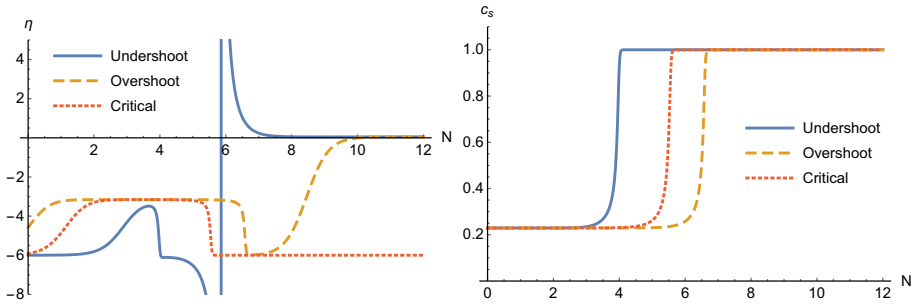

Figure 5.7: The evolution of η and c_s in the k-essence non-attractor model.

10, $M = 5 \times 10^{-5}$, $V_0 = 6.25 \times 10^{-4}$, while v and β are given by the relation in (5.63). Initially inflaton field is set to roll up the hilltop potential from $\phi_i = 2 \times 10^{-6}$. Then via varying the initial field velocity, we find different transition behaviours. The numerical solutions of background dynamics are shown here. Figure 5.6 gives us the phase space diagram. In Figure 5.7, we focus on the evolution of two parameters: the second slow-roll parameter η, which is important for the non-attractor behaviour, and the sound speed c_s, which tells if inflaton field is canonical or not.

From these figures, we can see a generic pattern for the transition process: after the non-attractor I stage ($\eta \simeq -6$), inflation first enters the non-attractor II phase ($\eta \simeq -3$), and later as shown by the evolution of c_s, the canonical transition happens. Here we introduce a critical field velocity $\dot{\phi}_c$, for which inflaton can just reach the top of the potential and will stay there forever. Then accordingly the numerical analysis can be classified into

three representative cases:

- *Undershoot* (blue curves). This corresponds to the case where the initial field velocity is smaller than $|\dot{\phi}_c|$. After a very short non-attractor II phase, in the canonical non-attractor regime, inflaton stops somewhere before reaching the top of the potential and then rolls backward to initiate the slow-roll phase. At the turning point, since $\dot{\phi} = 0$, we have $\epsilon = 0$ and $\eta = \infty$.

- *Critical case* (red curves). The initial field velocity is set to be the critical value. In this case, after the canonical transition, the system reaches an eternal non-attractor stage with $\eta = -6$ and $c_s = 1$.

- *Overshoot* (orange curves). This is the case where the initial field velocity is larger than $|\dot{\phi}_c|$. As we see, here the non-attractor I stage is very short, while the non-attractor II phase lasts for a longer time, during which the inflaton field rolls over the top of the potential. After this, inflation goes into the canonical non-attractor regime and then transits to the slow-roll stage as we discussed before.

In these three cases, only *undershoot* and *overshoot* can give us successful "non-attractor to slow-roll" transition. Although the details can be very different, both these two numerical results verify the evolution in Figure 5.5 and the qualitative description there, i.e. in these non-canonical models the canonical transition always occurs before the relaxation to slow-roll. This holds true at least for our choice of parameters which are consistent with [43]. It would be interesting to see whether it is also true for other values of the parameters; however, we do not go further in this direction here. In the following rough calculation of non-Gaussianity, we shall use this general transition behaviour as the basic setup and refer to these two cases (overshoot and undershoot) for details.

5.3.2 Non-Gaussianities

With the above background analysis, we are ready to study the primordial perturbations. At first glance, a full calculation could be very difficult, since the transition behaviour is quite complicated. Numerical calculation also faces a technical UV-convergence problem because the non-attractor phase is rather short.

However, the problem can be simplified if we focus on the generic pattern of the transition. As we see, the main difficulty comes from the occurrence

of the non-attractor II phase, during which we have $\eta = -3$. If this period lasts for a long time (as in the overshoot case), we cannot get a scale-invariant power spectrum for curvature modes that are leaving the horizon during this period. This can be interesting for the research of features in the primordial perturbations, but in this paper we keep focusing on the behaviour of non-Gaussianity during the transition. And for the analysis of the bispectrum, it is the canonical transition that plays a crucial role here.

Therefore we propose the following limit case for analytical study: The non-attractor II phase is so short such that its effect can be neglected. In this approximation, before the slow-roll attractor, η can always be seen as -6 and the canonical transition occurs at some time in this stage. In principle this does not agree with the numerical results since it breaks the relation (5.64), but it can be seen as an approximated description of the undershoot case.

Based on the qualitative analysis above, next we focus on the modes which exit the Hubble radius during the non-attractor I stage, and do the back-of-the-envelope estimates for the non-Gaussianities. The starting point is the cubic action for a general k-essence field in the comoving gauge [192, 193]. Since $\epsilon \ll 1$ always holds true during the whole transition process, again we can focus on the decoupling limit with only three operators left

$$S_3 \supset \int dtd^3x \left[-\frac{a^3\epsilon}{c_s^2}\Xi\frac{\dot{\mathcal{R}}^3}{H} - 3\frac{a^3\epsilon}{c_s^4}(1-c_s^2)\mathcal{R}\dot{\mathcal{R}}^2 + \frac{a^3\epsilon}{2c_s^2}\frac{d}{dt}\left(\frac{\eta}{c_s^2}\right)\mathcal{R}^2\dot{\mathcal{R}}\right] . \quad (5.65)$$

The coefficient of the $\dot{\mathcal{R}}^3$ term is given by

$$\Xi \equiv 1 - \frac{1}{c_s^2} + \frac{2\lambda}{\Sigma} = \left(\frac{2\alpha-1}{3} - \frac{1}{c_s^2}\right)(1-c_s^2) , \quad (5.66)$$

where (5.57), (5.58), (5.59), (5.61) and (5.62) are used for the second equality. Before the canonical transition we have $\Xi = 2(c_s^2-1)/3c_s^2$. This coefficient and the one for the second term in (5.65) both vanish after the canonical transition. At the same time, the following field redefinition is also considered in [184]

$$\mathcal{R} = \mathcal{R}_n + \frac{\eta}{4c_s^2}\mathcal{R}_n^2 + \frac{1}{c_s^2 H}\mathcal{R}_n\dot{\mathcal{R}}_n , \quad (5.67)$$

which can give large non-Gaussianity in the non-attractor I phase. However, since this term should be evaluated in the slow-roll stage where $\eta \simeq 0$ and $\dot{\mathcal{R}} \simeq 0$, its contribution can be neglected. For the last operator in (5.65), again we re-express it via integration by part

$$-\int dtd^3x \frac{d}{dt}\left[\frac{a^3\epsilon}{6c_s^2}\frac{d}{dt}\left(\frac{\dot{\eta}}{c_s^2}\right)\right]\mathcal{R}^3 + \text{surface term} . \quad (5.68)$$

Plugging in the numerical solution, we confirm that the effective coupling here is also negligible during the transitions as in the canonical case.

The difference from the canonical case arises due to a couple of interaction terms in the Lagrangian that are unique for the non-canonical models. Let us estimate their contributions. The first term in (5.65) gives the bispectrum of

$$B_{\dot{\mathcal{R}}^3}(k_1,k_2,k_3) = 12\Im\Bigg[\mathcal{R}_{k_1}(\tau_0)\mathcal{R}_{k_2}(\tau_0)\mathcal{R}_{k_3}(\tau_0) \times\int_{-\infty}^{\tau_c}\frac{a\epsilon d\tau}{c_s^2 H}\,\Xi(\tau)\mathcal{R}'^*_{k_1}(\tau)\mathcal{R}'^*_{k_2}(\tau)\mathcal{R}'^*_{k_3}(\tau)\Bigg], \quad (5.69)$$

where τ_c is the conformal time at the canonical transition, and τ_0 is the one at the beginning of the slow-roll phase. Since Ξ vanishes after the canonical transition, the in-in integral stops at τ_c. Another subtlety here is the mode function $\mathcal{R}_k$. Since there is a sudden change of c_s around the transition, in principle one has to use the general slow-roll formalism to solve its behaviour, taking into account the discontinuity around the canonical transition. However, since the integral above vanishes right after the canonical transition, the mode function after transition becomes irrelevant for that integral; and it is easy to check that it does not affect the prefactors $\mathcal{R}_{k_i}(\tau_0)$ in (5.69) at leading order either. Therefore, for a rough estimate, here we take the following zeroth order approximation

$$\mathcal{R}_k = \frac{H}{\sqrt{4\epsilon c_s k^3}}(1+ic_s k\tau)e^{-ic_s k\tau} \qquad \mathcal{R}'_k = \frac{H}{\sqrt{4\epsilon c_s k^3}}c_s^2 k^2\tau e^{-ic_s k\tau} - \frac{3}{\tau}\mathcal{R}_k \quad (5.70)$$

Since we mainly care about the modes crossing the Hubble radius during the initial non-attractor phase, we have $-k\tau_0 \ll -k\tau_c \ll 1$. Meanwhile in this limited case we assume $\eta = -6$ before the time τ_0, which means for this whole period $\epsilon(\tau) = \epsilon_0\tau^6/\tau_0^6$. As a result, the bispectrum becomes

$$B_{\dot{\mathcal{R}}^3}(k_1,k_2,k_3) = (2\pi)^4\left(\frac{H^2}{8\pi^2\epsilon_0 c_s}\right)^2\frac{3(c_s^2-1)}{4c_s^2}\left(\frac{\tau_0}{\tau_c}\right)^6\frac{k_1^3+k_2^3+k_3^3}{k_1^3k_2^3k_3^3}, \quad (5.71)$$

which is in the local shape. As we see, when $\tau_0 = \tau_c$ it returns to the previous result in [184]. However, if the canonical transition occurs ΔN e-folds before the slow-roll phase, $(\tau_0/\tau_c)^6$ would give a suppression factor $\sim e^{-6\Delta N}$. Correspondingly in the squeezed limit, we get the following amplitude of non-Gaussianity

$$\frac{3}{5}f_{\rm NL}^{\dot{\mathcal{R}}^3} = \frac{3}{2c_s^2}(c_s^2-1)\left(\frac{\tau_0}{\tau_c}\right)^6 \sim -\frac{3}{2c_s^2}(1-c_s^2)e^{-6\Delta N}\,. \quad (5.72)$$

This suppression is caused by the super-Hubble evolution of the curvature perturbation after the canonical transition. Since $\mathcal{R}$ keeps growing until the end of the non-attractor phase, the difference between $\mathcal{R}(\tau_c)$ and $\mathcal{R}(\tau_0)$ yields the suppression factor above.

With a similar procedure, the second term in (5.65) gives

$$\begin{aligned} B_{\mathcal{R}\dot{\mathcal{R}}^2}(k_1,k_2,k_3) &= (2\pi)^4\Big(\frac{H^2}{8\pi^2\epsilon_0 c_s}\Big)^2\Big(\frac{\tau_0}{\tau_c}\Big)^3 \\ &\quad\times\Big[3\left(\frac{\tau_0}{\tau_c}\right)^3-2\Big]\frac{3(1-c_s^2)}{8c_s^2}\frac{k_1^3+k_2^3+k_3^3}{k_1^3k_2^3k_3^3}\,, \end{aligned} \tag{5.73}$$

Therefore, it is still in the local form and the final amplitude of non-Gaussianity is given by

$$\frac{3}{5}f_{\rm NL}^{\mathcal{R}\dot{\mathcal{R}}^2}=\frac{3}{4c_s^2}(1-c_s^2)\Big(\frac{\tau_0}{\tau_c}\Big)^3\Big[3\left(\frac{\tau_0}{\tau_c}\right)^3-2\Big]\sim-\frac{3}{2c_s^2}(1-c_s^2)e^{-3\Delta N}\,, \tag{5.74}$$

where in the last step we ignored the $e^{-6\Delta N}$ suppression term. Again, the above result agrees with the one in [184] when $\tau_0=\tau_c$. In general, the duration of the non-attractor stage after the canonical transition can be $\Delta N\sim\mathcal{O}(1)$, thus the large non-Gaussianity generated in the non-attractor stage can be suppressed a lot. Summing up the leading terms of two contributions above, we get the following overall amplitude

$$\frac{3}{5}f_{\rm NL}\sim-\frac{3}{2c_s^2}e^{-3\Delta N}\,. \tag{5.75}$$

This estimate shows us how the non-Gaussianity generated in the initial non-attractor stage is suppressed after the canonical transition. Notice that the sound speed is determined by the model parameters, while the duration of the non-attractor III stage is related to the choice of initial conditions, thus c_s and ΔN are two independent parameters. Thus, we conclude that, it is still possible to have large non-Gaussianity in single field inflation.

5.4 Conclusion and discussion

In this paper, we investigated the production of primordial non-Gaussianities from models of non-attractor inflation. We revisited various non-attractor models constructed in the literature in order to understand the evolution of large local non-Gaussianity when the models undergo the transition from the non-attractor phase to slow-roll phase. The purpose of this study is

less of trying to present these fine-tuned toy-models as phenomenological candidates for data fitting, rather trying to understand more precisely the physical implications of Maldacena's single field consistency relation and various counter-examples that have been constructed.

Comparing with previous studies, we pay special attention to the transition period from the non-attractor phase to the conventional slow-roll phase. Such a transition is necessary for these models to have sufficient efolds or have the correct amplitude of density perturbations. We considered two types of non-attractor inflation, which are driven by a canonical scalar field and a non-canonical k-essence field, respectively.

For models with canonical kinetic terms, we consider two different evolutionary processes after the non-attractor phase: smooth transition and sharp transition. Through the calculation of both in-in and δN formalism, we find that a full consideration of the transition process generically suppresses the local non-Gaussianity generated in the non-attractor phase, but Maldacena's consistency condition is still violated. In the smooth transition, the super-horizon modes continue evolving after the non-attractor phase, and the $\mathcal{O}(1)$ non-Gaussian signals are completely erased during the transition period and the final $f_{\rm NL}$ at the end of inflation is slow-roll suppressed. Meanwhile for sharp transition, the final amplitude of the local non-Gaussianity generated in the non-attractor phase depends on the details of the transition process. In the extremal cases where the curvature perturbation freezes immediately right after the non-attractor phase, we get the maximum possibility of local non-Gaussianity, which recovers the original result in the non-attractor phase $f_{\rm NL} = 5/2$.

For models with non-canonical kinetic terms, although similar situation applies to one of the terms in the Lagrangian, the non-Gaussianities coming from two other terms, which are unique to non-canonical models, survive. Nonetheless, our rough estimations of this case show that the effect of smooth transition is still non-negligible. In addition to the contribution $\sim 1/c_s^2$ obtained in the previous studies, the transition period contributes to an extra suppression factor due to mode evolution outside the horizon during the transition phase. Since these two contributions are independent of each other, the conclusion, that the large local non-Gaussianity can be obtained in such single field models, remains the same; but the expression of $f_{\rm NL}$ should be revised.

As a final remark, we note that, recently, Ref. [194] argued that the $\mathcal{O}(1)$ local bispectrum generated from the canonical non-attractor inflation model, as calculated in Ref. [42], is not locally observable. The study of

Ref. [194] focuses on the non-attractor phase. Here we will not analyze their argument in detail which is beyond the scope of this paper. For our purpose, we simply point out that one of the main differences between their work and ours is that we have analyzed in details the subsequent transition process from the non-attractor phase to the standard single field slow-roll inflation, in order to be able to discuss the observability at all. As we have concluded, the final $f_{\rm NL}$ can range anywhere between zero and a value much larger than 1. If the value of $f_{\rm NL}$ is much larger than $1-n_s$, these local bispectra should be in principle observable. At the reheating surface, these local bispectra are indistinguishable from those arising from models in which we replace the single field non-attractor phase with a multifield phase and use the multifield phase to generate the same amount of primordial local bispectra.

6 Non-Gaussianity in general single field matter bounce

Abstract: We extend the matter bounce scenario to a more general theory in which the background dynamics and cosmological perturbations are generated by a k-essence scalar field with an arbitrary sound speed. When the sound speed is small, the curvature perturbation is enhanced, and the tensor-to-scalar ratio, which is excessively large in the original model, can be sufficiently suppressed to be consistent with observational bounds. Then, we study the primordial three-point correlation function generated during the matter-dominated contraction stage and find that it only depends on the sound speed parameter. Similar to the canonical case, the shape of the bispectrum is mainly dominated by a local form, though for some specific sound speed values a new shape emerges and the scaling behaviour changes. Meanwhile, a small sound speed also results in a large amplitude of non-Gaussianities, which is disfavored by current observations. As a result, it does not seem possible to suppress the tensor-to-scalar ratio without amplifying the production of non-Gaussianities beyond current observational constraints (and vice versa). This suggests an extension of the previously conjectured no-go theorem in single field nonsingular matter bounce cosmologies, which rules out a large class of models. However, the non-Gaussianity results remain as a distinguishable signature of matter bounce cosmology and have the potential to be detected by observations in the near future.

Keywords: Alternative to inflation, primordial non-Gaussianity, cosmological perturbation theory

Based on:

Y. Li, J. Quintin, D.-G. Wang, Y.-F. Cai
Matter bounce cosmology with a generalized single field: non-Gaussianity and an extended no-go theorem
JCAP 1703 (2018), no. 03 031, [arXiv:1612.02036].

6.1 Introduction

Matter bounce cosmology [31] is a very early universe structure formation scenario alternative to the paradigm of inflationary cosmology (see, e.g., [195] for a review of inflation, its problems and its alternatives). The idea is that quantum fluctuations exit the Hubble radius in a matter-dominated contracting phase before the Big Bang, which generates a scale-invariant power spectrum of curvature perturbations [29, 30]. The contracting phase is then followed by a bounce and the standard phases of hot Big Bang cosmology. This construction solves the usual problems of standard Big Bang cosmology such as the horizon and flatness problems, but in addition, it is free of the trans-Planckian corrections that plague inflationary cosmology [26], and one can naturally avoid reaching a singularity at the time of the Big Bang (contrary to standard[1] inflation [25, 197]) under the assumption that new physics appears at high energy scales [31, 195]. Nonsingular bounces can be constructed in various ways using matter violating the Null Energy Condition (NEC), with a modified gravity action, or within a quantum theory of gravity (see the reviews [27, 28, 31, 198, 199] and references therein).

A typical way of constructing a nonsingular matter bounce cosmology is to assume the existence of a new scalar field. With a canonical Lagrangian, the oscillation of the scalar field can drive a matter-dominated contracting phase when the ratio of the pressure to the energy density averages zero. As the energy scale of the universe increases, new terms can appear in the Lagrangian that violate the NEC and drive a nonsingular bounce. For example, using a Galileon scalar field [200] (or equivalently, in Horndeski theory [201]), one can construct a stable NEC violating nonsingular bounce [202–207] that may be free of ghost and gradient instabilities [208, 209] (see, however, the difficulties in doing so as pointed out by [210–213]).

To distinguish the matter bounce scenario from inflation observationally, studying primordial non-Gaussianities is a useful tool[2]. In the case of inflation, after the calculation of the bispectra generated in single field slow-roll models [39], there have been many studies in the past decade trying to extend the simplest result, which largely enriched the phenomenology of nonlinear perturbations (see [37, 38] for reviews). In particular,

[1] The singularity before inflation could be avoided with, for example, bounce inflation (e.g., [196]).

[2] Another observable quantity, besides non-Gaussianities, that would allow one to differentiate between inflation and the matter bounce scenario is the running of the scalar spectral index (see [214, 215]).

one important progress has been to generalize the canonical inflaton to a k-essence scalar field [91, 92], such as k-inflation [216, 217] and DBI models [95, 96], which are collectively known as general single field inflation [193]. In these models, due to the effects of a small sound speed, the amplitude of the bispectrum is enhanced and interesting shapes emerge [37, 38, 94, 192, 193, 218]. In a matter-dominated contracting phase, the calculation of the bispectrum has only been done by [186] for the original matter bounce model with a canonical scalar field. A natural extension is thus to consider a k-essence scalar field[3] similarly to what has been done in inflationary cosmology, especially since the appearance of a noncanonical field is quite common in the literature of nonsingular bouncing cosmology in order to violate the NEC as explained above. Because the perturbations behave differently in matter bounce cosmology compared to inflation, in particular due to the growth of curvature perturbations on super-Hubble scales during the matter-dominated contracting phase, the canonical matter bounce yields non-Gaussianities with negative sign and order one amplitude, which differs from the results in canonical single field inflation. It would be interesting to explore how these non-Gaussianity results change when one generalizes the original matter bounce scenario to be based on a k-essence scalar field.

Besides non-Gaussianity, another interesting observable for very early universe models is the tensor-to-scalar ratio r. In the original matter bounce scenario, this ratio is predicted to be very large [225, 226]. Indeed, the scalar and tensor power spectra share the same amplitude, and accordingly, the tensor-to-scalar ratio is naturally of order unity [227]. This is well beyond the current observational bound from the Cosmic Microwave Background (CMB), which states that $r < 0.07$ at 95% confidence [228].

A resolution to this problem is to allow for the growth of curvature perturbations during the bounce phase, which suppresses the tensor-to-scalar ratio. However, curvature perturbations tend to remain constant through the bounce phase on super-Hubble scales [207, 229]. In fact, amplification can only be achieved under some tuning of the parameters, and the overall growth is still limited[4] [227]. Yet, if the scalar modes are amplified,

[3]This could be easily further generalized to a Galileon field [219], which has also been done for inflation (see, e.g., [220–224]).

[4]The studies of Refs. [207, 227, 229] have been carried out for models where the nonsingular bounce is attributed to a noncanonical scalar field. Loop quantum cosmology (LQC) provides an alternative class of nonsingular bouncing models that could suppress r during the bounce. In LQC, the amplitude of the suppression depends on the equation of state during the bounce; if it is close to zero, then the suppression is very strong

another problem follows in that it leads to the production of large non-Gaussianities [227], a problem that might be generic to a large class of nonsingular bounces [232, 233]. Again, these large non-Gaussianities are excluded by current measurements from the CMB [109]. This leads to conjecture that single field matter bounce cosmology suffers from a no-go theorem [227], which states that one cannot satisfy the bound on r without violating the bounds on non-Gaussianities and vice versa.

There is another way to suppress the tensor-to-scalar ratio if the sound speed of the perturbations can be smaller than the speed of light during the matter-dominated contracting phase. For example, in the ΛCDM bounce scenario [230] (and its extension [234]; see the review [215]), if there exists a form of dark matter with a small sound speed that dominates the contracting phase when the scale-invariant power spectra are generated, then the tensor-to-scalar ratio is already suppressed proportionally to the sound speed. Therefore, this provides another motivation to study non-Gaussianities when the sound speed is small during the matter-dominated contracting phase. An immediate question is whether the no-go theorem still holds true in this case or whether it can be circumvented. In this work, we want to explore this possibility of having a k-essence scalar field that would mimic dust-like matter with a small sound speed at low energies and that could play the role of the NEC violating scalar field during the bounce.

In this paper, we will evaluate the bispectrum produced by a k-essence scalar field in a matter-dominated contracting universe. This more general setup will yield richer features, which have the potential to be detected by future non-Gaussianity observations. In particular, the shapes, amplitudes, and scaling behaviors will be studied systematically. We will show that a small sound speed implies a large amplitude associated with the three-point function. Accordingly, we will claim that the no-go theorem is not circumvented but rather extended: in single field matter bounce cosmology, one cannot suppress the tensor-to-scalar ratio, either from the onset of the initial conditions in the matter contracting phase or from the amplification of the curvature perturbations during the bouncing phase, without producing large non-Gaussianities.

The outline of the paper is as follows. In section 6.2, we first introduce the background dynamics of the matter bounce scenario and introduce the class of k-essence scalar field models that we study in this paper. In section 6.3, we calculate the power spectra of curvature perturbations and ten-

(see [226, 230, 231] and references therein for a discussion of LQC effects in nonsingular bouncing cosmology).

sor modes and show how a small sound speed coming from the k-essence scalar field allows for the suppression of the tensor-to-scalar ratio. We then consider the primordial non-Gaussianity in section 6.4. Using the in-in formalism, we evaluate every contribution to the three-point function and give a detailed analysis of the size and shapes of the resulting bispectrum. In section 6.5, we compute the amplitude parameter of non-Gaussianities in different limits and finally combine these results with the bound on the sound speed from section 6.3 to show that the no-go theorem in matter bounce cosmology is extended. We summarize our results in section 6.6. Throughout this paper, we use the mostly plus metric convention, and we define the reduced Planck mass to be $M_{\rm pl} = (8\pi G_{\rm N})^{-1/2}$, where $G_{\rm N}$ is Newton's gravitational constant.

6.2 Setup and background dynamics

The idea of the matter bounce scenario is to begin with a matter-dominated contracting phase. At the background level, this corresponds to having a scale factor as a function of physical time given by

$$a(t) = a_B \left(\frac{t - \tilde{t}_B}{t_B - \tilde{t}_B} \right)^{2/3} , \tag{6.1}$$

and the Hubble parameter follows,

$$H(t) = \frac{2}{3(t - \tilde{t}_B)} , \tag{6.2}$$

where t_B corresponds to the time of the beginning of the bounce phase and $\tilde{t}_B$ corresponds to the time at which the singularity would occur if no new physics appeared at high energy scales. Accordingly, a_B is the value of the scale factor at t_B. In terms of the conformal time τ defined by $d\tau = a^{-1}dt$, the scale factor is given by

$$a(\tau) = a_B \left(\frac{\tau - \tilde{\tau}_B}{\tau_B - \tilde{\tau}_B} \right)^2 , \tag{6.3}$$

where τ_B and $\tilde{\tau}_B$ are the conformal times corresponding to t_B and $\tilde{t}_B$. Throughout the rest of this paper, the scale factor is normalized such that $a_B = 1$.

One can define the usual "slow-roll" parameters of inflation by

$$\epsilon \equiv -\frac{\dot{H}}{H^2} = \frac{3}{2}(1 + w) , \qquad \eta \equiv \frac{\dot{\epsilon}}{H\epsilon} , \tag{6.4}$$

where a dot denotes a derivative with respect to physical time, and $w \equiv p/\rho$ is the equation of state parameter with p and ρ denoting pressure and energy density, respectively. In the case of the matter bounce, the matter contracting phase implies that pressure vanishes, which is to say that

$$w = 0 \ , \qquad \epsilon = \frac{3}{2} \ , \qquad \eta = 0 \ . \tag{6.5}$$

If the pressure does not vanish exactly but is still very small, i.e. $|p/\rho| \ll 1$, then the values for w, ϵ, and η in equation (6.5) are only valid as leading order approximations, and they will be time dependent rather than constant. In this paper, we will work in the limit where equation (6.5) is valid.

In the usual matter bounce scenario, one would introduce a canonical scalar field to drive the matter-dominated contracting phase and describe the cosmological fluctuations. In this paper, we aim for more generality and assume that the perturbations are introduced by a k-essence scale field ϕ with Lagrangian density of the form[5]

$$\mathcal{L}_\phi = P(X, \phi) \ , \tag{6.6}$$

where $X \equiv -\partial_\mu \phi \partial^\mu \phi / 2$, and we assume that the scalar field is minimally coupled to gravity. The energy density and pressure of this scalar field are then given by

$$\rho = 2XP_{,X} - P \ , \qquad p = P \ , \tag{6.7}$$

where a comma denotes a partial derivative, e.g. $P_{,X} \equiv \partial P / \partial X$. Thus, the Friedmann equations read

$$3M_{\rm pl}^2 H^2 = 2XP_{,X} - P \ , \qquad M_{\rm pl}^2 \dot{H} = -XP_{,X} \ . \tag{6.8}$$

Since we want a matter-dominated contracting phase, the pressure of the scalar field should vanish (at least in average), and $\rho = 2XP_{,X} \propto a^{-3}$.

It is helpful to have one specific example where a k-essence field drives the matter contraction. Let us consider the following Lagrangian density:

$$\mathcal{L}_\phi = K(X) = \frac{1}{8}(X - c^2)^2 \ . \tag{6.9}$$

This type of Lagrangian belongs to a subclass of k-essence models $P(X, \phi)$ where the kinetic terms $K(X)$ are separate from the potential terms $V(\phi)$,

[5] For an introduction to such a Lagrangian in early universe cosmology with the derivation of the background equations of motion and the definition of the different parameters, see, e.g., [192, 193, 216, 217].

i.e. $P(X,\phi) = K(X) - V(\phi)$. Moreover, the above Lagrangian has vanishing potential. Then, the ghost condensate solution is given by $X = c^2$ and $\phi(t) = ct + \pi(t)$, with $\dot{\pi}(t) \ll c$. In this case, the background equations yield $p \simeq 0$ and $\rho \sim \dot{\pi} \propto a^{-3}$, which exactly corresponds to a matter-dominated universe. More details about this model can be found in [235]. We note that there should be also other forms of $P(X,\phi)$ that can drive a matter contraction, and remarkably, the analysis that follows in this paper is done in a *model-independent* way and does *not* rely on the specific model of equation (6.9).

The sound speed and another "slow-roll" parameter are defined by[6]

$$c_s^2 \equiv \frac{\partial p}{\partial \rho} = \frac{P_{,X}}{P_{,X} + 2XP_{,XX}} \ , \qquad s \equiv \frac{\dot{c}_s}{c_s H} \ . \tag{6.10}$$

Calculations will be done for a general sound speed, but as we will argue, we will be interested in the small sound speed limit, which can be realized with the appropriate form for $P(X,\phi)$. For instance, the explicit example given by equation (6.9) yields $\simeq \dot{\pi}/c \ll 1$. Furthermore, we will generally assume later that the sound speed remains nearly constant, which is to say that $|s| \ll 1$. We also define two other variables for later convenience,

$$\Sigma \equiv XP_{,X} + 2X^2 P_{,XX} = \frac{M_{\rm pl}^2 H^2 \epsilon}{2} \ , \tag{6.11}$$

and

$$\lambda \equiv X^2 P_{,XX} + \frac{2}{3} X^3 P_{,XXX} = \frac{X}{3}\Sigma_{,X} - \frac{1}{3}\Sigma \ . \tag{6.12}$$

The ratio λ/Σ will be of particular interest in the following sections. For inflation, it depends on the specific realization of the general single field, such as DBI and k-inflation models. For the matter bounce scenario, it can be obtained in an approximately model-independent way. The detailed calculation is in Appendix 6.A, where we find that the ratio λ/Σ can be expressed in terms of the sound speed, as shown by equation (6.81).

6.3 Mode functions and two-point correlation functions

We begin with an action of the form

$$S = \int d^4x \ \sqrt{-g} \left(\frac{1}{2} M_{\rm pl}^2 R + \mathcal{L}_\phi \right) \ , \tag{6.13}$$

[6] We assume that the cosmological perturbations will remain adiabatic throughout the matter-dominated contracting phase.

where g is the determinant of the metric tensor and R is the Ricci scalar. Importantly, we assume that the matter Lagrangian $\mathcal{L}_\phi$ has the general form of equation (6.6), but we do not restrict our attention to any specific model. By perturbing up to second order the above action, one finds[7]

$$S_2 = \int d\tau d^3x \; z^2 \left[\zeta'^2 - c_s^2(\nabla\zeta)^2\right] \; , \tag{6.14}$$

where $\zeta(\tau, x)$ denotes the curvature perturbation in the comoving gauge, i.e. on slices where fluctuations of the scalar field vanish ($\delta\phi = 0$). Also, a prime represents a derivative with respect to conformal time, $\nabla = \partial_i$ is the spatial gradient, and we define $z^2 \equiv 2\epsilon a^2 M_{\rm pl}^2/c_s^2$. Transforming to Fourier space, the second-order perturbed action becomes

$$S_2 = \int d\tau \int \frac{d^3k}{(2\pi)^3} \; z^2 \left[\zeta'(\mathbf{k})\zeta'(-\mathbf{k}) - c_s^2 k^2 \zeta(\mathbf{k})\zeta(-\mathbf{k})\right] \; , \tag{6.15}$$

where $k^2 \equiv \mathbf{k}\cdot\mathbf{k} = |\mathbf{k}|^2$. Upon quantization of the curvature perturbation, one has

$$\hat{\zeta}(\tau, \mathbf{k}) = \hat{a}_{\mathbf{k}}^\dagger u_k(\tau) + \hat{a}_{-\mathbf{k}} u_k^*(\tau) \; , \tag{6.16}$$

where the annihilation and creation operators satisfy the usual commutation relation $[\hat{a}_{\mathbf{k}}, \hat{a}_{\mathbf{k}'}^\dagger] = (2\pi)^3\delta^{(3)}(\mathbf{k} - \mathbf{k}')$. The equation of motion of the mode function is then given by

$$v_k'' + \left(c_s^2 k^2 - \frac{z''}{z}\right) v_k = 0 \; , \tag{6.17}$$

where the mode function is rescaled as $v_k = z u_k$ (v_k is called the Mukhanov-Sasaki variable). Together with the commutation relation $[\hat{\zeta}(\mathbf{k}_1), \hat{\zeta}'(\mathbf{k}_2)] = (2\pi)^3\delta^{(3)}(\mathbf{k}_1 + \mathbf{k}_2)$, one finds (see, e.g., [186])

$$u_k(\tau) = \frac{iA[1 - ic_s k(\tau - \tilde{\tau}_B)]}{2\sqrt{\epsilon c_s k^3}(\tau - \tilde{\tau}_B)^3} e^{ic_s k(\tau - \tilde{\tau}_B)} \tag{6.18}$$

$$u_k'(\tau) = \frac{iA}{2\sqrt{\epsilon c_s k^3}} \left(\frac{-3[1 - ic_s k(\tau - \tilde{\tau}_B)]}{(\tau - \tilde{\tau}_B)^4} + \frac{c_s^2 k^2}{(\tau - \tilde{\tau}_B)^2}\right) e^{ic_s k(\tau - \tilde{\tau}_B)} \tag{6.19}$$

to be the solution to the equation of motion (6.17) in the context of a matter-dominated contracting universe as described in the previous section. Here, A is a normalization constant that is determined by the quantum

[7] Again, see, e.g., [37, 192, 193, 217] for a derivation of the perturbation equations in k-essence early universe cosmology.

vacuum condition at Hubble radius crossing in the contracting phase, which is given by $A = (\tau_B - \tilde{\tau}_B)^2/M_{\rm pl}$.

The general two-point correlation functions are given by

$$\langle \hat{\zeta}(\tau_1, \mathbf{k}_1)\hat{\zeta}(\tau_2, \mathbf{k}_2)\rangle = (2\pi)^3\delta(\mathbf{k}_1 + \mathbf{k}_2)u^*_{k_1}(\tau_1)u_{k_1}(\tau_2) \ , \tag{6.20}$$

$$\langle \hat{\zeta}(\tau_1, \mathbf{k}_1)\hat{\zeta}'(\tau_2, \mathbf{k}_2)\rangle = (2\pi)^3\delta(\mathbf{k}_1 + \mathbf{k}_2)u^*_{k_1}(\tau_1)u'_{k_1}(\tau_2) \ , \tag{6.21}$$

and in particular, the power spectrum, evaluated at the bounce point τ_B (well after Hubble radius exit), is given by

$$\langle \hat{\zeta}(\tau_B, \mathbf{k})\hat{\zeta}(\tau_B, \mathbf{k}')\rangle = (2\pi)^3\delta^{(3)}(\mathbf{k} + \mathbf{k}')\frac{2\pi^2}{k^3}\mathcal{P}_\zeta(\tau_B, k) \ , \tag{6.22}$$

where

$$\mathcal{P}_\zeta(\tau_B, k) = \frac{A^2}{8\pi^2\epsilon c_s(\tau_B - \tilde{\tau}_B)^6} = \frac{1}{12\pi^2 c_s M^2_{\rm pl}(\tau_B - \tilde{\tau}_B)^2} \ . \tag{6.23}$$

The scale invariance of the power spectrum in matter bounce cosmology is thus explicit from the above.

The above focused only on the scalar perturbations, but as mentioned in the introduction, the matter bounce scenario also generates a scale-invariant power spectrum of tensor perturbations. Considering the transverse and traceless perturbations to the spatial metric, $\delta g_{ij} = a^2 h_{ij}$, which can be decomposed as

$$h_{ij}(\tau, x) = h_+(\tau, x)e^+_{ij} + h_\times(\tau, x)e^\times_{ij} \tag{6.24}$$

with two fixed polarization tensors e^+_{ij} and $e^\times_{ij}$, the second-order perturbed action has contributions of the form

$$S_2 \supset \frac{M^2_{\rm pl}}{4}\int d\tau d^3x \ a^2\left[h'^2 - (\nabla h)^2\right] \tag{6.25}$$

for each polarization state h_+ and $h_\times$. By normalizing each state as $\mu = aM_{\rm pl}h/2$, the second-order perturbed action is of canonical form (μ is the Mukhanov-Sasaki variable), and the resulting equation of motion for each state is

$$\mu''_k + \left(k^2 - \frac{a''}{a}\right)\mu_k = 0 \ , \tag{6.26}$$

where the equation is written in Fourier space. Since $a \sim \tau^2$ in a matter-dominated contracting phase, one has $a''/a = 2/\tau^2$, and so, one expects a

scale-invariant power spectrum just as in de Sitter space. The tensor power spectrum is given by

$$\mathcal{P}_{\rm t} = 2\mathcal{P}_h = 2\left(\frac{2}{aM_{\rm pl}}\right)^2 \frac{k^3}{2\pi^2}|\mu_k|^2 \ , \tag{6.27}$$

where the first factor of 2 accounts for the two polarizations + and ×, and the factor $[2/(aM_{\rm pl})]^2$ comes from the normalization of μ. Upon matching with quantum vacuum initial conditions at Hubble radius crossing similar to the above treatment for scalar modes, one finds the power spectrum of tensor modes at the bounce point to be given by

$$\mathcal{P}_{\rm t}(\tau_B, k) = \frac{2}{\pi^2 M_{\rm pl}^2(\tau_B - \tilde{\tau}_B)^2} \ , \tag{6.28}$$

which is indeed independent of scale.

The tensor-to-scalar ratio is then defined to be

$$r \equiv \frac{\mathcal{P}_{\rm t}}{\mathcal{P}_\zeta} \ . \tag{6.29}$$

It follows from equations (6.23) and (6.28) that

$$r = 24c_s \tag{6.30}$$

in the context of matter bounce cosmology with a general k-essence scalar field[8]. On one hand, this highlights the problem of standard matter bounce cosmology, which is driven by a canonical scalar field with $c_s = 1$, in which case $r = 24$. On the other hand, the above result provides a natural mechanism to suppress the tensor-to-scalar ratio provided the k-essence scalar field has an appropriately small sound speed. For example, satisfying the observational bound [228] $r < 0.07$ at 95% confidence imposes a bound on the sound speed of the order of

$$c_s \lesssim 0.0029 \ . \tag{6.31}$$

6.4 Non-Gaussianity

The previous section showed that a k-essence scalar field could yield a small tensor-to-scalar ratio in the context of the matter bounce scenario. This is

[8]Of course, this assumes that the perturbations remain constant on super-Hubble scales after the matter contraction phase, in particular through the bounce and until the beginning of the radiation-dominated expanding phase of standard Big Bang cosmology.

done at the expense of having a small sound speed. In what follows, the goal is to compute the bispectrum and see how a small sound speed affects the results.

6.4.1 Cubic action

To evaluate the three-point correlation function, we must expand the action (6.13) up to third order. Let us recall the result of [193], the third-order interaction action of a general single scalar field[9],

$$\begin{aligned} S_3 = \int dt d^3x \, \Big\{ & -a^3 \Big[\Sigma\Big(1-\frac{1}{c_s^2}\Big)+2\lambda\Big]\frac{\dot\zeta^3}{H^3} + \frac{a^3\epsilon}{c_s^4}(\epsilon-3+3c_s^2)\zeta\dot\zeta^2 \\ & + \frac{a\epsilon}{c_s^2}(\epsilon-2s+1-c_s^2)\zeta(\partial\zeta)^2 - 2a\frac{\epsilon}{c_s^2}\dot\zeta(\partial\zeta)(\partial\chi) + \frac{a^3\epsilon}{2c_s^2}\frac{d}{dt}\left(\frac{\eta}{c_s^2}\right)\zeta^2\dot\zeta \\ & + \frac{\epsilon}{2a}(\partial\zeta)(\partial\chi)\partial^2\chi + \frac{\epsilon}{4a}(\partial^2\zeta)(\partial\chi)^2 + 2f(\zeta)\left.\frac{\delta L}{\delta\zeta}\right|_1 \Big\} \, , \end{aligned} \tag{6.32}$$

where it is understood that $(\partial\zeta)^2 = \partial_i\zeta\partial^i\zeta$, $(\partial\zeta)(\partial\chi) = \partial_i\zeta\partial^i\chi$, $\partial^2\zeta = \partial_i\partial^i\zeta$, and where we define χ such that $\partial^2\chi = a^2\epsilon\dot\zeta$. Also, we have

$$\left.\frac{\delta L}{\delta\zeta}\right|_1 = a\left(\frac{d\partial^2\chi}{dt} + H\partial^2\chi - \epsilon\partial^2\zeta\right) \, , \tag{6.33}$$

$$\begin{aligned} f(\zeta) = {} & \frac{\eta}{4c_s^2}\zeta^2 + \frac{1}{c_s^2H}\zeta\dot\zeta + \frac{1}{4a^2H^2}\{-(\partial\zeta)(\partial\zeta) + \partial^{-2}[\partial_i\partial_j(\partial^i\zeta\partial^j\zeta)]\} \\ & + \frac{1}{2a^2H}\{(\partial\zeta)(\partial\chi) - \partial^{-2}[\partial_i\partial_j(\partial^i\zeta\partial^j\chi)]\} \, , \end{aligned} \tag{6.34}$$

where ∂^{-2} is the inverse Laplacian.

The first and second terms in the last line of equation (6.32) can be reexpressed as

$$\frac{\epsilon}{2a}(\partial\zeta)(\partial\chi)\partial^2\chi + \frac{\epsilon}{4a}(\partial^2\zeta)(\partial\chi)^2 = -\frac{a^3\epsilon^3}{2}\zeta\dot\zeta^2 + \frac{\epsilon}{2a}\zeta(\partial_i\partial_j\chi)(\partial^i\partial^j\chi) + \mathcal{K} \, , \tag{6.35}$$

where the boundary term is given by

$$\mathcal{K} = \partial_i\left[\zeta(\partial^i\chi)(\partial^2\chi) + \frac{1}{2}(\partial^i\zeta)(\partial\chi)^2 - \zeta(\partial^i\partial^j\chi)(\partial_j\chi)\right] \, . \tag{6.36}$$

[9] From here on, we take $M_{\rm pl} = 1$ for convenience.

Since the $\partial_i[...]$ term above does not contribute to the three-point function, the third-order action, equation (6.32), is equivalent to

$$S_3 = \int dtd^3x \left\{ -a^3\left[\Sigma\left(1-\frac{1}{c_s^2}\right)+2\lambda\right]\frac{\dot{\zeta}^3}{H^3} + \frac{a^3\epsilon}{c_s^4}(\epsilon-3+3c_s^2)\zeta\dot{\zeta}^2 \right.$$
$$+ \frac{a\epsilon}{c_s^2}(\epsilon-2s+1-c_s^2)\zeta(\partial\zeta)^2 - 2a\frac{\epsilon}{c_s^2}\dot{\zeta}(\partial\zeta)(\partial\chi) + \frac{a^3\epsilon}{2c_s^2}\frac{d}{dt}\left(\frac{\eta}{c_s^2}\right)\zeta^2\dot{\zeta}$$
$$\left. - \frac{a^3\epsilon^3}{2}\zeta\dot{\zeta}^2 + \frac{\epsilon}{2a}\zeta(\partial_i\partial_j\chi)(\partial^i\partial^j\chi) + 2f(\zeta)\left.\frac{\delta L}{\delta\zeta}\right|_1 \right\} . \tag{6.37}$$

In the case of a canonical field with $c_s = 1$, this action returns to equation (15) of [186]. Meanwhile, as usual the last term in this action is removed by performing the field redefinition

$$\zeta \to \tilde{\zeta} + f(\tilde{\zeta}) , \tag{6.38}$$

where $\tilde{\zeta}$ denotes the field after redefinition.

6.4.2 Contributions to the shape function

In this section, we calculate the three-point correlation function using the in-in formalism (to leading order in perturbation theory; see, e.g., [37–39] for the methodology),

$$\langle O(t)\rangle = -2\,\Im\int_{-\infty}^{t} d\bar{t}\ \langle 0|O(t)L_{\rm int}(\bar{t})|0\rangle , \tag{6.39}$$

where O represents a set of operators of the form $\hat{\zeta}^3$ in our case of interest. Then, the shape function, $\mathcal{A}$, is defined such that[10]

$$\langle\zeta_{\mathbf{k}_1}\zeta_{\mathbf{k}_2}\zeta_{\mathbf{k}_3}\rangle = (2\pi)^7\delta^{(3)}\left(\mathbf{k}_1+\mathbf{k}_2+\mathbf{k}_3\right)\frac{\mathcal{P}_\zeta^2}{\prod_i k_i^3}\mathcal{A}(\mathbf{k}_1,\mathbf{k}_2,\mathbf{k}_3) . \tag{6.40}$$

In what follows, we list all the contributions to the shape function coming from the field redefinition and the interaction action (6.37). It is easy to check that, when taking the limit $c_s = 1$, one recovers the results of [186] for the matter bounce with a canonical scalar field as expected.

- Contribution from the field redefinition

[10] We use $\zeta_{\mathbf{k}}$ to refer to $\hat{\zeta}(\tau,\mathbf{k}_i)$ to simplify the notation from here on.

In momentum space, the field redefinition can be written as

$$\zeta_{\mathbf{k}} \rightarrow \tilde{\zeta}_{\mathbf{k}} + \int \frac{d^3k_1}{(2\pi)^3}\left[-\frac{3}{2c_s^2} - \frac{3\epsilon}{4}\left(\frac{\mathbf{k}_1\cdot(\mathbf{k}-\mathbf{k}_1)}{k_1^2} - \frac{(\mathbf{k}\cdot\mathbf{k}_1)[\mathbf{k}\cdot(\mathbf{k}-\mathbf{k}_1)]}{k^2k_1^2}\right)\right]\tilde{\zeta}_{\mathbf{k}_1}\tilde{\zeta}_{\mathbf{k}-\mathbf{k}_1}\ . \tag{6.41}$$

This redefinition has the following contribution to the three-point correlation function,

$$\langle\zeta_{\mathbf{k}_1}\zeta_{\mathbf{k}_2}\zeta_{\mathbf{k}_3}\rangle_{\rm redef} = \int \frac{d^3\mathbf{k}'}{(2\pi)^3}\left[-\frac{3}{2c_s^2} - \frac{3\epsilon}{4}\left(\frac{\mathbf{k}'\cdot(\mathbf{k}_3-\mathbf{k}')}{k'^2} - \frac{(\mathbf{k}_3\cdot\mathbf{k}')(\mathbf{k}_3\cdot[\mathbf{k}_3-\mathbf{k}'])}{k_3^2k'^2}\right)\right] \times(\zeta_{\mathbf{k}_1}\zeta_{\mathbf{k}_2}\zeta_{\mathbf{k}'}\zeta_{\mathbf{k}_3-\mathbf{k}'}) + \text{perms.}\ , \tag{6.42}$$

and accordingly, the contribution to the shape function is

$$\mathcal{A}_{\rm redef} = \Big(\frac{3\epsilon}{16} - \frac{3}{4c_s^2}\Big)\sum_i k_i^3 + \frac{3\epsilon}{64}\sum_{i\neq j}k_ik_j^2 - \frac{3\epsilon}{64\prod_i k_i^2}\Big(\sum_{i\neq j}k_i^7k_j^2 + \sum_{i\neq j}k_i^6k_j^3 - 2\sum_{i\neq j}k_i^5k_j^4\Big) \tag{6.43}$$

When $c_s^2 \ll 1$, this contribution is enhanced compared to the canonical case.

- Contribution from the $\zeta\dot{\zeta}^2$ term

  The term $\zeta\dot{\zeta}^2$ in equation (6.37) yields the following contribution to the bispectrum

$$\langle\zeta_{\mathbf{k}_1}\zeta_{\mathbf{k}_2}\zeta_{\mathbf{k}_3}\rangle_{\zeta\dot{\zeta}^2} = -4(2\pi)^3\delta\Big(\mathbf{k}_1+\mathbf{k}_2+\mathbf{k}_3\Big)\,\Im\int_{-\infty}^{\tau_B}d\bar{\tau}\, a^2\Big[\frac{\epsilon}{c_s^4}(\epsilon-3+3c_s^2) - \frac{\epsilon^3}{2}\Big]u_{k_1}^*(\tau_B)u_{k_2}^*(\tau_B)u_{k_3}^*(\tau_B) \times u_{k_1}(\bar{\tau})u'_{k_2}(\bar{\tau})u'_{k_3}(\bar{\tau}) + \text{perm.}\ . \tag{6.44}$$

To leading order in $c_sk_i(\tau_B-\tilde{\tau}_B) \ll 1$, i.e. on scales larger than the sound Hubble radius[11], and recalling the solutions for u_k and u'_k

[11] This is also called the Jeans radius; see [230, 236] for an explicit definition of this scale and its role in matter bounce cosmology when $c_s \neq 1$.

[equations (6.18) and (6.19)], we get the following contribution to the shape function,

$$\mathcal{A}_{\zeta\dot{\zeta}^2} = -\frac{c_s^2}{8}\left[\frac{1}{c_s^4}(\epsilon - 3 + 3c_s^2) - \frac{\epsilon^2}{2}\right]\sum_i k_i^3 \ . \tag{6.45}$$

Again, when $c_s^2 \ll 1$, this contribution is enhanced compared to the canonical case.

- Contribution from the $\dot{\zeta}\partial\zeta\partial\chi$ term

  A similar computation for this term yields the following contribution to the shape function

$$\mathcal{A}_{\dot{\zeta}\partial\zeta\partial\chi} = -\frac{\epsilon}{8}\sum_i k_i^3 + \frac{\epsilon}{8\prod_i k_i^2}\Big(\sum_{i\neq j} k_i^7 k_j^2 - \sum_{i\neq j} k_i^4 k_j^5\Big). \tag{6.46}$$

  We note that this contribution is independent of c_s.

6.4.2.1 Contribution from the $\zeta(\partial_i\partial_j\chi)^2$ term

For this term, the contribution to the shape function is given by

$$\begin{aligned}\mathcal{A}_{\zeta(\partial_i\partial_j\chi)^2} =& -\frac{c_s^2\epsilon^2}{32}\sum_i k_i^3 + \frac{c_s^2\epsilon^2}{64}\sum_{i\neq j} k_i^2 k_j + \frac{c_s^2\epsilon^2}{64\prod_i k_i^2} \\ &\times\Big(\sum_i k_i^9 - \sum_{i\neq j} k_i^6 k_j^3 + 3\sum_{i\neq j} k_i^5 k_j^4 - 3\sum_{i\neq j} k_i^7 k_j^2\Big) \ .\end{aligned} \tag{6.47}$$

When $c_s^2 \ll 1$, this contribution is suppressed compared to the canonical case.

- Contribution from the $\dot{\zeta}^3$ term

  The $\dot{\zeta}^3$ term is a new element in the Lagrangian caused by the non-trivial sound speed, which does not show up in the cubic action of canonical fields. Its contribution to the bispectrum is

$$\begin{aligned}\langle\zeta_{\mathbf{k}_1}\zeta_{\mathbf{k}_2}\zeta_{\mathbf{k}_3}\rangle_{\dot{\zeta}^3} =& -12(2\pi)^3\delta^{(3)}(\mathbf{k}_1+\mathbf{k}_2+\mathbf{k}_3)\ \mathrm{Im}\int_{-\infty}^{\tau_B} d\bar{\tau} \\ &\Big(-\frac{aM_{\rm pl}^2\epsilon}{Hc_s^2}\Big)\Big(1-\frac{1}{c_s^2}+2\frac{\lambda}{\Sigma}\Big)u_{k_1}^*(\tau_B)u_{k_2}^*(\tau_B)u_{k_3}^*(\tau_B) \\ &\times u_{k_1}'(\bar{\tau})u_{k_2}'(\bar{\tau})u_{k_3}'(\bar{\tau}) \ ,\end{aligned} \tag{6.48}$$

where we have used the expression for Σ, equation (6.11). Then the contribution to the shape function is expressed as

$$\mathcal{A}_{\dot{\zeta}^3} = -\frac{9}{2}\left(1 - \frac{1}{c_s^2} + 2\frac{\lambda}{\Sigma}\right)\sum_i k_i^3 \ . \tag{6.49}$$

Since this is a new contribution compared to the canonical case, it vanishes for $c_s^2 = 1$. Indeed, when $c_s^2 = 1$, $\lambda/\Sigma \simeq (1 - c_s^2)/(6c_s^2) = 0$ (see equation (6.81) in Appendix 6.A) and $1 - 1/c_s^2 = 0$. We note though that when $c_s^2 \ll 1$, this contribution is large.

- Secondary contributions

  The contribution from the term

  $$\frac{a^3\epsilon}{2c_s^2}\frac{d}{dt}\Big(\frac{\eta}{c_s^2}\Big)\zeta^2\dot{\zeta}$$

  in equation (6.37) is exactly zero since $\eta = 0$ during the matter contraction. We can also neglect the contribution from the term

  $$\frac{a\epsilon}{c_s^2}(\epsilon - 2s + 1 - c_s^2)\zeta(\partial\zeta)^2$$

  since the leading order term of the resulting bispectrum is proportional to $c_s^2 k_i^2(\tau_B - \tilde{\tau}_B)^2$, which means that it is suppressed outside the sound Hubble radius.

The above results differ from the ones of general single field inflation. As pointed out in [186], two main reasons account for the different non-Gaussianities between matter bounce cosmology and inflation. First, here the "slow-roll" parameter ϵ is of order one rather than being close to zero, so the amplitudes are larger and the higher-order terms in ϵ are not suppressed. Second, curvature perturbations grow on super-Hubble scales in a matter-dominated contracting universe, and this behaviour manifests itself in the integral of equation (6.39), while for inflation, ζ usually remains constant after horizon-exit, so there is no such contribution.

In what follows, we summarize the above results and give a detailed analysis of the bispectrum. In particular, the differences with the canonical single field matter bounce scenario are discussed.

6.4.3 Summary of results

One can gather all the contributions above and get the total shape function,

$$\begin{aligned}\mathcal{A}_{\rm tot} = & \left(-\frac{105}{32}+\frac{39}{16c_s^2}+\frac{9c_s^2}{128}\right)\sum_i k_i^3+\frac{3}{256}(3c_s^2+6)\sum_{i\neq j}k_i^2k_j \\ & +\frac{3}{256\prod_i k_i^2}\left[3c_s^2\sum_i k_i^9+(10-9c_s^2)\sum_{i\neq j}k_i^7k_j^2\right. \\ & \left.-(3c_s^2+6)\sum_{i\neq j}k_i^6k_j^3+(9c_s^2-4)\sum_{i\neq j}k_i^5k_j^4\right] , \end{aligned} \tag{6.50}$$

where we have used $\epsilon = 3/2$ and $\lambda/\Sigma = (1-c_s^2)/6c_s^2$ for the matter contraction stage. Now the only free parameter in the total shape function is the sound speed c_s. In what follows, we shall discuss several interesting aspects of this result.

6.4.3.1 Amplitude

The size of non-Gaussianity is depicted by the dimensionless amplitude parameter

$$f_{\rm NL}(\mathbf{k}_1,\mathbf{k}_2,\mathbf{k}_3) = \frac{10}{3}\frac{\mathcal{A}_{\rm tot}(\mathbf{k}_1,\mathbf{k}_2,\mathbf{k}_3)}{\sum_i k_i^3} . \tag{6.51}$$

As one can see in equation (6.50), for most values of $c_s \in (0,1]$, the first term dominates the total shape function, and roughly, $f_{\rm NL}$ becomes

$$f_{\rm NL} \simeq -\frac{175}{16}+\frac{65}{8c_s^2}+\frac{15c_s^2}{64} , \tag{6.52}$$

which yields $f_{\rm NL} < 0$ for $0.87 \lesssim c_s \leqslant 1$ and $f_{\rm NL} > 0$ for $c_s \lesssim 0.87$. Thus, besides the negative amplitude in the canonical case [186], a small sound speed in matter bounce cosmology can produce a positive $f_{\rm NL}$. In the next section, we shall further discuss its behaviour in different limits to confront observations.

6.4.3.2 Shape

The shape of non-Gaussianity is described by the dimensionless shape function

$$\mathcal{F}(k_1/k_3, k_2/k_3) = \frac{\mathcal{A}_{\rm tot}}{k_1k_2k_3} . \tag{6.53}$$

Then, the first term in equation (6.50) gives exactly the form of the local shape. Thus, when the prefactor of the first term is nonvanishing ($c_s \not\approx 0.87$), the shape function is dominated by the local form, while the remaining terms just give some corrections. The total shape of non-Gaussianity is shown in the left panel of Figure 6.1, which looks very similar to the plots in [186] for the canonical matter bounce except that the amplitude is much larger here with c_s small.

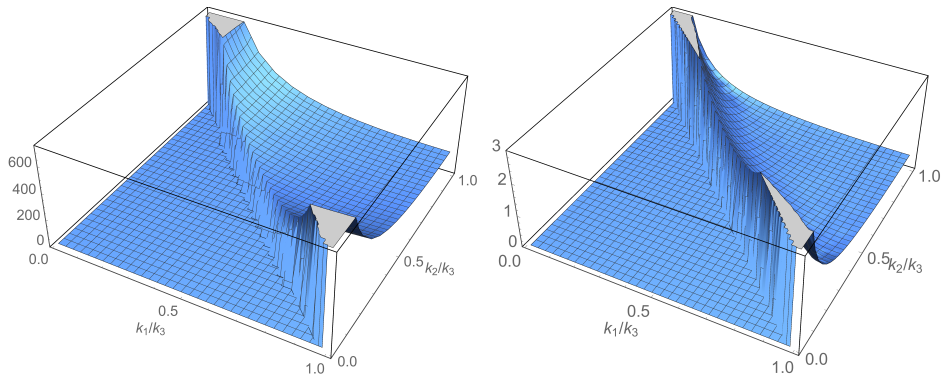

Figure 6.1: The shape of $\mathcal{F}(k_1/k_3, k_2/k_3)$ for $c_s = 0.2$ (left panel) and $c_s = 0.87$ (right panel).

At the same time, this result differs from the one of general single field inflation, where the equilateral form dominates the shape of non-Gaussianity for $c_s \ll 1$ [193]. This is mainly caused by the different generation mechanisms of non-Gaussianity in these two scenarios. For the matter bounce scenario, the growth of curvature perturbations after Hubble radius exit makes a significant contribution to the final bispectrum. Meanwhile, the local form is usually thought to be generated on super-Hubble scales since "local" means that the non-Gaussianity at one place is *disconnected* with the one at other places. For general single field inflation, the dominant contribution is due to the enhanced interaction at horizon-crossing. Thus, these two scenarios behave quite differently with a small sound speed.

It is also interesting to note that for $c_s \approx 0.87$, the first term in equation (6.50) vanishes, so the shape function is dominated by the remaining terms. The shape of non-Gaussianity is plotted in the right panel of Figure 6.1 for this case, which is a new form different from the local one. To the best of our knowledge, no other scenario can give rise to such a kind of shape, thus it can be seen as a distinguishable signature of matter bounce cosmology for probes of non-Gaussianity.

6.4.3.3 The squeezed limit

Usually people are interested in the squeezed limit of the bispectrum ($k_1 \ll k_2 = k_3 = k$), since its scaling behaviour is helpful for clarifying the shapes of non-Gaussianity analytically. Here in the squeezed limit ($k_1/k \to 0$), the dimensionless shape function can be expanded as

$$\mathcal{F}(k_1/k_3, k_2/k_3) \simeq \frac{3}{8}\left(-\frac{33}{2}+\frac{13}{c_s^2}\right)\frac{k}{k_1}+\frac{3}{64}\left(1+6c_s^2\right)\frac{k_1}{k}+\mathcal{O}\left(\left(\frac{k_1}{k}\right)^2\right) \ . \quad (6.54)$$

The leading order term gives the scaling $\mathcal{F} \sim k/k_1$ and

$$\langle \zeta_{\mathbf{k}_1}\zeta_{\mathbf{k}_2}\zeta_{\mathbf{k}_3}\rangle_{\text{squeezed}} \sim \frac{1}{k_1^3} \ , \quad (6.55)$$

which is consistent with the dominant local form. The only exception is when the coefficient of the first term vanishes ($c_s = \sqrt{26/33}$) and another scaling, $\mathcal{F} \sim k_1/k$, follows from the next-to-leading order term.

6.5 Amplitude parameter of non-Gaussianities and implication for the no-go theorem

There are three forms of the amplitude parameter f_{NL} that are of particular interest for cosmological observations. They are called the "local form", the "equilateral form", and the "folded form". The local form requires that one of the three momentum modes exits the Hubble radius much earlier than the other two, e.g., $k_1 \ll k_2 = k_3$. In this limit, one can simplify the total shape function, equation (6.50), to find

$$f_{\text{NL}}^{\text{local}} \simeq -\frac{165}{16}+\frac{65}{8c_s^2} \ . \quad (6.56)$$

The equilateral form requires that the three momenta form an equilateral triangle, i.e. $k_1 = k_2 = k_3$. In this case, we obtain

$$f_{\text{NL}}^{\text{equil}} \simeq -\frac{335}{32}+\frac{65}{8c_s^2}+\frac{45c_s^2}{128} \ . \quad (6.57)$$

The folded form has $k_1 = 2k_2 = 2k_3$, hence

$$f_{\text{NL}}^{\text{folded}} \simeq -\frac{37}{4}+\frac{65}{8c_s^2} \ . \quad (6.58)$$

As a result, in the limit where $c_s^2 \ll 1$, we find that

$$f_{\rm NL}^{\rm local} \approx f_{\rm NL}^{\rm equil} \approx f_{\rm NL}^{\rm folded} \approx \frac{65}{8c_s^2} \gg 1 \ . \tag{6.59}$$

Let us recall from section 6.3 that in order to satisfy the observational bound on the tensor-to-scalar ratio, we must impose $c_s \lesssim 0.0029$. This immediately implies

$$f_{\rm NL}^{\rm local} \approx f_{\rm NL}^{\rm equil} \approx f_{\rm NL}^{\rm folded} \gtrsim 9.55 \times 10^5 \gg 1 \ . \tag{6.60}$$

This amplitude of primordial non-Gaussianity is clearly ruled out according to the observations [109],

$$f_{\rm NL}^{\rm local} = 0.8 \pm 5.0 \ , \quad f_{\rm NL}^{\rm equil} = -4 \pm 43 \ , \quad f_{\rm NL}^{\rm ortho} = -26 \pm 21 \ , \tag{6.61}$$

thus ruling out the viability of the class of models studied here.

Alternatively, if one requires that, e.g., $-9.2 \lesssim f_{\rm NL}^{\rm local} \lesssim 10.8$ (i.e., imposing $f_{\rm NL}^{\rm local}$ to be within the measured 2σ error bars), then one would need[12] $c_s \gtrsim 0.62$. However, this lower bound on the sound speed yields a tensor-to-scalar ratio $r \gtrsim 14.88$, which is again clearly ruled out by observations [228].

In summary, there is no region of parameter space where c_s can give a good, small tensor-to-scalar ratio (i.e., of order 0.1 at most) and good, small non-Gaussianities (i.e., of order 10 at most). Therefore, independent of what happens during the bounce, we extend the no-go theorem conjectured in [227] to the following one:

No-Go Theorem. *For quantum fluctuations generated during a matter-dominated contracting phase, an upper bound on the tensor-to-scalar ratio (r) is equivalent to a lower bound on the amount of primordial non-Gaussianities ($f_{\rm NL}$). Furthermore, if*

- *the matter contraction phase is due to a single (not necessarily canonical) scalar field,*
- *the same single scalar field allows for the violation of the NEC to produce a nonsingular bounce,*
- *and General Relativity holds at all energy scales,*

then satisfying the current observational upper bound on the tensor-to-scalar ratio cannot be done without contradicting the current observational upper bounds on $f_{\rm NL}$ (and vice versa).

[12] Note that this constraint does not exclude $c_s \approx 0.87$, for which the new shape of non-Gaussianity in the right panel of Figure 6.1 emerges.

6.6 Conclusions and discussion

In this paper, we computed the two- and three-point correlation functions produced by a generic k-essence scalar field in a matter-dominated contracting universe. Comparing the power spectra of scalar and tensor modes, we found that the tensor-to-scalar ratio can be appropriately suppressed if the sound speed associated with the k-essence scalar field is sufficiently small. In turn, we showed that the amplitude of the bispectrum is amplified by the smallness of the sound speed[13]. As a result, it seems incompatible to suppress the tensor-to-scalar ratio below current observational bounds without producing excessive non-Gaussianities. This leads us to extend the conjecture of the no-go theorem, which effectively rules out a large class of nonsingular matter bounce models.

Although this seriously constrains nonsingular matter bounce cosmology as a viable alternative scenario to inflation, there remain several classes of models that are not affected by this no-go theorem. Indeed, one could still evade the no-go theorem assuming certain modified gravity models as stated in [227] (see references therein) or with the introduction of one or several new fields. For example, in the matter bounce curvaton scenario [239] (see also [202, 240, 241] for other nonsingular bouncing models using the curvaton mechanism) and in the two-field matter bounce scenario [242], entropy modes are generated by the presence of an additional scalar field, which are then converted to curvature perturbations. In both models near the bounce, the kinetic term of the entropy field varies rapidly, which acts as a tachyonic-like mass that amplifies (in a controlled way) the entropy fluctuations while not affecting the tensor modes. As a result, the tensor-to-scalar ratio is suppressed (see [28, 226] for reviews of this process). Furthermore, the production of non-Gaussianities in the matter bounce curvaton scenario has been estimated in [239], and it indicated that sizable, negative non-Gaussianities appeared, yet still in agreement with current observations. Accordingly, such a curvaton scenario does not appear to suffer from a no-go theorem. However, there still remains to do an appropriate extensive analysis of the production of non-Gaussianities when general multifields are included in the matter bounce scenario.

[13] With a small sound speed, one may also reach the strong coupling regime where the perturbative analysis breaks down. This is known as the strong coupling problem [237, 238], which affects many non-inflationary scenarios (see in particular Appendix C of [237], which focuses on non-attractor models). It represents a general independent theoretical constraint, but in the context of the matter bounce scenario, our no-go theorem is more constraining due to current observational bounds.

A similar curvaton mechanism is used in the new Ekpyrotic model [243, 244] (extended in [245–248]), which generates a nearly scale-invariant power spectrum of curvature perturbations. In this case, however, the smallness of the observed tensor-to-scalar ratio must be attributed to the fact that the tensor modes have a blue power spectrum when they exit the Hubble radius in a contracting phase with $w \gg 1$. The new Ekpyrotic model originally predicted large non-Gaussianities [249–253] (see also the reviews [254, 255]), but some more recent extensions can resolve this issue [256–260]. Thus, here as well, it appears that these types of models do not suffer from a similar no-go theorem[14].

We note that one might be able to prove the no-go conjecture of this paper borrowing similar techniques to the effective field theory of inflation [94], i.e. by constructing an effective field theory of nonsingular bouncing cosmology (e.g., see the recent work of [212, 213]). In complete generality, this could allow us to find the exact and explicit relation between the tensor-to-scalar ratio (which involves the power spectra of curvature and tensor modes) and the bispectrum. In fact, the goal would be to find a consistency relation for the three-point function in single field nonsingular bouncing cosmology similar to what has been done in inflation [39, 40, 262]. This will be explored in a follow-up study.

Finally, we would like to emphasize that, for matter bounce cosmology, although the simplest k-essence model is ruled out by the no-go theorem, the bispectrum with $c_s \neq 1$ (as an independent result of this paper) remains to be a probable target for future probes of non-Gaussianity. This possibility relies on the aforementioned bouncing models that can evade the no-go theorem with other mechanisms. In those cases, a nontrivial sound speed may still lead to the same behaviour of non-Gaussianities found in this paper, which potentially can be detected by future observations. Particularly, we predict a new shape with an amplitude still consistent with current observational limits, which can serve as the distinctive signature of matter bounce cosmology and help us distinguish it from other very early universe theories.

[14]Furthermore, Ekpyrotic models are robust against the growth of anisotropies in a contracting universe. This is another challenge with the matter bounce scenario (see [205, 261]) that will have to be overcome to have a viable theory.

Appendix

6.A The ratio λ/Σ

Let us recall the definition of Σ and λ in equations (6.11) and (6.12). Their ratio is thus given by

$$\frac{\lambda}{\Sigma} = \frac{1}{3}\left(X\frac{\Sigma_{,X}}{\Sigma} - 1\right) \ . \tag{6.62}$$

Recalling the definition of c_s^2 in equation (6.10), we note that

$$\Sigma = X(P_{,X} + 2XP_{,XX}) = X\frac{P_{,X}}{c_s^2} \ . \tag{6.63}$$

Also, recalling the expression for ρ and p in equation (6.7), we find that $2XP_{,X} = \rho + p$, and so, the above expression for Σ becomes

$$\Sigma = \frac{\rho + p}{2c_s^2} \ . \tag{6.64}$$

Consequently,

$$X\frac{\Sigma_{,X}}{\Sigma} = X\frac{\rho_{,X} + p_{,X}}{\rho + p} - 2X\frac{c_s, X}{c_s} \ . \tag{6.65}$$

Working in the limit where $p = 0$, we note that $\rho = 2XP_{,X}$, and so, $p_{,X} = P_{,X} = \rho/(2X)$, which implies that $p_{,X}/\rho = 1/(2X)$. Also, $\rho_{,X} = p_{,X}/c_s^2$ from the definition of the sound speed, and thus,

$$\frac{\rho_{,X}}{\rho} = \frac{p_{,X}}{\rho c_s^2} = \frac{1}{2c_s^2 X} \ . \tag{6.66}$$

Therefore, equation (6.65) in the limit where $p = 0$ becomes

$$X\frac{\Sigma_{,X}}{\Sigma} = \frac{1}{2c_s^2} + \frac{1}{2} - 2X\frac{c_s, X}{c_s} \ . \tag{6.67}$$

Alternatively, one can evaluate the ratio λ/Σ as

$$\frac{\lambda}{\Sigma} = \frac{1}{3}\left(\frac{\Sigma_{,X}}{\Sigma}X - 1\right) = \frac{1}{3}\left(\frac{\dot{\Sigma}}{\Sigma}\frac{X}{\dot{X}} - 1\right) \ . \tag{6.68}$$

Since we can write $\Sigma = H^2 M_{\rm pl}^2 \epsilon/c_s^2$ and recalling the definition of the slow-roll parameters in section 6.2, we get

$$\frac{\dot{\Sigma}}{H\Sigma} = -2\epsilon + \eta - 2s \ . \tag{6.69}$$

Now, we note that we can write

$$\eta = \frac{\dot{\epsilon}}{H\epsilon} = \frac{\ddot{H}}{H\dot{H}} - 2\frac{\dot{H}}{H^2} = \frac{\ddot{H}}{H\dot{H}} + 2\epsilon \ . \tag{6.70}$$

Also, the Friedmann equation $M_{\rm pl}^2\dot{H} = -XP_{,X}$ implies that

$$\frac{\ddot{H}}{H\dot{H}} = \frac{1}{H}\left(\frac{\dot{X}}{X} + \frac{\dot{P}_{,X}}{P_{,X}}\right) \ , \tag{6.71}$$

and so,

$$\frac{\dot{X}}{HX} = \eta - 2\epsilon - \frac{\dot{P}_{,X}}{P_{,X}} \ . \tag{6.72}$$

Therefore, combining equation (6.69) and the above yields

$$\frac{\dot{\Sigma}}{\Sigma}\frac{X}{\dot{X}} = \frac{-2\epsilon + \eta - 2s}{-2\epsilon + \eta - \frac{\dot{P}_{,X}}{P_{,X}}} \ . \tag{6.73}$$

In the limit where $p = 0$, we recall that $\epsilon = 3/2$ and $\eta = 0$, and as a result,

$$\frac{\dot{\Sigma}}{\Sigma}\frac{X}{\dot{X}} = \frac{3 + 2s}{3 + \frac{\dot{P}_{,X}}{P_{,X}}} \ . \tag{6.74}$$

Comparing the above with equation (6.67), since $(\dot{\Sigma}/\Sigma)(X/\dot{X}) = X\Sigma_{,X}/\Sigma$, we find

$$\frac{3 + 2s}{3 + \frac{\dot{P}_{,X}}{P_{,X}}} = \frac{1}{2c_s^2} + \frac{1}{2} - 2X\frac{c_s, X}{c_s} \ , \tag{6.75}$$

but

$$-2X\frac{c_s, X}{c_s} = -2\frac{X}{\dot{X}}\frac{\dot{c}_s}{c_s} = -2s\frac{HX}{\dot{X}} = \frac{-2s}{\eta - 2\epsilon - \frac{\dot{P}_{,X}}{P_{,X}}} \ , \tag{6.76}$$

where the last equality follows from equation (6.72). Thus, equation (6.75), with $\epsilon = 3/2$ and $\eta = 0$, leaves us with

$$\frac{3}{3 + \frac{\dot{P}_{,X}}{P_{,X}}} = \frac{1}{2c_s^2} + \frac{1}{2} \ , \tag{6.77}$$

and consequently,

$$\frac{\dot{P}_{,X}}{P_{,X}} = -3\left(\frac{1 - c_s^2}{1 + c_s^2}\right) \ . \tag{6.78}$$

As a result, equation (6.74) becomes

$$\frac{\dot{\Sigma}}{\Sigma}\frac{X}{\dot{X}} = X\frac{\Sigma_{,X}}{\Sigma} = \frac{1}{2c_s^2}\left(1+\frac{2}{3}s\right)(1+c_s^2)\ , \tag{6.79}$$

and in the end, (6.68) is equivalent to

$$\frac{\lambda}{\Sigma} = \frac{1}{3}\left[\frac{1}{2c_s^2}\left(1+\frac{2}{3}s\right)(1+c_s^2)-1\right]\ . \tag{6.80}$$

In the limit where $|s| \ll 1$, this reduces to

$$\frac{\lambda}{\Sigma} \simeq \frac{1}{3}\left[\frac{1+c_s^2}{2c_s^2}-1\right] = \frac{1-c_s^2}{6c_s^2}\ . \tag{6.81}$$

In comparison, DBI inflation has $\lambda/\Sigma = (1-c_s^2)/(2c_s^2)$ (see [193]).

Bibliography

[1] A. H. Guth, *The Inflationary Universe: A Possible Solution to the Horizon and Flatness Problems*, *Phys. Rev.* **D23** (1981) 347–356.

[2] A. D. Linde, *A New Inflationary Universe Scenario: A Possible Solution of the Horizon, Flatness, Homogeneity, Isotropy and Primordial Monopole Problems*, *Phys. Lett.* **108B** (1982) 389–393.

[3] A. A. Starobinsky, *A New Type of Isotropic Cosmological Models Without Singularity*, *Phys. Lett.* **B91** (1980) 99–102. [,771(1980)].

[4] K. Sato, *First Order Phase Transition of a Vacuum and Expansion of the Universe*, *Mon. Not. Roy. Astron. Soc.* **195** (1981) 467–479.

[5] L. Z. Fang, *Entropy Generation in the Early Universe by Dissipative Processes Near the Higgs' Phase Transitions*, *Phys. Lett.* **B95** (1980) 154–156.

[6] A. Albrecht and P. J. Steinhardt, *Cosmology for Grand Unified Theories with Radiatively Induced Symmetry Breaking*, *Phys. Rev. Lett.* **48** (1982) 1220–1223.

[7] **Planck** Collaboration, Y. Akrami et al., *Planck 2018 results. X. Constraints on inflation*, `arXiv:1807.06211`.

[8] **Planck** Collaboration, Y. Akrami et al., *Planck 2018 results. ix. constraints on primordial non-gaussianity*, `arXiv:1905.05697`.

[9] A. Einstein, *The Foundation of the General Theory of Relativity*, *Annalen Phys.* **49** (1916), no. 7 769–822.

[10] G. Lemaitre, *A Homogeneous Universe of Constant Mass and Growing Radius Accounting for the Radial Velocity of Extragalactic Nebulae*, *Annales de la Société Scientifique de Bruxelles* **47A** (1927) 49–59.

[11] E. Hubble, *A relation between distance and radial velocity among extra-galactic nebulae*, *Proceedings of the national academy of sciences* **15** (1929), no. 3 168–173.

[12] A. Friedmann, *On the curvature of space*, *Z. Phys.* **10** (1922) 377–386. [Gen. Rel. Grav.31,1991 (1999)].

[13] W. De Sitter, *On the relativity of inertia. remarks concerning einstein's latest hypothesis*, *Proc. Kon. Ned. Acad. Wet* **19** (1917), no. 2 1217–1225.

[14] W. De Sitter, *On the curvature of space*, in *Proc. Kon. Ned. Akad. Wet*,

vol. 20, pp. 229–243, 1917.

[15] R. A. Alpher, H. Bethe, and G. Gamow, *The origin of chemical elements*, *Physical Review* **73** (1948), no. 7 803.

[16] F. L. Bezrukov and M. Shaposhnikov, *The Standard Model Higgs boson as the inflaton*, *Phys. Lett. B* **659** (2008) 703–706, [arXiv:0710.3755].

[17] R. Kallosh and A. Linde, *Universality Class in Conformal Inflation*, *JCAP* **1307** (2013) 002, [arXiv:1306.5220].

[18] R. Kallosh, A. Linde, and D. Roest, *Superconformal Inflationary α-Attractors*, *JHEP* **11** (2013) 198, [arXiv:1311.0472].

[19] D. Baumann and L. McAllister, *Inflation and String Theory*. Cambridge Monographs on Mathematical Physics. Cambridge University Press, 2015.

[20] E. J. Copeland, A. R. Liddle, D. H. Lyth, E. D. Stewart, and D. Wands, *False vacuum inflation with Einstein gravity*, *Phys. Rev.* **D49** (1994) 6410–6433, [astro-ph/9401011].

[21] K. Freese, J. A. Frieman, and A. V. Olinto, *Natural inflation with pseudo - Nambu-Goldstone bosons*, *Phys. Rev. Lett.* **65** (1990) 3233–3236.

[22] H. Ooguri and C. Vafa, *On the Geometry of the String Landscape and the Swampland*, *Nucl. Phys.* **B766** (2007) 21–33, [hep-th/0605264].

[23] N. Arkani-Hamed, L. Motl, A. Nicolis, and C. Vafa, *The String landscape, black holes and gravity as the weakest force*, *JHEP* **06** (2007) 060, [hep-th/0601001].

[24] G. Obied, H. Ooguri, L. Spodyneiko, and C. Vafa, *De Sitter Space and the Swampland*, arXiv:1806.08362.

[25] A. Borde, A. H. Guth, and A. Vilenkin, *Inflationary space-times are incompletein past directions*, *Phys. Rev. Lett.* **90** (2003) 151301, [gr-qc/0110012].

[26] J. Martin and R. H. Brandenberger, *The TransPlanckian problem of inflationary cosmology*, *Phys. Rev.* **D63** (2001) 123501, [hep-th/0005209].

[27] R. Brandenberger and P. Peter, *Bouncing Cosmologies: Progress and Problems*, arXiv:1603.05834.

[28] Y.-F. Cai, *Exploring Bouncing Cosmologies with Cosmological Surveys*, *Sci. China Phys. Mech. Astron.* **57** (2014) 1414–1430, [arXiv:1405.1369].

[29] D. Wands, *Duality invariance of cosmological perturbation spectra*, *Phys. Rev.* **D60** (1999) 023507, [gr-qc/9809062].

[30] F. Finelli and R. Brandenberger, *On the generation of a scale invariant spectrum of adiabatic fluctuations in cosmological models with a contracting phase*, *Phys. Rev.* **D65** (2002) 103522, [hep-th/0112249].

[31] R. H. Brandenberger, *The Matter Bounce Alternative to Inflationary Cosmology*, arXiv:1206.4196.

[32] M. Sasaki, *Large Scale Quantum Fluctuations in the Inflationary Universe*, *Prog. Theor. Phys.* **76** (1986) 1036.

[33] V. F. Mukhanov, *Quantum Theory of Gauge Invariant Cosmological Perturbations*, *Sov. Phys. JETP* **67** (1988) 1297–1302. [Zh. Eksp. Teor.

Fiz.94N7,1(1988)].

[34] V. F. Mukhanov, H. A. Feldman, and R. H. Brandenberger, *Theory of cosmological perturbations. Part 1. Classical perturbations. Part 2. Quantum theory of perturbations. Part 3. Extensions*, *Phys. Rept.* **215** (1992) 203–333.

[35] N. Bartolo, E. Komatsu, S. Matarrese, and A. Riotto, *Non-Gaussianity from inflation: Theory and observations*, *Phys. Rept.* **402** (2004) 103–266, [astro-ph/0406398].

[36] M. Liguori, E. Sefusatti, J. R. Fergusson, and E. P. S. Shellard, *Primordial non-Gaussianity and Bispectrum Measurements in the Cosmic Microwave Background and Large-Scale Structure*, *Adv. Astron.* **2010** (2010) 980523, [arXiv:1001.4707].

[37] X. Chen, *Primordial Non-Gaussianities from Inflation Models*, *Adv. Astron.* **2010** (2010) 638979, [arXiv:1002.1416].

[38] Y. Wang, *Inflation, Cosmic Perturbations and Non-Gaussianities*, *Commun. Theor. Phys.* **62** (2014) 109–166, [arXiv:1303.1523].

[39] J. M. Maldacena, *Non-Gaussian features of primordial fluctuations in single field inflationary models*, *JHEP* **05** (2003) 013, [astro-ph/0210603].

[40] P. Creminelli and M. Zaldarriaga, *Single field consistency relation for the 3-point function*, *JCAP* **0410** (2004) 006, [astro-ph/0407059].

[41] W. H. Kinney, *Horizon crossing and inflation with large eta*, *Phys. Rev.* **D72** (2005) 023515, [gr-qc/0503017].

[42] M. H. Namjoo, H. Firouzjahi, and M. Sasaki, *Violation of non-Gaussianity consistency relation in a single field inflationary model*, *Europhys. Lett.* **101** (2013) 39001, [arXiv:1210.3692].

[43] X. Chen, H. Firouzjahi, M. H. Namjoo, and M. Sasaki, *A Single Field Inflation Model with Large Local Non-Gaussianity*, *Europhys. Lett.* **102** (2013) 59001, [arXiv:1301.5699].

[44] T. Bringmann, P. Scott, and Y. Akrami, *Improved constraints on the primordial power spectrum at small scales from ultracompact minihalos*, *Phys. Rev. D* **85** (2012) 125027, [arXiv:1110.2484].

[45] Y.-F. Cai, X. Tong, D.-G. Wang, and S.-F. Yan, *Primordial Black Holes from Sound Speed Resonance during Inflation*, *Phys. Rev. Lett.* **121** (2018), no. 8 081306, [arXiv:1805.03639].

[46] Y.-F. Cai, C. Chen, X. Tong, D.-G. Wang, and S.-F. Yan, *When Primordial Black Holes from Sound Speed Resonance Meet a Stochastic Background of Gravitational Waves*, *Phys. Rev. D* **100** (2019), no. 4 043518, [arXiv:1902.08187].

[47] A. Achúcarro and G. A. Palma, *The string swampland constraints require multi-field inflation*, *JCAP* **1902** (2019) 041, [arXiv:1807.04390].

[48] R. Bravo, G. A. Palma, and S. Riquelme, *A Tip for Landscape Riders: Multi-Field Inflation Can Fulfill the Swampland Distance Conjecture*, arXiv:1906.05772.

[49] C. Gordon, D. Wands, B. A. Bassett, and R. Maartens, *Adiabatic and entropy perturbations from inflation*, *Phys. Rev.* **D63** (2001) 023506, [astro-ph/0009131].

[50] S. Groot Nibbelink and B. J. W. van Tent, *Density perturbations arising from multiple field slow roll inflation*, hep-ph/0011325.

[51] S. Groot Nibbelink and B. J. W. van Tent, *Scalar perturbations during multiple field slow-roll inflation*, *Class. Quant. Grav.* **19** (2002) 613–640, [hep-ph/0107272].

[52] A. Achucarro, J.-O. Gong, S. Hardeman, G. A. Palma, and S. P. Patil, *Features of heavy physics in the CMB power spectrum*, *JCAP* **1101** (2011) 030, [arXiv:1010.3693].

[53] J.-O. Gong and T. Tanaka, *A covariant approach to general field space metric in multi-field inflation*, *JCAP* **1103** (2011) 015, [arXiv:1101.4809]. [Erratum: JCAP1202,E01(2012)].

[54] D. H. Lyth and D. Wands, *Generating the curvature perturbation without an inflaton*, *Phys. Lett. B* **524** (2002) 5–14, [hep-ph/0110002].

[55] T. Moroi and T. Takahashi, *Effects of cosmological moduli fields on cosmic microwave background*, *Phys. Lett. B* **522** (2001) 215–221, [hep-ph/0110096]. [Erratum: Phys.Lett.B 539, 303–303 (2002)].

[56] X. Chen and Y. Wang, *Large non-Gaussianities with Intermediate Shapes from Quasi-Single Field Inflation*, *Phys. Rev.* **D81** (2010) 063511, [arXiv:0909.0496].

[57] X. Chen and Y. Wang, *Quasi-Single Field Inflation and Non-Gaussianities*, *JCAP* **1004** (2010) 027, [arXiv:0911.3380].

[58] D. Baumann and D. Green, *Signatures of Supersymmetry from the Early Universe*, *Phys. Rev.* **D85** (2012) 103520, [arXiv:1109.0292].

[59] N. Arkani-Hamed and J. Maldacena, *Cosmological Collider Physics*, arXiv:1503.08043.

[60] A. J. Tolley and M. Wyman, *The Gelaton Scenario: Equilateral non-Gaussianity from multi-field dynamics*, *Phys. Rev.* **D81** (2010) 043502, [arXiv:0910.1853].

[61] A. Achucarro, J.-O. Gong, S. Hardeman, G. A. Palma, and S. P. Patil, *Mass hierarchies and non-decoupling in multi-scalar field dynamics*, *Phys. Rev.* **D84** (2011) 043502, [arXiv:1005.3848].

[62] A. Achucarro, J.-O. Gong, S. Hardeman, G. A. Palma, and S. P. Patil, *Effective theories of single field inflation when heavy fields matter*, *JHEP* **05** (2012) 066, [arXiv:1201.6342].

[63] S. Renaux-Petel and K. Turzynski, *Geometrical Destabilization of Inflation*, *Phys. Rev. Lett.* **117** (2016), no. 14 141301, [arXiv:1510.01281].

[64] S. Renaux-Petel, K. Turzyński, and V. Vennin, *Geometrical destabilization, premature end of inflation and Bayesian model selection*, *JCAP* **1711** (2017), no. 11 006, [arXiv:1706.01835].

[65] S. Garcia-Saenz and S. Renaux-Petel, *Flattened non-Gaussianities from the*

effective field theory of inflation with imaginary speed of sound, *JCAP* **1811** (2018), no. 11 005, [arXiv:1805.12563].

[66] O. Grocholski, M. Kalinowski, M. Kolanowski, S. Renaux-Petel, K. Turzyński, and V. Vennin, *On backreaction effects in geometrical destabilisation of inflation*, *JCAP* **1905** (2019), no. 05 008, [arXiv:1901.10468].

[67] M. Cicoli, V. Guidetti, and F. G. Pedro, *Geometrical Destabilisation of Ultra-Light Axions in String Inflation*, *JCAP* **1905** (2019), no. 05 046, [arXiv:1903.01497].

[68] A. R. Brown, *Hyperbolic Inflation*, *Phys. Rev. Lett.* **121** (2018), no. 25 251601, [arXiv:1705.03023].

[69] S. Mizuno and S. Mukohyama, *Primordial perturbations from inflation with a hyperbolic field-space*, *Phys. Rev.* **D96** (2017), no. 10 103533, [arXiv:1707.05125].

[70] T. Bjorkmo and M. C. D. Marsh, *Hyperinflation generalised: from its attractor mechanism to its tension with the 'swampland conditions'*, *JHEP* **04** (2019) 172, [arXiv:1901.08603].

[71] J. Fumagalli, S. Garcia-Saenz, L. Pinol, S. Renaux-Petel, and J. Ronayne, *Hyper non-Gaussianities in inflation with strongly non-geodesic motion*, arXiv:1902.03221.

[72] T. Bjorkmo, R. Z. Ferreira, and M. C. D. Marsh, *Mild Non-Gaussianities under Perturbative Control from Rapid-Turn Inflation Models*, arXiv:1908.11316.

[73] R. Kallosh, A. Linde, and D. Roest, *Universal Attractor for Inflation at Strong Coupling*, *Phys. Rev. Lett.* **112** (2014), no. 1 011303, [arXiv:1310.3950].

[74] R. Kallosh and A. Linde, *Escher in the Sky*, *Comptes Rendus Physique* **16** (2015) 914–927, [arXiv:1503.06785].

[75] A. Achúcarro, R. Kallosh, A. Linde, D.-G. Wang, and Y. Welling, *Universality of multi-field α-attractors*, *JCAP* **1804** (2018), no. 04 028, [arXiv:1711.09478].

[76] P. Christodoulidis, D. Roest, and E. I. Sfakianakis, *Angular inflation in multi-field α-attractors*, arXiv:1803.09841.

[77] A. Linde, D.-G. Wang, Y. Welling, Y. Yamada, and A. Achúcarro, *Hypernatural inflation*, *JCAP* **1807** (2018), no. 07 035, [arXiv:1803.09911].

[78] A. Achúcarro, V. Atal, C. Germani, and G. A. Palma, *Cumulative effects in inflation with ultra-light entropy modes*, *JCAP* **1702** (2017), no. 02 013, [arXiv:1607.08609].

[79] A. Achúcarro, E. J. Copeland, O. Iarygina, G. A. Palma, D.-G. Wang, and Y. Welling, *Shift-Symmetric Orbital Inflation: single field or multi-field?*, arXiv:1901.03657.

[80] A. Achúcarro, G. A. Palma, D.-G. Wang, and Y. Welling, *Origin of*

ultra-light fields during inflation and their suppressed non-Gaussianity, arXiv:1908.06956.

[81] A. Achúcarro and Y. Welling, *Orbital Inflation: inflating along an angular isometry of field space*, arXiv:1907.02020.

[82] Y. Welling, *A simple, exact, model of quasi-single field inflation*, arXiv:1907.02951.

[83] S. Garcia-Saenz, S. Renaux-Petel, and J. Ronayne, *Primordial fluctuations and non-Gaussianities in sidetracked inflation*, *JCAP* **1807** (2018), no. 07 057, [arXiv:1804.11279].

[84] T. Bjorkmo, *Rapid-Turn Inflationary Attractors*, *Phys. Rev. Lett.* **122** (2019), no. 25 251301, [arXiv:1902.10529].

[85] P. Christodoulidis, D. Roest, and E. I. Sfakianakis, *Attractors, Bifurcations and Curvature in Multi-field Inflation*, arXiv:1903.03513.

[86] P. Christodoulidis, D. Roest, and E. I. Sfakianakis, *Scaling attractors in multi-field inflation*, arXiv:1903.06116.

[87] M. D. Schwartz, *Quantum Field Theory and the Standard Model*. Cambridge University Press, 3, 2014.

[88] S. R. Coleman, J. Wess, and B. Zumino, *Structure of phenomenological Lagrangians. 1.*, *Phys. Rev.* **177** (1969) 2239–2247.

[89] J. Callan, Curtis G., S. R. Coleman, J. Wess, and B. Zumino, *Structure of phenomenological Lagrangians. 2.*, *Phys. Rev.* **177** (1969) 2247–2250.

[90] S. Weinberg, *Effective Field Theory for Inflation*, *Phys. Rev.* **D77** (2008) 123541, [arXiv:0804.4291].

[91] C. Armendariz-Picon, V. F. Mukhanov, and P. J. Steinhardt, *A Dynamical solution to the problem of a small cosmological constant and late time cosmic acceleration*, *Phys. Rev. Lett.* **85** (2000) 4438–4441, [astro-ph/0004134].

[92] C. Armendariz-Picon, V. F. Mukhanov, and P. J. Steinhardt, *Essentials of k essence*, *Phys. Rev.* **D63** (2001) 103510, [astro-ph/0006373].

[93] V. Assassi, D. Baumann, D. Green, and L. McAllister, *Planck-Suppressed Operators*, *JCAP* **1401** (2014) 033, [arXiv:1304.5226].

[94] C. Cheung, P. Creminelli, A. L. Fitzpatrick, J. Kaplan, and L. Senatore, *The Effective Field Theory of Inflation*, *JHEP* **03** (2008) 014, [arXiv:0709.0293].

[95] E. Silverstein and D. Tong, *Scalar speed limits and cosmology: Acceleration from D-cceleration*, *Phys. Rev.* **D70** (2004) 103505, [hep-th/0310221].

[96] M. Alishahiha, E. Silverstein, and D. Tong, *DBI in the sky*, *Phys. Rev.* **D70** (2004) 123505, [hep-th/0404084].

[97] L. Senatore and M. Zaldarriaga, *The Effective Field Theory of Multifield Inflation*, *JHEP* **04** (2012) 024, [arXiv:1009.2093].

[98] A. Achúcarro, G. Pimentel, and D.-G. Wang *In preparation* (2020).

[99] T. Banks, M. Dine, P. J. Fox, and E. Gorbatov, *On the possibility of large axion decay constants*, *JCAP* **0306** (2003) 001, [hep-th/0303252].

[100] A. Nicolis and F. Piazza, *Spontaneous Symmetry Probing*, *JHEP* **06** (2012) 025, [arXiv:1112.5174].

[101] A. Achúcarro, D.-G. Wang, Y. Welling, and A. Westphal, *Inflation in coset space*, *In preparation* (2020).

[102] N. Arkani-Hamed, D. Baumann, H. Lee, and G. L. Pimentel, *The Cosmological Bootstrap: Inflationary Correlators from Symmetries and Singularities*, arXiv:1811.00024.

[103] B. Finelli, G. Goon, E. Pajer, and L. Santoni, *Soft Theorems For Shift-Symmetric Cosmologies*, *Phys. Rev.* **D97** (2018), no. 6 063531, [arXiv:1711.03737].

[104] B. Finelli, G. Goon, E. Pajer, and L. Santoni, *The Effective Theory of Shift-Symmetric Cosmologies*, *JCAP* **1805** (2018), no. 05 060, [arXiv:1802.01580].

[105] D.-G. Wang, *On the inflationary massive field with a curved field manifold*, *JCAP* **01** (2020) 046, [arXiv:1911.04459].

[106] Y.-F. Cai, X. Chen, M. H. Namjoo, M. Sasaki, D.-G. Wang, and Z. Wang, *Revisiting non-Gaussianity from non-attractor inflation models*, *JCAP* **1805** (2018), no. 05 012, [arXiv:1712.09998].

[107] Y.-B. Li, J. Quintin, D.-G. Wang, and Y.-F. Cai, *Matter bounce cosmology with a generalized single field: non-Gaussianity and an extended no-go theorem*, *JCAP* **1703** (2017), no. 03 031, [arXiv:1612.02036].

[108] **Planck** Collaboration, P. A. R. Ade et al., *Planck 2015 results. XX. Constraints on inflation*, *Astron. Astrophys.* **594** (2016) A20, [arXiv:1502.02114].

[109] **Planck** Collaboration, P. A. R. Ade et al., *Planck 2015 results. XVII. Constraints on primordial non-Gaussianity*, *Astron. Astrophys.* **594** (2016) A17, [arXiv:1502.01592].

[110] S. Ferrara, R. Kallosh, A. Linde, and M. Porrati, *Minimal Supergravity Models of Inflation*, *Phys. Rev.* **D88** (2013), no. 8 085038, [arXiv:1307.7696].

[111] S. Cecotti and R. Kallosh, *Cosmological Attractor Models and Higher Curvature Supergravity*, *JHEP* **05** (2014) 114, [arXiv:1403.2932].

[112] M. Galante, R. Kallosh, A. Linde, and D. Roest, *Unity of Cosmological Inflation Attractors*, *Phys. Rev. Lett.* **114** (2015), no. 14 141302, [arXiv:1412.3797].

[113] S. Ferrara and R. Kallosh, *Seven-Disk Manifold, α-attractors and B-modes*, arXiv:1610.04163.

[114] R. Kallosh, A. Linde, T. Wrase, and Y. Yamada, *Maximal Supersymmetry and B-Mode Targets*, *JHEP* **04** (2017) 144, [arXiv:1704.04829].

[115] R. Kallosh, A. Linde, D. Roest, and Y. Yamada, *$\overline{D3}$ induced geometric inflation*, *JHEP* **07** (2017) 057, [arXiv:1705.09247].

[116] N. Bartolo, S. Matarrese, and A. Riotto, *Adiabatic and isocurvature perturbations from inflation: Power spectra and consistency relations*, *Phys.*

Rev. **D64** (2001) 123504, [astro-ph/0107502].

[117] Z. Lalak, D. Langlois, S. Pokorski, and K. Turzynski, *Curvature and isocurvature perturbations in two-field inflation*, *JCAP* **0707** (2007) 014, [arXiv:0704.0212].

[118] C. M. Peterson and M. Tegmark, *Testing Two-Field Inflation*, *Phys. Rev.* **D83** (2011) 023522, [arXiv:1005.4056].

[119] Y. Welling, *Multiple Field Inflation and Signatures of Heavy Physics in the CMB*, arXiv:1502.04369.

[120] T. Kobayashi and S. Mukohyama, *Effects of Light Fields During Inflation*, *Phys. Rev.* **D81** (2010) 103504, [arXiv:1003.0076].

[121] S. Renaux-Petel and K. Turzynski, *On reaching the adiabatic limit in multi-field inflation*, *JCAP* **1506** (2015), no. 06 010, [arXiv:1405.6195].

[122] S. Cremonini, Z. Lalak, and K. Turzynski, *On Non-Canonical Kinetic Terms and the Tilt of the Power Spectrum*, *Phys. Rev.* **D82** (2010) 047301, [arXiv:1005.4347].

[123] S. Cremonini, Z. Lalak, and K. Turzynski, *Strongly Coupled Perturbations in Two-Field Inflationary Models*, *JCAP* **1103** (2011) 016, [arXiv:1010.3021].

[124] C. van de Bruck and M. Robinson, *Power Spectra beyond the Slow Roll Approximation in Theories with Non-Canonical Kinetic Terms*, *JCAP* **1408** (2014) 024, [arXiv:1404.7806].

[125] R. Kallosh and A. Linde, *Multi-field Conformal Cosmological Attractors*, *JCAP* **1312** (2013) 006, [arXiv:1309.2015].

[126] A. A. Starobinsky, S. Tsujikawa, and J. Yokoyama, *Cosmological perturbations from multifield inflation in generalized Einstein theories*, *Nucl. Phys.* **B610** (2001) 383–410, [astro-ph/0107555].

[127] F. Di Marco, F. Finelli, and R. Brandenberger, *Adiabatic and isocurvature perturbations for multifield generalized Einstein models*, *Phys. Rev.* **D67** (2003) 063512, [astro-ph/0211276].

[128] J. Ellis, M. A. G. García, D. V. Nanopoulos, and K. A. Olive, *Two-Field Analysis of No-Scale Supergravity Inflation*, *JCAP* **1501** (2015) 010, [arXiv:1409.8197].

[129] S. Ferrara, R. Kallosh, and A. Linde, *Cosmology with Nilpotent Superfields*, *JHEP* **10** (2014) 143, [arXiv:1408.4096].

[130] M. Dias, J. Frazer, and D. Seery, *Computing observables in curved multifield models of inflation?A guide (with code) to the transport method*, *JCAP* **1512** (2015), no. 12 030, [arXiv:1502.03125].

[131] D. S. Salopek and J. R. Bond, *Nonlinear evolution of long wavelength metric fluctuations in inflationary models*, *Phys. Rev.* **D42** (1990) 3936–3962.

[132] M. Sasaki and E. D. Stewart, *A General analytic formula for the spectral index of the density perturbations produced during inflation*, *Prog. Theor. Phys.* **95** (1996) 71–78, [astro-ph/9507001].

[133] A. A. Starobinsky, *Multicomponent de Sitter (Inflationary) Stages and the Generation of Perturbations*, *JETP Lett.* **42** (1985) 152–155. [Pisma Zh. Eksp. Teor. Fiz.42,124(1985)].

[134] M. Sasaki and T. Tanaka, *Superhorizon scale dynamics of multiscalar inflation*, *Prog. Theor. Phys.* **99** (1998) 763–782, [gr-qc/9801017].

[135] H.-C. Lee, M. Sasaki, E. D. Stewart, T. Tanaka, and S. Yokoyama, *A New delta N formalism for multi-component inflation*, *JCAP* **0510** (2005) 004, [astro-ph/0506262].

[136] Y. Yamada, *U(1) symmetric α-attractors*, arXiv:1802.04848.

[137] P. Agrawal, G. Obied, P. J. Steinhardt, and C. Vafa, *On the Cosmological Implications of the String Swampland*, *Phys. Lett.* **B784** (2018) 271–276, [arXiv:1806.09718].

[138] A. G. Muslimov, *On the Scalar Field Dynamics in a Spatially Flat Friedman Universe*, *Class. Quant. Grav.* **7** (1990) 231–237.

[139] J. E. Lidsey, *The Scalar field as dynamical variable in inflation*, *Phys. Lett.* **B273** (1991) 42–46.

[140] E. J. Copeland, E. W. Kolb, A. R. Liddle, and J. E. Lidsey, *Reconstructing the inflation potential, in principle and in practice*, *Phys. Rev.* **D48** (1993) 2529–2547, [hep-ph/9303288].

[141] X. Chen, G. A. Palma, W. Riquelme, B. Scheihing Hitschfeld, and S. Sypsas, *Landscape tomography through primordial non-Gaussianity*, *Phys. Rev.* **D98** (2018), no. 8 083528, [arXiv:1804.07315].

[142] D. H. Lyth and Y. Rodriguez, *The Inflationary prediction for primordial non-Gaussianity*, *Phys. Rev. Lett.* **95** (2005) 121302, [astro-ph/0504045].

[143] C. T. Byrnes, K.-Y. Choi, and L. M. H. Hall, *Conditions for large non-Gaussianity in two-field slow-roll inflation*, *JCAP* **0810** (2008) 008, [arXiv:0807.1101].

[144] C. T. Byrnes and G. Tasinato, *Non-Gaussianity beyond slow roll in multi-field inflation*, *JCAP* **0908** (2009) 016, [arXiv:0906.0767].

[145] C. T. Byrnes and K.-Y. Choi, *Review of local non-Gaussianity from multi-field inflation*, *Adv. Astron.* **2010** (2010) 724525, [arXiv:1002.3110].

[146] M. Dias, J. Frazer, and M. c. D. Marsh, *Seven Lessons from Manyfield Inflation in Random Potentials*, *JCAP* **1801** (2018), no. 01 036, [arXiv:1706.03774].

[147] T. Bjorkmo and M. C. D. Marsh, *Manyfield Inflation in Random Potentials*, *JCAP* **1802** (2018), no. 02 037, [arXiv:1709.10076].

[148] S. C. Hotinli, J. Frazer, A. H. Jaffe, J. Meyers, L. C. Price, and E. R. M. Tarrant, *Effect of reheating on predictions following multiple-field inflation*, *Phys. Rev.* **D97** (2018), no. 2 023511, [arXiv:1710.08913].

[149] D. Seery and J. E. Lidsey, *Primordial non-Gaussianities from multiple-field inflation*, *JCAP* **0509** (2005) 011, [astro-ph/0506056].

[150] J. Chluba, J. Hamann, and S. P. Patil, *Features and New Physical Scales in Primordial Observables: Theory and Observation*, *Int. J. Mod. Phys.* **D24**

(2015), no. 10 1530023, [arXiv:1505.01834].

[151] P. D. Meerburg et al., *Primordial Non-Gaussianity*, arXiv:1903.04409.

[152] V. Assassi, D. Baumann, and D. Green, *On Soft Limits of Inflationary Correlation Functions*, *JCAP* **1211** (2012) 047, [arXiv:1204.4207].

[153] E. Sefusatti, J. R. Fergusson, X. Chen, and E. P. S. Shellard, *Effects and Detectability of Quasi-Single Field Inflation in the Large-Scale Structure and Cosmic Microwave Background*, *JCAP* **1208** (2012) 033, [arXiv:1204.6318].

[154] T. Noumi, M. Yamaguchi, and D. Yokoyama, *Effective field theory approach to quasi-single field inflation and effects of heavy fields*, *JHEP* **06** (2013) 051, [arXiv:1211.1624].

[155] H. Lee, D. Baumann, and G. L. Pimentel, *Non-Gaussianity as a Particle Detector*, *JHEP* **12** (2016) 040, [arXiv:1607.03735].

[156] P. D. Meerburg, M. Münchmeyer, J. B. Muñoz, and X. Chen, *Prospects for Cosmological Collider Physics*, *JCAP* **1703** (2017), no. 03 050, [arXiv:1610.06559].

[157] X. Chen, Y. Wang, and Z.-Z. Xianyu, *Standard Model Background of the Cosmological Collider*, *Phys. Rev. Lett.* **118** (2017), no. 26 261302, [arXiv:1610.06597].

[158] X. Chen, Y. Wang, and Z.-Z. Xianyu, *Standard Model Mass Spectrum in Inflationary Universe*, *JHEP* **04** (2017) 058, [arXiv:1612.08122].

[159] A. Hook, J. Huang, and D. Racco, *Searches for other vacua II: A new Higgstory at the cosmological collider*, arXiv:1907.10624.

[160] S. Kumar and R. Sundrum, *Cosmological Collider Physics and the Curvaton*, arXiv:1908.11378.

[161] L.-T. Wang and Z.-Z. Xianyu, *In Search of Large Signals at the Cosmological Collider*, arXiv:1910.12876.

[162] X. Chen, *Primordial Features as Evidence for Inflation*, *JCAP* **1201** (2012) 038, [arXiv:1104.1323].

[163] X. Chen, M. H. Namjoo, and Y. Wang, *Models of the Primordial Standard Clock*, *JCAP* **1502** (2015), no. 02 027, [arXiv:1411.2349].

[164] X. Chen, M. H. Namjoo, and Y. Wang, *Quantum Primordial Standard Clocks*, *JCAP* **1602** (2016), no. 02 013, [arXiv:1509.03930].

[165] X. Chen, A. Loeb, and Z.-Z. Xianyu, *Unique Fingerprints of Alternatives to Inflation in the Primordial Power Spectrum*, *Phys. Rev. Lett.* **122** (2019), no. 12 121301, [arXiv:1809.02603].

[166] T. Krajewski, K. Turzyński, and M. Wieczorek, *On preheating in α-attractor models of inflation*, *Eur. Phys. J.* **C79** (2019), no. 8 654, [arXiv:1801.01786].

[167] M. Dias, J. Frazer, A. Retolaza, M. Scalisi, and A. Westphal, *Pole N-flation*, *JHEP* **02** (2019) 120, [arXiv:1805.02659].

[168] O. Iarygina, E. I. Sfakianakis, D.-G. Wang, and A. Achucarro, *Universality and scaling in multi-field α-attractor preheating*, *JCAP* **1906** (2019), no. 06

027, [arXiv:1810.02804].

[169] F. G. Pedro and A. Westphal, *Flattened Axion Monodromy Beyond Two Derivatives*, arXiv:1909.08100.

[170] D. Chakraborty, R. Chiovoloni, O. Loaiza-Brito, G. Niz, and I. Zavala, *Fat Inflatons, Large Turns and the η-problem*, arXiv:1908.09797.

[171] S. Garcia-Saenz, L. Pinol, and S. Renaux-Petel, *Revisiting non-Gaussianity in multifield inflation with curved field space*, arXiv:1907.10403.

[172] C. P. Burgess, M. Cicoli, F. Quevedo, and M. Williams, *Inflating with Large Effective Fields*, *JCAP* **1411** (2014) 045, [arXiv:1404.6236].

[173] R. Klein, D. Roest, and D. Stefanyszyn, *Symmetry Breaking Patterns for Inflation*, *JHEP* **06** (2018) 006, [arXiv:1712.05760].

[174] H. An, M. McAneny, A. K. Ridgway, and M. B. Wise, *Quasi Single Field Inflation in the non-perturbative regime*, *JHEP* **06** (2018) 105, [arXiv:1706.09971].

[175] X. Tong, Y. Wang, and S. Zhou, *On the Effective Field Theory for Quasi-Single Field Inflation*, *JCAP* **1711** (2017), no. 11 045, [arXiv:1708.01709].

[176] J. Fumagalli, S. Renaux-Petel, and J. W. Ronayne, *Higgs vacuum (in)stability during inflation: the dangerous relevance of de Sitter departure and Planck-suppressed operators*, arXiv:1910.13430.

[177] E. Pajer, G. L. Pimentel, and J. V. S. Van Wijck, *The Conformal Limit of Inflation in the Era of CMB Polarimetry*, *JCAP* **1706** (2017), no. 06 009, [arXiv:1609.06993].

[178] J. J. Sakurai, *Modern Quantum Mechanics (Revised Edition)*. Addison-Wesley Publishing Company, 1994.

[179] N. Dalal, O. Dore, D. Huterer, and A. Shirokov, *The imprints of primordial non-gaussianities on large-scale structure: scale dependent bias and abundance of virialized objects*, *Phys. Rev.* **D77** (2008) 123514, [arXiv:0710.4560].

[180] S. Matarrese and L. Verde, *The effect of primordial non-Gaussianity on halo bias*, *Astrophys. J.* **677** (2008) L77–L80, [arXiv:0801.4826].

[181] M. Biagetti, *The Hunt for Primordial Interactions in the Large Scale Structures of the Universe*, *Galaxies* **7** (2019), no. 3 71, [arXiv:1906.12244].

[182] **Planck** Collaboration, P. A. R. Ade et al., *Planck 2015 results. XIII. Cosmological parameters*, *Astron. Astrophys.* **594** (2016) A13, [arXiv:1502.01589].

[183] J. Martin, H. Motohashi, and T. Suyama, *Ultra Slow-Roll Inflation and the non-Gaussianity Consistency Relation*, *Phys. Rev.* **D87** (2013), no. 2 023514, [arXiv:1211.0083].

[184] X. Chen, H. Firouzjahi, E. Komatsu, M. H. Namjoo, and M. Sasaki, *In-in and δN calculations of the bispectrum from non-attractor single-field inflation*, *JCAP* **1312** (2013) 039, [arXiv:1308.5341].

[185] Q.-G. Huang and Y. Wang, *Large Local Non-Gaussianity from General Single-field Inflation*, *JCAP* **1306** (2013) 035, [arXiv:1303.4526].

[186] Y.-F. Cai, W. Xue, R. Brandenberger, and X. Zhang, *Non-Gaussianity in a Matter Bounce*, *JCAP* **0905** (2009) 011, [arXiv:0903.0631].

[187] S. Mooij and G. A. Palma, *Consistently violating the non-Gaussian consistency relation*, *JCAP* **1511** (2015), no. 11 025, [arXiv:1502.03458].

[188] E. Pajer and S. Jazayeri, *Systematics of Adiabatic Modes: Flat Universes*, *JCAP* **1803** (2018), no. 03 013, [arXiv:1710.02177].

[189] R. Bravo, S. Mooij, G. A. Palma, and B. Pradenas, *A generalized non-Gaussian consistency relation for single field inflation*, *JCAP* **1805** (2018), no. 05 024, [arXiv:1711.02680].

[190] Y.-F. Cai, J.-O. Gong, D.-G. Wang, and Z. Wang, *Features from the non-attractor beginning of inflation*, *JCAP* **1610** (2016), no. 10 017, [arXiv:1607.07872].

[191] D. H. Lyth, K. A. Malik, and M. Sasaki, *A General proof of the conservation of the curvature perturbation*, *JCAP* **0505** (2005) 004, [astro-ph/0411220].

[192] D. Seery and J. E. Lidsey, *Primordial non-Gaussianities in single field inflation*, *JCAP* **0506** (2005) 003, [astro-ph/0503692].

[193] X. Chen, M.-x. Huang, S. Kachru, and G. Shiu, *Observational signatures and non-Gaussianities of general single field inflation*, *JCAP* **0701** (2007) 002, [hep-th/0605045].

[194] R. Bravo, S. Mooij, G. A. Palma, and B. Pradenas, *Vanishing of local non-Gaussianity in canonical single field inflation*, arXiv:1711.05290.

[195] R. H. Brandenberger, *Introduction to Early Universe Cosmology*, *PoS* **ICFI2010** (2010) 001, [arXiv:1103.2271].

[196] Y. Wan, T. Qiu, F. P. Huang, Y.-F. Cai, H. Li, and X. Zhang, *Bounce Inflation Cosmology with Standard Model Higgs Boson*, *JCAP* **1512** (2015), no. 12 019, [arXiv:1509.08772].

[197] A. Borde and A. Vilenkin, *Eternal inflation and the initial singularity*, *Phys. Rev. Lett.* **72** (1994) 3305–3309, [gr-qc/9312022].

[198] M. Novello and S. E. P. Bergliaffa, *Bouncing Cosmologies*, *Phys. Rept.* **463** (2008) 127–213, [arXiv:0802.1634].

[199] D. Battefeld and P. Peter, *A Critical Review of Classical Bouncing Cosmologies*, *Phys. Rept.* **571** (2015) 1–66, [arXiv:1406.2790].

[200] A. Nicolis, R. Rattazzi, and E. Trincherini, *The Galileon as a local modification of gravity*, *Phys. Rev.* **D79** (2009) 064036, [arXiv:0811.2197].

[201] G. W. Horndeski, *Second-order scalar-tensor field equations in a four-dimensional space*, *Int. J. Theor. Phys.* **10** (1974) 363–384.

[202] T. Qiu, J. Evslin, Y.-F. Cai, M. Li, and X. Zhang, *Bouncing Galileon Cosmologies*, *JCAP* **1110** (2011) 036, [arXiv:1108.0593].

[203] D. A. Easson, I. Sawicki, and A. Vikman, *G-Bounce*, *JCAP* **1111** (2011) 021, [arXiv:1109.1047].

[204] Y.-F. Cai, D. A. Easson, and R. Brandenberger, *Towards a Nonsingular Bouncing Cosmology*, *JCAP* **1208** (2012) 020, [arXiv:1206.2382].

[205] Y.-F. Cai, R. Brandenberger, and P. Peter, *Anisotropy in a Nonsingular Bounce*, *Class. Quant. Grav.* **30** (2013) 075019, [arXiv:1301.4703].

[206] M. Osipov and V. Rubakov, *Galileon bounce after ekpyrotic contraction*, *JCAP* **1311** (2013) 031, [arXiv:1303.1221].

[207] L. Battarra, M. Koehn, J.-L. Lehners, and B. A. Ovrut, *Cosmological Perturbations Through a Non-Singular Ghost-Condensate/Galileon Bounce*, *JCAP* **1407** (2014) 007, [arXiv:1404.5067].

[208] A. Ijjas and P. J. Steinhardt, *Classically stable nonsingular cosmological bounces*, *Phys. Rev. Lett.* **117** (2016), no. 12 121304, [arXiv:1606.08880].

[209] A. Ijjas and P. J. Steinhardt, *Fully stable cosmological solutions with a non-singular classical bounce*, *Phys. Lett.* **B764** (2017) 289–294, [arXiv:1609.01253].

[210] M. Libanov, S. Mironov, and V. Rubakov, *Generalized Galileons: instabilities of bouncing and Genesis cosmologies and modified Genesis*, *JCAP* **1608** (2016), no. 08 037, [arXiv:1605.05992].

[211] T. Kobayashi, *Generic instabilities of nonsingular cosmologies in Horndeski theory: A no-go theorem*, *Phys. Rev.* **D94** (2016), no. 4 043511, [arXiv:1606.05831].

[212] Y. Cai, Y. Wan, H.-G. Li, T. Qiu, and Y.-S. Piao, *The Effective Field Theory of nonsingular cosmology*, *JHEP* **01** (2017) 090, [arXiv:1610.03400].

[213] P. Creminelli, D. Pirtskhalava, L. Santoni, and E. Trincherini, *Stability of Geodesically Complete Cosmologies*, *JCAP* **1611** (2016), no. 11 047, [arXiv:1610.04207].

[214] J.-L. Lehners and E. Wilson-Ewing, *Running of the scalar spectral index in bouncing cosmologies*, *JCAP* **1510** (2015), no. 10 038, [arXiv:1507.08112].

[215] Y.-F. Cai, A. Marciano, D.-G. Wang, and E. Wilson-Ewing, *Bouncing cosmologies with dark matter and dark energy*, *Universe* **3** (2016), no. 1 1, [arXiv:1610.00938].

[216] C. Armendariz-Picon, T. Damour, and V. F. Mukhanov, *k - inflation*, *Phys. Lett.* **B458** (1999) 209–218, [hep-th/9904075].

[217] J. Garriga and V. F. Mukhanov, *Perturbations in k-inflation*, *Phys. Lett.* **B458** (1999) 219–225, [hep-th/9904176].

[218] J. Noller and J. Magueijo, *Non-Gaussianity in single field models without slow-roll*, *Phys. Rev.* **D83** (2011) 103511, [arXiv:1102.0275].

[219] C. Deffayet, X. Gao, D. A. Steer, and G. Zahariade, *From k-essence to generalised Galileons*, *Phys. Rev.* **D84** (2011) 064039, [arXiv:1103.3260].

[220] T. Kobayashi, M. Yamaguchi, and J. Yokoyama, *G-inflation: Inflation driven by the Galileon field*, *Phys. Rev. Lett.* **105** (2010) 231302, [arXiv:1008.0603].

[221] C. Burrage, C. de Rham, D. Seery, and A. J. Tolley, *Galileon inflation*,

JCAP **1101** (2011) 014, [arXiv:1009.2497].

[222] P. Creminelli, G. D'Amico, M. Musso, J. Norena, and E. Trincherini, *Galilean symmetry in the effective theory of inflation: new shapes of non-Gaussianity*, *JCAP* **1102** (2011) 006, [arXiv:1011.3004].

[223] T. Kobayashi, M. Yamaguchi, and J. Yokoyama, *Generalized G-inflation: Inflation with the most general second-order field equations*, *Prog. Theor. Phys.* **126** (2011) 511–529, [arXiv:1105.5723].

[224] X. Gao and D. A. Steer, *Inflation and primordial non-Gaussianities of 'generalized Galileons'*, *JCAP* **1112** (2011) 019, [arXiv:1107.2642].

[225] Y.-F. Cai, T.-t. Qiu, R. Brandenberger, and X.-m. Zhang, *A Nonsingular Cosmology with a Scale-Invariant Spectrum of Cosmological Perturbations from Lee-Wick Theory*, *Phys. Rev.* **D80** (2009) 023511, [arXiv:0810.4677].

[226] Y.-F. Cai, J. Quintin, E. N. Saridakis, and E. Wilson-Ewing, *Nonsingular bouncing cosmologies in light of BICEP2*, *JCAP* **1407** (2014) 033, [arXiv:1404.4364].

[227] J. Quintin, Z. Sherkatghanad, Y.-F. Cai, and R. H. Brandenberger, *Evolution of cosmological perturbations and the production of non-Gaussianities through a nonsingular bounce: Indications for a no-go theorem in single field matter bounce cosmologies*, *Phys. Rev.* **D92** (2015), no. 6 063532, [arXiv:1508.04141].

[228] **BICEP2, Keck Array** Collaboration, P. A. R. Ade et al., *Improved Constraints on Cosmology and Foregrounds from BICEP2 and Keck Array Cosmic Microwave Background Data with Inclusion of 95 GHz Band*, *Phys. Rev. Lett.* **116** (2016) 031302, [arXiv:1510.09217].

[229] B. Xue, D. Garfinkle, F. Pretorius, and P. J. Steinhardt, *Nonperturbative analysis of the evolution of cosmological perturbations through a nonsingular bounce*, *Phys. Rev.* **D88** (2013) 083509, [arXiv:1308.3044].

[230] Y.-F. Cai and E. Wilson-Ewing, *A ΛCDM bounce scenario*, *JCAP* **1503** (2015), no. 03 006, [arXiv:1412.2914].

[231] E. Wilson-Ewing, *Separate universes in loop quantum cosmology: framework and applications*, *Int. J. Mod. Phys.* **D25** (2016), no. 08 1642002, [arXiv:1512.05743].

[232] X. Gao, M. Lilley, and P. Peter, *Production of non-gaussianities through a positive spatial curvature bouncing phase*, *JCAP* **1407** (2014) 010, [arXiv:1403.7958].

[233] X. Gao, M. Lilley, and P. Peter, *Non-Gaussianity excess problem in classical bouncing cosmologies*, *Phys. Rev.* **D91** (2015), no. 2 023516, [arXiv:1406.4119].

[234] Y.-F. Cai, F. Duplessis, D. A. Easson, and D.-G. Wang, *Searching for a matter bounce cosmology with low redshift observations*, *Phys. Rev.* **D93** (2016), no. 4 043546, [arXiv:1512.08979].

[235] C. Lin, R. H. Brandenberger, and L. Perreault Levasseur, *A Matter Bounce By Means of Ghost Condensation*, *JCAP* **1104** (2011) 019,

[arXiv:1007.2654].

[236] J. Quintin and R. H. Brandenberger, *Black hole formation in a contracting universe*, *JCAP* **1611** (2016) 029, [arXiv:1609.02556].

[237] D. Baumann, L. Senatore, and M. Zaldarriaga, *Scale-Invariance and the Strong Coupling Problem*, *JCAP* **1105** (2011) 004, [arXiv:1101.3320].

[238] A. Joyce and J. Khoury, *Strong Coupling Problem with Time-Varying Sound Speed*, *Phys. Rev.* **D84** (2011) 083514, [arXiv:1107.3550].

[239] Y.-F. Cai, R. Brandenberger, and X. Zhang, *The Matter Bounce Curvaton Scenario*, *JCAP* **1103** (2011) 003, [arXiv:1101.0822].

[240] S. Alexander, Y.-F. Cai, and A. Marciano, *Fermi-bounce cosmology and the fermion curvaton mechanism*, *Phys. Lett.* **B745** (2015) 97–104, [arXiv:1406.1456].

[241] A. Addazi, S. Alexander, Y.-F. Cai, and A. Marciano, *Dark matter and baryogenesis in the Fermi-bounce curvaton mechanism*, *Chin. Phys.* **C42** (2018), no. 6 065101, [arXiv:1612.00632].

[242] Y.-F. Cai, E. McDonough, F. Duplessis, and R. H. Brandenberger, *Two Field Matter Bounce Cosmology*, *JCAP* **1310** (2013) 024, [arXiv:1305.5259].

[243] J.-L. Lehners, P. McFadden, N. Turok, and P. J. Steinhardt, *Generating ekpyrotic curvature perturbations before the big bang*, *Phys. Rev.* **D76** (2007) 103501, [hep-th/0702153].

[244] E. I. Buchbinder, J. Khoury, and B. A. Ovrut, *New Ekpyrotic cosmology*, *Phys. Rev.* **D76** (2007) 123503, [hep-th/0702154].

[245] T. Qiu, X. Gao, and E. N. Saridakis, *Towards anisotropy-free and nonsingular bounce cosmology with scale-invariant perturbations*, *Phys. Rev.* **D88** (2013), no. 4 043525, [arXiv:1303.2372].

[246] M. Li, *Note on the production of scale-invariant entropy perturbation in the Ekpyrotic universe*, *Phys. Lett.* **B724** (2013) 192–197, [arXiv:1306.0191].

[247] M. Li, *Entropic mechanisms with generalized scalar fields in the Ekpyrotic universe*, *Phys. Lett.* **B741** (2015) 320–326, [arXiv:1411.7626].

[248] E. Wilson-Ewing, *Ekpyrotic loop quantum cosmology*, *JCAP* **1308** (2013) 015, [arXiv:1306.6582].

[249] E. I. Buchbinder, J. Khoury, and B. A. Ovrut, *On the initial conditions in new ekpyrotic cosmology*, *JHEP* **11** (2007) 076, [arXiv:0706.3903].

[250] E. I. Buchbinder, J. Khoury, and B. A. Ovrut, *Non-Gaussianities in new ekpyrotic cosmology*, *Phys. Rev. Lett.* **100** (2008) 171302, [arXiv:0710.5172].

[251] J.-L. Lehners and P. J. Steinhardt, *Non-Gaussian density fluctuations from entropically generated curvature perturbations in Ekpyrotic models*, *Phys. Rev.* **D77** (2008) 063533, [arXiv:0712.3779]. [Erratum: Phys. Rev.D79,129903(2009)].

[252] J.-L. Lehners and P. J. Steinhardt, *Intuitive understanding of non-gaussianity in ekpyrotic and cyclic models*, *Phys. Rev.* **D78** (2008)

023506, [arXiv:0804.1293]. [Erratum: Phys. Rev.D79,129902(2009)].

[253] J.-L. Lehners and S. Renaux-Petel, *Multifield Cosmological Perturbations at Third Order and the Ekpyrotic Trispectrum*, *Phys. Rev.* **D80** (2009) 063503, [arXiv:0906.0530].

[254] J.-L. Lehners, *Ekpyrotic and Cyclic Cosmology*, *Phys. Rept.* **465** (2008) 223–263, [arXiv:0806.1245].

[255] J.-L. Lehners, *Ekpyrotic Non-Gaussianity: A Review*, *Adv. Astron.* **2010** (2010) 903907, [arXiv:1001.3125].

[256] A. Fertig, J.-L. Lehners, and E. Mallwitz, *Ekpyrotic Perturbations With Small Non-Gaussian Corrections*, *Phys. Rev.* **D89** (2014), no. 10 103537, [arXiv:1310.8133].

[257] A. Ijjas, J.-L. Lehners, and P. J. Steinhardt, *General mechanism for producing scale-invariant perturbations and small non-Gaussianity in ekpyrotic models*, *Phys. Rev.* **D89** (2014), no. 12 123520, [arXiv:1404.1265].

[258] A. M. Levy, A. Ijjas, and P. J. Steinhardt, *Scale-invariant perturbations in ekpyrotic cosmologies without fine-tuning of initial conditions*, *Phys. Rev.* **D92** (2015), no. 6 063524, [arXiv:1506.01011].

[259] A. Fertig and J.-L. Lehners, *The Non-Minimal Ekpyrotic Trispectrum*, *JCAP* **1601** (2016), no. 01 026, [arXiv:1510.03439].

[260] A. Fertig, J.-L. Lehners, E. Mallwitz, and E. Wilson-Ewing, *Converting entropy to curvature perturbations after a cosmic bounce*, *JCAP* **1610** (2016), no. 10 005, [arXiv:1607.05663].

[261] A. M. Levy, *Fine-tuning challenges for the matter bounce scenario*, *Phys. Rev.* **D95** (2017), no. 2 023522, [arXiv:1611.08972].

[262] C. Cheung, A. L. Fitzpatrick, J. Kaplan, and L. Senatore, *On the consistency relation of the 3-point function in single field inflation*, *JCAP* **0802** (2008) 021, [arXiv:0709.0295].

Summary

Where do we come from?

The quest for the origin of everything has puzzled all the curious minds since our ancestors looked up the starry sky in wonder.

What is the fundamental law of nature?

To get a complete answer, from philosophers in ancient Greece to theoretical physicists today, numerous brilliant thinkers have stepped on "the greatest adventure that the human mind has ever begun"[1].

Excitingly, the modern advances of primordial cosmology are building the link between these two most fascinating questions in the history of human civilization. In the current understanding, our Universe originated from a small patch with a hot and dense state 13.8 billion years ago. From the recent developments of fundamental physics, we further speculate that the cosmic expansion was exponentially rapid within the first fraction of a second after the Big Bang. This theoretical proposal, called cosmic inflation, provides a successful description for the earliest stage of the Universe. Meanwhile, during this inflation stage quantum fluctuations can become the initial seeds of cosmic inhomogeneities, which later evolve into galaxies, clusters and large scale structures. Thus it is remarkable that through today's astronomical observations, we can trace the imprints in primordial inhomogeneities left by physics processes during inflation. As a result, primordial cosmology has become an exciting research area for theoretical physicists, where one can hunt for the fundamental laws of physics that govern the earliest moment in our Universe.

Motivated by the big picture above, this thesis is dedicated to exploring the theories of the primordial Universe and their connections with astro-

[1]Quoted from Richard Feynman, *The Feynman Lectures on Physics, Volume III.*

nomical observations.

The first part of the thesis focuses on so-called inflationary curved field spaces. To understand how inflation happens, typically we require a driver called the inflaton field, and it may move in a multi-dimensional field space which in general is curved. Thus the geometry of this internal space can be seen as one particular example of new physics effects during inflation.

In Chapter 2, we investigate a class of inflation models called α-attractors. Here the magic of the hyperbolic field space is demonstrated explicitly in the two-field extension of these models. With its effects, the model predictions of single field α-attractors are almost unaffected, even when the multi-field effects become significant. This work complements the previous single-field analysis of α-attractor models, and also highlights the role of the hyperbolic geometry of the field space.

Chapter 3 proposes another class of cosmological models called "shift-symmetric orbital inflation", where the inflaton circles along an "angular" direction in a general field space. Again the multi-field effects are significant in these models, but in the end we still find single-field like predictions. This work corresponds to a less explored regime in multi-field inflation where the extra field is light but significantly coupled to the inflaton.

While most of the previous analysis of the internal spaces are relying on specific models, Chapter 4 is dedicated to a more general question: what are the model-independent observational signatures of these inflationary curved field spaces? Here I try to answer this question using the non-Gaussian phenomenology of massive fields during inflation, and find the fingerprints of these internal spaces which can be tested in future observations.

The second part of the thesis studies the phenomenology of one very important observable – primordial non-Gaussianity, which captures the deviation from the Gaussian statistics of primordial inhomogeneities. These signals are worth searching for, as a wealth of early-time information is believed to be encoded in the cosmological triangle patterns.

Chapter 5 revisits the non-Gaussianities generated in non-attractor inflation. This class of models are well known to violate Maldacena's consistency relation in the framework of single-field inflation, which has received much attention and investigation. Through careful calculation, we explicitly show what happens to this famous counter-example when realistic and complete models of non-attractor inflation are considered.

Chapter 6 studies the non-Gaussian phenomenology of an alternative to

inflation – matter bounce cosmology. We begin with a generalized single-field setup. The non-Gaussian signals generated here can be used to distinguish this alternative scenario from inflation. Moreover, we propose a no-go theorem which rules out many alternative models with the current observational constraints.

What's next? This thesis aims to push the frontier of the primordial cosmology. Needless to say, this is a research area under fast development: many interesting theoretical ideas are emerging; and upcoming observational experiments may tell us more about the earliest stage of the Universe. To further explore the new physics effects in the primordial era, the following topics are worthy of deep consideration in the coming years.

- *Internal symmetries* usually play an important role in the fundamental realizations of inflation, and they may also be closely related to the effective field theory, the geometry of the field space and new phenomenology. To hunt for signatures of underlying symmetries during inflation, it is interesting to perform more systematic investigations.

- *Scattering amplitudes* research provides new perspectives and powerful tools in the modern study of quantum field theory. One may wonder whether similar approaches can be applied for bootstrapping correlators in cosmology. While some pioneering studies have appeared recently, this is a brand new area with many open opportunities.

- *Large scale structure surveys* are expected to produce massive amounts of data for cosmology in the near future. Theorists are needed to gain better understanding of the new observational windows for non-Gaussianities and other primordial signals, and also get prepared for possible new discoveries.

Just as it goes[2]:

The way ahead is a long, long one, oh!
I will seek the Truth high and low.

[2]Qu Yuan (c. 340–278 BC), *The Lament*.

Samenvatting

Waar komen we vandaan?

De zoektocht naar de oorsprong van alles heeft generaties van nieuwsgierige mensen aan het denken gezet, al sinds onze voorouders verwonderd de sterrenhemel bestudeerden.

Wat zijn de fundamentele natuurwetten?

Om hier een volledig antwoord op te krijgen zijn tal van briljante denkers, van filosofen in het oude Griekenland tot aan theoretische natuurkundigen vandaag, 'het grootste avontuur dat de menselijke geest ooit is begonnen'[1] aangegaan.

Het is intrigerend dat de moderne kosmologie gedreven wordt door deze twee fascinerende vragen.De huidige wetenschappelijke opvatting is dat ons universum 13,8 miljard jaar geleden is ontstaan uit een piepklein volume dat zich in een zeer hete en dichte toestand bevond. Daarbij volgt uit bepaalde theoretische overwegingen dat het heelal de eerste fractie van een seconde na de oerknal exponentieel uitdijt. Dit theoretische model, kosmische inflatie genaamd, geeft een succesvolle beschrijving voor het vroege heelal. Tegelijkertijd vormen kwantumfluctuaties, die tijdens de periode van inflatie ontstaan, de zaadjes van kosmische inhomogeniteiten, die later evolueren tot sterrenstelsels, clusters en grootschalige structuren. Het is dus opmerkelijk dat we met behulp van astronomische observaties de fysische processen kunnen achterhalen die tijdens inflatie hebben plaatsgevonden. Als gevolg hiervan is de kosmologie een spannend onderzoeksgebied geworden voor theoretische natuurkundigen, waar men kan jagen op de fundamentele natuurkundige wetten die het vroege universum beheersten.

Met dit als motivatie, is dit proefschrift gewijd aan het onderzoeken voor theorieën van het vroege universum en hun verbinding met astronomische waarnemingen.

[1] Aangehaald door Richard Feynman, *The Feynman Lectures on Physics, Volume III.*

Het eerste deel van het proefschrift richt zich op inflatie in gekromde veldruimtes. Om te begrijpen hoe inflatie plaatsvindt, hebben we meestal een veld nodig dat de inflatie aandrijft. Dit veld wordt het inflatonveld genoemd en het kan in een multi-dimensionale veldruimte bewegen, die over het algemeen gekromd is. De geometrie van deze interne ruimte kan worden gezien als een bijzonder voorbeeld van nieuwe fysische effecten tijdens inflatie.

In Hoofdstuk 2 onderzoeken we een klasse van inflatiemodellen genaamd α-attractors. Hier wordt de magie van de hyperbolische veldruimte expliciet gedemonstreerd in de twee-velduitbreiding van deze modellen. Door de hyperbolische kromming blijven de voorspellingen van single-field α-attractors vrijwel onveranderd, zelfs wanneer de multi-field effecten significant sterker worden. Mijn werk vormt een aanvulling op de eerdere analyse van single-field α-attractor-modellen en benadrukt de rol van de hyperbolische geometrie van de veldruimte.

Hoofdstuk 3 introduceert een nieuwe klasse van kosmologische modellen, genaamd 'shift-symmetric orbital inflation', waarbij het inflaton in een algemene veldruimte in de 'hoek richting' beweegt. Wederom zijn de multi-field effecten significant in deze modellen, maar uiteindelijk vinden we nog steeds single-field-achtige voorspellingen. Mijn onderzoek focust op een minder bestudeerd regime in inflatie met meerdere velden, waarbij het extra veld licht is, maar tegelijkertijd aanzienlijk gekoppeld aan het inflaton.

Terwijl de meeste eerdere studies van de interne veldruimtes gebaseerd zijn op specifieke modellen, is Hoofdstuk 4 daarentegen gewijd aan een meer algemene vraag: wat zijn de model-onafhankelijke signalen van deze gekromde veldruimtes in inflatie? Hier probeer ik deze vraag te beantwoorden met behulp van de niet-Gaussische signalen gecreëerd door de aanwezige velden tijdens inflatie, en vind dat de vingerafdrukken van deze interne ruimtes kunnen worden getest in toekomstige waarnemingen.

Het tweede deel van het proefschrift bestudeert de fenomenologie van een zeer belangrijke observable - 'primordial non-Gaussianities', die de afwijking van de Gaussische verdeling van de vroege inhomogeniteiten meet. Deze signalen zijn het zoeken waard, omdat wordt aangenomen dat een schat aan informatie uit het vroege universum in de kosmologische driehoekspatronen is bevat.

Hoofdstuk 5 gaat opnieuw in op de non-Gaussianities die worden gegenereerd bij 'non-attractor-inflation'. Van deze klasse modellen is bekend dat

ze de 'single field consistency relation' van Maldacena schenden, en hebben daardoor veel bekendheid gekregen. Door een zorgvuldige berekening laten we expliciet zien wat er met dit beroemde tegenvoorbeeld gebeurt wanneer realistische en volledige modellen van non-attractor-inflation worden doorgerekend.

Hoofdstuk 6 bestudeert de niet-Gaussische fenomenologie van een alternatief voor inflatie - 'matter-bounce cosmology'. We beginnen met een algemene theorie met één veld. De hier geproduceerde niet-Gaussische signalen kunnen worden gebruikt om dit alternatieve scenario van inflatie te onderscheiden. Bovendien komen we tot een no-go-stelling die veel alternatieve modellen met de huidige staat van waarnemingen uitsluit.

Wat komt hierna? Dit proefschrift heeft tot doel de grens van de oerkosmologie te verleggen. Dit is een onderzoeksgebied dat zich snel ontwikkelt: er ontstaan veel interessante theoretische ideeën; en aankomende experimenten kunnen ons meer vertellen over de vroegste fase van het heelal. Om de nieuwe fysische effecten in het oertijdperk verder te verkennen, zijn de volgende onderwerpen de komende jaren de aandacht waard.

- *Interne symmetrieën* spelen gewoonlijk een belangrijke rol bij de fundamentele realisaties van inflatie, en ze kunnen ook nauw in verband staan met een effectieve veldentheorie, de geometrie van de veldruimte en nieuwe fenomenologie. Om te zoeken naar waarneembare effecten van onderliggende symmetrieën tijdens inflatie, is het interessant om meer systematisch onderzoek te doen.

- Het *scattering amplitudes* programma biedt nieuwe perspectieven en krachtige hulpmiddelen in de moderne kwantumveldentheorie. Men kan zich afvragen of vergelijkbare methodes kunnen worden toegepast voor 'bootstrapping-correlators' in de kosmologie. Hoewel er onlangs enkele baanbrekende werken zijn verschenen, is dit een gloednieuw gebied met veel open vragen.

- *Large scale structure* onderzoeken zullen naar verwachting in de nabije toekomst enorme hoeveelheden gegevens voor kosmologie opleveren. Theoretici zijn nodig om de nieuwe waarnemingsmogelijkheden voor non-Gaussianities en andere oersignalen beter te begrijpen en zich ook voor te bereiden op mogelijke nieuwe ontdekkingen.

Net zoals het gaat[2]:

De weg voor ons is een lange, lange, oh!
Ik zal de waarheid hoog en laag zoeken.

[2]Qu Yuan (c. 340–278 BC), *The Lament*.

List of publications

- Oksana Iarygina, Evangelos I. Sfakianakis, Dong-Gang Wang, Ana Achúcarro, *Multi-field inflation and preheating in asymmetric α-attractors*, arXiv: 2005.00528.
- Dong-Gang Wang, *On the inflationary massive field with a curved field manifold*, *JCAP* 2001 (2020) no.01, 046.
- Ana Achúcarro, Gonzalo Palma, Dong-Gang Wang, Yvette Welling, *Origin of ultra-light fields during inflation and their suppressed non-Gaussianity*, arXiv: 1908.06956.
- Yi-Fu Cai, Chao Chen, Xi Tong, Dong-Gang Wang, Sheng-Feng Yan, *When Primordial Black Holes from Sound Speed Resonance Meet a Stochastic Background of Gravitational Waves*, *Phys. Rev.* D **100**, 043518 (2019).
- Ana Achúcarro, Ed Copeland, Oksana Iarygina, Gonzalo Palma, Dong-Gang Wang, Yvette Welling, *Shift-symmetric orbital inflation: single field or multi-field?*, *Phys. Rev.* D *Rapid Communications*, **102**, 021302(R) (2020).
- Oksana Iarygina, Evangelos I. Sfakianakis, Dong-Gang Wang, Ana Achúcarro, *Universality and scaling in multi-field α-attractor preheating*, *JCAP* 1906 (2019) no.06, 027.
- Yi-Fu Cai, Xi Tong, Dong-Gang Wang, Sheng-Feng Yan, *Primordial black holes from sound speed resonance during inflation*, *Phys.Rev.Lett.* **121**, 081306 (2018).
- Andrei Linde, Dong-Gang Wang, Yvette Welling, Yusuke Yamada, Ana Achúcarro, *Hypernatural Inflation*, *JCAP* 1807 (2018) no.07, 035.

- Yi-Fu Cai, Xingang Chen, Mohammed Hossein Namjoo, Misao Sasaki, Dong-Gang Wang, Ziwei Wang, *Revisiting non-Gaussianity from non-attractor inflation models*, *JCAP* 1805 (2018) no.05, 012.

- Ana Achúcarro, Renata Kallosh, Andrei Linde, Dong-Gang Wang, Yvette Welling, *Universality of multi-field alpha-attractors*, *JCAP* 1804 (2018) no.04, 028.

- Yu-Bin Li, Jerome Quintin, Dong-Gang Wang and Yi-Fu Cai, *Matter bounce cosmology with a generalized single field: non-Gaussianity and an extended no-go theorem*, *JCAP* 1703 (2017) no.03, 013.

- Yi-Fu Cai, Antonino Marciano, Dong-Gang Wang and Edward Wilson-Ewing, *Bouncing cosmologies with dark matter and dark energy*, *Universe* **3**, 1 (2017).

- Yi-Fu Cai, Jinn-Ouk Gong, Dong-Gang Wang and Ziwei Wang, *Features from the non-attractor beginning of inflation*, *JCAP* 1610 (2016) no.10, 017.

- Fa Peng Huang, Youping Wan, Dong-Gang Wang, Yi-Fu Cai and Xinmin Zhang, *Hearing the echoes of electroweak baryogenesis with gravitational wave detectors*, *Phys. Rev.* D *Rapid Communications* **94**, 041702(R) (2016).

- Yi-Fu Cai, Francis Duplessis, Damien Easson and Dong-Gang Wang, *Search for a matter bounce cosmology with low redshift observations* , *Phys. Rev.* D **93**, 043546 (2016).

- Dong-Gang Wang, Yang Zhang and J. Chen, *Vacuum and Gravitons of Relic Gravitational Waves, and Regularization of Spectrum and Energy-Momentum Tensor*, *Phys. Rev.* D **94**, 044033 (2016).

- Dong-Gang Wang, Yi-Fu Cai, W. Zhao and Y. Zhang, *Scale-dependent CMB power asymmetry from primordial speed of sound and a generalized δN formalism*, *JCAP* 1602 (2016) no.02, 019.

Curriculum Vitae

I was born in 1991, in Guangrao in Shandong Province, a county town in East China. There, I attended primary school and middle school, and spent a lot time reading and dreaming, which in some sense planted the seeds for my interests in physics and astronomy.

In 2006, I left my hometown and went to the Shengli No.1 High School in the city of Dongying. In 2009, I went to China University of Petroleum, Beijing. This turned out to be a poor decision, as engineering was not my passion, while my dream of physics and astronomy kept calling me. So, later, I decided to pursue a new career towards the stars above, instead of the oil beneath the ground. After my undergraduate study I earned admission to the University of Science and Technology of China (USTC), being exempted from the postgraduate entrance examination.

From 2013, I did my master study in the Department of Astronomy at USTC, and started to work on cosmology under the supervision of Prof. Yang Zhang. I became intrigued by the question how galaxies originated from quantum fluctuations in the very early Universe, and devoted myself to this research area. In 2015, I met and started my collaborations with Prof. Yi-Fu Cai, who joined USTC as a new faculty member at that time and sparked my interest in the modern frontier of cosmology.

In 2016, I obtained a de Sitter Fellowship from Leiden University and came to the Netherlands for my PhD. There I became affiliated with Leiden Observatory and Lorentz Institute for Theoretical Physics, and started conducting theoretical research in primordial cosmology under the supervision of Prof. Ana Achúcarro. My PhD training motivated me to systematically look into high energy physics effects in consistent theories of cosmic inflation and also focus on their detectability in astronomical observations.

From October 2020, I will be a postdoctoral researcher in the theoretical cosmology group of Dr. Enrico Pajer in the Department of Applied Mathematics and Theoretical Physics at the University of Cambridge.

Acknowledgements

The four year's journey for my PhD in Leiden is coming to an end, and I cannot imagine I would have gotten this far without the support of many people.

Ana, I won't simply say "thank you" here, since it cannot express how grateful I truly am. To me, what you have done in the past 4 years is much more than mentoring a PhD student on specific projects. Academically, you showed me how to figure out physically important problems and develop exciting ideas with scientific rigor. Because of your support, I was also able to get in touch with so many brilliant cosmologists, and step on an upward trajectory for career. Psychologically, you have helped me through the darkest moments in my PhD life, and guided me to find the strength within myself. It is hard to describe how tremendously you have influenced me on the way to become a good cosmologist and a better person. No doubt you are the best supervisor that I could have hoped for.

Yifu, it was fantastic to keep collaborating with you and your group at USTC even after I had graduated. I really appreciate your generous and long-term support for my research, career development and life, which has turned out to be very important for my PhD period. Needless to say, I was very fortunate to meet you when I started my journey in cosmology.

I would like to thank my collaborators during my PhD: Ed Copeland, Chao Chen, Xingang Chen, Oksana Iarygina, Renata Kallosh, Yubin Li, Andrei Linde, Mohammed Hossein Namjoo, Gonzalo Palma, Guilherme Pimentel, Jerome Quintin, Misao Sasaki, Evangelos Sfakianakis, Xi Tong, Ziwei Wang, Yvette Welling, Yusuke Yamada, Sheng-Feng Yan. There was a lot of fun in our collaborations, and it would be impossible to finish those cool projects without you!

I am also grateful to my colleagues at the Leiden Observatory and the Lorentz Institute for creating a warm environment. Many thanks, Koen, for your kind and continuous support. Special thanks to the Leiden cosmology

gang members Yashar, Guadalupe, Omar, Matteo, Simone, Valeri, and also my office mates Margot, Vivianni, Alessandro and Shunsheng. Thank you, Yvette, for helping me with the Dutch summary of this thesis. Certainly I should also acknowledge the efficient and friendly administrative support from Marjan, Alexandra, Evelijn and Fran.

Meanwhile it was a great pleasure to be part of the Dutch theoretical cosmology community, and I really enjoyed our monthly THC meetings. Special thanks to Horng Sheng Chia, Perseas Christodoulidis, Garret Goon, Leihua Liu, Enrico Pajer and Diederik Roest. The discussions with you have been illuminating and helpful. I am also indebted to many other cosmology colleagues outside the Netherlands, including but not limited to Vicente Atal, Andrea Fuster, Cristiano Germani, Jinn-Ouk Gong, Bin Hu, Chunshan Lin, Sebastien Renaux-Petel, Krzysztof Turzynski, Yi Wang, Alexander Westphal and Edward Wilson-Ewing.

Life is full of ups and downs, and it would be difficult to handle them without the company of friends outside of cosmology, thus I would like to express my sincere gratitudes to Chao Fan, Qi Zhang, Yuanhao Guo, Junjie Mao, Zhihong You, Shizhe Zhang, Xuechen Zheng, Fangyou Gao, Mingyuan Wang, Zhenfeng Sheng, Feng Jiang, Yun Tian, Chunmiao Ye, Yuhan Sun, Xuxing Lu, Jiangnan Ding, Junxiang Yao, Yu Liu, Zujia Lu, Peng Cheng, Yongliang Hao, Maolin Zhang, members of the Leiden Science China community and USTC Alumni Association in the Netherlands, and many others.

At last I am deeply indebted to my family, especially to my parents. Your unconditional love is always the solid backing for me and the invaluable treasure in my life. This thesis is dedicated to you.